Université de Montréal

Rôle physiologique de la MAP kinase atypique ERK3 : Analyse génétique et étude de l'expression génique chez la souris

par

Benjamin Turgeon

Programme de biologie moléculaire
Faculté des études supérieures

Thèse présentée à la Faculté des études supérieures
en vue de l'obtention du grade de Philosophiæ Doctor (Ph.D.)
en biologie moléculaire

Janvier, 2007

Université de Montréal
Faculté des études supérieures

Cette thèse intitulée :

Rôle physiologique de la MAP kinase atypique ERK3 : Analyse génétique et étude de l'expression génique chez la souris

présentée par :
Benjamin Turgeon

a été évaluée par un jury composé des personnes suivantes :

……Jacques Drouin, Ph.D……
président rapporteur

……Sylvain Meloche, Ph.D……
directeur de recherche

……...…Jean Vacher, D. Sc……
membre du jury

……Jean Charron, Ph.D……
examinateur externe

……Philippe Roux, Ph.D……
représentant du doyen

Thèse acceptée le 23 juillet 07

RÉSUMÉ

Les MAP (*mitogen-activated protein kinases*) kinases sont des protéines kinases à spécificité Ser/Thr qui définissent des voies de signalisation impliquant un module caractéristique de trois kinases activées de façon séquentielles par phosphorylation. L'implication de ces voies de signalisation dans une multitude de processus cellulaires, leur conservation au cours de l'évolution ainsi que l'effet dramatique de la perte de la plupart de ces isoformes pour le développement murin témoigne de leur importance biologique. ERK3 (extracellular signal-regulated kinase 3) fait partie cette grande famille qui comprend 14 gènes chez l'humain. ERK3 se distingue des autres MAP kinases par certaines caractéristiques structurales et un mode de régulation atypique. Par ailleurs, plusieurs controverses sont associées à l'étude de ERK3, dont l'existence d'isoformes, sa localisation subcellulaire ainsi que son activité catalytique, expliquant en partie pourquoi sa fonction reste inconnue 15 ans après sa découverte. Dans le but de comprendre la fonction de ERK3, j'ai créé un modèle animal pour permettre l'étude de son rôle biologique sans être limité par ces controverses ou encore par ses caractéristiques moléculaires atypiques.

Dans un premier temps, j'ai isolé, séquencé et caractérisé un ADNc encodant la protéine ERK3 murine. Cet ADNc a permis d'étudier l'expression de l'ARNm de *Erk3* chez la souris et de caractériser son produit comme étant une protéine de 100 kDa. Par ailleurs, l'analyse des séquences de l'ARNm ainsi que d'une partie du gène *Erk3* de rat a permis de confirmer une erreur dans la séquence de l'ADNc de *Erk3* de rat publiée. Enfin, le gène *Erk3* murin a été localisé sur le chromosome 9 du génome murin. De façon importante, ce travail a fourni les premières évidences expérimentales que ERK3 est une protéine de 100 kDa chez les mammifères, permettant de résoudre la controverse de l'existence d'un gène encodant une isoforme de 62 kDa.

Dans une deuxième étape, j'ai isolé par clonage moléculaire le gène murin encodant ERK3 et déterminé sa structure. Le gène est divisé en 6 exons dont un exon non-codant situé dans la partie 5' du gène, à une dizaine de kilobases (kb) du premier exon codant. Par ailleurs, l'analyse des séquences génomiques chez l'humain révèle que la structure de ce gène est très bien conservée entre la souris et l'homme. De plus, la structure exon/intron est conservée entre les gènes *ERK3* et *ERK4* humain, démontrant que ces deux gènes sont paralogues. Finalement, cette analyse du génome humain a révélé six pseudogènes de *ERK3*. Ainsi, ces analyses confirment l'existence d'un seul gène encodant la protéine ERK3.

Dans un troisième temps, j'ai généré un modèle d'invalidation génique de ERK3 chez la souris par remplacement de sa partie codante par le gène rapporteur *LacZ*. L'étude de l'expression de ce transgène au cours du développement foetal indique que le gène *Erk3* est exprimé de façon importante dans les cellules possédant un réticulum endoplasmique (RE) spécialisé et très développé comme les cellules épithéliales et musculaires. De plus, l'expression de ce gène est régulée dans l'espace et le temps au cours du développement de plusieurs tissus, suggérant un rôle important de ERK3 lors de l'ontogénie. En accord avec cette idée, l'invalidation de ce gène mène à la mortalité néonatale. Celle-ci est causée par une détresse respiratoire à la naissance ainsi qu'à une incapacité des nouveaux-nés à téter. Par ailleurs, la perte de fonction du gène *Erk3* est associée à un retard de croissance *in utero* ainsi qu'à une tolérance anormale au glucose chez les nouveaux-nés.

En conclusion, mes travaux font la lumière sur la controverse associée à l'existence de plusieurs isoformes de ERK3. De façon importante, mes études ont également permis de mettre en évidence l'importance biologique de ERK3 pour la première fois et d'associer la perte de fonction de ce gène à des états pathologiques.

Mots clés: MAPK, ERK3, clonage moléculaire, localisation chromosomique, invalidation génique, détresse respiratoire, incapacité téter, retard de croissance, intolérance au glucose, mortalité néonatale.

SUMMARY

Mitogen-activated protein (MAP) kinases are a superfamily of serine/threonine kinases that play a major role in transducing extracellular chemical and physical signals into intracellular responses. The high relevance of these pathways is depicted by their involvement in a large number of cellular processes, their high conservation through evolution as well as the dramatic effects resulting from gene inactivation of these enzymes in mice. Extracellular signal-regulated kinase (ERK) 3 is an atypical member of this superfamily that encodes 14 genes in human. However, it possesses many structural and regulatory features that make it unique among the MAP kinase family. Since its discovery 15 year ago, ERK3 study has been impaired by many controversies concerning the existence of isoforms, its subcellular localization as well as its putative kinase activity. As a consequence, ERK3 biological function remains elusive. With the aim to understand ERK3 function, I have created an animal model to allow the study of its biological function without the limitations associated with its atypical character or controversies related to the study of its molecular biology.

First, I cloned, sequenced and characterized a mouse homolog of ERK3. The cDNA isolated allowed the study of *Erk3* mRNA expression in mouse and the characterization of its product as a protein of 100 kDa. Furthermore, the analysis of *Erk3* mRNA and gene sequences in rat has revealed a cloning artefact in the rat cDNA sequence previously published. Finally, the *Erk3* gene was mapped to mouse chromosome 9. Importantly, these results provide several lines of evidence to support the existence of a unique *Erk3* gene product of 100 kDa in mammalian cells, resolving the controversy of the existence of an ERK3 isoform of 62 kDa.

Second, I characterized the genomic loci encoding ERK3 in mice and humans. Molecular cloning and sequencing reveal that the mouse *Erk3* gene spans more than 20 kb and is split into six exons. Its structure is similar to the human *MAPK6* gene, which extends over 40 kb. In humans, database analysis has revealed the presence of six *MAPK6* processed pseudogenes. Furthermore, *ERK3* structure is conserved with that of *ERK4,* indicating that these genes are paralogs. This analysis confirms the existence of a single functional gene encoding ERK3.

Finally, the *Erk3* gene was inactivated in mouse by knock-in of the *LacZ* reporter gene. Expression studies using the *LacZ* reporter revealed that *Erk3* is strongly expressed in muscle tissues as well as in the epithelium of multiple organs during development. Interestingly, *Erk3* expression is regulated in time and space in multiple organs at various stages of their development, suggesting an important role of ERK3 for mouse ontogeny. Targeted inactivation

of *Erk3* is associated with respiratory failure or inability to feed after birth, leading to neonatal death. Furthermore, loss of ERK3 results into intrauterine growth restriction, consistent with an important role of ERK3 during development. In addition, newborn homozygous mutants have an impaired glucose tolerance after birth. These data represent the first genetic evidence of an essential role of ERK3 for normal mouse development.

Keywords: MAPK, ERK3, molecular cloning, chromosomal mapping, gene knockout, respiratory distress, inability to feed, intrauterine growth restriction, glucose tolerance, neonatal death.

TABLE DES MATIÈRES

LISTE DES TABLEAUX

LISTE DES FIGURES

LISTE DES SIGLES ET ABRÉVIATIONS

Abréviation	Signification
a.a.	Acides aminés
Ach	Acetylcholine
ACTB	Actin beta
ADN	Acide désoxyribonucléique
ADNc	ADN complémentaire
Ala	Alanine
Arg	Arginine
ARNm	Acide ribonucléique messager
ATP	Adenosine triphosphate
ATt-20	Atomic test tube 20
BAC	Bacterial artificial chromosome
BDNF	Brain derived neurotrophic factor
BMK	Big MAP kinase
bp	Base pair
BSA	Bovine serum albumin
β-Gal	Beta-galactosidase
Cdc7	Cell division cycle 7
CE	Cornified envelope
CEBP	CCAAT/enhancer binding protein
CK1	Caseine kinase 1
cpm	Count per million
CP	Choroid plexus
CRM1	Chromosome region maintenance 1
CSAIDS	Cytokine suppressive anti-inflammatory drugs
DA	Ductus arteriosus
DMBA	7,12-dimethylbenz(*a*)anthracene
DN	Double négatif
DP	Double positif
dpc	Day post coitum

E	Embryonic
EGF	Epithelial growth factor
E-M	Epithéliomésenchymateuse
ERGIC	ER-Golgi intermediate compartment
ERK	Extracelllular signal-regulated kinase
ES	Embryonic stem
EST	Expressed sequence tag
F5	Factor V
F7	Factor VII
FISH	Fluorescent *in-situ* hybridisation
FGF	Fibroblast growth factor
FMN	Facial motor nucleus
GABA	Gamma-aminobutyric acid
GAPDH	Glyceraldehyde-3-phosphate dehydrogenase
GFP	Green fluorescent protein
Glu	Glutamic acid
Gly	Glycine
GPCR	G-protein coupled receptor
Grb2	Growth factor receptor-bound protein 2
H&E	Hematoxylin and eosin
HGF	Hepatocyte growth factor
HMN	Hypoglossal motor nucleus
IGF	Insulin-like growth factor
IL-2	Interleukin-2
IUGR	Intrauterine growth restriction
JNK	c-Jun N-terminal kinase
kDa	Kilodaltons
KO	Knockout
LINE	Long interspersed nuclear element
LPS	Lipopolysaccharides
LTR	Long terminal repeat

MAGUK	Membrane associated guanylate kinase
MAP2	Microtubule-associated protein 2
MAPK	Mitogen-activated protein kinase
MAPKAPK	MAP kinase-activated protein kinase
MBP	Myelin basic protein
MEF	Mouse embryonic fibroblasts
MEF2C	Myocyte-specific enhancer factor 2C
MEK	MAP-ERK kinase
MK5	MAPKAPK5
MKK	Map kinase kinase
MKKK	Map kinase kinase kinase
MKP	MAP kinase phosphatases
MPTP	1-methyl 4-phenyl 1,2,3,6-tetrahydropyridine
mM	Milimolar
ml	Mililiter
µg	Micrograms
µl	Microliter
µM	Micromolar
NCBI	National center for biological information
NEK2	NIMA related expressed kinase 2
Neo	Neomycin
ng	Nanogram
NGF	Nerve growth factor
NIMA	Never in mitosis A
NLK	Nemo-like kinase
NMJ	Neuromuscular junction
NTD	Neural tube defects
ORF	Open reading frame
OT	Outflow tract
PBS	Phosphate buffered saline
PCR	Polymmerase chain reaction
PDA	Patent ductus arteriosus
PDGF	Platelet derived growth factor

pFRG	Parafacial respiratory group
PGF	Prostaglandine
PKA	Protein kinase A
PKC	Protein kinase C
PMA	4α-Phorbol 12-myristate 13-acetate
PN	Pneumocytes
PRL	Prolactine
Pro	Proline
PTP	Protein tyrosine phosphatase
RA	Retinoic acid
Rb	Retinoblastoma
RDS	Respiratory distress syndrome
RE	Réticulum endoplasmique
RCPG	Récepteur couplé aux protéines G
rpL32	Ribosomal protein L32
RT	Reverse transcriptase
RTK	Récepteur tyrosine kinase
SAP	Stress-activated protein
SDS	Sodium dodecyl sulfate
Ser	Sérine
SF	Scatter factor
SINE	Small interspersed nuclear element
Src	Sarcoma kinase
TAK	TGF-β activated protein
TAP	Tandem affinity purification
Taq	Thermophilus aquaticus
TBS	Tris-buffered saline
TCF	Ternary complex factor
TGF	Tumor growth factor
Th	T helper
TMN	Trigeminal motor nucleus
Tnf	Tumor necrosis factor
Thr	Thréonine

Tyr	Tyrosine
TPA	Tetradecanoyl phorbol acetate
TEWL	Transepidermal water loss
UTR	Untranslated region
UV	Ultra-Violet
VEGF	Vascular endothelial growth factor
VLM	Ventrolateral medulla
WNT	Wingless/Int factor
WT	Wild-type
X-Gal	5-bromo-4-chloro-3-indolyl-b–galactopyranoside

Je dédis cette thèse à mon père, de qui j'ai hérité l'âme d'un biologiste,
De même qu'à tous ceux qui vont la lire, par intérêt.

Le savant n'est pas l'homme qui fournit les vraies réponses.
C'est celui qui pose les vraies questions. (Claude Lévi-Strauss)

REMERCIEMENTS

Un parcours scientifique ne s'effectue jamais en solitaire, je tiens à remercier toutes les personnes qui ont contribué de près ou de loin à l'avancement de mes recherches, ainsi que ceux et celles qui m'ont soutenu et fait confiance. Merci pour votre patience et votre tolérance envers mes nombreux retards associés aux imprévus de l'expérimentation en laboratoire.

Je remercie le Dr Sylvain Meloche pour l'accueil dans son équipe, pour le traitement particulier dont il m'a fait part, pour la grande confiance démontrée envers mes aptitudes, son esprit juste, ainsi que son énorme motivation pour les projets sur lesquels nous avons eu la chance de travailler. Je remercie le Dr Marc K. Saba-El-Leil pour m'avoir supervisé à mes débuts dans le laboratoire, pour avoir contribué au développement de mon autonomie expérimentale et intellectuelle, de même que pour les corrections de certains chapitres.

J'aimerais remercier les membres du laboratoire avec qui j'ai partagé des moments inoubliables au cours de ces nombreuses années. Je tiens à exprimer mon immense gratitude à Philippe Coulombe (maintenant Ph.D) pour la correction de la thèse, de m'avoir accompagné dans mon cheminement scientifique en tant que guide et modèle, et pour les moments partagés entre amis. Merci à Justine Rousseau, ma protégée, avec qui j'ai partagé la passion de projets communs et qui m'a permis de rédiger une partie de la thèse dans un endroit calme et chaleureux. Merci à Valérie Paquet et Kim Lévesque pour l'aide technique.

Ma reconnaissance va également à ma famille, mes parents et mes trois frères, qui n'ont pas toujours compris en quoi j'étudiais, mais qui n'ont cependant jamais douté de mes aptitudes à poursuivre et terminer mon doctorat. Merci à tante Rachel pour son attention spéciale, son support et pour le prêt de sa voiture pour me rendre au labo tard le soir. Je remercie Marco pour son support moral et une amitié inconditionnelle. Merci à Geoffrey et Jean-René pour leur support, leur amitié et pour avoir été là à des moments critiques de mon cheminement.

Un merci particulier à mon rayon de soleil Diana Paola pour la correction de la thèse, ses commentaires ainsi qu'un support moral qui a fait toute la différence en fin de thèse et particulièrement dans ma vie.

J'aimerais finalement remercier les membres du jury pour avoir accepté de réviser cette thèse de doctorat.

CHAPITRE 1

INTRODUCTION : SECTION 1

ERK3, une MAP kinases atypique dans un monde classique

MISE EN SITUATION

Cette thèse de doctorat, qui se divise en 5 chapitres, décrit le clonage et l'analyse du gène *Erk3* murin, le clonage et l'analyse d'un ADNc de ERK3 murin, la détermination de sa localisation chromosomique de même que l'effet de l'inactivation de ce gène chez la souris.

Le chapitre 1 est une revue de la littérature qui est divisée en deux parties. La première section traite des voies MAP kinases, principalement en termes de leur importance physiologique chez la souris. Par ailleurs, cette section adresse le contexte scientifique associé à l'étude de ERK3 de façon à situer le projet recherche. La section suivante est une revue des phénotypes et défauts associés à la mortalité néonatale chez les mutants de souris.

1.1 Un quart de siècle de MAP kinases

La phosphorylation des protéines sur des résidus sérine (Ser), thréonine (Thr) ou tyrosine (Tyr) est située au cœur des processus de régulation des activités cellulaires. Le grand nombre de gènes encodant les enzymes responsables des évènements de phosphorylation démontre l'importance de cette modification post-traductionnelle. Ainsi, plus de 2% du génome de plusieurs organismes encodent des protéines kinases [1]. L'importance de ces gènes est de plus illustrée par leur conservation élevée au cours de l'évolution. Par exemple, le génome murin contient 510 des 518 kinases retrouvées chez l'humain [2].

Un des rôles majeurs des kinases intracellulaires est leur participation aux cascades d'événements par lesquels les cellules répondent aux messages extracellulaires. Ces cascades d'événements, appelées voies de signalisations, correspondent à l'interprétation des signaux moléculaires reçus par la cellule. Plusieurs de ces voies sont définies par une famille d'enzymes appelées MAP kinases (Mitogen activated protein kinases), qui possèdent une spécificité pour les acides aminés (a.a.) Ser et Thr. Une voie MAP kinase typique se caractérise par son architecture définie par un module de trois kinases, elles-mêmes activées de façon séquentielle par phosphorylation : une MAP kinase kinase kinase (MKKK), une MAK kinase kinase (MKK) et la MAP kinase elle-même (Figure 1).

Il existe plusieurs modules MAP kinases et une multitude d'évènements pouvant activer ces voies, la réponse associée à l'activation d'un module MAP kinase spécifique étant dépendant du contexte cellulaire. L'implication de ces voies de signalisation dans un grand nombre de processus cellulaires de même que leur conservation au cours de l'évolution témoigne de leur importance pour les systèmes biologiques.

1.1.1 La naissance d'un dogme

L'étude des MAP kinases s'est faite à des vitesses fort différentes au cours des années, en relation directe avec les techniques disponibles. Plusieurs ères sont associées à l'étude des MAP kinases : l'ère biochimique, l'ère du clonage moléculaire et l'ère post-génomique. N'étant pas mutuellement exclusives, chacune a contribué à forger notre vision scientifique des voies MAP kinases et de leurs rôles en biologie.

1.1.1.1 L'origine: Une «activité» MAP kinase

La naissance de la recherche sur les MAP kinase remonte au début des années 80, alors qu'on s'intéressait aux substrats de kinases à spécificité tyrosine, comme les récepteurs

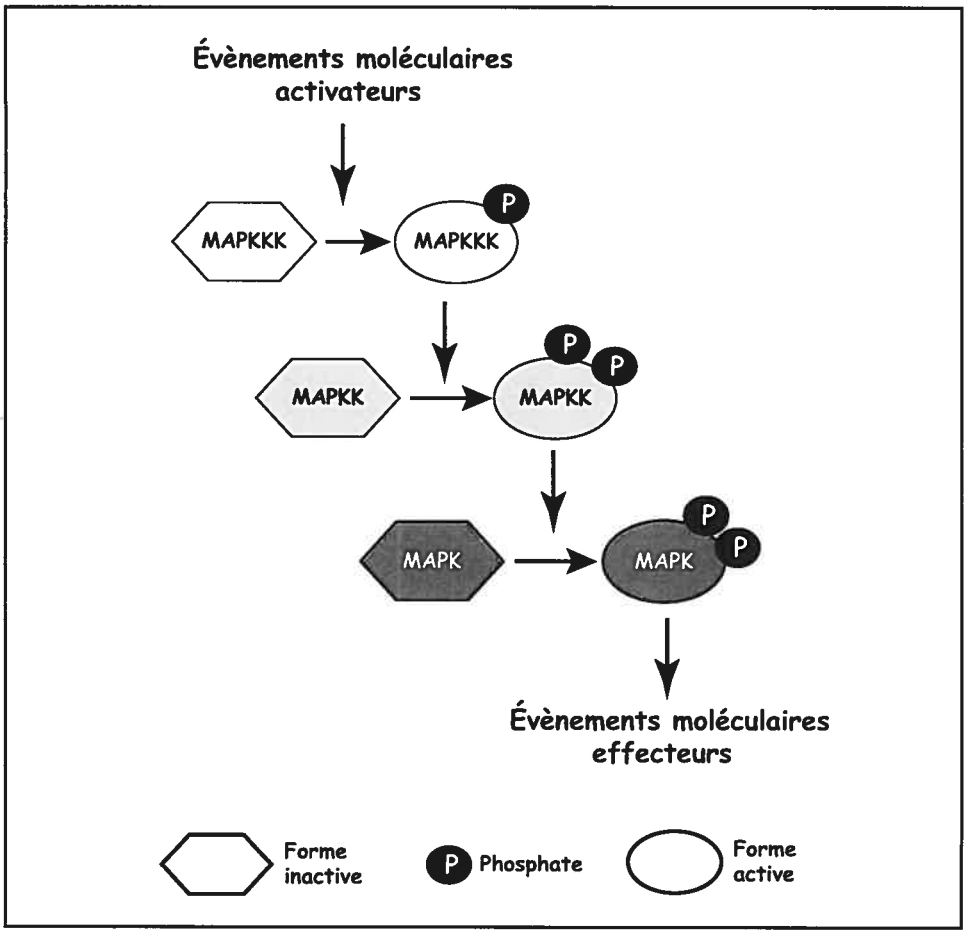

Figure 1: Organisation d'un module MAP kinase typique. L'activation de la MAPK résulte d'une cascade d'évènements de phosphorylation. Adaptée de [44].

des facteurs de croissance ou certains oncogènes, dans le but de comprendre leur mécanisme d'action. Ainsi, la stimulation de fibroblastes quiescents par le EGF, PDGF, TPA ou le sérum bovin, s'accompagnait de la phosphorylation en tyrosine d'une protéine d'environs 42 kDa [3-6]. Ces évènements de phosphorylation étaient observés dans des fibroblastes de plusieurs espèces [7, 8], suggérant que la phosphorylation de cette protéine, appelée pp42, était un évènement précoce conservé dans la réponse aux mitogènes.

Par ailleurs, cet intérêt pour la phosphorylation en réponse à des signaux extracellulaires, dont l'insuline, impliquait également la recherche d'activités kinases pouvant être modifiées en réponse à ces signaux. Ainsi, une entité appelée MAP kinase pour *microtubule-associated protein kinase*, était reconnue pour être activée en réponse à l'insuline [9, 10]. Cette activité kinase était mesurée par la phosphorylation de la protéine MAP2, d'où le nom MAP kinase. Cette MAP kinase, spécifique aux résidus Ser/Thr, était elle-même phosphorylée en Tyr et Thr en réponse à l'insuline [11]. Ceci suggérait que cette enzyme était une composante

importante de la cascade de phosphorylation impliquée dans la réponse à l'insuline, mais également en réponse à d'autres signaux extracellulaires mitogéniques. En effet, cette activité kinase était aussi activée par plusieurs mitogènes polypeptidiques ou non-peptidiques [12]. La purification partielle de cette activité a permis sa caractérisation, révélant une enzyme biochimiquement différente des autres kinases connues de l'époque [13, 14].

La phosphorylation en tyrosine de cette MAP kinase en réponse à l'insuline ainsi que sa masse moléculaire, d'environ 42 kDa, suggérait fortement que pp42 était la MAP kinase à spécificité Ser/Thr activée par plusieurs signaux mitogéniques. La caractérisation biochimique de pp42 en comparaison avec MAP kinase en réponse aux signaux mitogéniques, incluant le séquençage partiel de séquences polypeptidiques, confirma que pp42 était bel et bien MAP kinase [15]. Le terme MAP kinase prenait alors un deuxième sens pour *mitogen-activated protein kinase*. Cette définition est d'ailleurs celle utilisée aujourd'hui pour décrire la famille MAP kinase.

L'ADNc de cette protéine fut par la suite isolé par clonage moléculaire et l'enzyme a été renommé ERK1 pour *extracellular signal-regulated kinase* 1 [16]. À cette époque, on était loin de penser que le rôle de cette enzyme dépasserait le simple médiateur intracellulaire des facteurs de croissance. L'étude de la voie de signalisation définie par ERK1 est à l'origine de l'élaboration du dogme MAP kinases.

1.1.1.2 La voie MAP kinase : élaboration du dogme

L'étude des MAP kinases connue un développement fulgurant suite au clonage moléculaire d'ADNc encodant des protéines apparentées à ERK1. La connaissance de ces ADNc a ensuite rendu possible le clonage de plusieurs autres membres de la famille MAP kinase. Finalement, l'utilisation de protéine recombinante permis la caractérisation de l'architecture de la voie MAP kinase ainsi que ses mécanismes de régulation. Parallèlement, des protéines responsables de l'activation de MAP kinase ont été découvertes et caractérisées.

De MAP kinase à MAP kinases. La connaissance d'une séquence nucléotidique de l'ADNc de ERK1 a permis le clonage de plusieurs autres membres de la famille MAP kinase : ERK2 et ERK3 en 1991 [17], $p63^{MAPK}$/ERK4 en 1992 [18], ERK5 en 1995 [19, 20] et ERK7 en 1999 [21]. Par ailleurs, des kinases ayant des particularités de structure et de régulation semblables à ERK1 furent découvertes. Ainsi, deux nouvelles familles de MAP kinases, JNK et $p38^{MAPK}$ furent identifiées et caractérisées [22].

Le module MAP kinase. Des activités kinases activatrices de l'activité MAP kinase ont été caractérisées biochimiquement et isolées par clonage moléculaire [23]. Par contre, l'existence de modules MAP kinases spécifiques a d'abord été reconnu chez la levure, où l'architecture de la voie MAP kinase en module de trois kinases a été proposée [24]. Les protéines situées en amont du module MAP kinase sont également retrouvées chez les mammifères, indiquant la conservation de l'architecture du module MAP kinase au cours de l'évolution [25]. Les MKK définissent une grande famille de kinases, alors que les MKKK forment un groupe hétérogène d'enzymes appartenant à différentes familles de gènes [25]. Quatre modules de ce type ont d'ailleurs été caractérisés chez les mammifères : la voie ERK1/2, la voie JNK, la voie $p38^{MAPK}$ et la voie ERK5 (voir ci-bas).

Régulation de l'activité MAP kinases. En absence de signaux activateurs, les MAP kinases ont une activité catalytique difficilement détectable. De façon similaire, l'activité d'une MAP kinase recombinante produite en bactérie est plutôt faible. On connaît depuis longtemps l'importance de la phosphorylation pour l'activité ERK ainsi que les sites phosphorylés de la kinase active [11 , 26]. Depuis, des études structurales de plusieurs MAP kinases, dont les formes inactive et active de ERK2, ont permis une meilleure compréhension de leur activation [27]. L'activité catalytique MAP kinase est régulée par phosphorylation d'une séquence peptidique appelée la boucle d'activation. Les résidus Thr et Tyr du motif TXY (ou X est un résidu variable) situés dans cette boucle sont les sites accepteurs de la double phosphorylation par les MAPK kinases. Les changements de conformation associés à l'activation enzymatique requièrent absolument la double phosphorylation. Ainsi, la phosphorylation du résidu Thr est importante pour modifier la géométrie du site actif, donc de l'activité catalytique. Par ailleurs, la phosphorylation du résidu Tyr augmente l'accessibilité aux substrats. Dans le cas de ERK2, la double phosphorylation active l'enzyme plus de 1000 fois [27]. Une caractéristique intéressante de la nécessité de phosphorylation double dans la boucle d'activation est que la substitution de la Thr et Tyr par des résidus acidiques (phospho-mimétiques) ne résulte pas en une forme constitutivement active de l'enzyme. Seulement les résidus Thr et Tyr phosphorylés peuvent induire les changements de conformation appropriés pour l'activation de la MAP kinase. Par ailleurs. C'est probablement pour cette raison que les MAP kinases non jamais été identifié comme des oncogènes [25].

L'inactivation des MAP kinases se fait par déphosphorylation, principalement par un groupe spécialisé de phosphatases appelées MKPs (*MAP kinase phosphatases*). Jusqu'à présent, plus de 10 MKPs ont été identifiées [28]. Les MKPs font partie de la grande famille PTP (*protein tyrosine phosphatase*) et ont une spécificité envers les résidues phosphotyrosine et phosphothréonine. La déphosphorylation d'un seul site du motif TXY est suffisante pour rendre la kinase inactive, et d'autres phosphatases à spécificité unique peuvent également

déphophoryler et inactiver les MAP kinases [27].

Spécificité. Les MAP kinases sont des kinases à spécificité Ser/Thr, i.e, elles catalysent l'ajout d'un phosphate sur des résidus Ser ou Thr de protéines cibles. Leurs substrats sont phosphorylés sur des séquences similaires ayant le motif peptidique Ser/Thr-Pro (S/TP). L'activité catalytique MAP kinase est donc *proline directed.* Puisque cette séquence peptidique peut être retrouvée dans un nombre important de substrats potentiels, plusieurs déterminants existent pour contrôler la spécificité des MAP kinases. Parmi ceux-ci on retrouve la présence de site d'amarrage sur les substrats [29] ainsi que l'existence de protéine d'échafaudage [30].

Localisation subcellulaire. La fonction des MAP kinases comme protéine de signalisation implique la réponse à des signaux extracellulaires et leur transduction dans la cellule. Étant donné que les substrats de MAP kinases peuvent se retrouver dans le cytoplasme et dans le noyau, le contrôle spatial est un mode important de la régulation des MAP kinases [31]. Notamment, il a été montré que la phosphorylation des MAP kinases ERK1/2 favorise leur translocation nucléaire [32]. Les protéines d'échafaudage sont également impliquées dans le contrôle de la localisation subcellulaire des MAP kinases activées [30].

1.1.2 Les MAP kinases à l'ère post-génomique

Le séquençage du génome humain a récemment permis de définir son kinome, i,e, le catalogue de tous les gènes possédant un domaine kinase. Bien que tous les membres de la famille MAP kinase étaient déjà connus à ce moment, cette analyse a permis de confirmer leur organisation en une grande famille de 14 gènes subdivisés en 7 sous-familles. Ces protéines sont représentées à la figure 2. De plus, l'analyse de différents génomes a permis de comparer la conservation des MAP kinases entre diverses espèces. Par exemple, chacun de ces gènes possède un orthologue hautement conservé chez la souris (voir ci-bas). Une classification des MAP kinases en deux groupes a récemment été suggérée, basée sur leur mode d'activation [33]. Les MAP kinases conventionnelles sont activées selon un mode dit classique, i.e, par double phosphorylation par un membre de la famille MAPKK. Par contre, les MAP kinases atypiques présentent un mode de régulation différent de celui des MAP kinases conventionnelles.

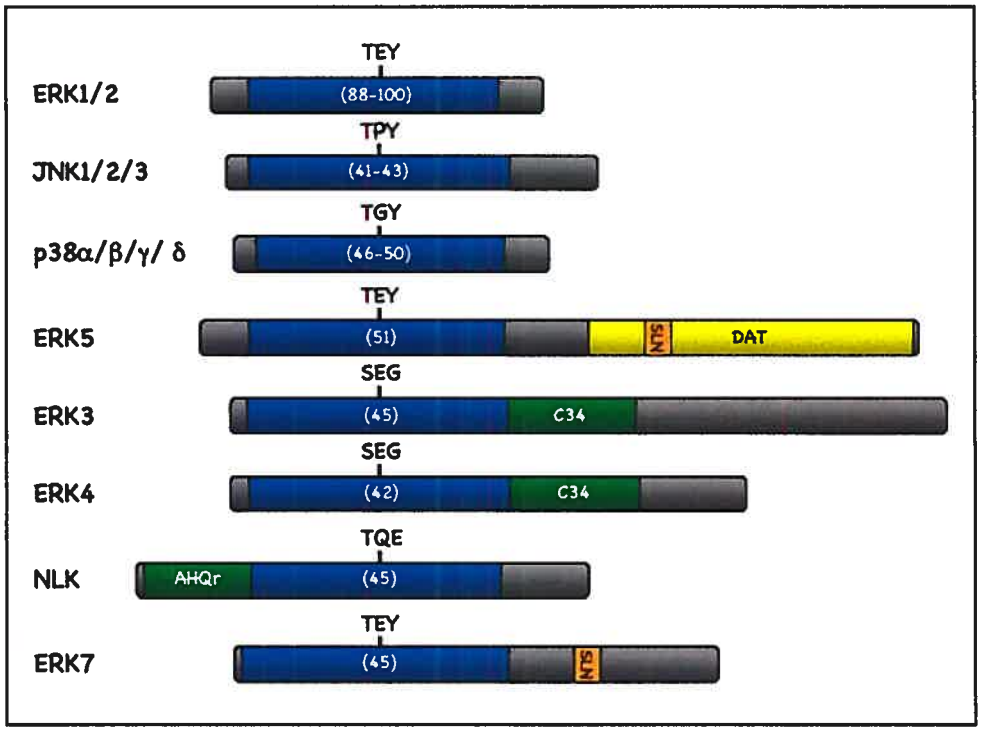

Figure 2: Représentation schématique des membres de la grande famille MAP kinase chez les mammifères. Les isoformes d'une même sous-famille (à l'exeption de ERK4 de la sous-famille ERK3) ne sont pas représentées par simplicité. Le pourcentage d'identité protéique dans le domaine catalytique (bleu) est indiqué par rapport à ERK1. (DAT: domaine d'activation transcriptionnel; SLN: signal de localisation nucléaire; C34: Région conservée ERK3/4; AHQr: région riche en résidus Ala/His/Gln). Adaptée de [33].

1.1.2.1 MAP kinases classiques

1.1.2.1.1 ERK1/2

La voie MAP kinase prototype ERK est celle définie par les isoformes ERK1/ERK2, qui sont encodées par deux gènes différents. L'étude de cette voie a grandement contribué à notre compréhension des voies MAP kinases, et est à l'origine du dogme MAP kinase. La grande variété de signaux capable d'activer cette voie explique en partie pourquoi elle est la mieux caractérisée de toutes les voies MAP kinases. La voie ERK est au cœur de la régulation de plusieurs processus cellulaires associés à la croissance, la différenciation et la survie [34].

Les MAP kinases de la voie ERK sont activées par double phosphorylation sur des résidus Tyr et Thr du motif TEY dans leur boucle d'activation. ERK1/2 sont activées par MEK1/2 et définissent un module classique (Figure 3). Cette voie est activée par une multitude de signaux extracellulaires incluant des hormones peptidiques, des facteurs de croissances

et des signaux de différenciation cellulaire et de survie [34]. Suite à l'activation des MAP kinases ERK1/2, des substrats situés dans plusieurs compartiments cellulaires peuvent être phosphorylés. Parmi ceux-ci on retrouve des protéines associées au cytosquelette, des enzymes, ainsi qu'une liste grandissante de facteurs de transcription [34].

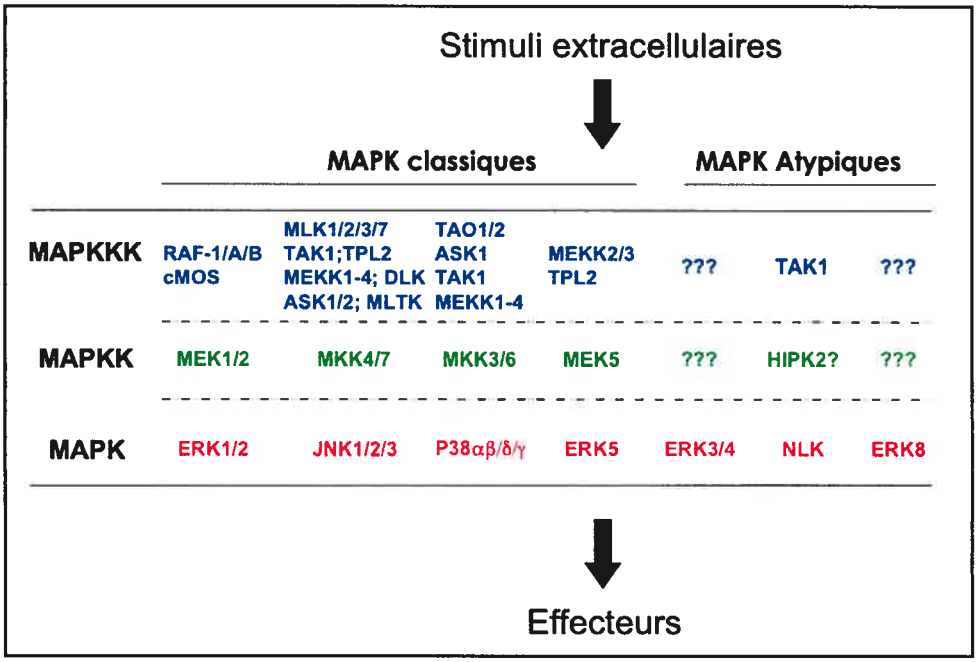

Figure 3: Voies MAP kinases chez l'humain. Les MAP kinases dites classiques sont activées par double phosphorylation par des membres de la famille MKK. Adaptée de [33].

1.1.2.1.2 JNKs

Chez les mammifères, il existe trois gènes encodant des isoformes de JNKs. De plus, chacun est sujet à l'épissage alternatif, résultant en la génération d'une dizaine d'isoformes [35]. La première isoforme de JNK a été originalement identifiée comme l'enzyme responsable de la phosphorylation de c-Jun en réponse aux UV [36, 37], ainsi que l'enzyme qui phosphoryle MAP2 suite au traitement à la cycloheximide chez le rat. L'activation de JNK par des stress cellulaires est à l'origine de l'appellation SAP kinases (stress-activated protein kinases). Les JNKs sont maintenant reconnues comme des régulateurs critiques de plusieurs processus cellulaires dont la survie, la mort cellulaire, la réparation de l'ADN et le métabolisme [38].

Les JNKs sont activées par double phosphorylation du motif TPY par MKK4/7 et définissent un module classique (Figure 3). La voie JNK est évidemment activée principalement par des stress cellulaires. Ces stress peuvent se présenter sous différentes formes : dommages à l'ADN, chocs osmotiques ou thermiques et les espèces oxygénées

réactives (H_2O_2). Des ligands extracellulaires peuvent également activer la voie JNK via les récepteurs membranaires de différentes familles incluant les récepteurs du TNFα, les récepteurs couplés aux protéines G (GCPR), les récepteurs à activité tyrosine kinase (RTK) ainsi que les récepteurs des cytokines. Bien que les JNKs puissent phosphoryler des protéines cytoplasmiques, leurs substrats sont majoritairement des facteurs de transcription [25].

1.1.2.1.3 p38^{MAPK}

La première isoforme de p38^{MAPK} a initialement été identifiée comme la protéine phosphorylée en tyrosine en réponse aux lipopolysaccharides, ou LPS [39]. Cet homologue de Hog1 chez la levure, une MAP kinase activée par les stress osmotiques, a également été découvert suite à la recherche de cibles des inhibiteurs de l'inflammation appelés CSAIDs pour *cytokine suppressive anti-inflammatory drugs* [40]. Chez les mammifères, la sous-famille p38^{MAPK} est définie par quatre gènes encodant p38alpha, beta, delta et gamma. Comme pour les gènes JNKs, plusieurs isoformes de P38^{MAPK} peuvent être issues d'un même gène [41]. Cependant, seulement les isoformes alpha/beta sont sensibles aux CSAIDs. La caractérisation de la voie p38^{MAPK} est issue principalement de l'étude de ces deux isoformes.

p38^{MAPK} est activée par la double phosphorylation du motif TGY dans sa boucle d'activation. P38^{MAPK} définit un module classique (Figure 3) et est activée par MKK3/6 en réponse à une multitude de signaux. Parmi ceux-ci on retrouve les inducteurs de stress cellulaires (rayonnements UV, les chocs osmotiques ou à la chaleur, les LPS, l'inhibition de la synthèse protéique), des récepteurs membranaires dont les récepteurs des cytokines ainsi que des GPCR. Suite à l'activation de p38^{MAPK}, plusieurs substrats sont spécifiquement phosphorylés, dont des kinases incluant certain membres de la famille MAPKAP kinase (*MAP kinase activated protéine kinases*) et plusieurs facteurs de transcriptions, notamment MEF2C et SAP-1 [41].

1.1.2.1.4 ERK5

ERK5 est la plus grosse des MAP kinases, d'où son nom alternatif BMK, pour *Big MAP kinase* [19, 20]. Bien que ERK5 soit considérée comme une MAP kinase conventionnelle, certaines caractéristiques la distinguent des autres MAP kinases. Tout d'abord, ERK5 est une protéine bifonctionnelle [42]. Sa partie N-terminale contient le domaine kinase, alors que sa partie C-terminale présente un domaine de transactivation transcriptionnel (Figure 2). De plus, un motif régulateur de l'activité kinase de ERK5 est également retrouvé dans sa partie C-terminale. Ainsi, la phosphorylation du résidu Ser^{486} permet l'interaction avec une protéine de la famille 14-3-3 et la stabilisation de la forme inactive de ERK5. La déphosphorylation

de cette sérine est d'ailleurs un préalable pour son activation dans certaines conditions [43]. Finalement, la protéine ERK5 est également retrouvée chez le poisson zèbre [44] et le ver [45] et probablement chez la drosophile.

ERK5 possède le motif activateur caractéristique ERK (Thr-Glu-Tyr) et défini un module qui respecte l'architecture classique de la voie MAP kinase (Figure 3). D'ailleurs, ERK5 a été découverte entre autres par l'interaction avec son activateur MEK5 [19]. Ce module est activé par plusieurs agents mitogéniques comme le EGF, le NGF, le BDNF, le VEGF, le FGF2 et les esters de phorbol. La voie ERK5 est également activée par des agents générateurs de stress cellulaires incluant le sorbitol, l'H_2O_2 et l'irradiation aux U.V. [46].

1.1.2.2 MAP kinases atypiques

1.1.2.2.1 ERK3/ERK4

ERK3 et ERK4 sont les produits de gènes paralogues et partagent plusieurs caractéristiques atypiques de structure. En effet, toutes deux possèdent le motif SEG en remplacement du motif TXY conservé chez les MAP kinases, ce qui suggère que ERK3 et ERK4 sont régulées de façons différentes des MAP kinases conventionnelles. De plus, chacune possède une extension C-terminale de fonction inconnue (Figure 2).

Depuis leur identification au début des années 90, la fonction de ERK3 et ERK4 est restée peu caractérisée comparativement aux MAP kinases classiques. Récemment, ces deux protéines ont été décrites comme des activateurs biologiques de MAPKAPK5 ou simplement MK5 [47-50]. Ainsi, toutes deux peuvent s'associer à MK5 et provoquer sa redistribution cellulaire. De plus, la diminution des niveaux de ERK3 ou ERK4 s'accompagne d'une diminution de l'activité endogènes de MK5 [47-50]. MK5 fait partie d'une famille de kinases connue comme des substrats de MAP kinases classiques et fut initialement isolée comme un substrat de $p38^{MAPK}$ *in vitro* [51]. Par contre, l'activation de MK5 est spécifique à ERK3 et ERK4 *in vivo* [47-50]. Toutefois, l'importance de cette activation est inconnue, puisque la fonction de MK5 demeure elle aussi peu caractérisée.

Jusqu'à présent, très peu d'études ont traité de ERK4, qui reste la MAP kinase la moins étudiée de toute la famille. À l'inverse, plusieurs études ont adressé des questions quant à la biologie de ERK3. Toutefois, plusieurs controverses sont associées à ces recherches. Ces controverses, de même que les caractéristiques structurales et de régulation particulières à ERK3 sont présentées à la section 1.2.

1.1.2.2.2 ERK7/ERK8

ERK7 et ERK8 sont les dernières MAP kinases identifiées par clonage moléculaire chez les mammifères. ERK7 fut d'abord identifiée chez le rat par clonage moléculaire [21] et ERK8 fut ensuite clonée chez l'humain par son homologie de séquence à ERK7 [52]. Fait intéressant, les deux protéines sont le produit de gènes orthologues, donc les deux protéines ne se retrouvent pas chez une même espèce [44]. Cependant, elles partagent une identité protéique de seulement 69% (82% dans le domaine kinase), ce qui est faible en comparaison aux orthologues de MAP kinases classiques. La protéine ERK7 est également retrouvée chez le poisson, la mouche et le ver [44]. ERK7 et ERK8 possèdent plusieurs caractéristiques qui les différencient des MAP kinases classiques.

ERK7 et ERK8 possèdent le motif activateur TEY. Cependant, ERK7 est constitutivement phosphorylée sur sa boucle d'activation et un mutant inactif n'est pas phosphorylé *in vivo* [53]. Ceci suggère que ERK7 s'active par autophosphorylation. En accord avec cette idée, l'expression de ERK7/8 en bactérie résulte en des kinases actives, indiquant que contrairement au MAP kinases classiques, l'autophosphorylation pourrait être un mode de régulation important de leur activité [53, 54]. Un mode de régulation atypique a de plus été décrit pour ERK7. Ainsi, les niveaux protéiques de ERK7 sont régulés par le système ubiquitine-protéasome. [55]. Les signaux responsables de la régulation de ERK7 restent toutefois inconnus.

Tout comme les autres MAP kinases atypiques, ERK7 et ERK8 possèdent une grande région C-terminale (Figure 2). Des études de mutagenèse suggèrent que ce domaine est important pour la localisation subcellulaire de ERK7, son activité constitutive et sa capacité à diminuer la prolifération cellulaire [21, 53]. Pour sa part, la région C-terminale de ERK8 est importante pour son interaction avec Src [52] et son activation par le proto-oncogène RET [56]. De plus, la partie C-terminale de ERK8, plutôt que son activité kinase, est associée à l'inhibition des récepteurs nucléaires en réponse aux glucocorticoïdes [57].

Bien que ERK7 et ERK8 présentent une identité protéique faible qui prédit des fonctions uniques pour ces deux protéines, certaines évidences suggèrent toutefois qu'elles pourraient avoir une fonction biologique conservée. Ainsi, elles partagent des caractéristiques de régulation qui impliquent leurs régions C-terminales plutôt que leurs domaines kinases. De plus, certains substrats de ERK7 peuvent également être phosphorylés par ERK8 [54]. Finalement, toutes deux sont des régulateurs négatifs des récepteurs nucléaires, même si leurs mécanismes d'action semblent êtres différents [57, 58].

1.1.2.2.3 NLK

NLK a été initialement isolée suite à la recherche de nouveaux membres de la famille ERK par une approche de clonage moléculaire utilisant le PCR dégénéré [59]. Toutefois, l'identité importante que cette kinase partage avec la protéine Nemo de drosophile lui a valu le nom de *Nemo-like kinase.* NLK partage une identité protéique de 45% avec ERK2 dans le domaine kinase. NLK n'a été officiellement acceptée dans la grande famille des MAP kinase que très récemment [60]. NLK est considérée comme une MAP kinase atypique pour plusieurs raisons incluant des caractéristiques structurales et sa localisation subcellulaire. De plus, la voie définie par NLK est différente de celle du module MAP kinase classique.

NLK se distingue des MAP kinases classique tout d'abord par l'absence du motif TXY dans la boucle d'activation, qui est remplacé par le motif TQE. Ce motif est toutefois important pour l'activité catalytique de NLK [59]. Ainsi, la mutation de la Thr^{286} résulte en une perte d'activité d'autophosphorylation. De plus, NLK possède une extension C-terminale, comme les autres MAP kinases atypiques, mais également une extension N-terminale (Figure 2). Sa fonction demeure toutefois inconnue. Enfin, contrairement aux MAP kinases classiques ERK1/2, NLK est retrouvé principalement dans le compartiment nucléaire [59].

La protéine TAK1, en collaboration avec une protéine d'interaction appelée TAB1, est un activateur de NLK [61]. De manière intéressante, TAK1 est une MAPKKK pour les voies JNK et $p38^{MAPK}$ (Figure 3). Récemment, la kinase HIPK2 a été suggérée comme étant la MAPKK de NLK [62]. La voie NLK pourrait donc posséder un module d'activation composé de trois kinases, similaire au MAP kinases classiques. L'importance de ce module a été démontrée pour la régulation négative de l'activité transcriptionnelle de β-catenine/ TCF et un régulateur négatif de la voie Wnt [61]. En accord avec cette idée, ce module est activé par Wnt5a, un membre non-canonique de la famille Wnt. D'ailleurs, l'activation de la voie NLK par Wnt5a est un mécanisme important dans l'antagonisme de la voie canonique Wnt/β-catenine [63]. L'activation du module NLK ne se limite toutefois pas aux Wnt non-canoniques. Ainsi, Wnt1 peut également activer NLK pour induire un mécanisme de rétro-inhibition [64] et pour inhiber l'activité du proto oncogène c-Myb [62, 65].

1.1.3 Rôles physiopathologiques : Des souris et des MAP kinases

L'utilisation de lignées cellulaires établies comme modèles d'étude a été un facteur déterminant pour comprendre plusieurs aspects de la biologie moléculaire des MAP kinases, tels que l'identification des signaux activateurs, l'architecture du module, les modes de régulation, l'identification de substrats ainsi que les réponses cellulaires associées

à l'activation des MAP kinases. De plus, l'étude des MAP kinases a bénéficié d'analyses fonctionnelles chez plusieurs organismes modèles. Ainsi, des études faites chez la levure, le ver, la drosophile, le xénope et le poisson zèbre, ont contribué de façon importante à notre compréhension des modules MAP kinases dans un contexte physiologique [25].

Il a cependant fallu attendre la génération des premiers mutants murins de MAP kinase, ou de modulateur de l'activité MAP kinase, pour confirmer leur importance biologique chez les mammifères. Ces modèles ont contribué à mettre en évidence le rôle des voies MAP kinases pour le développement normal et plusieurs fonctions physiologiques (Tableau I), mais également leur implication dans plusieurs désordres pathologiques. De plus, l'analyse de ces mutants a permis de définir un rôle spécifique de certaines isoformes d'une même sous famille de MAP kinases.

1.1.3.1 Mutants JNKs

Les gènes *Jnks* ont été les premiers à être invalidés chez la souris, expliquant le nombre élevé d'études rapportant l'utilisation de mutants au locus *Jnks*. Peu de phénotypes sont associés à l'inactivation individuelle de chacun de ces trois gènes, ce qui suggère qu'ils ne sont pas nécessaires pour le développement normal ou qu'une forme de redondance existe entre ces isoformes. Par contre, la génération de mutants composés est associée à la létalité à différents stades du développement, ce qui indique que la voie JNK est essentielle pour le développement murin. Les rôles de JNK dans le développement des lymphocytes T et certaines pathologies ont également été révélés par l'analyse de ces mutants de souris.

Développement. Les souris déficientes pour *Jnk1*, *Jnk2*, ou *Jnk3* sont viables et ne développent aucune anomalie limitant leur survie [66-69]. Par contre, plusieurs analyses des souris double mutantes pour *Jnk1* et *Jnk2* indiquent un rôle important de la voie JNK dans plusieurs stades du développement. Tout d'abord, la perte combinée de JNK1 et JNK2 est associée à des défauts de développement du système nerveux. En effet, des problèmes d'exencéphalie et de fermeture du tube neural ont été observés chez ces souris [70, 71]. Ces anomalies impliquent des défauts d'apoptose dans certaines régions du système nerveux à des stades bien précis du développement. De plus, le dosage génique semble important pour cette condition, indiquant que les niveaux de JNKs sont critiques pour le développement neural [70]. En accord avec un rôle de JNK dans l'apoptose, des fibroblastes embryonnaires mutants *Jnk1/2* sont résistants à l'apoptose induite par certains stress apoptotiques.

Plusieurs autres défauts embryonnaires on été observés chez les mutants composés des loci *Jnk1/2*. Tout d'abord, la perte d'un allèle *Jnk1* en absence des deux allèles *Jnk2*

résulte en des défauts de fermeture de la fissure optique et des anomalies aux yeux, dont des malformations du cristallin [72]. Ces défauts confirment l'importance de JNK pour les processus morphogéniques tel qu'initialement observé chez la drosophile [73]. Par ailleurs, il a été observé que les souris déficientes en JNK1/2 présentent des retards de développement de l'épithélium dans plusieurs tissus dont l'épiderme, l'intestin et les poumons [74].

Les phénotypes associés à la délétion combinée de *Jnk1/2* ne peuvent toutefois pas expliquer la mort de ces embryons au cours de l'embryogenèse, suggérant que les JNKs sont importantes pour d'autres processus essentiels au cours du développement. Ainsi, la perte de c-Jun, un substrat de JNK, est associée à la mortalité embryonnaire résultant de défauts de développement du foie foetal et d'érythropoïèse [75]. Ce phénotype à également été décrit en l'absence de MKK4 [76], un activateur de la voie JNK, suggérant que des problèmes d'érythropoïèse pourraient également être la cause de la mortalité des souris JNK1/2 mutantes. L'analyse des souris mutantes pour la voie JNK confirme toutefois leurs rôles essentiels et redondants dans le développement embryonnaire.

Réponse immunitaire. Le développement des lymphocytes T (thymocytes) en réponse à des signaux thymiques consiste en une sélection positive et négative de façon à générer deux populations de lymphocytes : les lymphocytes effecteurs CD4+ et les lymphocytes cytotoxiques CD8+ [77]. L'analyse de différents modèles murins indique un rôle de la voie JNK dans le développement thymocytaire. Ainsi, l'inhibition de la voie JNK par l'expression transgénique d'un dominant négatif JNK (forme non-activable) est associée à une réduction de la déplétion de thymocyte, indiquant un rôle de cette voie dans la sélection négative [78]. De plus, les thymocytes des mutants *Jnk1* (-/-) ou double hétérozygote *Jnk1/Jnk2* présentent des défauts d'apoptose dans certaines conditions [79]. La diminution d'activité ou des niveaux d'expression de JNK est donc en accord avec un rôle de JNK dans le développement des thymocytes.

Les phénotypes lymphocytaires des mutants aux loci *Jnks* sont toutefois beaucoup plus importants en périphérie que dans le compartiment thymique. Après avoir quitté le thymus, les lymphocytes CD4+ peuvent être différenciés en cellules activées Th1 ou Th2, qui se distinguent l'une de l'autre par le répertoire de cytokines sécrétées et leurs fonctions spécialisées dans la réponse immunitaire [77]. L'implication de JNK dans l'activation des lymphocytes T et la production d'interleukine 2 (IL-2) est connue depuis longtemps [80]. L'analyse des modèles de mutants *Jnks* a par ailleurs révélé leur importance dans la différenciation des lymphocytes CD4+. En absence de JNK1, les cellules CD4+ produisent des cytokines associées aux cellules Th2 dans des conditions favorables à l'activation de cellules Th1 [69]. L'incapacité à générer une défense Th1 appropriée dans les mutants *Jnk1*

semble d'ailleurs être responsable de l'incapacité de ces souris à répondre à une infection contre le pathogène *L. major* [81]. Par contre, la perte de JNK2 résulte une réponse Th1 exacerbée, mais une différenciation normale des Th2 [67]. De plus, la perte combinée de JNK1 et JNK2 dans les cellules CD4+, est associée à un profile Th2 favorisé, de même que l'inhibition de la voie JNK par l'expression transgénique d'un dominant négatif JNK [82]. Ces observations démontrent l'importance de la voie JNK dans la différenciation de cellules CD4+ de même que le rôle non redondant des isoformes JNK1 et JNK2 dans ce processus.

Les cellules CD8+ présentent également des défauts en absence de JNK spécifiques. La perte de JNK1 dans les cellules CD8+ conduit à une diminution de prolifération suite à leur activation [83, 84]. Au contraire, l'inactivation de *Jnk2* est associée à un nombre anormalement élevé de cellules CD8+ après activation [83, 84]. Les JNKs possèdent donc des fonctions importantes pour la réponse immunitaire, telles que révélées par les défauts de développement et d'activation des lymphocytes T en leur absence. Alors que certaines de ces fonctions pourraient être redondantes à certains niveaux du développement des cellules T, l'analyse de mutants pour les gènes *Jnk1/2* indique des fonctions spécifiques pour chacun de ces gènes. L'analyse de ces mutants indique donc un rôle important de *Jnk* pour la différenciation des cellules T effectrices et une réponse immunitaire appropriée et suggère que les souris déficientes en JNK sont immunocompromises.

Fonction neurale. L'activité JNK est principalement associée à JNK1 dans le cerveau [85]. L'analyse des souris déficientes en JNK1 a révélé l'absence de la commissure antérieure, une structure riche en axone qui relie les deux lobes temporaux. Ceci est causé par une dégénérescence neuronale associée à un problème de maintenance des processus axonaux qui est conséquente d'une instabilité des microtubules [86]. Cette instabilité est associée à l'hypophosphorylation de MAP2, une protéine stabilisatrice des microtubules. La protéine MAP2 est également importante pour l'élongation dentritique [87]. D'ailleurs, des défauts liés aux structures dentritiques sont également observés dans le cervelet et le cortex moteur du cerveau des souris *Jnk1* (-/-) [85].

Pathologies. L'analyse des souris mutantes pour les locus *Jnks* a permis de mettre en évidence l'importance de la voie JNK en réponse aux stress neurodégénératifs. Tout d'abord, les souris déficientes en JNK3 sont résistantes au traitement par l'acide kainique, un agent excitotoxique qui induit l'apoptose dans les neurones [66]. Ces souris sont également résistantes à la neurotoxine MPTP, qui reproduit la neurodégénerescence reliée à la maladie de Parkinson [88]. Les souris *Jnk2* (-/-) sont elles aussi résistantes à la destruction de neurones dopaminergiques induite par le traitement au MPTP. De manière intéressante, la protection neuronale est supérieure dans les doubles mutants *Jnk2/3* qu'à celle des mutants uniques

[88]. De plus, l'inactivation de *Jnk3* protège contre l'apoptose neuronale suite à l'ischémie-hypoxie cérébrale [89]. Alors que l'isoforme JNK1 est importante pour la fonction neuronale, les isoformes JNK2 et JNK3 semble donc impliquées dans l'apoptose neuronale induite par des stress.

En plus d'un rôle dans la fonction neuronale et la dégénérescence, la voie JNK est physiologiquement importante pour le contrôle métabolique lié au diabète. La résistance à l'insuline causant le diabète de type II reliée à l'obésité est associée à une suractivation des voies de stress, dont la voie JNK [90]. L'analyse de mutant pour la voie JNK a confirmé son rôle dans la résistance à l'insuline associée à l'obésité. En effet, les souris déficientes en JNK1 sont plus sensibles à l'insuline dans un modèle d'obésité. Ainsi, la perte de JNK1 réduit l'obésité, l'hyperglycémie ainsi que l'hyperinsulinémie dans un modèle d'obésité [91]. De manière similaire, la résistance à l'insuline est diminuée chez les souris déficientes en JIP1, une protéine d'échafaudage importante pour la signalisation par JNK1 [92]. Ce phénotype n'a pas été observé pour les souris déficientes en JNK2, suggérant un rôle spécifique de JNK1 dans cette pathologie [93], ou encore un profil d'expression différent dans les tissus sensibles à l'insuline.

L'étude des mutants pour les gènes *Jnks* a également confirmé leur importance pour des pathologies ayant une composante inflammatoire. L'utilisation de cellules déficientes en JNK1 ou JNK2 confirme le rôle de ces enzymes dans l'inflammation, tel qu'observée par l'utilisation d'inhibiteur spécifique de cette voie MAP kinase [94]. Dans un modèle d'inflammation arthritique murin, la perte de JNK2 réduit l'érosion des cartilages et des protéoglycans [95]. Par ailleurs, l'implication de JNK dans l'artérosclérose, une maladie ayant une composante inflammatoire, a également été suggérée par l'étude d'un mutant murin *Jnk*. Ainsi l'inactivation de *Jnk*2 dans les macrophages est suffisante pour réduire le processus de formation de plaques d'athérome [96].

L'importance de JNK dans le cancer est plutôt controversée. Bien que des inhibiteurs de JNK puissent empêcher la réparation de l'ADN suite aux dommages induit par la chimiothérapie, l'inhibition de JNK pourrait diminuer l'apoptose induite dans les cellules ciblées par les agents chimiothérapeutiques. Des études impliquant des mutants murins de *Jnk1* ou *Jnk2* dans certains modèles de carcinogenèse ont révélé des résultats plus surprenant quant au rôle de JNK dans le cancer. Ainsi la perte de JNK1 augmente l'incidence de tumeurs [97], alors que l'invalidation de *Jnk2* diminue l'apparition de tumeurs [98]. L'analyse des souris mutantes au locus *Jnks* est donc en accord avec l'idée que l'inhibition de la voie JNK est un couteau à deux tranchants.

La génération et la caractérisation des mutants des gènes *Jnks* chez la souris a donc contribuée grandement à définir le rôle des voies JNK chez les mammifères. De plus, bien que l'analyse de ces mutants ait confirmé la redondance de ces gènes, elle a également révélé des fonctions spécifiques pour chacune de ces isoformes dans plusieurs processus physiologiques normaux et pathologiques chez les mammifères. Ainsi, les gènes *Jnks* s'avèrent importants pour le développement, la fonction neurale, la réponse immunitaire et certaines pathologies.

1.1.3.2 Mutants ERK1/2

Comme pour la sous-famille JNK, l'analyse de souris mutantes au loci *Erk1/2* a permis une meilleure compréhension du rôle physiologique et physiopathologique de la voie prototype ERK. Les phénotypes associés à la perte de fonction de *Erk1* ou *Erk2* mpntre une forme de redondance de ces isoformes lors du développement, mais suggèrent également des rôles spécifiques dans le développement embryonnaire et immunitaire ainsi que certaines pathologies chez la souris.

Développement. Un rôle crucial de la voie ERK dans le développement des vertébrés a d'abord été suggéré par des expériences chez le xénope, où l'inhibition de la voie ERK conduit à des défauts d'induction du mésoderme [99, 100]. L'invalidation de *Erk1* chez la souris n'est toutefois associée à aucun défaut de développement [101]. Par contre, les souris déficientes en ERK2 meurent au cours du développement embryonnaire, suggérant que ERK2 peut compenser pour la perte de ERK1. Bien que l'analyse d'embryons déficients en ERK2 au jour embryonnaire (E) 7.5 suggère des défauts du mésoderme [102], ces observations pourraient être une conséquence de défauts affectant le développement extra-embryonnaire. Ainsi, des analyses effectuées sur des embryons au jour E6.5 ont démontré l'absence de structures extra-embryonnaires dont le cône ectoplacentaire, qui précèdent le développement du mésoderme [103]. Un défaut du développement des trophoblastes serait responsable de ce problème, mais également de malformations du placenta mises en évidence avant le jour E11.5 [103, 104]. Par ailleurs, la perte de MEK1, un activateur de ERK1/2, est également associée à des défauts de placenta et la mort à un stade précoce du développement [105], confirmant le rôle de la voie ERK pour le développement placentaire.

La voie ERK est également importante dans le développement des lymphocytes T dans le thymus. La perte de ERK1 est associée à un défaut de différenciation des thymocytes double négatif (DN) CD4-/CD8- en cellules double positive (DP) CD4+/CD8+. De plus, ERK1 est également critique pour la maturation de cellules DP en simple positive CD4+ [101]. Toutefois, la différenciation et l'activation des lymphocytes T ne sont pas affectées dans ces mutants *Erk1* [106]. ERK2 est également important pour la sélection positive,

tel que révélé par l'analyse de souris dont l'allèle *Erk2* est inactivé spécifiquement dans le compartiment thymocytaire. En effet, la perte conditionnelle de ERK2 est associée à une diminution de la progression des thymocytes DN en DP, de même qu'a un ratio de CD4+/ CD8+ anormal [107].

Fonction neurale. L'analyse de souris déficientes en ERK1 a permis de mettre en évidence un rôle de la voie ERK1/2 dans la fonction neurale. Bien que ces souris se développent normalement, des différences d'apprentissage ont été observées entre les souris mutantes et normales. Ainsi, les mutants *Erk1* (-/-) développent une mémoire à long-terme plus rapidement que les souris témoins lorsque soumis à des tests d'apprentissage [108]. Par contre, la perte de ERK1 est associée à une suractivation de ERK2, un phénomène d'ailleurs observé dans la plupart des cellules [108]. Le blocage pharmacologique de l'activation de ERK2 dans les mutants *Erk1*(-/-) rétablit l'apprentissage normal de ces souris [108], indiquant que le phénomène est associé à l'augmentation de l'activité ERK2 plutôt qu'à un rôle spécifique de ERK1. Par ailleurs, l'inactivation du gène *Erk1* est associée à l'augmentation de la signalisation dopaminergique dans le cerveau, ce qui explique une plus grande dépendance de ces souris aux psychotropes [108, 109].

Pathologie. La mortalité embryonnaire associée à l'invalidation du gène *Erk2* limite l'étude de cette MAP kinase dans le développement pathologique. L'importance de la voie ERK a donc été adressée par l'étude des souris déficientes en ERK1. Tout d'abord, ces études révèlent l'importance de ERK1 dans l'obésité. En effet, l'adipogenèse est affecée en absence de ERK1 [110]. Ainsi, les souris *Erk1* (-/-) ont une masse adipeuse réduite en association avec un nombre réduit d'adipocytes. En conséquence, ces souris sont résistantes à l'obésité induite par une diète riche en gras [110]. Par ailleurs, l'inhibition pharmacologique de ERK2 n'affecte pas la formation d'adipocytes, suggérant un rôle spécifique de ERK1 dans l'adipogenèse et l'obésité.

En plus de mettre en évidence un rôle de ERK1 dans l'obésité, l'étude des souris déficientes en ERK1 a également permis de confirmer son rôle dans le cancer. Ainsi, il fut démontré que la perte de ERK1 diminue l'incidence de carcinomes de la peau induits par le DMBA/TPA. Cette différence pourrait être causée par un déséquilibre entre la prolifération et l'apoptose des kératinocytes déficients en ERK1 [111]. Par ailleurs, les dommages générés à la peau par le TPA sont moins importants chez les souris mutantes, suggérant que ERK1 est importante pour l'homéostasie de la peau [111].

Les mutants murins des gènes *Erk1* et *Erk2* ont été d'une grande importance dans l'étude du rôle physiologique de la voie MAP kinase ERK chez les mammifères. De plus, ces

mutants devraient permettre l'étude de la fonction spécifique de chacune de ces deux enzymes, longtemps considérées comme moléculairement redondantes. Ainsi le rôle spécifique de ERK2 à été suggéré pour le développement extra-embryonnaire alors que ERK1 semble jouer un rôle unique dans l'homéostasie de tissues spécifiques. La génération de mutation additionnelle du gène *Erk2* sera nécessaire pour comprendre son rôle chez l'adulte.

1.1.3.3 Mutants p38^{MAPK}

L'utilisation d'inhibiteurs de la voie p38^{MAPK} a été d'une grande importance pour déterminer l'implication de cette voie dans plusieurs processus cellulaires. Par contre, la spécificité de chacune des isoformes n'a pu être adressée qu'avec la génération de mutants murins pour chacun de ces loci encodant des isoformes p38. En plus de confirmer la redondance de ces gènes et l'importance de cette voie MAP kinase dans la réponse inflammatoire, les mutants murins des gènes encodant les isoformes de p38^{MAPK} ont permis de mettre en évidence un rôle important de cette voie dans le développement embryonnaire.

Développement. L'invalidation des gènes encodant p38β, p38γ, p38δ, ou p38γ/δ combinées, résulte en des souris viables et sans problèmes de développement [112, 113]. Par contre, l'inactivation de *p38*α est létale, indiquant un rôle essentiel pour le développement murin qui ne peut être compensé par les autres isoformes. Les souris déficientes en p38α meurent à mi-gestation [114-117]. Une cause de mortalité est associée à des défauts du placenta [115, 117]. En effet, les placentas *p38*α (-/-) présentent des anomalies du labyrinthe placentaire qui résultent d'une angiogenèse anormale [115]. L'importance de p38α dans le développement placentaire a de plus été démontrée par l'analyse d'embryons chimériques. En effet, le développement des embryons *p38*α (-/-) peut être rescapé dans un environnement extra-embryonnaire non-mutant. Ces embryons ne présentent pas de retard de croissance et survivent au moins jusqu'à terme sans défauts apparents [117], remettant en question les défauts d'érythropoïèse également observés en absence de p38α [116]. Ceci suggère que certaines isoformes de p38^{MAPK} peuvent compenser pour la perte de p38α dans le développement embryonnaire mais pas pour le développement du placenta. Les défauts de placenta associés à la double délétion de MKK3/6, les kinases activatrices de p38^{MAPK}, sont également compatibles avec l'idée que la voie p38^{MAPK} est essentielle pour le développement [118].

Pathologies. La voie p38^{MAPK} a été découverte comme la cible d'agents anti-inflammatoires, suggérant un rôle de p38^{MAPK} comme médiateur de l'inflammation. Seulement deux isoformes de p38, p38α/β, sont sensibles aux CSAIDs. L'analyse des mutants murins pour ces loci suggère toutefois que p38α est l'isoforme importante dans

le processus inflammatoire. Ainsi, la production de cytokines en réponse au LPS n'est pas affectée dans les souris déficientes en p38β [113]. De plus, l'absence de p38β ne diminue pas l'inflammation dans un modèle murin d'arthrite et de maladie inflammatoire de l'intestin [113]. Ces observations indiquent que p38α peut compenser pour la perte de p38β lors de l'inflammation. Ces expériences n'ont pu être reproduites chez les souris déficientes en p38α à cause de la mortalité précoce de ces souris. Par contre, l'analyse de cellules mutantes pour p38α, différenciées in vitro, a confirmé que cette isoforme est une composante essentielle de la réponse aux cytokines inflammatoires [114].

Un rôle de p38α dans la survie des cardiomyocytes suite à des stress a également été suggéré par l'utilisation de souris mutante pour ce locus. L'inactivation conditionnelle du gène de p38α dans le tissu cardiaque est compatible avec le développement normal de ces souris [119]. Par contre, ces souris présentent une réponse anormale à l'hypertrophie cardiaque induite par des stress. Ainsi, l'augmentation de pression ventriculaire cardiaque est associée à une fibrose cardiaque massive, une apoptose des cardiomyocytes ainsi que l'augmentation de la mortalité chez ces mutant de p38α [119].

La génération de mutants pour chacun des gènes de la sous-famille $p38^{MAPK}$ a permis de mettre en évidence le rôle important de p38α dans le développement et comme médiateur de l'inflammation. La génération de mutants additionnels ainsi que l'analyse des mutants disponibles devraient permettre de mettre en évidence le rôle spécifique de ces isoformes dans le développement normal et pathologique.

1.1.3.4 Mutants ERK5

Comparativement aux autres MAP kinases, une multitude de mutant murin ont jusqu'à maintenant été générés pour le gène *Erk5*. L'analyse de ces mutants a révélé le rôle de cette MAP kinase dans la vascularisation, autant chez l'adulte que durant le développement embryonnaire. L'importance de la voie ERK5 dans la progression tumorale a également été mise à jour grâce à ces mutants.

Développement. La perte de ERK5 se fait sentir très tôt dans le développement. Des défauts cardiaques observés chez les embryons mutants sont incompatibles avec le développement des embryons *Erk5* (-/-) qui meurent au début de l'organogenèse [120-122]. Les embryons déficients en ERK5 présentent également des défauts vasculaires dans les tissus embryonnaires et extra-embryonnaires [120-122]. Bien que la vascularisation soit normale, le remodelage et/ou le maintient du système vasculaire (angiogenèse) est compromis chez les souris *Erk5* (-/-) [120, 121]. Les défauts observés chez les embryons

mutants ne sont toutefois pas une conséquence des défauts extra-embryonnaires. Ainsi, la délétion conditionnelle de *Erk5* uniquement dans l'embryon résulte également en des défauts cardiaques, du système vasculaire et la mort au jour E9.5-10.5 [123]. Par ailleurs, l'inactivation conditionnelle de *Erk5* dans le compartiment endothélial phénocopie la perte de ERK5 [124]. Par contre, l'inactivation conditionnelle dans les cardiomyocytes n'est pas incompatible avec le développement normal, confirmant que les défauts cardiaques résultent d'un problème vasculaire et que ERK5 n'est pas essentiel pour le développement des cardiomyocytes [124]. L'importance de la voie ERK5 dans le développement embryonnaire est par ailleurs supportée par les phénocopies des souris déficientes pour l'activateur connu de ERK5, MEK5 [125], ou déficientes pour un substrat de ERK5, la protéine MEF2C [126-128].

Bien que l'inactivation de ce gène soit létale, cela n'a pas limité l'exploration de sa fonction chez l'adulte. Ainsi, l'inactivation conditionnelle du gène *Erk5* chez l'adulte résulte également en des problèmes du système cardiovasculaire [124]. L'intégrité de la barrière endothéliale est perturbée en absence de ERK5, conséquemment à une augmentation d'apoptose des cellules endothéliales. L'analyse de cellules déficientes en ERK5 a permis de démontrer l'importance de cette voie dans la survie spécifique des cellules endothéliales, mais pas pour la survie de fibroblastes embryonnaires [124].

Pathologie. Étant donné l'importance de ERK5 dans le développement vasculaire, l'importance de cette voie dans la progression tumorale est de grand intérêt. Ainsi, la délétion conditionnelle de *Erk5* chez l'adulte protège les souris du développement tumoral dans plusieurs modèles d'induction de tumeur [129]. Par ailleurs, plusieurs mutants conditionnels de *Erk5* on été générés dans le compartiment cardiaque, neural, hépatique et l'épithélium de certain tissus sécrétoires. Ces souris se développent bien dans des conditions normales. Par contre, ces mutants n'ont été soumis à aucun stress [123].

L'étude de ces mutants aura permis de mettre en évidence l'importance physiologique de la voie ERK5 dans l'intégrité vasculaire embryonnaire, extraembryonnaire et même chez l'adulte. L'absence de phénotypes dans plusieurs de ces mutants a également permis de démontrer que cette voie MAP kinase est dispensable pour le développement de la plupart des tissus chez la souris [123]. L'étude de ces mutants dans des conditions spécifiques pourrait permettre de découvrir de nouvelle fonction de cette voie MAP kinase.

1.1.3.5 Mutants des MAP kinases atypiques NLK, ERK7, ERK3 et ERK4

Les voies définies par les MAP kinases atypiques sont moins bien caractérisées au niveau moléculaire que les MAP kinases classiques. Ce constat fait les frais de la compréhension limitée du rôle de ces enzymes. Par contre la délétion des gènes encodant ces membres atypiques MAP kinases devrait permettre une meilleure compréhension de la fonction de ces gènes. La délétion de NLK a d'ailleurs révélé un rôle important de cette enzyme dans le développement de la moëlle osseuse [130]. À l'exception de NLK, l'inactivation des MAP kinases atypiques n'a pas été rapportée chez la souris.

1.1.4. Conclusion

La recherche sur les MAP kinases effectuée durant les 25 dernières années s'est principalement concentrée sur les membres conventionnels et leurs voies définies en un module de trois kinases : MAPKKK-MAPKK-MAP Kinase. Bien qu'il existe plusieurs gènes MAP kinases, les modèles moléculaires actuels regroupent celles-ci dans un nombre limité de voies MAP kinases chez les mammifères [33, 44]. En conséquence, la contribution des membres d'une même sous-famille pour une voie donnée est mal comprise. De plus, les voies définies par les MAP kinases dites atypiques restent peu caractérisées.

L'inactivation des gènes MAP kinases a contribué à notre compréhension du rôle de ces voies de signalisation dans le développement normal. De plus, l'étude de mutant MAP kinase a permis de mettre en évidence la fonction spécifique de certains membres d'une même sous-famille. Les mutations générées ne permettent toutefois pas de distinguer le rôle spécifique des isoformes issues de l'épissage alternatif d'un même gène. L'étude de mutants murins de MAP kinases a également permis de caractériser l'implication des MAP kinases dans plusieurs états pathologiques. L'importance de l'étude de ces mutants murins se traduit par le développement de composé inhibiteurs des voies MAP kinase qui montrent un potentiel pour pour le traitement de plusieurs maladies chez l'humain [131].

Tableau I Sommaire des phénotypes associés à l'invalidation génique des MAP kinases chez la souris

Gène	Protéine	Localisation	Mutation	Létalité	Phénotypes rapportés		Références
MAP kinases classiques					Systèmes touchés	Processus perturbés	
Sous-famille ERK							
Mapk3	ERK1	Chr 7	Nulle	Viable	Immunitaire	Maturation des thymocytes	[101]
Mapk1	ERK2	Chr 16	Nulle	E6.5-E7.5	Placenta	Développement des trophoblastes	[103], [104]
			Nulle	E7.5	Mésoderme	Différenciation du mésoderme	[102]
			Cond-Tcell	Viable	Immunitaire	Maturation des thymocytes	[107]
Sous-famille JNK							
Mapk8	JNK1	Chr 16	Nulle	Viable	Immunitaire	Activation des cellules TH2	[69]
Mapk9	JNK2	Chr 11	Nulle-LacZ	Viable	Immunitaire	Activation des cellules TH1	[67], [68]
Mapk10	JNK3	Chr 5	Nulle	Viable			[66]
Mapk8/9	JNK1/JNK2		Composées	E11.5	Neurologique	Apoptose Neuronale	[70], [71]
Sous-famille p38							
Mapk11	p38beta	Chr 15	Nulle	Viable			[113]
Mapk12	p38gamma	Chr 15	Nulle	Viable			[112]
Mapk13	p38delta	Chr 17	Nulle	Viable			[112]
Mapk14	p38alpha	Chr 17	Nulle/Nulle LacZ	E10.5-E11.5	Placenta	Angiogenèse du labyrinthe	[115], [117]
			Nulle	E11.5-E12.5	Hematopoïétique	Érythropoïèse	[116]
Mapk12/13	gamma/delta		Composées	Viable			[112]
Sous famille ERK5							
Mapk7	ERK5	Chr 11	Nulle	E9.5-E10.5	Placenta/Cardiaque	Angiogenèse	[120], [121], [122]
			Cond-endo	E9.5-E10.5	Vasculaire	Angiogenèse	[124]
			Cond-emb	E9.5-E10.5	Vasclulaire	Angiogenèse	[123]
			Cond-adulte	3-4 semaines**	Vasculaire	Intégrité endothéliale	[124]
MAP kinases atypiques							
Sous-famille ERK7							
Mapk15	ERK7*	Chr 15					Non-publié
Sous-famille ERK3							
Mapk4	ERK4	Chr 18	Nulle-GFP	Viable			Rousseau et al. non-publié
Mapk6	ERK3	Chr 9	Nulle-LacZ	Néonatal			Chapître 4
Sous-famille NLK							
Nlk	NLK	Chr 11	Nulle-LacZ	4-6 semaines	Hématopoïétique	Défauts de moëlle osseuse	[130]

E: jour embryonnaire; Cond: Conditionelle; endo: endothélial; emb: compartiment embryonnaire; Chr: Chromosome
*Chez l'humain, la protéine encodée par *MAPK15* est appelée ERK8. **Post induction.

1.2 La MAP kinase atypique ERK3

Contrairement aux MAP kinases conventionnelles, pour lesquelles la recherche s'est faite à une vitesse impressionnante, l'élucidation de la voie impliquant ERK3 a été plutôt lente. Cette voie reste d'ailleurs l'une des moins bien caractérisées de toutes les voies MAP kinase. Ce constat résulte en partie des nombreuses controverses liées à l'étude de ERK3, mais également de ses caractéristiques atypiques de régulation.

1.2.1 Un historique de controverses

La découverte de ERK3 remonte au début des années 90, à l'époque même de l'identification des premières MAP kinases par clonage moléculaire. Plusieurs études ont depuis adressé directement la biologie moléculaire de cette MAP kinase atypique (Figure 4).

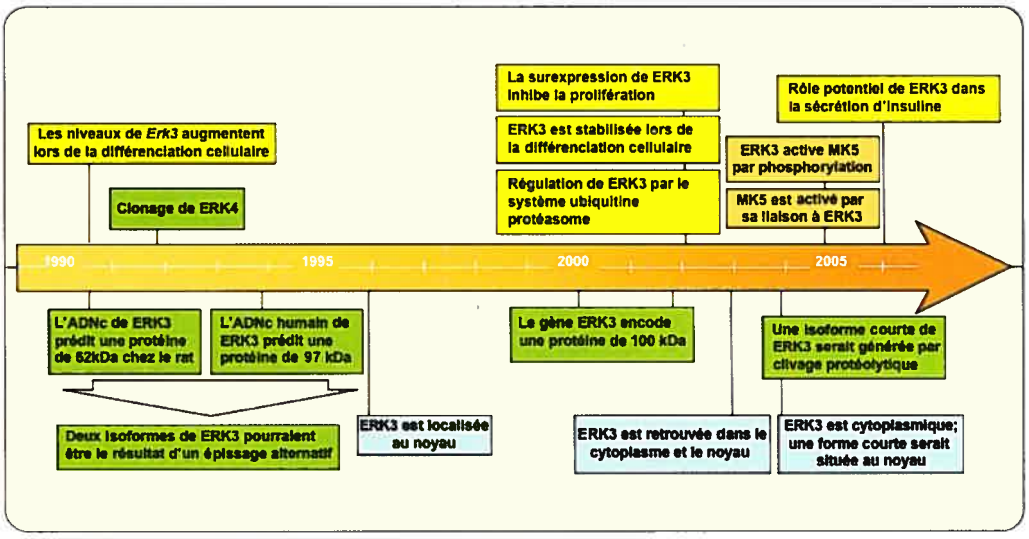

Figure 4: Chronologie des principales études adressant la biologie moléculaire de la MAP kinase atypique ERK3 depuis son identification en 1991. Plusieurs controverses sont associées à l'étude de ERK3 quant à l'existence d'isoformes, sa localisation subcellulaire ainsi que le mode d'activation de la kinase MK5.

Bien que ces recherches aient permis de mettre en évidence le caractère atypique de ERK3, plusieurs de ces études sont par contre associées à des controverses concernant l'existence d'isoformes de ERK3, sa localisation cellulaire ainsi que ses substrats. Ces controverses expliquent en partie pourquoi la voie définie par ERK3 est restée peu caractérisée.

1.2.1.1 Clonage de ERK3 : une controverse d' isoformes

Le premier ADNc encodant ERK3 a été cloné à partir d'une banque d'ADNc de cerveau de rat, grâce à son homologie de séquence à *Erk1*. La séquence de cet ADNc prédisait une proteine de 546 a.a et d'environ 62 kDa. ERK3 se différenciait par une extension C-terminale plus longue que ERK1, mais également par l'absence du motif TXY retrouvé dans le domaine catalytique de ERK1/2 [17].

La découverte d'ADNc encodant des homologues potentiels de ERK3 chez l'humain s'ensuivit. Le premier ADNc humain rapporté a également été isolé à partir de son homologie à *Erk1* et prédisait une protéine de 63 kDa. Appelée à l'origine $p63^{MAPK}$ [18], la protéine encodée par cette séquence a depuis été renommée ERK4 [132]. Elle est le produit d'un gène paralogue à celui de ERK3 (voir chapître 3), partage 70% d'identité protéique avec ERK3 dans la région catalytique et, tout comme ERK3, ne possède pas le motif d'activation TXY retrouvé chez les MAP kinases classiques. Deux groupes, incluant le nôtre, ont rapporté le clonage d'un ADNc humain possédant une séquence orthologue à celle de ERK3 de rat [133, 134]. Par contre, la séquence de ces ADNc prédisait une protéine de 721 a.a (97 kDa). En plus de posséder un domaine C-terminal plus long, la séquence primaire de ERK3 humain divergeait de celle de rat dans la région C-terminale. Par contre, les séquences protéiques des domaines kinase étaient identiques [134].

Des anticorps générés contre la protéine ERK3 humaine ont permis de détecter des protéines de 62 et 97 kDa à partir d'extrait d'une lignée cellulaire humaine, suggérant l'existence de deux isoformes de ERK3 chez les mammifères [134]. Cette observation a d'ailleurs conduit à l'hypothèse que ces deux protéines étaient issues de l'épissage alternatif du même gène [135]. Par contre, des analyses d'hybridations ont suggéré l'existence de plusieurs séquences apparentées à celle de ERK3 dans le génome humain [17, 133]. Les deux isoformes auraient donc également pu être le produit de deux gènes de séquence fortement conservées. Toutefois, l'hybridation de différentes sondes provenant de l'ADNc humain à de l'ARN de différents tissus ou lignées cellulaires suggérait l'existence d'un seul transcrit de ERK3 [134], amenant un doute raisonnable quant à l'existence de deux isoformes de ERK3. En accord avec cette idée, le clonage moléculaire d'un ADNc de ERK3 chez la souris ainsi que des analyses génomiques prédisent l'existence d'un produit de gène unique de 100 kDa (voir chapitre 2 et 3).

Il a récemment été suggéré que le clivage protéolytique de la région C-terminale serait responsable de la génération d'une protéine ERK3 de plus faible poids moléculaire. Ces observations ont été faites lors de surexpression d'une forme de ERK3 recombinante dans un modèle cellulaire [136]. Bien que l'existence d'une telle isoforme reste à être clairement démontrée, ceci pourrait expliquer pourquoi deux isoformes de ERK3 sont encore détectées par l'utilisation d'anticorps commerciaux. L'existence d'une isoforme de ERK3 de plus petite taille est donc encore aujourd'hui un sujet d'actualité.

1.2.1.2 Localisation subcellulaire: nucléaire, cytoplasmique ou les deux?

Plusieurs études ont adressé directement ou indirectement la localisation de la protéine ERK3 dans plusieurs types cellulaires. Les conclusions tirées de ces études ne permettent toutefois pas de comprendre sa localisation subcellulaire. Il a d'abord été suggéré que ERK3 est une protéine constitutivement nucléaire [135]. Par contre, des expériences d'immunolocalisation faite dans notre laboratoire indiquent que ERK3 (recombinant et endogène) est distribuée dans le cytoplasme ainsi que dans le noyau de plusieurs modèles cellulaires [137]. Par ailleurs, une étude récente indique qu'une forme recombinante de ERK3 est exclue du noyau [50]. La protéine ERK3 endogène a aussi été localisée par microscopie confocale dans un compartiment intermédiaire séparant le Réticulum endoplasmique (RE) et le golgi, une structure connu sous le nom de ERGIC pour *endoplasmic reticulum-golgi intermediate compartment* [136]. Par ailleurs, l'existence d'une forme tronquée de ERK3 recombinant, observée au noyau, a également été décrite [136]. Par contre, cette donnée n'est pas corroborée par l'étude de la protéine ERK3 endogène. La localisation subcellulaire de ERK3 demeure donc sujet à controverse.

1.2.1.3 La controverse des substrats

La controverse des substrats de ERK3 n'est pas récente et les premières études ayant adressé la question ont rapporté des résultats plutôt contradictoires. Par exemple, il a été suggéré que ERK3 peut phosphoryler *in vitro* un substrat connu de MAP kinases, la protéine MBP [134, 138], Cependant, notre laboratoire ainsi que d'autres équipes ont démontré que plusieurs substrats de MAP kinase classiques tel que MAP2, c-jun, tal-1, MyoD, Elk1 ou MBP ne sont pas phosphorylés par ERK3 *in vitro* [135].

Une interaction entre ERK3 et la protéine kinase MK5 à récemment été décrite. Cette protéine faisant partie d'une famille de substrats de MAP kinase, la capacité de ERK3 a phosphoryler cette protéine a donc été adressée [49, 50]. Bien que ces deux études démontrent que ERK3 est un régulateur positif de l'activité biologique de MK5, la capacité

de ERK3 à phosphoryler cette protéine reste controversée. Ainsi, une relation enzyme-substrat classique entre ERK3 et MK5 semble être responsable de l'activation de MK5 [49]. Par contre, l'activation de MK5 pourrait également s'expliquer par l'augmentation de l'autophosphorylation de MK5 suite à son interaction avec ERK3. [50]. Bien que cette question demeure ouverte, plusieurs résultats suggèrent toutefois que ERK3 est un régulateur biologique de MK5, indiquant que ces protéines font partie d'une même voie de signalisation (voir ci-bas).

En conséquence, la connaissance limitée des substrats de ERK3 demeure un obstacle important quant à l'étude de l'activité catalytique de ERK3 qui demeure, elle aussi, un sujet de controverse.

1.2.2 ERK3 l'atypique : structure et régulation

Plusieurs évidences structurales démontrent que ERK3 fait partie de la grande famille des MAP kinases. Le domaine kinase de ERK3 partage près de 50% d'identité protéique avec celui de ERK1 [17, 133, 134, 139] et l'identité protéique peut atteindre jusqu'à 83% dans certains sous-domaine, alors qu'elle n'est même pas de 20 % entre ERK1 et PKA [135]. De plus, la longueur des sous-domaines est conservée [17]. ERK3 possède également les séquences signatures de la famille des MAP kinases [140]. ERK3 définit donc une sous-famille de MAP kinase, mais ses caractéristiques de structure, de régulation et potentiellement de spécificité la distinguent des autres MAP kinases conventionnelles.

1.2.2.1 Caractéristiques structurales

Domaine kinase. ERK3 présente deux distinctions biochimiques importantes dans la région catalytique. Premièrement, la séquence Ser-Glu-Gly remplace le motif Thr-X-Tyr dans la boucle d'activation du domaine kinase. La phosphorylation de la tyrosine de ce motif, fortement conservée chez les autres MAP kinases, est importante pour induire l'activation de ERK2 ainsi que la liaison au substrat [141]. Cette substitution de la tyrosine en glycine suggère donc un mode de régulation différent pour ERK3. D'ailleurs, ERK3 est un faible substrat pour les membres de la famille MEK [142, 143].

La seconde particularité de ERK3 est la séquence Ser-Pro-Arg en remplacement du motif Ala-Pro-Glu dans le sous domaine VIII du domaine catalytique. Le résidu glutamate du motif (A-P-E) est très conservé chez les protéines kinases. Comme ERK3, les isoformes de la famille caséine kinase I (CKI) ne possèdent pas d'acide glutamique dans leur sous-domaine VIII [60]. L'analyse de la structure crystaline de ERK2 indique que ce résidu Glu

est important pour la stabilisation de la région c-terminal du domaine kinase [144]. Par contre, la résolution de la structure de caséine kinase I, qui ne possède pas le résidu Glu, suggère un mécanisme différent pour stabiliser le domaine kinase [145]. Ceci suggère que la substitution du résidu glutamate n'est pas incompatible avec une activité protéine kinase de ERK3. D'ailleurs, ERK3 est capable de s'autophosphoryler *in vitro* [135, 146]. De plus, des études de chimérisme entre le domaine kinase de ERK3 et ERK2 sont en faveur d'un domaine kinase fonctionnel chez ERK3 [147].

Extension C-terminale. Une caractéristique structurale importante qui différencie ERK3 des MAP kinases classiques est la présence d'un grand domaine C-terminal. Alors que le domaine C-terminal de ERK5 lui confère une activité transcriptionnelle et celui de ERK7 est associé à un rôle antiprolifératif (voir ci-haut), la fonction de la région C-terminale de ERK3 reste peu caractérisée et aucun domaine connu n'y est retrouvé. Par contre, des résultats récents suggèrent que ce domaine pourrait être important pour la fonction de ERK3. Tout d'abord, des motifs de localisation subcellulaire y sont retrouvés. Ainsi, une région d'export nucléaire [137] ainsi qu'un signal de localisation au Golgi y sont retrouvés [136]. Ces signaux semblent d'ailleurs importants pour la localisation subcellulaire de ERK3 puisque des troncations de la région C-terminale de ERK3 résulte en un enrichissement dans le compartiment nucléaire [135-137]. Ensuite, il a récemment été démontré que certaines régions du domaine C-terminal médient l'association de ERK3 avec des partenaires d'interaction comme MK5 [49, 50] ainsi qu'avec un régulateur du cycle cellulaire, la cycline D3 [148]. Finalement, certains motifs contenus dans le domaine C-terminal pourraient être responsable de la génération d'une isoforme courte de ERK3 par clivage protéolytique [136]. Ainsi, le domaine C-terminal de ERK3 est important pour sa localisation subcellulaire, pour des interactions protéines-protéines et potentiellement pour la génération d'une isoforme plus courte.

1.2.2.2 Régulation

Les particularités structurales au niveau du domaine kinase de ERK3 suggèrent que cette protéine possèdent des différences de spécificité et de régulation par rapport aux autres MAP kinases. Cependant, peu de données sont disponibles quant à la régulation de l'activité catalytique de ERK3. Par contre, une mode de régulation important semble être le contrôle des niveaux d'expression de ERK3. Finalement, comme pour les autres MAP kinases, des changements de sa localisation subcellulaire pourraient également contribuer à la régulation de ERK3.

Activité catalytique. Le principal site phosphoaccepteur susceptible de réguler ERK3 est la Ser^{189} du motif S-E-G, qui se retrouve à une position équivalente à la Thr^{183} du motif activateur T-X-Y de ERK2. Des études ont démontré que ERK3 pouvait s'autophosphoryler sur cette sérine [135], confirmant que ERK3 possède une activité catalytique. Par contre, il a été observé que la Ser^{189} de ERK3 est constitutivement phosphorylée dans plusieurs lignées cellulaires en absence de facteurs de croissance. Cette phosphorylation n'est pas modifiée par l'addition de facteurs de croissance ou chez un mutant catalytiquement inactif de ERK3 [149]. Une protéine possédant une activité kinase envers la Ser^{189} de ERK3 a été décrite, mais l'identité de cette kinase demeure inconnue [150]. Finalement des études récentes suggèrent que la mutation de cette sérine n'est pas importante pour la localisation cellulaire de ERK3 [135-137]. Par contre, la phosphorylation de la Ser^{189} de ERK3 semble être nécessaire pour la pleine activation de MK5 in vitro [50].

Des facteurs pouvant augmenter l'expression de ERK3 ont été rapportés, tel certains gangliosides, la prolactine et le NGF (voir ci-bas). Par contre, leurs effets sur l'activité kinase de ERK3 n'ont pu être évalués, faute de substrats. Une étude récente suggère toutefois que le PMA pourrait être un activateur potentiel de ERK3. En effet, la phosphorylation de ERK3 en sérine est augmentée suite à la stimulation d'une lignée cellulaire épithéliale pancréatique (RINm5F) par le PMA [151]. Les sites précis de phosphorylation ne sont pas connus, ni les enzymes responsables de cette phosphorylation. Par contre, des inhibiteurs de la protéine kinase C (PKC) bloquent cette phosphorylation de ERK3 [151], suggérant une implication de PKC pour la phosphorylation de ERK3 en sérine.

Expression. Contrairement aux autres MAP kinases, dont les niveaux cellulaires ne sont pas limitant pour leur activité, l'activité biologique de ERK3 pourrait être régulée par son abondance cellulaire. En effet, plusieurs études révèlent que les niveaux de ERK3 peuvent être augmentés par des signaux extracellulaires, de même que par certains stress cellulaires. De plus, des expériences effectuées dans notre laboratoire indiquent que la modulation de la demi-vie de ERK3 représente également un mode de contrôle de son expression.

La régulation des niveaux d'expression de l'ARNm de ERK3 est connue depuis longtemps. Il a en effet été observé au début des années 90 que la différenciation cellulaire de cellules P19 (embryocarcinome) s'accompagnait d'une augmentation des niveaux de l'ARNm de ERK3 [17]. Depuis, plusieurs études ont rapporté des variations d'expression de l'ARNm de ERK3 en réponse à différents signaux extracellulaires. L'expression de *Erk3* est différemment régulée par la prolactine (PRL) et la prostaglandine F2 α (PGF2α) dans le corpus luteum de la rate [152]. La PRL induit également l'expression de *Erk3* dans les îlots pancréatiques en culture [153]. Le collagène de type IV ainsi que certaines isoformes

du FGF2 peuvent également moduler l'expression de *Erk3* de façon positive ou négative, respectivement [154, 155]. Des stress intracellulaires peuvent également accroître l'expression de *Erk3*. Ainsi, l'inhibition du protéasome dans plusieurs types cellulaires [156], ou encore le traitement des cellules Raji (lymphocyte B) par certains gangliosides [157], sont associés à l'augmentation des niveaux d'expression de *Erk3*. Les mécanismes responsables de la hausse d'expression de l'ARNm de ERK3 sont inconnus, mais pourraient impliquer les MAP kinases p38α ou β. En effet, l'induction d'expression de *Erk3* par des inhibiteurs du protéasome est bloquée par des inhibiteur de la voie $p38^{MAPK}$ [156], suggérant un rôle de ces enzymes dans la régulation d'expression de *Erk3*.

Le mode de régulation de ERK3 le plus caractérisé demeure néanmoins la modulation de sa demi-vie. ERK3 possède une demi-vie de seulement 30 min, alors que celle des MAP kinases classiques comme ERK1 est de plusieurs heures [158]. De plus, ERK3 est constitutivement dégradée dans les lignées cellulaires en croissance exponentielle. Fait intéressant, l'addition d'un épitope d'une certaine longueur en N-terminal de ERK3 bloque sa dégradation et favorise son expression ectopique [159, 160]. Cette observation est à l'origine de la démonstration que les niveaux de ERK3 sont régulés par le système ubiquitine-protéasome [160]. Ainsi, ERK3 est polyubiquitinée *in vivo* et dégradée par le protéasome. L'activité catalytique de ERK3, sa phosphorylation sur la Ser^{189} ou la présence de la région C-terminale n'influence pas la demi-vie de ERK3. Par contre, deux régions (dégrons) situées dans la partie N-terminale de la protéine sont importantes pour l'ubiquitination et la dégradation de ERK3 [160]. La caractérisation des sites d'ubiquitination responsables de la dégradation de ERK3 indique que ERK3 est ubiquitinée sur son extrémité N-terminale, plutôt que sur des lysines internes. D'ailleurs, ERK3 est la première protéine pour laquelle ce mode particulier d'ubiquitination a été prouvé de manière directe par spectropmétrie de masse [160].

L'importance de cet aspect de la régulation de ERK3 pour sa fonction reste toutefois peu caractérisée. Ainsi les signaux de croissance, de dommage à l'ADN ainsi qu'un stress d'hypoxie ne modifient pas la demi-vie de ERK3. Cependant, la stabilisation de ERK3 accompagne la différenciation des cellules C2C12 et PC12 (voir ci-bas). De plus, la surexpression de mutants non-dégradables de ERK3 inhibe la prolifération cellulaire [158]. Ainsi, le contrôle de la demi-vie de ERK3 pourrait être important pour son activité biologique.

Localisation subcellulaire. Plusieurs évidences suggèrent que la redistribution de ERK3 dans un compartiment cellulaire pourrait être un mode de régulation. Tout d'abord, le transport de ERK3 ectopique du noyau au cytoplasme est médié par un mécanisme actif. Bien que le mécanisme d'import reste peu caractérisé, le mécanisme d'export implique

la protéine exportatrice CRM1. D'ailleurs, ERK3 est la première MAP kinase ayant été démontré comme pouvant s'associer avec CRM1 [137]. De plus, lors de coexpression avec MK5, l'interaction avec MK5 enrichie ERK3 dans le cytoplasme [49]. Ensuite, la délétion de la partie C-terminale de ERK3 résulte en un enrichissement au noyau [136, 137]. Il a été récemment démontré que la localisation de ERK3 dans le compartiment ERGIC dépend de l'état prolifératif de la cellule [136].

Bien que la localisation cellulaire de ERK3 reste un sujet controversé, les résultats expérimentaux suggèrent toutefois que l'activité catalytique de ERK3 ou sa phosphorylation sur la Ser^{189} n'influence pas sa localisation subcellulaire [50, 136, 137]. De plus, aucun signal extracellulaire capable de modifier la localisation de ERK3 n'a encore été identifié. ERK3 se distingue donc des MAP kinases classiques puisque sa localisation subcellulaire ne semble pas dépendante de la phosphorylation de sa boucle d'activation.

La signification de la régulation de localisation subcellulaire de ERK3 reste peu caractérisée. Par contre, il est à noter que l'inhibition du transport nucléocytoplasmique de ERK3 est associée à une diminution de sa capacité à inhiber la prolifération cellulaire (voir ci-bas), suggérant que des mécanismes impliqués dans la localisation cellulaire de ERK3 sont importants pour sa fonction.

1.2.2.3 Spécificité de substrat

Les MAP kinases ont une spécificité pour les séquences peptidiques contenant une proline et sont donc des kinases *proline directed*. La structure tridimensionnelle de ERK3, modélisée par analogie à celle de ERK2, suggère que ERK3 possède un spécificité complètement différente des autres MAP kinases [33]. Ainsi, il a été suggéré que ERK3 pourrait avoir une préférence pour des substrats déjà phosphorylés et ainsi être une kinase *phosphate directed*. Il existe plusieurs kinases ayant ce genre de spécificité dans le kinome comme la caséine kinase I (CKI), qui partage certaines caractéristiques structurales avec ERK3 [145]. L'hypothèse que ERK3 possède une spécificité pour les peptides phosphorylés reste cependant à être vérifiée expérimentalement.

Des résultats récents obtenus dans notre laboratoire suggèrent que ERK3 phosphoryle directement MK5, tel que proposé précédemment [48]. La boucle d'activation de MK5 contient une thréonine qui doit être phosphorylée pour l'activation de MK5. Cette Thr est suivie d'un résidu Pro. Il reste cependant à identifier le site de phosphorylation de MK5 par ERK3.

1.2.3 Fonction biologique de ERK3

Jusqu'à maintenant, la fonction biologique de ERK3 est demeurée inconnue. L'ARNm de ERK3 est retrouvé à différents niveaux d'expression dans la plupart des organes chez les rongeurs et l'humain, prédisant un rôle ubiquitaire pour cette protéine [17, 133, 134]. De plus, la protéine est détectée dans plusieurs lignées cellulaires [134-136]. Par ailleurs, aucune étude n'a permis de démontrer le rôle de ERK3 comme molécule de signalisation cellulaire et la question de la fonction cellulaire de ERK3 n'a été adressée que partiellement. Par contre, plusieurs hypothèses intéressantes quant à la fonction de ERK3 ont été suggérées.

1.2.3.1 Développement

Plusieurs évidences suggèrent que ERK3 pourrait être importante pour le développement. Premièrement, une augmentation de ERK3 au cours de la différenciation cellulaire fut observée dans plusieurs modèles cellulaires. Ainsi, l'expression de *Erk3* augmente lors de la différenciation des cellules P19 en cellules musculaires ou neuronales [17]. L'augmentation de *Erk3* a également été observée lors de la différenciation des cellules Raji [157] et d'oligodendrocytes primaires [161]. Enfin, les niveaux d'expression de la protéine sont augmentés lors de la différenciation de PC12 en neurone et de C2C12 en cellules musculaires [158].

L'expression de ERK3 au cours du développement embryonnaire est également en accord avec un rôle de ERK3 dans le développement. Ainsi, *Erk3* est fortement exprimée dans le tissu neural de l'embryon du poisson zèbre, suggérant un rôle de ERK3 au cours du développement du cerveau [162]. De plus, l'expression de ERK3 varie au cours du développement de plusieurs organes chez le rat, connaissant une expression plus forte en fin de gestation, plutôt que chez l'adulte [163]. Par ailleurs, lors du développement du poumon de rat, l'expression temporelle de ERK3 corrèle avec la différenciation des pneumocytes au niveau distal ainsi que de l'épithélium broncho-épithélial proximal en fin de gestation [163].

Finalement, ERK3 est un activateur physiologique de MK5. Un rôle de MK5 dans le développement embryonnaire a été suggéré par l'observation que l'inactivation du gène de MK5 chez la souris est associée à la mortalité embryonnaire dans un fond génétique enrichie en C57BL/6 [50]. ERK3 a récemment été décrit comme un régulateur positif de l'activité de MK5, indiquant que ces deux protéines font partie d'une même voie de signalisation [49, 50]. En accord avec cette idée, les ARNm de ERK3 et MK5 sont co-exprimés dans certain tissus au cours du développement embryonnaire murin [50]. De plus, des fibroblastes embryonnaires

déficients en ERK3 présentent une activité MK5 diminuée. À l'inverse, une forte diminution de l'expression de ERK3 est observée dans des fibroblastes embryonnaires dépourvus de MK5 [49, 50]. Bien que le rôle précis de MK5 dans le développement reste inconnu, il semble que l'intégrité de la voie ERK3-MK5 soit importante pour le développement embryonnaire.

1.2.3.2 Cycle cellulaire

Plusieurs évidences expérimentales suggèrent que ERK3 pourrait jouer un rôle dans la régulation du cycle cellulaire dans certains contextes. Tout d'abord, l'expression de mutants non-dégradables de ERK3 bloque la prolifération cellulaire dans plusieurs modèles cellulaires [158]. En accord avec un rôle de ERK3 comme régulateur négatif de la prolifération, l'accumulation de ERK3 est associée à l'arrêt du cycle cellulaire, mesuré par l'apparition de $p21^{CIP1}$, lors de la différenciation musculaire [158]. Le mécanisme d'action de ERK3 sur le cycle cellulaire reste toutefois à être déterminé, mais pourrait impliquer un régulateur du cycle cellulaire, la cyclin D3. En effet, ERK3 a récemment été identifiée comme une protéine pouvant interagir *in vitro* et *in vivo* avec cyclin D3 [148]. Par ailleurs, les auteurs d'une étude récente suggèrent un rôle de ERK3 dans la ségrégation du Golgi lors de la mitose. En effet, la variation de la localisation de ERK3 entre le Golgi et le noyau varie en fonction du cycle cellulaire [136]. Cette hypothèse reste toutefois à être vérifiée. Bien que ces résultats expérimentaux suggèrent un rôle de ERK3 dans le cycle cellulaire, les données disponibles ne permettent pas de savoir si ERK3 joue un rôle positif ou négatif sur la prolifération cellulaire dans des conditions physiologiques.

1.2.3.3 Sécrétion d'insuline

Une étude récente suggère un rôle de ERK3 dans la sécrétion d'insuline [151]. En effet, la diminution de l'expression de ERK3 par des oligonucléotides antisens dans des îlots pancréatiques isolés de rate gestante fut accompagnée d'une diminution de la production d'insuline induite par le glucose. Ceci a été reproduit dans un modèle cellulaire, où la suppression de l'expression de ERK3 fut associée a une diminution de sécrétion d'insuline dans les cellules RINm5F stimulées par le PMA. Le rôle moléculaire précis de ERK3 dans la production d'insuline est peu caractérisé, mais pourrait impliquer l'interaction et la phosphorylation de la protéine MAP2 [151]. MAP2 est une protéine potentiellement impliquée dans le contrôle de l'exocytose de l'insuline [164]. Bien que l'interaction directe entre ces deux protéines reste à être démontrée, la diminution de la phosphorylation de MAP2 en Ser suite à la diminution des niveaux d'expression de ERK3 suggère que MAP2 pourrait être un substrat de ERK3 dans le contrôle de la production d'insuline [151].

1.2.4 Conclusion

ERK3 est l'un des premiers membres de la famille MAP kinase identifiée par clonage moléculaire dont l'étude a été limitée par plusieurs controverses. Plusieurs caractéristiques de structure et de régulation lui confèrent un caractère atypique. ERK3 contient un motif SEG en remplacement du motif TXY hautement conservé chez les MAP kinases et présente une extension C-terminale de fonction indéterminée. De plus, les mécanismes responsables de son activité catalytique restes inconnus. Par contre, plusieurs données indiquent que ERK3 pourrait être régulée au niveau de son expression. L'influence de ces caractéristiques sur la fonction de ERK3 est toutefois incomprise, sa fonction demeurant inconnue.

1.3 Contexte du projet de recherche

1.3.1 Limitations liées à l'étude de ERK3

Plusieurs limitations sont associées à l'étude de la fonction de ERK3. Tout d'abord, ERK3 possède des caractéristiques structurales et de régulation qui la distingue des autres MAP kinases. Ces différences structurales particulières prédisent une activité et un mode de régulation différent pour ERK3. Ainsi, ERK3 est régulée au niveau de son expression et pourrait avoir une spécificité pour des substrats déjà phosphorylés. Ensuite, plusieurs controverses sont liées à l'étude de ERK3 : l'existence d'isoformes, sa localisation subcellulaire ainsi que ses substrats potentiels. Ces controverses sont associées à l'utilisation de modèles cellulaires comme modèles d'études, mais également au fait que la recherche sur ERK3 s'est faite dans le cadre proposé par la recherche sur les MAP kinases conventionnelles. Finalement, ERK3 n'est pas retrouvée chez les organismes modèles comme la levure, le ver et la mouche. Ces modèles se sont avérés des outils majeurs dans l'étude des MAP kinases classiques. En conséquence, la fonction de ERK3 reste incomprise 15 ans après sa découverte.

1.3.2 Un modèle d'invalidation génique de ERK3 chez la souris

La compréhension complète du rôle physiologique d'une protéine kinase dépend de la génération et l'analyse d'organismes mutants pour cette kinase, mutation résultant en la perte de fonction ou empêchant son activation. La plupart des gènes encodant des membres de la grande famille MAP kinase ont ainsi été invalidé chez la souris et l'analyse de ces mutants a démontré la pertinence de cette approche pour l'étude de cette famille de gènes. De plus, cette approche permet de contourner les limitations liées à ERK3 comme ses caractéristiques atypiques et les controverses associées à l'étude de sa fonction.

1.3.2.1 Objectif général

La génération d'une mutation «perte de fonction» du gène *Erk3* chez la souris permettrait de vérifier l'hypothèse que ERK3 est important pour le développement murin. Ainsi, l'objectif général de cette thèse était de générer un modèle d'invalidation génique de *Erk3* chez la souris dans le but de mettre en évidence son rôle biologique.

1.3.2.2 Objectifs spécifiques

Objectif spécifique I. L'invalidation d'un gène implique tout d'abord la connaissance de sa structure, ou organisation intron/exon. Dans le cas particulier de ERK3, l'existence de plusieurs gènes encodant cette protéine a été proposée. Le premier objectif spécifique était donc d'isoler et caractériser la structure du ou des gènes pouvant encoder des isoformes de ERK3 de façon à résoudre cette controverse.

Objectif spécifique II. L'étude du rôle physiologique d'un gène nécessite une connaissance de son profil expression. Dans le but de mettre en évidence le rôle de ERK3 dans le développement, le second objectif était d'étudier l'expression du (des) gène (s) *Erk3* au cours du développement murin.

Objectif spécifique III. La mise en évidence de la fonction biologique d'un gène implique la caractérisation des phénotypes associés à son inactivation. Le dernier objectif était donc de créer un allèle nul du gène *Erk3* dans des cellules embryonnaires souches de souris, générer des souris homozygotes pour cette mutation et caractériser les phénotypes associés à la perte de ERK3 chez ces souris mutantes.

En plus de mettre en évidence la fonction biologique de ERK3 et vérifier l'hypothèse que ERK3 est important pour le développement de la souris, la génération d'un modèle murin déficient en ERK3 représente un modèle de choix pour d'étude de cette MAP kinase atypique.

1.4 Références

1 Goldberg, J. M., Manning, G., Liu, A., Fey, P., Pilcher, K. E., Xu, Y. and Smith, J. L. (2006) The dictyostelium kinome--analysis of the protein kinases from a simple model organism. PLoS Genet **2**, e38

2 Caenepeel, S., Charydczak, G., Sudarsanam, S., Hunter, T. and Manning, G. (2004) The mouse kinome: discovery and comparative genomics of all mouse protein kinases. Proc Natl Acad Sci U S A **101**, 11707-11712

3 Cooper, J. A., Sefton, B. M. and Hunter, T. (1984) Diverse mitogenic agents induce the phosphorylation of two related 42,000-dalton proteins on tyrosine in quiescent chick cells. Mol Cell Biol **4**, 30-37

4 Gilmore, T. and Martin, G. S. (1983) Phorbol ester and diacylglycerol induce protein phosphorylation at tyrosine. Nature **306**, 487-490

5 Bishop, R., Martinez, R., Nakamura, K. D. and Weber, M. J. (1983) A tumor promoter stimulates phosphorylation on tyrosine. Biochem Biophys Res Commun **115**, 536-543

6 Nakamura, K. D., Martinez, R. and Weber, M. J. (1983) Tyrosine phosphorylation of specific proteins after mitogen stimulation of chicken embryo fibroblasts. Mol Cell Biol **3**, 380-390

7 Kohno, M. (1985) Diverse mitogenic agents induce rapid phosphorylation of a common set of cellular proteins at tyrosine in quiescent mammalian cells. J Biol Chem **260**, 1771-1779

8 Cooper, J. A. and Hunter, T. (1985) Major substrate for growth factor-activated protein-tyrosine kinases is a low-abundance protein. Mol Cell Biol **5**, 3304-3309

9 Ray, L. B. and Sturgill, T. W. (1987) Rapid stimulation by insulin of a serine/threonine kinase in 3T3-L1 adipocytes that phosphorylates microtubule-associated protein 2 in vitro. Proc Natl Acad Sci U S A **84**, 1502-1506

10 Sturgill, T. W. and Ray, L. B. (1986) Muscle proteins related to microtubule associated protein-2 are substrates for an insulin-stimulatable kinase. Biochem Biophys Res Commun **134**, 565-571

11 Ray, L. B. and Sturgill, T. W. (1988) Insulin-stimulated microtubule-associated protein kinase is phosphorylated on tyrosine and threonine in vivo. Proc Natl Acad Sci U S A **85**, 3753-3757

12 Hoshi, M., Nishida, E. and Sakai, H. (1988) Activation of a Ca2+-inhibitable protein kinase that phosphorylates microtubule-associated protein 2 in vitro by growth factors, phorbol esters, and serum in quiescent cultured human fibroblasts. J Biol Chem **263**, 5396-5401

13 Hoshi, M., Nishida, E. and Sakai, H. (1989) Characterization of a mitogen-activated, Ca2+-sensitive microtubule-associated protein-2 kinase. Eur J Biochem **184**, 477-486

14 Ray, L. B. and Sturgill, T. W. (1988) Characterization of insulin-stimulated microtubule-associated protein kinase. Rapid isolation and stabilization of a novel serine/threonine kinase from 3T3-L1 cells. J Biol Chem **263**, 12721-12727

15 Rossomando, A. J., Payne, D. M., Weber, M. J. and Sturgill, T. W. (1989) Evidence that pp42, a major tyrosine kinase target protein, is a mitogen-activated serine/threonine protein kinase. Proc Natl Acad Sci U S A **86**, 6940-6943

16 Boulton, T. G., Yancopoulos, G. D., Gregory, J. S., Slaughter, C., Moomaw, C., Hsu, J. and Cobb, M. H. (1990) An insulin-stimulated protein kinase similar to yeast kinases involved in cell cycle control. Science **249**, 64-67

17 Boulton, T. G., Nye, S. H., Robbins, D. J., Ip, N. Y., Radziejewska, E., Morgenbesser, S. D., DePinho, R. A., Panayotatos, N., Cobb, M. H. and Yancopoulos, G. D. (1991) ERKs: a family of protein-serine/threonine kinases that are activated and tyrosine phosphorylated in response to insulin and NGF. Cell **65**, 663-675

18 Gonzalez, F. A., Raden, D. L., Rigby, M. R. and Davis, R. J. (1992) Heterogeneous expression of four MAP kinase isoforms in human tissues. FEBS Lett **304**, 170-178

19 Zhou, G., Bao, Z. Q. and Dixon, J. E. (1995) Components of a new human protein kinase signal transduction pathway. J Biol Chem **270**, 12665-12669

20 Lee, J. D., Ulevitch, R. J. and Han, J. (1995) Primary structure of BMK1: a new mammalian map kinase. Biochem Biophys Res Commun **213**, 715-724

21 Abe, M. K., Kuo, W. L., Hershenson, M. B. and Rosner, M. R. (1999) Extracellular signal-regulated kinase 7 (ERK7), a novel ERK with a C-terminal domain that regulates its activity, its cellular localization, and cell growth. Mol Cell Biol **19**, 1301-1312

22 Kyriakis, J. M. and Avruch, J. (2001) Mammalian mitogen-activated protein kinase signal transduction pathways activated by stress and inflammation. Physiol Rev **81**, 807-869

23 Crews, C. M. and Erikson, R. L. (1993) Extracellular signals and reversible protein phosphorylation: what to Mek of it all. Cell **74**, 215-217

24 Herskowitz, I. (1995) MAP kinase pathways in yeast: for mating and more. Cell **80**, 187-197

25 Widmann, C., Gibson, S., Jarpe, M. B. and Johnson, G. L. (1999) Mitogen-activated protein kinase: conservation of a three-kinase module from yeast to human. Physiol Rev **79**, 143-180

26 Payne, D. M., Rossomando, A. J., Martino, P., Erickson, A. K., Her, J. H., Shabanowitz, J., Hunt, D. F., Weber, M. J. and Sturgill, T. W. (1991) Identification of the regulatory phosphorylation sites in pp42/mitogen-activated protein kinase (MAP kinase). Embo J **10**, 885-892

27 English, J., Pearson, G., Wilsbacher, J., Swantek, J., Karandikar, M., Xu, S. and Cobb, M. H. (1999) New insights into the control of MAP kinase pathways. Exp Cell Res **253**, 255-270

28 Theodosiou, A. and Ashworth, A. (2002) MAP kinase phosphatases. Genome Biol **3**, REVIEWS3009

29 Biondi, R. M. and Nebreda, A. R. (2003) Signalling specificity of Ser/Thr protein kinases through docking-site-mediated interactions. Biochem J **372**, 1-13

30 Dard, N. and Peter, M. (2006) Scaffold proteins in MAP kinase signaling: more than simple passive activating platforms. Bioessays **28**, 146-156

31 Kondoh, K., Torii, S. and Nishida, E. (2005) Control of MAP kinase signaling to the nucleus. Chromosoma **114**, 86-91

32 Volmat, V. and Pouyssegur, J. (2001) Spatiotemporal regulation of the p42/p44 MAPK pathway. Biol Cell **93**, 71-79

33 Coulombe, P. and Meloche, S. (2006) Atypical mitogen-activated protein kinases: Structure, regulation and functions. Biochim. Biophys. Acta doi:10.1016/ j.bbamcr.2006.11.001

34 Rubinfeld, H. and Seger, R. (2005) The ERK cascade: a prototype of MAPK signaling. Mol Biotechnol **31**, 151-174

35 Gupta, S., Barrett, T., Whitmarsh, A. J., Cavanagh, J., Sluss, H. K., Derijard, B. and Davis, R. J. (1996) Selective interaction of JNK protein kinase isoforms with transcription factors. Embo J **15**, 2760-2770

36 Kyriakis, J. M., Banerjee, P., Nikolakaki, E., Dai, T., Rubie, E. A., Ahmad, M. F., Avruch, J. and Woodgett, J. R. (1994) The stress-activated protein kinase subfamily of c-Jun kinases. Nature **369**, 156-160

37 Derijard, B., Hibi, M., Wu, I. H., Barrett, T., Su, B., Deng, T., Karin, M. and Davis, R. J. (1994) JNK1: a protein kinase stimulated by UV light and Ha-Ras that binds and phosphorylates the c-Jun activation domain. Cell **76**, 1025-1037

38 Karin, M. and Gallagher, E. (2005) From JNK to pay dirt: jun kinases, their biochemistry, physiology and clinical importance. IUBMB Life **57**, 283-295

39 Han, J., Lee, J. D., Bibbs, L. and Ulevitch, R. J. (1994) A MAP kinase targeted by endotoxin and hyperosmolarity in mammalian cells. Science **265**, 808-811

40 Lee, J. C., Laydon, J. T., McDonnell, P. C., Gallagher, T. F., Kumar, S., Green, D., McNulty, D., Blumenthal, M. J., Heys, J. R., Landvatter, S. W. and et al. (1994) A protein kinase involved in the regulation of inflammatory cytokine biosynthesis. Nature **372**, 739-746

41 Zarubin, T. and Han, J. (2005) Activation and signaling of the p38 MAP kinase pathway. Cell Res **15**, 11-18

42 Kasler, H. G., Victoria, J., Duramad, O. and Winoto, A. (2000) ERK5 is a novel type of mitogen-activated protein kinase containing a transcriptional activation domain. Mol Cell Biol **20**, 8382-8389

43 Zheng, Q., Yin, G., Yan, C., Cavet, M. and Berk, B. C. (2004) 14-3-3beta binds to big mitogen-activated protein kinase 1 (BMK1/ERK5) and regulates BMK1 function. J Biol Chem **279**, 8787-8791

44 Krens, S. F., Spaink, H. P. and Snaar-Jagalska, B. E. (2006) Functions of the MAPK family in vertebrate-development. FEBS Lett **580**, 4984-4990

45 Watanabe, N., Nagamatsu, Y., Gengyo-Ando, K., Mitani, S. and Ohshima, Y. (2005) Control of body size by SMA-5, a homolog of MAP kinase BMK1/ERK5, in C. elegans. Development **132**, 3175-3184

46 Wang, X. and Tournier, C. (2006) Regulation of cellular functions by the ERK5 signalling pathway. Cell Signal **18**, 753-760

47 Kant S, Schumacher S, Singh MK, Kispert A, Kotlyarov A and M., G. (2006) Characterization of the atypical map kinase ERK4 and its activation of the MAPK-activated protein kinase MK5. J Biol Chem **281**, 35511-35519

48 Aberg E, Perander M, Johansen B, Julien C, Meloche S, Keyse SM and OM., S. (2006) Regulation of MAPK-activated protein kinase 5 activity and subcellular localization by the atypical MAP kinase ERK4/MAPK4. J Biol Chem **281**, 35499-35510

49 Seternes, O. M., Mikalsen, T., Johansen, B., Michaelsen, E., Armstrong, C. G., Morrice, N. A., Turgeon, B., Meloche, S., Moens, U. and Keyse, S. M. (2004) Activation of MK5/PRAK by the atypical MAP kinase ERK3 defines a novel signal transduction pathway. Embo J **23**, 4780-4791

50 Schumacher, S., Laass, K., Kant, S., Shi, Y., Visel, A., Gruber, A. D., Kotlyarov, A. and Gaestel, M. (2004) Scaffolding by ERK3 regulates MK5 in development. Embo J **23**, 4770-4779

51 Gaestel, M. (2006) MAPKAP kinases - MKs - two's company, three's a crowd. Nat Rev Mol Cell Biol **7**, 120-130

52 Abe, M. K., Saelzler, M. P., Espinosa, R., 3rd, Kahle, K. T., Hershenson, M. B., Le Beau, M. M. and Rosner, M. R. (2002) ERK8, a new member of the mitogen-activated protein kinase family. J Biol Chem **277**, 16733-16743

53 Abe, M. K., Kahle, K. T., Saelzler, M. P., Orth, K., Dixon, J. E. and Rosner, M. R. (2001) ERK7 is an autoactivated member of the MAPK family. J Biol Chem **276**, 21272-21279

54 Klevernic, I. V., Stafford, M. J., Morrice, N., Peggie, M., Morton, S. and Cohen, P. (2006) Characterization of the reversible phosphorylation and activation of ERK8. Biochem J **394**, 365-373

55 Kuo, W. L., Duke, C. J., Abe, M. K., Kaplan, E. L., Gomes, S. and Rosner, M. R. (2004) ERK7 expression and kinase activity is regulated by the ubiquitin-proteosome pathway. J Biol Chem **279**, 23073-23081

56 Iavarone, C., Acunzo, M., Carlomagno, F., Catania, A., Melillo, R. M., Carlomagno, S. M., Santoro, M. and Chiariello, M. (2006) Activation of the Erk8 mitogen-activated protein (MAP) kinase by RET/PTC3, a constitutively active form of the RET proto-oncogene. J Biol Chem **281**, 10567-10576

57 Saelzler, M. P., Spackman, C. C., Liu, Y., Martinez, L. C., Harris, J. P. and Abe, M. K. (2006) ERK8 down-regulates transactivation of the glucocorticoid receptor through Hic-5. J Biol Chem **281**, 16821-16832

58 Henrich, L. M., Smith, J. A., Kitt, D., Errington, T. M., Nguyen, B., Traish, A. M. and Lannigan, D. A. (2003) Extracellular signal-regulated kinase 7, a regulator of hormone-dependent estrogen receptor destruction. Mol Cell Biol **23**, 5979-5988

59 Brott, B. K., Pinsky, B. A. and Erikson, R. L. (1998) Nlk is a murine protein kinase related to Erk/MAP kinases and localized in the nucleus. Proc Natl Acad Sci U S A **95**, 963-968

60 Manning, G., Whyte, D. B., Martinez, R., Hunter, T. and Sudarsanam, S. (2002) The protein kinase complement of the human genome. Science **298**, 1912-1934

61 Ishitani, T., Ninomiya-Tsuji, J., Nagai, S., Nishita, M., Meneghini, M., Barker, N., Waterman, M., Bowerman, B., Clevers, H., Shibuya, H. and Matsumoto, K. (1999) The TAK1-NLK-MAPK-related pathway antagonizes signalling between beta-catenin and transcription factor TCF. Nature **399**, 798-802

62 Kanei-Ishii, C., Ninomiya-Tsuji, J., Tanikawa, J., Nomura, T., Ishitani, T., Kishida, S., Kokura, K., Kurahashi, T., Ichikawa-Iwata, E., Kim, Y., Matsumoto, K. and Ishii, S. (2004) Wnt-1 signal induces phosphorylation and degradation of c-Myb protein via TAK1, HIPK2, and NLK. Genes Dev **18**, 816-829

63 Ishitani, T., Kishida, S., Hyodo-Miura, J., Ueno, N., Yasuda, J., Waterman, M., Shibuya, H., Moon, R. T., Ninomiya-Tsuji, J. and Matsumoto, K. (2003) The TAK1-NLK mitogen-activated protein kinase cascade functions in the Wnt-5a/Ca(2+) pathway to antagonize Wnt/beta-catenin signaling. Mol Cell Biol **23**, 131-139

64 Smit, L., Baas, A., Kuipers, J., Korswagen, H., van de Wetering, M. and Clevers, H. (2004) Wnt activates the Tak1/Nemo-like kinase pathway. J Biol Chem **279**, 17232-17240

65 Kurahashi, T., Nomura, T., Kanei-Ishii, C., Shinkai, Y. and Ishii, S. (2005) The Wnt-NLK signaling pathway inhibits A-Myb activity by inhibiting the association with coactivator CBP and methylating histone H3. Mol Biol Cell **16**, 4705-4713

66 Yang, D. D., Kuan, C. Y., Whitmarsh, A. J., Rincon, M., Zheng, T. S., Davis, R. J., Rakic, P. and Flavell, R. A. (1997) Absence of excitotoxicity-induced apoptosis in the hippocampus of mice lacking the Jnk3 gene. Nature **389**, 865-870

67 Sabapathy, K., Hu, Y., Kallunki, T., Schreiber, M., David, J. P., Jochum, W., Wagner, E. F. and Karin, M. (1999) JNK2 is required for efficient T-cell activation and apoptosis but not for normal lymphocyte development. Curr Biol **9**, 116-125

68 Yang, D. D., Conze, D., Whitmarsh, A. J., Barrett, T., Davis, R. J., Rincon, M. and Flavell, R. A. (1998) Differentiation of CD4+ T cells to Th1 cells requires MAP kinase JNK2. Immunity **9**, 575-585

69 Dong, C., Yang, D. D., Wysk, M., Whitmarsh, A. J., Davis, R. J. and Flavell, R. A. (1998) Defective T cell differentiation in the absence of Jnk1. Science **282**, 2092-2095

70 Sabapathy, K., Jochum, W., Hochedlinger, K., Chang, L., Karin, M. and Wagner, E. F. (1999) Defective neural tube morphogenesis and altered apoptosis in the absence of both JNK1 and JNK2. Mech Dev **89**, 115-124

71 Kuan, C. Y., Yang, D. D., Samanta Roy, D. R., Davis, R. J., Rakic, P. and Flavell, R. A. (1999) The Jnk1 and Jnk2 protein kinases are required for regional specific apoptosis during early brain development. Neuron **22**, 667-676

72 Weston, C. R., Wong, A., Hall, J. P., Goad, M. E., Flavell, R. A. and Davis, R. J. (2003) JNK initiates a cytokine cascade that causes Pax2 expression and closure of the optic fissure. Genes Dev **17**, 1271-1280

73 Stronach, B. E. and Perrimon, N. (1999) Stress signaling in Drosophila. Oncogene **18**, 6172-6182

74 Weston, C. R., Wong, A., Hall, J. P., Goad, M. E., Flavell, R. A. and Davis, R. J. (2004) The c-Jun NH2-terminal kinase is essential for epidermal growth factor expression during epidermal morphogenesis. Proc Natl Acad Sci U S A **101**, 14114-14119

75 Hilberg, F., Aguzzi, A., Howells, N. and Wagner, E. F. (1993) c-jun is essential for normal mouse development and hepatogenesis. Nature **365**, 179-181

76 Ganiatsas, S., Kwee, L., Fujiwara, Y., Perkins, A., Ikeda, T., Labow, M. A. and Zon, L. I. (1998) SEK1 deficiency reveals mitogen-activated protein kinase cascade crossregulation and leads to abnormal hepatogenesis. Proc Natl Acad Sci U S A **95**, 6881-6886

77 Flavell, R. A., Li, B., Dong, C., Lu, H. T., Yang, D. D., Enslen, H., Tournier, C., Whitmarsh, A., Wysk, M., Conze, D., Rincon, M. and Davis, R. J. (1999) Molecular basis of T-cell differentiation. Cold Spring Harb Symp Quant Biol **64**, 563-571

78 Rincon, M., Whitmarsh, A., Yang, D. D., Weiss, L., Derijard, B., Jayaraj, P., Davis, R. J. and Flavell, R. A. (1998) The JNK pathway regulates the In vivo deletion of immature CD4(+)CD8(+) thymocytes. J Exp Med **188**, 1817-1830

79 Sabapathy, K., Kallunki, T., David, J. P., Graef, I., Karin, M. and Wagner, E. F. (2001) c-Jun NH2-terminal kinase (JNK)1 and JNK2 have similar and stage-dependent roles in regulating T cell apoptosis and proliferation. J Exp Med **193**, 317-328

80 Su, B., Jacinto, E., Hibi, M., Kallunki, T., Karin, M. and Ben-Neriah, Y. (1994) JNK is involved in signal integration during costimulation of T lymphocytes. Cell **77**, 727-736

81 Constant, S. L., Dong, C., Yang, D. D., Wysk, M., Davis, R. J. and Flavell, R. A. (2000) JNK1 is required for T cell-mediated immunity against Leishmania major infection. J Immunol **165**, 2671-2676

82 Dong, C., Yang, D. D., Tournier, C., Whitmarsh, A. J., Xu, J., Davis, R. J. and Flavell, R. A. (2000) JNK is required for effector T-cell function but not for T-cell activation. Nature **405**, 91-94

83 Arbour, N., Naniche, D., Homann, D., Davis, R. J., Flavell, R. A. and Oldstone, M. B. (2002) c-Jun NH(2)-terminal kinase (JNK)1 and JNK2 signaling pathways have divergent roles in CD8(+) T cell-mediated antiviral immunity. J Exp Med **195**, 801-810

84 Conze, D., Krahl, T., Kennedy, N., Weiss, L., Lumsden, J., Hess, P., Flavell, R. A., Le Gros, G., Davis, R. J. and Rincon, M. (2002) c-Jun NH(2)-terminal kinase (JNK)1 and JNK2 have distinct roles in CD8(+) T cell activation. J Exp Med **195**, 811-823

85 Bjorkblom, B., Ostman, N., Hongisto, V., Komarovski, V., Filen, J. J., Nyman, T. A., Kallunki, T., Courtney, M. J. and Coffey, E. T. (2005) Constitutively active cytoplasmic c-Jun N-terminal kinase 1 is a dominant regulator of dendritic architecture: role of microtubule-associated protein 2 as an effector. J Neurosci **25**, 6350-6361

86 Chang, L., Jones, Y., Ellisman, M. H., Goldstein, L. S. and Karin, M. (2003) JNK1 is required for maintenance of neuronal microtubules and controls phosphorylation of microtubule-associated proteins. Dev Cell **4**, 521-533

87 Harada, A., Teng, J., Takei, Y., Oguchi, K. and Hirokawa, N. (2002) MAP2 is required for dendrite elongation, PKA anchoring in dendrites, and proper PKA signal transduction. J Cell Biol **158**, 541-549

88 Hunot, S., Vila, M., Teismann, P., Davis, R. J., Hirsch, E. C., Przedborski, S., Rakic, P. and Flavell, R. A. (2004) JNK-mediated induction of cyclooxygenase 2 is required for neurodegeneration in a mouse model of Parkinson's disease. Proc Natl Acad Sci U S A **101**, 665-670

89 Kuan, C. Y., Whitmarsh, A. J., Yang, D. D., Liao, G., Schloemer, A. J., Dong, C., Bao, J., Banasiak, K. J., Haddad, G. G., Flavell, R. A., Davis, R. J. and Rakic, P. (2003) A critical role of neural-specific JNK3 for ischemic apoptosis. Proc Natl Acad Sci U S A **100**, 15184-15189

90 Hotamisligil, G. S. (2003) Inflammatory pathways and insulin action. Int J Obes Relat Metab Disord **27 Suppl 3**, S53-55

91 Hirosumi, J., Tuncman, G., Chang, L., Gorgun, C. Z., Uysal, K. T., Maeda, K., Karin, M. and Hotamisligil, G. S. (2002) A central role for JNK in obesity and insulin resistance. Nature **420**, 333-336

92 Jaeschke, A., Czech, M. P. and Davis, R. J. (2004) An essential role of the JIP1 scaffold protein for JNK activation in adipose tissue. Genes Dev **18**, 1976-1980

93 Waetzig, V. and Herdegen, T. (2005) Context-specific inhibition of JNKs: overcoming the dilemma of protection and damage. Trends Pharmacol Sci **26**, 455-461

94 Han, Z., Boyle, D. L., Chang, L., Bennett, B., Karin, M., Yang, L., Manning, A. M. and Firestein, G. S. (2001) c-Jun N-terminal kinase is required for metalloproteinase expression and joint destruction in inflammatory arthritis. J Clin Invest **108**, 73-81

95 Han, Z., Chang, L., Yamanishi, Y., Karin, M. and Firestein, G. S. (2002) Joint damage and inflammation in c-Jun N-terminal kinase 2 knockout mice with passive murine collagen-induced arthritis. Arthritis Rheum **46**, 818-823

96 Ricci, R., Sumara, G., Sumara, I., Rozenberg, I., Kurrer, M., Akhmedov, A., Hersberger, M., Eriksson, U., Eberli, F. R., Becher, B., Boren, J., Chen, M., Cybulsky, M. I., Moore, K. J., Freeman, M. W., Wagner, E. F., Matter, C. M. and Luscher, T. F. (2004) Requirement of JNK2 for scavenger receptor A-mediated foam cell formation in atherogenesis. Science **306**, 1558-1561

97 Chen, N., Nomura, M., She, Q. B., Ma, W. Y., Bode, A. M., Wang, L., Flavell, R. A. and Dong, Z. (2001) Suppression of skin tumorigenesis in c-Jun NH(2)-terminal kinase-2-deficient mice. Cancer Res **61**, 3908-3912

98 She, Q. B., Chen, N., Bode, A. M., Flavell, R. A. and Dong, Z. (2002) Deficiency of c-Jun-NH(2)-terminal kinase-1 in mice enhances skin tumor development by 12-O-tetradecanoylphorbol-13-acetate. Cancer Res **62**, 1343-1348

99 Umbhauer, M., Marshall, C. J., Mason, C. S., Old, R. W. and Smith, J. C. (1995) Mesoderm induction in Xenopus caused by activation of MAP kinase. Nature **376**, 58-62

100 Gotoh, Y., Masuyama, N., Suzuki, A., Ueno, N. and Nishida, E. (1995) Involvement of the MAP kinase cascade in Xenopus mesoderm induction. Embo J **14**, 2491-2498

101 Pages, G., Guerin, S., Grall, D., Bonino, F., Smith, A., Anjuere, F., Auberger, P. and Pouyssegur, J. (1999) Defective thymocyte maturation in p44 MAP kinase (Erk 1) knockout mice. Science **286**, 1374-1377

102 Yao, Y., Li, W., Wu, J., Germann, U. A., Su, M. S., Kuida, K. and Boucher, D. M. (2003) Extracellular signal-regulated kinase 2 is necessary for mesoderm differentiation. Proc Natl Acad Sci U S A **100**, 12759-12764

103 Saba-El-Leil, M. K., Vella, F. D., Vernay, B., Voisin, L., Chen, L., Labrecque, N., Ang, S. L. and Meloche, S. (2003) An essential function of the mitogen-activated protein kinase Erk2 in mouse trophoblast development. EMBO Rep **4**, 964-968

104 Hatano, N., Mori, Y., Oh-hora, M., Kosugi, A., Fujikawa, T., Nakai, N., Niwa, H., Miyazaki, J., Hamaoka, T. and Ogata, M. (2003) Essential role for ERK2 mitogen-activated protein kinase in placental development. Genes Cells **8**, 847-856

105 Giroux, S., Tremblay, M., Bernard, D., Cardin-Girard, J. F., Aubry, S., Larouche, L., Rousseau, S., Huot, J., Landry, J., Jeannotte, L. and Charron, J. (1999) Embryonic death of Mek1-deficient mice reveals a role for this kinase in angiogenesis in the labyrinthine region of the placenta. Curr Biol **9**, 369-372

106 Nekrasova, T., Shive, C., Gao, Y., Kawamura, K., Guardia, R., Landreth, G. and Forsthuber, T. G. (2005) ERK1-deficient mice show normal T cell effector function and are highly susceptible to experimental autoimmune encephalomyelitis. J Immunol **175**, 2374-2380

107 Fischer, A. M., Katayama, C. D., Pages, G., Pouyssegur, J. and Hedrick, S. M. (2005) The role of erk1 and erk2 in multiple stages of T cell development. Immunity **23**, 431-443

108 Mazzucchelli, C., Vantaggiato, C., Ciamei, A., Fasano, S., Pakhotin, P., Krezel, W., Welzl, H., Wolfer, D. P., Pages, G., Valverde, O., Marowsky, A., Porrazzo, A., Orban, P. C., Maldonado, R., Ehrengruber, M. U., Cestari, V., Lipp, H. P., Chapman, P. F., Pouyssegur, J. and Brambilla, R. (2002) Knockout of ERK1 MAP kinase enhances synaptic plasticity in the striatum and facilitates striatal-mediated learning and memory. Neuron **34**, 807-820

109 Grueter, B. A., Gosnell, H. B., Olsen, C. M., Schramm-Sapyta, N. L., Nekrasova, T., Landreth, G. E. and Winder, D. G. (2006) Extracellular-signal regulated kinase 1-dependent metabotropic glutamate receptor 5-induced long-term depression in the bed nucleus of the stria terminalis is disrupted by cocaine administration. J Neurosci **26**, 3210-3219

110 Bost, F., Aouadi, M., Caron, L., Even, P., Belmonte, N., Prot, M., Dani, C., Hofman, P., Pages, G., Pouyssegur, J., Le Marchand-Brustel, Y. and Binetruy, B. (2005) The extracellular signal-regulated kinase isoform ERK1 is specifically required for in vitro and in vivo adipogenesis. Diabetes **54**, 402-411

111 Bourcier, C., Jacquel, A., Hess, J., Peyrottes, I., Angel, P., Hofman, P., Auberger, P., Pouyssegur, J. and Pages, G. (2006) p44 mitogen-activated protein kinase (extracellular signal-regulated kinase 1)-dependent signaling contributes to epithelial skin carcinogenesis. Cancer Res **66**, 2700-2707

112 Sabio, G., Arthur, J. S., Kuma, Y., Peggie, M., Carr, J., Murray-Tait, V., Centeno, F., Goedert, M., Morrice, N. A. and Cuenda, A. (2005) p38gamma regulates the localisation of SAP97 in the cytoskeleton by modulating its interaction with GKAP. Embo J **24**, 1134-1145

113 Beardmore, V. A., Hinton, H. J., Eftychi, C., Apostolaki, M., Armaka, M., Darragh, J., McIlrath, J., Carr, J. M., Armit, L. J., Clacher, C., Malone, L., Kollias, G. and Arthur, J. S. (2005) Generation and characterization of p38beta (MAPK11) gene-targeted mice. Mol Cell Biol **25**, 10454-10464

114 Allen, M., Svensson, L., Roach, M., Hambor, J., McNeish, J. and Gabel, C. A. (2000) Deficiency of the stress kinase p38alpha results in embryonic lethality: characterization of the kinase dependence of stress responses of enzyme-deficient embryonic stem cells. J Exp Med **191**, 859-870

115 Mudgett, J. S., Ding, J., Guh-Siesel, L., Chartrain, N. A., Yang, L., Gopal, S. and Shen, M. M. (2000) Essential role for p38alpha mitogen-activated protein kinase in placental angiogenesis. Proc Natl Acad Sci U S A **97**, 10454-10459

116 Tamura, K., Sudo, T., Senftleben, U., Dadak, A. M., Johnson, R. and Karin, M. (2000) Requirement for p38alpha in erythropoietin expression: a role for stress kinases in erythropoiesis. Cell **102**, 221-231

117 Adams, R. H., Porras, A., Alonso, G., Jones, M., Vintersten, K., Panelli, S., Valladares, A., Perez, L., Klein, R. and Nebreda, A. R. (2000) Essential role of p38alpha MAP kinase in placental but not embryonic cardiovascular development. Mol Cell **6**, 109-116

118 Brancho, D., Tanaka, N., Jaeschke, A., Ventura, J. J., Kelkar, N., Tanaka, Y., Kyuuma, M., Takeshita, T., Flavell, R. A. and Davis, R. J. (2003) Mechanism of p38 MAP kinase activation in vivo. Genes Dev **17**, 1969-1978

119 Nishida, K., Yamaguchi, O., Hirotani, S., Hikoso, S., Higuchi, Y., Watanabe, T., Takeda, T., Osuka, S., Morita, T., Kondoh, G., Uno, Y., Kashiwase, K., Taniike, M., Nakai, A., Matsumura, Y., Miyazaki, J., Sudo, T., Hongo, K., Kusakari, Y., Kurihara, S., Chien, K. R., Takeda, J., Hori, M. and Otsu, K. (2004) p38alpha mitogen-activated protein kinase plays a critical role in cardiomyocyte survival but not in cardiac hypertrophic growth in response to pressure overload. Mol Cell Biol **24**, 10611-10620

120 Yan, L., Carr, J., Ashby, P. R., Murry-Tait, V., Thompson, C. and Arthur, J. S. (2003) Knockout of ERK5 causes multiple defects in placental and embryonic development. BMC Dev Biol **3**, 11

121 Sohn, S. J., Sarvis, B. K., Cado, D. and Winoto, A. (2002) ERK5 MAPK regulates embryonic angiogenesis and acts as a hypoxia-sensitive repressor of vascular endothelial growth factor expression. J Biol Chem **277**, 43344-43351

122 Regan, C. P., Li, W., Boucher, D. M., Spatz, S., Su, M. S. and Kuida, K. (2002) Erk5 null mice display multiple extraembryonic vascular and embryonic cardiovascular defects. Proc Natl Acad Sci U S A **99**, 9248-9253

123 Hayashi, M. and Lee, J. D. (2004) Role of the BMK1/ERK5 signaling pathway: lessons from knockout mice. J Mol Med **82**, 800-808

124 Hayashi, M., Kim, S. W., Imanaka-Yoshida, K., Yoshida, T., Abel, E. D., Eliceiri, B., Yang, Y., Ulevitch, R. J. and Lee, J. D. (2004) Targeted deletion of BMK1/ERK5 in adult mice perturbs vascular integrity and leads to endothelial failure. J Clin Invest **113**, 1138-1148

125 Wang, X., Merritt, A. J., Seyfried, J., Guo, C., Papadakis, E. S., Finegan, K. G., Kayahara, M., Dixon, J., Boot-Handford, R. P., Cartwright, E. J., Mayer, U. and Tournier, C. (2005) Targeted deletion of mek5 causes early embryonic death and defects in the extracellular signal-regulated kinase 5/myocyte enhancer factor 2 cell survival pathway. Mol Cell Biol **25**, 336-345

126 Bi, W., Drake, C. J. and Schwarz, J. J. (1999) The transcription factor MEF2C-null mouse exhibits complex vascular malformations and reduced cardiac expression of angiopoietin 1 and VEGF. Dev Biol **211**, 255-267

127 Lin, Q., Lu, J., Yanagisawa, H., Webb, R., Lyons, G. E., Richardson, J. A. and Olson, E. N. (1998) Requirement of the MADS-box transcription factor MEF2C for vascular development. Development **125**, 4565-4574

128 Lin, Q., Schwarz, J., Bucana, C. and Olson, E. N. (1997) Control of mouse cardiac morphogenesis and myogenesis by transcription factor MEF2C. Science **276**, 1404-1407

129 Hayashi, M., Fearns, C., Eliceiri, B., Yang, Y. and Lee, J. D. (2005) Big mitogen-activated protein kinase 1/extracellular signal-regulated kinase 5 signaling pathway is essential for tumor-associated angiogenesis. Cancer Res **65**, 7699-7706

130 Kortenjann, M., Nehls, M., Smith, A. J., Carsetti, R., Schuler, J., Kohler, G. and Boehm, T. (2001) Abnormal bone marrow stroma in mice deficient for nemo-like kinase, Nlk. Eur J Immunol **31**, 3580-3587

131 English, J. M. and Cobb, M. H. (2002) Pharmacological inhibitors of MAPK pathways. Trends Pharmacol Sci **23**, 40-45

132 Meloche, S. (2002) Extracellular signal-regulated linase 4. In AfCS-Nature Molecule Pages, Nature publishing group

133 Meloche, S., Beatty, B. G. and Pellerin, J. (1996) Primary structure, expression and chromosomal locus of a human homolog of rat ERK3. Oncogene **13**, 1575-1579

134 Zhu, A. X., Zhao, Y., Moller, D. E. and Flier, J. S. (1994) Cloning and characterization of p97MAPK, a novel human homolog of rat ERK-3. Mol Cell Biol **14**, 8202-8211

135 Cheng, M., Boulton, T. G. and Cobb, M. H. (1996) ERK3 is a constitutively nuclear protein kinase. J Biol Chem **271**, 8951-8958

136 Bind, E., Kleyner, Y., Skowronska-Krawczyk, D., Bien, E., Dynlacht, B. D. and Sanchez, I. (2004) A novel mechanism for mitogen-activated protein kinase localization. Mol Biol Cell **15**, 4457-4466

137 Julien, C., Coulombe, P. and Meloche, S. (2003) Nuclear export of ERK3 by a CRM1-dependent mechanism regulates its inhibitory action on cell cycle progression. J Biol Chem **278**, 42615-42624

138 Sauma, S. and Friedman, E. (1996) Increased expression of protein kinase C beta activates ERK3. J Biol Chem **271**, 11422-11426

139 Turgeon, B., Saba-El-Leil, M. K. and Meloche, S. (2000) Cloning and characterization of mouse extracellular-signal-regulated protein kinase 3 as a unique gene product of 100 kDa. Biochem J **346 Pt 1**, 169-175

140 Kultz, D. (1998) Phylogenetic and functional classification of mitogen- and stress-activated protein kinases. J Mol Evol **46**, 571-588

141 Cobb, M. H. and Goldsmith, E. J. (1995) How MAP kinases are regulated. J Biol Chem **270**, 14843-14846

142 Robinson, M. J., Cheng, M., Khokhlatchev, A., Ebert, D., Ahn, N., Guan, K. L., Stein, B., Goldsmith, E. and Cobb, M. H. (1996) Contributions of the mitogen-activated protein (MAP) kinase backbone and phosphorylation loop to MEK specificity. J Biol Chem **271**, 29734-29739

143 English, J. M., Vanderbilt, C. A., Xu, S., Marcus, S. and Cobb, M. H. (1995) Isolation of MEK5 and differential expression of alternatively spliced forms. J Biol Chem **270**, 28897-28902

144 Zhang, F., Strand, A., Robbins, D., Cobb, M. H. and Goldsmith, E. J. (1994) Atomic structure of the MAP kinase ERK2 at 2.3 A resolution. Nature **367**, 704-711

145 Xu, R. M., Carmel, G., Sweet, R. M., Kuret, J. and Cheng, X. (1995) Crystal structure of casein kinase-1, a phosphate-directed protein kinase. Embo J **14**, 1015-1023

146 Coulombe, P. (2006) Étude de la régulation de la MAP kinase atypique ERK3 par le système ubiquitine protéasome. In Biologie Moléculaire, Université de Montréal, Montréal

147 Robinson, M. J., Xu Be, B. E., Stippec, S. and Cobb, M. H. (2002) Different domains of the mitogen-activated protein kinases ERK3 and ERK2 direct subcellular localization and upstream specificity in vivo. J Biol Chem **277**, 5094-5100

148 Sun, M., Wei, Y., Yao, L., Xie, J., Chen, X., Wang, H., Jiang, J. and Gu, J. (2006) Identification of extracellular signal-regulated kinase 3 as a new interaction partner of cyclin D3. Biochem Biophys Res Commun **340**, 209-214

149 Meloche, S., Turgeon, B., Coulombe, P. and Rodier, G. (2003) The atypical ERK3 subfamily of Mitogen-activated protein kinases. Transworld Research Network, Kerala, India.

150 Cheng, M., Zhen, E., Robinson, M. J., Ebert, D., Goldsmith, E. and Cobb, M. H. (1996) Characterization of a protein kinase that phosphorylates serine 189 of the mitogen-activated protein kinase homolog ERK3. J Biol Chem **271**, 12057-12062

151 Anhe, G. F., Torrao, A. S., Nogueira, T. C., Caperuto, L. C., Amaral, M. E., Medina, M. C., Azevedo-Martins, A. K., Carpinelli, A. R., Carvalho, C. R., Curi, R., Boschero, A. C. and Bordin, S. (2006) ERK3 associates with MAP2 and is involved in glucose-induced insulin secretion. Mol Cell Endocrinol **251**, 33-41

152 Stocco, C., Callegari, E. and Gibori, G. (2001) Opposite effect of prolactin and prostaglandin F(2 alpha) on the expression of luteal genes as revealed by rat cDNA expression array. Endocrinology **142**, 4158-4161

153 Bordin, S., Amaral, M. E., Anhe, G. F., Delghingaro-Augusto, V., Cunha, D. A., Nicoletti-Carvalho, J. E. and Boschero, A. C. (2004) Prolactin-modulated gene expression profiles in pancreatic islets from adult female rats. Mol Cell Endocrinol **220**, 41-50

154 Crowe, D. L. (2004) Induction of p97MAPK expression regulates collagen mediated inhibition of proliferation and migration in human squamous cell carcinoma lines. Int J Oncol **24**, 1159-1163

155 Quarto, N., Fong, K. D. and Longaker, M. T. (2005) Gene profiling of cells expressing different FGF-2 forms. Gene **356**, 49-68

156 Zimmermann, J., Lamerant, N., Grossenbacher, R. and Furst, P. (2001) Proteasome- and p38-dependent regulation of ERK3 expression. J Biol Chem **276**, 10759-10766

157 Kleines, M., Gartner, A., Ritter, K. and Schaade, L. (2000) Early steps in termination of the immortalization state in Burkitt lymphoma: induction of genes involved in signal transduction, transcription, and trafficking by the ganglioside IV(3)NeuAc-nLcOse(4)Cer. Biochim Biophys Acta **1492**, 139-144

158 Coulombe, P., Rodier, G., Pelletier, S., Pellerin, J. and Meloche, S. (2003) Rapid turnover of extracellular signal-regulated kinase 3 by the ubiquitin-proteasome pathway defines a novel paradigm of mitogen-activated protein kinase regulation during cellular differentiation. Mol Cell Biol **23**, 4542-4558

159 Mikalsen, T., Johannessen, M. and Moens, U. (2005) Sequence- and position-dependent tagging protects extracellular-regulated kinase 3 protein from 26S proteasome-mediated degradation. Int J Biochem Cell Biol **37**, 2513-2520

160 Coulombe, P., Rodier, G., Bonneil, E., Thibault, P. and Meloche, S. (2004) N-Terminal ubiquitination of extracellular signal-regulated kinase 3 and p21 directs their degradation by the proteasome. Mol Cell Biol **24**, 6140-6150

161 Scarlato, M., Beesley, J. and Pleasure, D. (2000) Analysis of oligodendroglial differentiation using cDNA arrays. J Neurosci Res **59**, 430-435

162 Krens, S. F., He, S., Spaink, H. P. and Snaar-Jagalska, B. E. (2006) Characterization and expression patterns of the MAPK family in zebrafish. Gene Expr Patterns

163 Kling, D. E., Brandon, K. L., Sollinger, C. A., Cavicchio, A. J., Ge, Q., Kinane, T. B., Donahoe, P. K. and Schnitzer, J. J. (2006) Distribution of ERK1/2 and ERK3 during normal rat fetal lung development. Anat Embryol (Berl) **211**, 139-153

164 Easom, R. A. (1999) CaM kinase II: a protein kinase with extraordinary talents germane to insulin exocytosis. Diabetes **48**, 675-684

INTRODUCTION : SECTION 2

MANUSCRIT EN PRÉPARATION

Revue des phénotypes de mortalité néonatale chez les mutants de souris : guide de survie

MISE EN SITUATION

L'analyse phénotypique de mutants de souris est souvent complexe pour les biologistes moléculaires, pour qui l'aisance expérimentale se situe à un niveau de complexité différent de celui de la physiologie animale. Je décrirai plus loin les effets de l'invalidation du gène *Erk3*, dont la principale conséquence est la mortalité néonatale. L'analyse de ce phénotype a représenté un défi considérable, puisque plusieurs anomalies touchant différents systèmes physiologiques peuvent être impliquées dans un tel phénotype.

Ce chapitre est le manuscrit d'une revue de la littérature sur le sujet non moins complexe des phénotypes de mortalité néonatale chez les mutants de souris. À ma connaissance, il n'existe aucune revue de ce type. De plus, le seul ouvrage traitant de ce sujet est le manuel d'analyse de phénotype intitulé; Mouse Phénotypes, aux éditions Cold Spring Harbor Laboratory Press (publié en 2005), qui ne décrit que très brièvement des avenues expérimentales envisageables suite à l'obtention de phénotypes de mortalité périnatale. Ce manuel est un guide général d'analyse de mutants qu'il est intéressant de posséder dans sa collection, mais qui ne traite que de façon trop superficielle les phénotypes périnataux.

J'ai donc écrit cette revue avec le but de palier à un manque dans le domaine des analyses phénotypiques. Il pourrait être soumis pour publication sous sa forme présente ou être complété de méthodes expérimentales et être publié sous forme de manuel. Je n'ai pas la prétention d'affirmer que cette revue est complète et parfaite. Mais je crois qu'elle est originale et je me console en me disant qu'elle pourra servir à deux choses : un guide pour les non-initiés de l'analyse phénotypique de mutants de souris ainsi que de référence de base pour l'écriture d'un ouvrage plus précis et complet.

24 hours to survive birth for mutant mice: from gene function to human diseases

Benjamin Turgeon and Sylvain Meloche

Institut de Recherche en Immunologie et Cancérologie and Departments of Pharmacology and Molecular Biology, Université de Montréal, Montreal, Quebec H3C 3J7, Canada

Running title: Interpreting neonatal lethal phenotypes in mutant mice

Corresponding author: Dr Sylvain Meloche
Institut de Recherche en Immunologie et Cancérologie
Université de Montréal
P.O. Box 6128, Station Centre-Ville
Montreal (Quebec) H3C 3J7
Canada
Tel.: (514) 343-6966
Fax: (514) 343-5839
E-mail: [redacted]

ABSTRACT

The mouse represents the model of choice to study the biological function of mammalian genes. Survey of mouse mutant databases reveals a surprisingly high number of mutations leading to neonatal death. However, the phenotypic characterization of such mutants remains a complex task. The variability in the time and causes of death as well as the large number of physiological systems involved renders the analysis of these mutants very challenging, even for initiated investigators. In this review, we highlight typical cases of neonatal lethal phenotypes and illustrate how analysis of the developmental timing and cause of death has helped identifying the physiological systems affected by the mutations. We discuss the relevance of these mutants for gene function studies and as models of human diseases. Importantly, we wish to provide a guide for analysis of neonatal phenotypes that will be helpful for dissecting out the function of specific genes during mouse development.

Keywords: mouse mutants; phenotype; neonatal lethality; gene function; human diseases

I. INTRODUCTION

The last 25 years have witnessed the enormous power of gene targeting for dissecting out the physiological functions of mammalian genes. More than 3000 knockout mouse models have been generated to date [1]. New targeting strategies have been developed to inactivate genes that should allow for the mutation of 70% of the mouse genome in the next 5 years, with the possible production of over 20,000 mutant lines of mice [2]. Although gene targeting techniques are straightforward and accessible to most laboratories, the largest investment of time and money in these projects is not in the generation of mutant mice but rather in their analysis. Indeed, unless a mutation causes a morphologically obvious phenotype, the analysis of a mutant phenotype can be very challenging. This is especially true for mutants dying perinatally with no overt phenotype, which represent a substantial proportion of lethal phenotypes in the mouse (Fig. 1). In these cases, death is sometimes seen as THE phenotype.

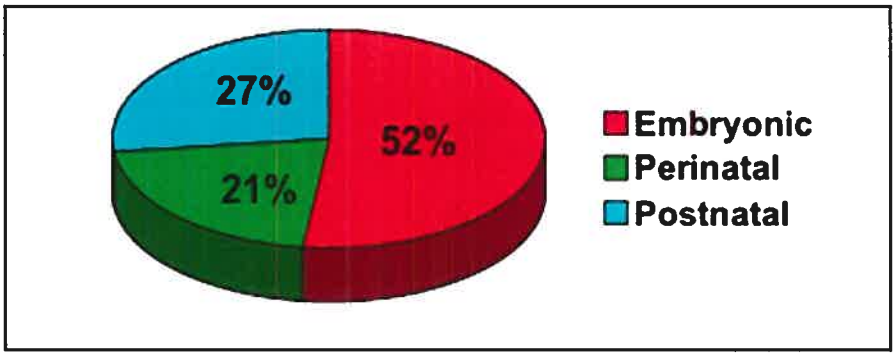

Fig. 1: Developmental timing of death in mice harboring lethal mutations. Calculations were made using the number of genotypes associated with lethality obtained from the Phenotype Ontology Database resource (www.informatics.jax.org).

One of the major problems in characterizing neonatal phenotypes is that death is usually not the consequence of a primary defect but rather the consequence of a physiological problem secondary to the primary defect, which is sometimes subtle (Fig. 2). The developmental timing of the neonatal lethality therefore represents an important clue to identify the underlying defects resulting from the mutation and, consequently, the biological

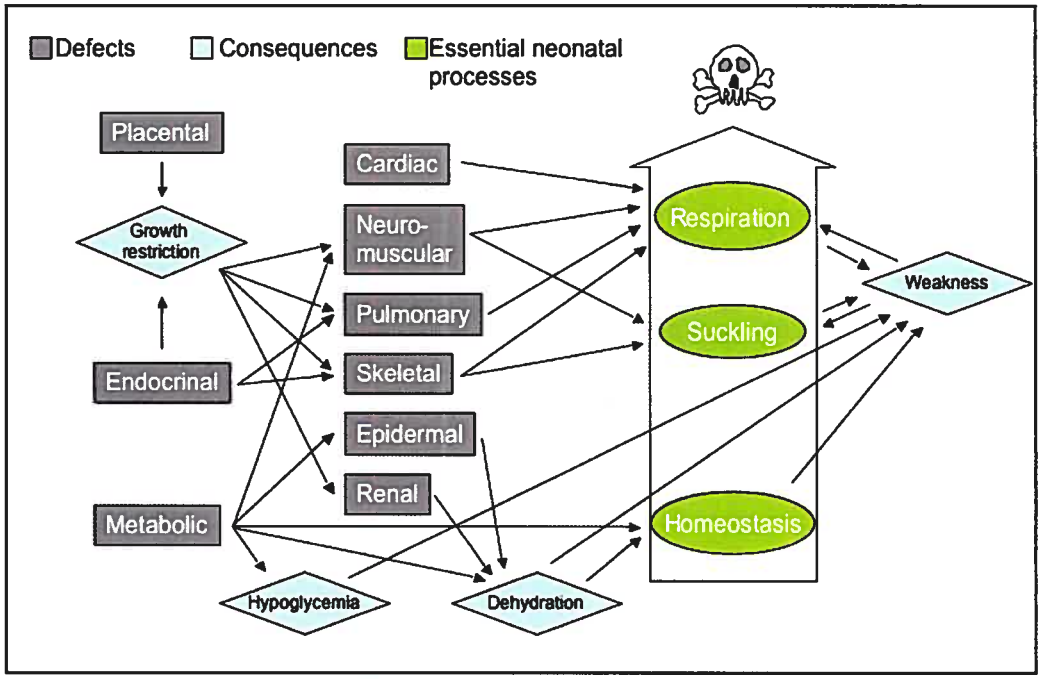

Fig. 2: Neonatal death in mutant mice: a biological complex network. The cause to effect relationship between organ defects and the affected physiological processes which are critical for neonatal survival.

function of the mutated gene. Death can occur at the end of fetal development, prior to birth - *fetal death*; immediately at birth or within one day - *neonatal death*; or after the first day of post-partum life - *postnatal death*. In more complex cases of *perinatal death*, the consequence of the mutation is fetal death as well as neonatal death among the mutant progeny. In addition to this complexity, it is becoming evident that a single gene mutation can produce a wide spectrum of developmental anomalies. Unless a gene is tissue-specific or conditionally inactivated in specific tissues, determining which physiological defect is responsible for death requires considerable efforts.

This review provides a guide for the analysis of neonatal lethal phenotypes in mouse mutants. We discuss studies where the biological functions of genes were revealed through the analysis of neonatal lethal phenotypes. We also highlight the importance of these mouse mutants as models of human neonatal syndromes. For simplicity, we focus on genes whose mutations have been reported to cause neonatal lethality due to specific defects rather than

gene mutants leading to pleiotropic lethal defects. It is virtually impossible to address all the causes of neonatal death in mouse mutants. Here, we describe the events that represent life-threatening challenges to the newborns during the first hours after birth, namely parturition, breathing, suckling and neonatal homeostasis (Fig. 3). Hopefully, the understanding of these simple examples will be useful for the analysis of more complex neonatal lethal phenotypes.

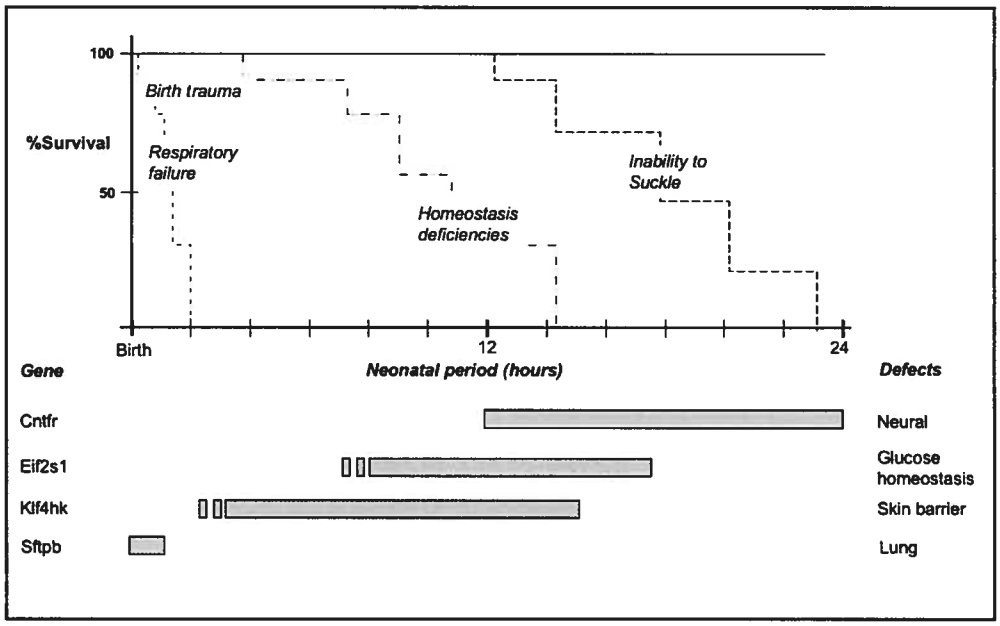

Fig. 3: Major causes of neonatal lethality in mouse mutant. Upper panel: survival curves predicted when essential neonatal physiological processes are impaired in newborn mutant mice (assuming a fully penetrant phenotype). Lower panel: examples of gene deletion models and the physiological defects that compromise neonatal survival. The grey lines represent the window of neonatal lethality.

II. SURVIVING PARTURITION

The first life-threatening event associated with neonatal survival is parturition itself. Although the euteria mammalian fetus is evolutionary adapted to support parturition, the stress encountered by the pups at parturition is high enough to cause lethal damage to abnormal pups. The aim of this section is not to dress the list of all neonatal lethal mutants presenting catastrophic or morphological defects. Instead, we wish to illustrate how analysis of such

mutants has allowed deciphering the function of genes involved in important embryonic processes, whose disruption results in neonatal death.

A. Morphological defects

Morphological defects usually lead to the exposure of internal components, such as neural or intestinal tissues. Such defects are problematic for newborn rodents for two reasons. First, exposed tissues can be lethally damaged during parturition, leading to birth trauma. Second, they can be eaten as the pups are being cleaned by the mother resulting into misinterpretation of the defects associated with the mutation. A good example is provided bythe *Cart1* gene knockout. Newborns were found to lack brain tissues and skull after birth. However, analysis of E18.5 fetuses revealed acrania as expected, but the brain was present, indicating that it had been cannibalized during parturition [3]. Exposure of the neural tissues can be a consequence of abnormal neural tube closure and mouse mutants are useful models of neural tube defects, which are relatively common in human (0.2-3.5 per 2000 pregnancies). More than 80 mutant mouse models present neural tube defects, and their characterization has helped understanding the molecular pathways involved in neural tube closure [4, 5].

Omphaloceles are also hazardous for the newborns and an exposed gut can be easily cannibalized by the mother, as was described for the *Rock1* gene deletion [6]. A number of gene deletions can lead to abnormal resorption of the midgut into the abdominal cavity during development, which usually results from the different developmental timing between genesis of the bowels and the overall growth of the embryo. The etiology of these anomalies is currently not well understood and mouse mutants with omphalocele represent unique models for the study of abdominal wall defects in human [7].

A number of mutations leading to severe morphological (catastrophic) defects have been described in the mouse. Most of these defects do not compromise embryonic survival

and are only revealed when the pups are found dead, or not found (cannibalized), after birth. One of the most dramatic examples is probably the *Shh* knockout. Some *Shh* mutant mice reach birth with a morphology very distinct from that of a normal pup, and they are likely eaten immediately after delivery [8]. Less severe, still impressive mutants include *Wnt5a* mutant mice, which are born with a dwarf appearance because of shortened jaws and limbs [9] and *Ctnnbip1* null mice, which lack the anterior structure of the head [10]. A total absence of limbs was described in *Fgf10* knockout, but death after birth was due to the absence of lungs in these mice [11, 12]. Knowing the precise cause of death associated with such catastrophic mutations has low experimental value, since the phenotype itself is being informative enough to define the biological function of the mutated gene. However, these examples illustrate how neonatal death in mutant mice can sometimes reveal gene functions that are essential for embryonic development such as those involved in embryonic patterning.

B. Hemorrhage

Failure in the establishment and maintenance of vascular circulation is an important cause of embryonic lethality in mouse mutants [13]. However, some mutations affecting vasculogenesis as well as hemostasis can by revealed by neonatal death resulting from birth trauma. The stress encountered at parturition leads to neonatal death of mice with a targeted deletion of *Itgav*, encoding the integrin alpha V isoform, which is essential for vasculogenesis in specific tissues. Death in these mice is due to intracranial and intestinal hemorrhage after birth [14]. The neonatal lethality of mice with a disruption of *Pdgfrb* (or its catalytic activity) is also associated with hemorrhage in multiple tissues after birth [15, 16]. Additional examples include the loss of function of *Cxcr4*, a gene important for gastrointestinal vascularisation. Deletion of this gene leads to intestinal hemorrhage and the mutants that reach term and are born cannot survive more than one hour [17].

Abnormal blood coagulation in mutant mice can also be revealed at birth as shown by inactivation of *Proc*, which encodes a master regulator of anticoagulation. Deletion of this gene leads to occlusion of the vasculature and results in fatal thrombosis and neonatal death. The trauma of birth is responsible for death during parturition and pups are either born dead or severely bruised in the head with subsequent death. However, pups are nursed normally and can survive up to 24 hours when delivered by cesarean section [18]. Inactivating mutations of coagulation factor genes can also result in neonatal death. Mice with a disruption of the *F5* (factor V) gene die within 2 hours of massive intra-abdominal hemorrhage [19],whereas *F7* (factor VII) knockout mice survive up to 24 hours after birth [20]. Mutant mice showing neonatal death due to defects in the procoagulant, anticoagulant, and fibrinolytic pathways represent models of coagulopaties in human. Furthermore, their study has brought the general concept that hemostasis is regulated in a tissue-specific manner [21].

III. THE FIRST BREATH OF AIR

Assuming that a pup is born without lethal morphological or hemostatic defects, its first extra-uterine challenge will be to breath. When the pups are being born, they remain cyanotic for a few minutes. This is a normal phase corresponding to the period of time between the arrest of placental oxygenation and the moment where breathing takes over. After a few breaths of air, the newborns acquire their characteristic pink color. However, the first breaths of air are critical and a large number of life-threatening anomalies that affect different physiological systems, in addition to the lungs, can interfere with normal breathing (Table 1).

A. Neuromuscular defects

Breathing is a physiological process governed by the brain that involves a rhythmic activity produced by a neural circuitry that develops before birth and is responsible for immediate breathing of the newborns. The respiratory center resides in the lower brainstem

and comprises rhythm generator neurons of the parafacial respiratory group (pFRG) and pattern generator neurons of the ventrolateral medulla (VLM). The respiratory rhythm is transmitted through the spinal motoneurons to the respiratory muscles: the diaphragm and intercostal muscles [22]. Defects of any of these structures can lead to respiratory failure.

1. Neural

Specific defects in the respiratory center lead to inadequate respiratory activity and a number of neonatal lethal mutants have been instrumental in the characterization of these structures. Inactivation of *Egr2*, which controls hindbrain segmentation, is associated with breathing instability and death a few hours after birth [23, 24]. In *Atp1a2* knockout mice, persistent depolarization of neurons in the brainstem results in absence of respiratory activity. These mice are akinesic, present gasping-like respiration and do not survive more than 10-15 min after birth [25, 26]. Neonatal death due to apnea can also result from abnormal neuronal oscillation patterns. Mice deficient for the *Mafb* gene suffer from central apnea, show gasping behavior and die within 2 hours after delivery [27]. Abnormal activity of inspiratory neurons in the medulla leads to central respiratory failure and neonatal death in the *Tlx3* [28] and *Pbx3* null mice [29], which represent models for congenital central hypoventilation syndrome. Depression of the respiratory center as a result of excessive glycinergic neurotransmission was described in the *Slc6a9* knockout mouse, a model of human glycine encephalopathy syndrome. These mice die between 6-14 hours after birth due to respiratory distress. In addition, inability to feed in association with bradykinesia was observed in these animals [30, 31]. These mutants, among others, have proven valuable to study developmental disorders of respiratory control in humans [32].

More general neural defects such as altered neurotransmission can also compromise neonatal survival by affecting respiration. For example, deletion of *Stxbp1*, an essential gene for all components of neurotransmitter release in the brain, leads to paralysis and immediate death after birth [33]. Targeted inactivation of *Kif1b*, which encodes a microtubule motor

protein important for axonal transport, is associated with an absence of expansion of the lungs and death within 30 minutes after delivery [34]. These mice display an abnormal curled posture (kyphosis) and dropping forelimbs, which is also a general indication of a neuromotor defect.

2. Neuromuscular junction

Proper muscle contraction to allow breathing is dependent on the development of a functional neuromuscular junction (NMJ). Genetic analysis in mice has provided key insights into the molecular control of neuromuscular synaptogenesis [35]. A defect at the NMJ is sufficient to cause neonatal lethality, as exemplified by the *Musk* and *Agrn* gene mutants. In the absence of any of these genes, the NMJ does not form, leading to akinesia. The lung remains collapsed due to the inability to breathe and mutants die immediately after birth [36, 37]. The phenocopy of these two mouse models has helped understanding the receptor-ligand relationship of the MuSK and Agrin proteins and their role for NMJ formation. Normal synaptic transmission at the NMJ is also important for respiration, as revealed by the inactivation of the *Scl5a7* gene that encodes a choline transporter. Insufficient acetycholine release at the NMJ of these mice results in limited capacity of movement and death within 1 hour of birth [38]. The absence of clustering of acetylcholine receptors at the NMJ resulting from disruption of *Rapsn* leads to a similar phenotype, and these mice die a few hours after birth from weak breathing [39].

3. Respiratory muscles

Inability to support the dramatic increase in muscular activity required for respiration immediately after birth leads to respiratory distress and neonatal death. Therefore mutations affecting muscle development as well as muscle function can challenge neonatal survival. The classical example is the targeted deletion of *Myog*, which encodes the muscle regulatory

factor Myogenin. These mice are unable to generate a force sufficient for respiration due to a severe reduction of respiratory muscles such as the diaphragm. They are immobile and cyanosed after birth, and die immediately [40, 41]. *Atp2a1* encodes a sarcoplasmic Ca^{2+} ATPase essential for the function of fast twitch type II muscular fibers. Mice deficient for this gene die of respiratory distress due to abnormal contraction of the diaphragm. They show gasping respirations, limited chest wall and limb movements, and die within 2 hours after birth [42].

Interestingly, muscle development can be affected by inadequate neuromuscular transmission and such phenotype is likely to be revealed by neonatal death. For example, the absence of the *Chat* gene, which is essential for acetylcholine synthesis, results in absence of synaptic transmission at the NMJ. *Chat*$^{-/-}$ mice lack any spontaneous movement and present kyphosis after birth, which is characteristic of neuromotor defects. In addition, these mutants display abnormal development of the diaphragm and intercostal muscles, defects that are directly responsible for respiratory failure and immediate death after birth [43]. Nerve defects associated with muscular dysfunction were also observed for a specific mutation in the *Nrg1* gene, which encodes a family of ligands important for synaptogenesis induction [44]. These gene targeting experiments emphasize the close relationship between nerve and muscle development, for which disturbance can be revealed by neonatal lethality.

B. Lung defects

Lung development is a complex process that can be divided into 4 specific stages in mice [45]. At the pseudoglandular stage (E9.5-E16.5), branching morphogenesis generates the respiratory tree. The canalicular stage follows (E16.5-E17.5), where the terminal bronchioles expand to form the respiratory ducts and sacs. Lung maturation at the saccular stage (E17.5-P5) is marked by the thinning of the mesenchyme, the differentiation of the specialized type I and II pneumocytes, which are involved in gas exchange and surfactant production

respectively, and the development of juxtaposed capillaries. Septation of the saccules that give rise to alveoli, only starts at postnatal day 5. Although the lungs have no survival value for embryonic development, many genes that are essential for early lung development are also required for embryonic development and deletion of these genes sometimes leads to death *in utero*. However, genes that are essential for morphogenesis, maturation or gas-exchange function of the lungs are usually revealed by respiratory distress at birth.

1. Branching morphogenesis

Elegant examples of abnormal branching morphogenesis are provided by disruption of genes involved in epithelial-mesenchymal interactions that govern lung ontogeny. Inactivation of these genes usually results in hypoplastic lungs, as shown for mouse mutant of *Wnt7b*, *Fgf9*, *Tcf21* or *Hhip* genes. *Wnt7b* mutants die rapidly after birth due to lack of branching, pulmonary hemorrhage and delayed epithelial differentiation [46]. Lack of extensive branching is also responsible for abnormally smaller lungs in *Fgf9* mutants. However, since normal epithelial differentiation occurs in the *Fgf9* mutant lungs, the mice are able to inflate their lungs and to breathe for a short period of time before dying [47]. Deletion of *Tcf21* leads to defective terminal branching, resulting in a lack of distal lung structures that is incompatible with lung inflation after birth [48]. Distal lung development in *Hhip* mutants occurs normally, which explains their ability to survive for a few hours. However, severe lobulation defects are observed in *Hhip*$^{-/-}$ lungs that seriously compromise normal respiration [49].

2. Lung maturation

Mutations affecting lung maturation can also challenge normal breathing, as illustrated in the *Nfib, Pdpn* and *Ndst1* knockout mouse models. Although these mutants make visible efforts to breathe, lung inflation is not sufficient to provide sufficient gas exchange in the lungs

and these mutants die within minutes after birth following a few agonal breaths. Lungs from mice deficient in *Nfib* are stuck at the pseudoglandular stage. They lack saccular structures and both type I and II pneumocytes [50, 51]. *Pdpn* mutants have abnormal saccules due to a blockade in type I pneumocyte differentiation and these mutants die within 10 min of birth [52]. Type II pneumocytes maturation is important for proper surfactant production and is impaired in *Ndst1* mutants. These mice experience severe respiratory difficulties and do not survive more than 10 hours postpartum [53].

Lung maturation is associated with apposition of blood vessels and respiratory epithelium. With the increased in blood flow accompanying birth, the vascular system must be well developed to allow proper gas exchange. Respiratory distress at birth and decreased survival was described in newborn deficient for *Nos3,* which encodes eNOS. Death within an hour of birth in these mutants was associated disrupted pulmonary vascular development. The lung pathology in these mutants resemble that of human infant with alveolar capillary dysplasia (ACD) [54].

Lung maturation can be delayed by factors extrinsic to the lung such as hormonal deficiencies. Glucocorticoid deficiency in the *Crh* mutant or absence of the glucocorticoid receptor (*Nr3c1* gene knockout) result in delayed lung maturation and mutant mice die a few hours after delivery [55, 56]. These examples show how hormonal defects can affect lung development and neonatal survival.

3. Gas exchange

Inadequate gas exchange in a morphologically normal lung can also impair respiratory functions. Indeed, successful adaptation to air breathing requires the appropriate production of surfactant from the mature lung, and clearance of the liquid in the lungs after birth. The prototypical example of surfactant deficiency is the deletion of the *Sftpb* gene,

which encodes surfactant protein B. In these mutants, respiratory failure associated with atelectasis results from the disruption of storage, routing and function of surfactant lipids. In the absence of surfactant, which decreases surface tension of the respiratory saccules, the lung cannot inflate and the animals remain cyanotic and die within minutes [58]. In addition to surfactant deficiency, inadequate lung clearance after birth is also associated with low survival of newborn mutant mice. This process is dependant of Na^+ absorption [59]. Mice with a deletion of *Scnn1a*, encoding the alpha subunit of an epithelial sodium transporter, are able to breathe and inflate their lungs after birth but die during the following 40 hours. Defective lung clearance in *Scnn1a*$^{-/-}$ mice results in liquid reaccumulation in the lungs few hours after birth, which interferes with adequate lung inflation [60].

4. Other respiratory defects

In addition to lung specific defects, obstruction of the upper airways is an unusual cause of respiratory distress. Nasal obstruction is incompatible with normal breathing since during attempted respiration, the tongue is pulled to the palate, resulting in obstruction of the oral airway. This leads to respiratory distress and death from asphyxia. A mouse mutant presenting this defect (choanal atresia) was described for a gene involved in retinoic acid biology. *Aldh1a3* null mutants show respiratory distress, are cyanosed and die within 10 hours after birth [61].

Mouse mutants presenting neonatal lethal phenotypes have therefore been of great value to reveal the function of genes essential for lung development and maturation. In addition, these mutants represent valuable models of congenital lung abnormalities and respiratory distress syndrome in human [62, 63].

C. Cardiovascular defects

The heart is the first organ to form in the embryo and the establishment of a normal circulatory function is a prerequisite for embryo survival. Heart development requires the coordinated differentiation of cells derived from different embryonic lineages: myocytes of the myocardium, endothelial cells of the endocardium, and cells of the neural crest that form the outflow tract [64]. A number of mutations have been engineered in mice that produce cardiovascular defects, which are often responsible for preterm lethality [65]. Histologically, there is no difference between the fetal and the postnatal heart. However, with the initiation of breathing at birth, dramatic changes occur in the circulatory system. The heart must also be strong enough to support the increased charge associated with newborn activity. Therefore, mutations leading to heart defects that are incompatible with the establishment of the respiratory circulation are responsible for congenital cyanosis, respiratory distress and, inevitably, neonatal death.

1. Outflow tract

Studies of neonatal lethal mutants have been particularly useful for the understanding of congenital heart disease in human, especially in the identification of genes involved in outflow tract formation [66]. Defects in outflow tract have been mainly attributed to abnormalities of cardiac neural crest cells, but also to cell autonomous endothelial defects. Ablation of the *Sema3c* gene results in outflow tract defects, such as persistent truncus arteriosus or interruption of the aortic arch. These mutants are cyanotic and die shortly after birth [67]. Aortic arch malformations were also observed in *Foxc2* mutant mice, which show gasping motion, cyanosis and collapsed lungs, resulting in death within 10 minutes after birth [68]. Endothelial defects leading to outflow tract abnormalities were described for a mutant of the *Plxnd1* gene. Interestingly, the related phenotypes of *Sema3c* and *Plxnd1* null mutants have helped integrating their gene products into a common signaling pathway important

for cardiovascular development [69]. Although most outflow tract defects are compatible with embryonic survival, failure of ductus arteriosus closure, that normally accompanies the initiation of breathing, disrupts pulmonary circulation and is incompatible with survival after birth (see below).

2. Ductus arteriosus

A frequent type of cardiovascular defects challenging neonatal survival involves the failure of cardiovascular remodeling after birth. With the initiation of respiration in the newborn, the transition from fetal (placental) circulation to respiratory circulation (increased blood flow in the lung) is dependant on the closure of a specialized vessel called the ductus arteriosus. The ductus arteriosus connects the pulmonary artery to the aorta and shunts pulmonary circulation to the systemic circulation in the fetus. Failure of the ductus arteriosus to close after birth threatens neonatal health as shown by respiratory complications in human newborns presenting a patent ductus arteriosus [70]. Initial closure of the ductus arteriosus is mediated by contraction of its thick muscular wall within 30 min after delivery with functional closure by 3 hours [71]. Genetic studies in the mouse have confirmed the importance of prostaglandins in the biology of ductus arteriosus closure. Deletion of *Ptger4*, which encodes a receptor for prostaglandin E_2 (PGE_2), leads to a defect of ductus arteriosus closure. Although initial ductal closure occurs in these mutants, they die between 24 and 48 hours after birth from lung oedema and congestive heart failure due to a reopening of the ductus arteriosus [72, 73]. Deficiencies in the synthesis of PGE_2 also lead to a patent ductus arteriosus in mice deficient in prostaglandin dehydrogenase (*Hpgd* gene), which die in a window of 12-24 hours [74]. Other deletion studies of the cyclooxygenase genes *Ptgs1* and *Ptgs2* indicate that patent ductus arteriosus leads to labored breathing, cyanosis, and death as soon as 30 minutes after birth, with no animal surviving for more than 12 hours [75].

D. Skeletal defects

The skeleton is made of two distinct tissues: cartilage and bone. Unlike other organs, it spreads throughout the entire body and is composed of more than 200 elements of various shapes [76]. It is not surprising that abnormal skeletal development in mutant mice can result in a wide spectrum of phenotypic outcomes ranging from slight anomalies to catastrophic damage in the fetus. Since a large number of these mutations are associated with death at birth, neonatal lethal phenotypes have therefore been useful to identify genes important in the various aspects of skeleton biology such as patterning and chondrogenesis [77, 78]. Mice deficient for *Runx2*, a candidate gene for cleidocranial dysplasia syndrome in human, illustrate well the importance of the skeletal system for neonatal survival. The skeleton of these mutants lacks ossification (bones), with the consequence that newborns show gasping respiration and die within 20 minutes after birth [79, 80]. Skeletal defects can threaten neonatal survival in various ways such as by failing to protect the newborn during parturition (leading to lethal damages) or by interfering with normal breathing.

1. Rib cage

The rib cage participates in respiration, principally by providing structural support to respiratory muscles. One would predict that defects in the rib cage would lead to respiratory distress and neonatal death. Indeed, targeted deletion of numerous genes involved in the induction of skeletal structures, morphogenesis and chondrogenesis, as well as production and remodeling of extracellular matrix components is associated with neonatal death. *Uncx4.1* is a homeobox gene that was found to be important for specification of skeletal elements derived from the lateral sclerotome, such as the proximal ribs. Knockout mutants have a distorted and smaller thoracic cavity that is associated with poor inflation of the lungs after birth. These mice present kyphosis (severe lordosis) and die shortly after birth [81, 82]. This phenotype is reminiscent of mutants with a *Tbx18* deletion that present an abnormally small rib cage

and die rapidly after a few irregular breaths [83]. A dismorphic rib cage is associated with respiratory failure in mice deficient for *Ctgf*, a gene essential for matrix remodeling during chondrogenesis [84]. Similar to lung development, hormonal deficiency can affect skeletal development, as shown by inactivation of the *Pthlh* gene, which encodes the parathyroid hormone-related peptide. *Pthlh*$^{-/-}$ mice die immediately after birth from respiratory distress due to abnormal ribs and sternum [85].

2. Vertebrae

Although a damaged rib cage can lead to respiratory distress at birth, a number of mutants present vertebral defects rather than rib malformations. Typical examples are the *Bapx1* and *Col2a1* gene mutations that result in lethal skeletal dysplasia. These mutants have abnormal vertebrae, lack intervertebral discs and die immediately after birth from respiratory failure, even though they have normal ribs [86-88]. It cannot be excluded that such skeletal defects can interfere with spine, nerves or even normal brain functions associated with breathing. However, unless neural defects are obvious, such as dorsal root ganglion fusion in the *Uncx4.1* mutant [82], the integrity of the spine and nerves is usually not addressed in skeletal mutants. As a consequence, neuronal malfunction could account for neonatal lethality in some cases of skeletal phenotypes. Nevertheless, neonatal lethal phenotypes have been useful to reveal genes essential for skeletal development that likely represent potential candidates for human skeletal genetic disorders [89].

IV. ABNORMAL FEEDING

Little or no milk in the stomach a few hours after birth is indicative of abnormal feeding. Complete inability to feed will obviously result in neonatal death due to absence of nourishment, but also because the liquid derived from the milk is essential for homeostastic processes in newborns [90]. Its absence leads to dehydration and intraperitoneal injection of saline usually rescues survival for many hours. Analysis of a number of neonatal lethal

mutants has revealed that normal fasting newborns die in a time window of 12-24 hours after birth [91-93]. Therefore, if death occurs before this period, it is unlikely that problems related to abnormal feeding are the primary cause of death. Abnormal feeding in neonatal mice can be the result of abnormal nursing or rejection by the mother. However, the major causes of inability to feed in mutant mice are associated with neuromuscular as well as craniofacial skeletal defects (Table 2).

A. Neuromuscular defects

Suckling is a complex process that involves many structures of the brain, nerves, as well as the muscles required to extract the milk [94]. Olfactants on the nipple are the primary sensory cue used in orientation and tactile sensation is required to initiate the suckling reflex. The suckling response includes nipple attachment, suckling with rhythmic movement of the jaw and tongue, and the stretch response [95]. These processes are regulated by complex interactions between sensory and motor neuronal pathways, which are linked to the central nervous system through the brainstem trigeminal complex. Motor neurons involved in feeding are located in the facial motor nucleus (face), trigeminal motor nucleus (jaws) and hypoglossal motor nucleus (tongue) [96]. Therefore, defect in any of these structures is likely to impair suckling and neonatal survival.

1. Olfaction

In newborn rodents, olfactory integrity is essential for the normal suckling behavior [97]. The importance of olfactory integrity for suckling is well illustrated by the knockout of *Edg2*, which encodes the lysophosphatidic acid receptor. These mutants present developmental abnormalities in the olfactory bulb and cerebral cortex, resulting in 50% neonatal lethality. Some of the mutant pups survive for a few days after birth depending on the milk content in the stomach, thereby establishing a good correlation between olfaction, milk content and survival

[98]. A similar example is provided by the targeted inactivation of *Ebf2*. These mutants show defects in the projection of olfactory neurons to the dorsal olfactory bulb resulting in lethality within one day, although some animals can survive for two days [99]. Severe loss of olfactory and autonomic neurons was described in mice deficient for the *Ascl1* gene, which do not survive more than 24 hours after birth [100]. This survival time is shorter than that of mouse models of anosmia, such as the *Cnga2* and *Gnal* knockouts. These two genes are involved in olfactant signal transduction. In their absence, the mice do not exhibit any odorant-evoked excitatory response and die within 2 days from a lack of feeding [101, 102]. It is interesting to note that is some cases of *Gnal* mutants, litter depletion increases survival of the mutant pups, by opposition to *Fyn* knockout pups, which require suckling littermates to stimulate the mother nipples in order to be able to suckle [103]. Although suckling is an olfactory-driven behavior, the timing of death as well as the partial survival of anosmic mice suggests that olfaction is more important in suckling maintenance than in the initial suckling reflex.

2. Sensory motor

Suckling, such as breathing, is regulated by the brainstem. It is therefore not surprising that defects in hindbrain development that affects respiratory rhythm, such as in the *Egf2* mutant (Table 1), also affect suckling activity. It is likely that such anomalies in the brainstem will result in respiratory failure. However, specific defects within the brainstem that affect suckling can also challenge neonatal survival. An elegant example is provided by the ablation of the *Cntfr* gene that encodes a receptor for ciliary neurotrophic factor. Homozygous mutants die within a window of 12-24 hours and cannot open their jaws, resulting in the inability to suckle. Lethality in these mutants was associated with severe motor neuron deficits in the brainstem nuclei that are associated with suckling [91].

The suckling behavior can be affected by sensory motor deficits revealed by the inability of mutant pups to reach the nipple, to open their jaws to suckle or both. Consequently,

a number of neonatal lethal mutants have helped to identify genes involved in sensory motor neuron development. Mouse mutants with severe sensory defects, such as *Grin2b* knockout mice, die within 24 hours even though they are normally nursed by their mother [104]. The primary sensory neurons do not interact with the brainstem trigeminal complex in these mice, explaining why sensory input does not induce suckling movement in mutant pups. Milder sensory phenotypes were described for *Bdnf* (brain-derived neurotrophic factor) knockout mice, which can survive up to 2 days with sensory neuron dysfunction [105].

The importance of the motor system is illustrated by the knockout of *Pip5k1c*, which encodes a phosphatidylinositol kinase essential for synaptic vesicle trafficking. Inability to feed in these mice is due to hypoactivity and results in death within 24 hours [106]. Defects at the NMJ are also associated with the inability to feed, although the majority of the mutations affecting NMJ functions lead to respiratory failure (see above). For example, inactivation of the *Chrng* gene, which encodes a fetal-type acetylcholine receptor, results in impaired breathing that compromises neonatal survival. However, mutants that can breathe, even irregularly, cannot feed and die within 2 days. These mice cannot move their hindlimbs and present the characteristic lunar shape of mouse mutants with neuromuscular defects [107]. In the *Pou4f1* mutant mice, motor defects are more severe and both the inability to open their jaws as well as characteristic uncoordinated limb and trunk movements are responsible for abnormal feeding [108, 109]. An additional example is provided by mice with a targeted deletion of *Nr2f1*, which display abnormal swallowing reflex and cannot survive more than 36 hours after birth. Inappropriate innervation of the pharynx and root of the tongue in these mutants likely results from death of neuronal precursor cells [110]. These examples illustrate the importance of peripheral sensory and motor neuron integrity for suckling and neonatal survival.

3. Hypothalamus

Lower milk intake can be influenced by the appetite of newborn pups as exemplified by deletion of *Hap1* gene. Ablation of this gene leads to early postnatal death and a correlation was made between milk intake and survival. However, the tactile sensation and motor control are normal in these mice [111, 112]. More recent work has revealed that reduced expression of Huntingtin-associated protein 1 decreases the levels of $GABA_A$ receptors in hypothalamic neurons [113], explaining the abnormal feeding behavior in *Hap1* mutant mice.

4. Muscles

Neuronal defects are the prevailing cause of abnormal feeding behavior in mutant mice. Although muscular deficiencies can be the associated with defective innervation, suckling impairment can also result from anomalies intrinsic to the muscles. For example, mouse mutants for *Jph1*, which encodes junctophilin, present an abnormal triad junction formation in the skeletal muscles of the face. This results in an inability to suckle due to impaired contractile activity of the jaws [114]. However, such examples are rare since most mutant mice presenting muscle phenotypes die of respiratory failure as described above.

B. Craniofacial defects

Abnormal suckling can be associated with skeletal defects resulting in facial malformations, the most common being a cleft of the secondary palate. Absence of the secondary palate in the mouth leads to a failure to suckle because of the absence of negative pressure in the oral cavity during the suckling process. Analysis of mutant mice has demonstrated that a cleft palate can result from intrinsic palatal shelves defective fusion or as a consequence of the abnormal development of craniofacial structures [115, 116].

The *Lhx8* knockout mouse is a good example of the importance of normal palatogenesis for neonatal survival. Disruption of *Lhx8*, which encodes a homeobox transcription factor expressed in palatal mesenchyme structures, results in a phenotype of cleft palate and the penetrance of the defect correlates well with neonatal death [117]. Other examples of intrinsic palatal defects thatlead to abnormal palate development include the disruption of the *Osr2* and *Tgfb3* genes. Failure of the palatal shelves to fuse in the *Tgfb3* mutant results in a cleft palate and death occurs within the normal window of non-feeding mice [118]. *Osr2* deficient mice also die within 24 hours, although in this case reduction of palatal mesenchymal proliferation is responsible for the cleft palate [119]. Isolated cleft palate is rare in mouse mutants and a large number of cleft palate phenotypes either result from abnormal tongue development, such as in *Foxf2* mutants [120], or develop secondary to craniofacial defects. Among the latter group are mutations in the Maguk family genes *Dlgh1*, *Cask* [121, 122] and homeobox genes *Hoxa2*, *Msx1* and *Dlx2* [123]. These mutants show inadequate development of neural crest derivatives.

It should be noted that neonatal death of certain mutants that present a cleft palate is not exclusively due to abnormal feeding but may be secondary to respiratory distress. For example, *Foxf2* null mutants die within 18 hours after birth because of abnormally air-distended gastrointestinal tract [120], which is also observed in the case of *Pax9* mutant mice [124]. Air distention of the belly likely leads to interference with normal breathing or with blood supply to the visceral organs. Fusion of the tongue with the palatal shelves in *Jag2* mutants is also associated with respiratory distress and early death of the newborns [125]. Therefore, the inability to suckle due to a cleft palate is not always the principal cause of death. Nevertheless, neonatal lethal mouse mutants presenting palatal defects represent useful models of cleft palate, a frequent malformation in human newborns [126].

C. Parental behavior

The newborns are totally dependant on their mother and abnormal nursing behavior obviously leads to neonatal death. Although rodent pups have some form of resistance to hypothermia, their survival outside a warm nest is greatly compromised. Analysis of a number of mutant mice suggests that the death time window of pups that are kicked-out of the nest by their mother is probably shorter than that of nested non-suckling newborns, although determining the precise window of death of fasting newborns outside a controlled environment is difficult because of ethical issues. As in many mammals, normal nursing by the mother is dependant of recognition of babies through vocalization. Absence or diminished vocalization due to inability to open their jaws could result in rejection by the mother.

V. HOMEOSTASIS DEFAULTS

During pregnancy, homeostasis of the fetus is critically dependent on the placenta, which is responsible for nutrient supply, metabolic exchange and waste disposal. After birth, the newborn must adapt quickly to metabolic needs and regulate its own homeostasis. Many mutations in mice that interfere with the state of equilibrium of various cellular functions and the chemical composition of fluids and tissues are therefore likely to remain silent during embryonic growth but can seriously challenge neonatal survival. Neonatal lethal phenotypes in mice have helped reveal the function of genes involved in energy homeostasis, fluid-electrolyte balance and metabolism, principally through symptoms such as hypoglycemia, dehydration (transepidermal water loss) and renal failure (Table 3).

A. Hypoglycemia

Glucose is an important energy source for neonates, which are in sudden demand of energy for their metabolic requirements. Soon after delivery, there is a period of starvation that follows the cessation of nutrient supply provided by maternal circulation. Gluconeogenesis

is not fully active in the immediate postnatal period [127]. During the period that precedes suckling, glucose must be produced to combat hypoglycemia mainly by glycogenolysis and mobilization of glycogen stores from the liver. Indeed, late in gestation, glycogen synthase expression is induced in the liver to promote the storage of glycogen that will allow survival of the newborn during post-natal starvation [128]. Hormonal control of this adaptation involves increased production of glucocorticoids, decreased insulin levels, and secretion of glucagons [129]. Furthermore, the newborns must adapt to self-nourishing and regulate energy utilization between feeding. Therefore, mutations that disrupt glucose homeostasis as well as normal development of the liver or pancreas are life threatening for the newborn because they challenge energy balance.

Following birth, transient hypoglycemia occurs until glycogenolysis and gluconeogenesis are activated in the liver [128]. An important source of glucose immediately after birth is therefore glycogen autophagy [130]. The study of a neonatal lethal mutant, the *Atg5* knockout mice, was instrumental to understand the importance of autophagy for neonatal energy needs. With the fall of glucose levels after birth, autophagy is induced in response to starvation and reaches a maximum at 3-6 hours post-partum. Autophagosome fusion is blocked in *Atg5* null mice that die within 12 hours of birth, with their energy status severely depressed [131]. A similar phenotype was observed in mice mutant for *Atg7*, confirming its role in early autophagy [132]. Analysis of these mutants has highlighted the essential role of autophagy to sustain life during the critical period of hypoglycemia that follows termination of placental nutrient supply.

The vulnerability of newborns to hypoglycemia is further demonstrated by the phenotype of mice mutant for genes involved in energy related functions of the liver, such as *Cebpa*, which encodes the transcriptional regulator CEBPα. *Cebpa*$^{-/-}$ neonates have reduced glucose levels and die within 8 hours of birth. The severe hypoglycemia observed in mutant mice results from the impairment of the liver to accumulate glycogen prior to birth

[133]. Similarly, mice expressing a non-phosphorylatable (S51A) mutant of eIF2α die from hypoglycemia associated with defective induction of gluconeogenesis.. These mice develop severe hypoglycemia within 6-8 hours, which is independent of suckling, and die within 18 hours of birth [134]. Although hypoglycemia can be life threatening during the first hours after birth, it is also hazardous later on, even after initiation of suckling. Inactivation of the *Arx* gene, which encodes a homeobox transcription factor leads to early-onset loss of pancreatic α-cells that produce glucagon [135]. These mice show a normal glycemia for 24 hours but then rapidly develop severe hypoglycemia and do not survive more than 2 days after birth, further illustrating the importance of glucose homeostasis for neonatal survival.

As a consequence, hypoglycemia in the newborn is a sometimes associated with cyanotic episodes, respiratory distress and abnormal feeding. Mice with a targeted deletion of the *Hmg1* gene show a moderate glucose homeostasis defect leading to early hypoglycemia. Soon after birth, these mice become lethargic and suckle very little, resulting in death within 24 hours despite normal nursing by the mother [136]. A similar behavior was observed in *Cebpa* mutant mice [133]. Cyanosis and lethargy was also associated with hypoglycemia with alteration at the *Ship2/Phox2a* loci [137]. Feeding was progressively less efficient in these mutants that were described as more insulin sensitive than controls.

B. Transepidermal water loss

The epidermis provides a water-impermeable barrier that prevents excessive loss of body fluids, a function that is critical for survival after birth. Impermeability is normally fully developed by E17 in the mouse [138]. The barrier function of the skin is conferred by a combination of the cornified envelope (CE) and intercorneocyte lipids within the outermost layer of the epidermis that work as bricks and mortar. Development of this specialized structure, called the stratum corneum, involves the formation of junctions between keratinocytes, accumulation of specialized keratin, formation of the cornified envelope, and extrusion of

specialized intercorneocyte lipids [139]. Gene mutations affecting skin development at any of these steps can result in transepidermal water loss and seriously affect neonatal survival.

The importance of skin barrier function for neonatal survival is well illustrated by the *Tgm1* gene knockout, which represents a model for human lamellar ichthyosis [140]. Deletion of this gene, which encodes transglutaminase 1, an enzyme that cross-link the cornified envelope, results in severe skin defects associated with an abnormal shiny skin and dehydration of the body extremities. *Tgm1* null mutants are less active than control littermates and die within 5 hours post-partum. A severe skin phenotype is also observed upon inactivation of the *Spink5* gene, which is associated with Netherton syndrome in humans [141, 142]. Deficiency of this gene, which encodes the serine protease inhibitor Lekt1, leads to degradation of desmoglein 1 as a result of epidermal protease hyperactivity. While the skin appears normal at birth in *Spink5* mutant mice, spontaneous detachment of the stratum corneum is observed within 30-60 minutes, which is responsible for the dry and wrinkled appearance of the skin. The important loss of water explains the short survival time, only 2 hours, of these mutants.

There is a growing list of mutant mouse strains with unsuspected defects in epidermal barrier function that die neonatally. For example, ablation of *Cldn1* leads to a 15% loss of weight in the first 15 hours after delivery due to loss of water through the skin. These mutants are weak and unable to feed and die within 24 hours [143]. The skin specific deletion of the *Scd2* gene encoding stearoyl-CoA desaturase 2 results in a similar phenotype of transepidermal water loss [144]. Whereas *Cldn1* deletion has revealed the importance of tight junctions in the epidermal barrier function, inactivation of *Scd2* results in defective lipid biosynthesis in the skin. Analysis of the neonatal lethal phenotype of *Klf4* mutants has revealed a novel function for this transcription factor in the acquisition of barrier function. These mice die within 15 hours of birth from a hypovolemic shock due to transepidermal water loss. It is unclear if the associated inability to feed in these mice is due to tongue defects or weakness [93]. This

array of mutant mouse models illustrates how neonatal phenotypes have contributed to the identification of new pathways involved in skin barrier acquisition and why they represent models of human skin disorders [145].

C. Renal failure

Neonatal lethality in mouse mutants has also allowed the identification of several genes important for development and function of the kidney, an organ that plays a crucial role in the regulation of fluid homeostasis. In fact, a large number of genes involved in genitourinary development were revealed by molecular genetic analysis of mutant mice with neonatal lethal phenotypes. Kidney development involves reciprocal interactions between the nephric duct epithelium and the metanephric mesenchyme. Signals from the mesenteric mesenchyme induce ureteric bud evagination from the nephric duct and its subsequent branching. In turn, newly formed ureter tips induce epithelial transition of the mesenchyme and differentiation into nephrons. The branches of the ureter give rise to the collecting ducts [146]. The importance of the genitourinary system for neonatal survival is revealed by the analysis of mice deficient for the homeobox gene *Emx2*, which lack all genitourinary structures and die soon after birth [147, 148].

Defects in development of the kidney proper, which range from kidney agenesis to kidney failure, can seriously compromise neonatal survival. Newborn mice with kidney anomalies have been shown to die during the first 2 days of life, with the timing of death that seems to be dependent on the severity of the defect. Inactivation of *Hs2st1*, *Wnt4* or *Ret* genes, which are essential for early development of the kidney, leads to kidney agenesis. Mice bearing these mutations do not survive for more than 24 hours after birth [149-151]. In mice deficient for *Itga8*, an integrin family member, absence of only one kidney in some mutants is associated with an additional day of survival [152]. Severe kidney defects were also described in a number of mutant mouse models. *Itga3* mutants feed normally but progressively become

weaker and dehydrated due to severe glomeruli defects, resulting in death within 24 hours of birth [153]. Deletion of *Pou3f3* results in small kidneys and death within 36 hours. These mice show a severe defect in the development and function of the nephron, which explains the decreased volume of urine observed as soon as 2 hours after birth [154]. Defects in the development of both the nephron and collecting ducts were described in mice deficient for *Foxd1*, which also die within 24 hours [155]. These examples illustrate how neonatal lethal phenotypes can reveal genitourinary tract defects, especially those affecting kidney ontology.

In addition to defects in kidney morphogenesis, deficiencies in kidney function such as impaired filtration barrier or electrolyte transport can also lead to neonatal death. For example, mice with a disruption of the *Nephs1* gene, which encodes Nephrin, present no gross morphological defects of the kidney and can feed normally. However, these mice develop massive proteinuria and edema and die within 24 hours after birth. Ultrastructure analysis revealed the absence of podocyte slit diaphragm in *Nephs1* mutant mice. These mice provide a model of congenital nephrotic syndrome in human [156, 157]. Mice deficient in the *Podxl* gene are anuric and die of acute renal failure within 24 hours. Podocytes of these mutant mice fail to form foot processes and slit diaphragms but instead form impermeable junctional complexes [158]. Altered electrolyte homeostasis was described for mice deficient for *Scnn1b*, which encodes a subunit of the epithelial sodium channel. Mutant mice consistently die between 10 to 48 hours after birth [159].

The kidney is the master regulator of normal fluid-electrolyte homeostasis in the body and these few examples emphasize the idea that even subtle kidney anomalies can affect neonatal survival. Neonatal lethal phenotypes in mutant mice have provided powerful models to get insight into normal nephrogenesis as well as into the pathogenesis of human renal diseases such as kidney agenesis, nephrotic syndromes and polycystic kidney disease [146, 160].

VI. CONCLUSIONS

Only a few organs have a high survival value *in utero*. However, defects in almost every physiological system appear to seriously challenge survival during the first 24 hours of post-partum life in mice. Indeed, the liver, the musculoskeletal system, the lungs, the urogenital system, the skin, and principally the nervous system, are highly sensitive to developmental perturbations that can affect neonatal survival. In addition, even minor defects in organs or processes that are essential for embryonic survival such as heart formation, erythropoiesis, vascular and placental development [13], can also impact on neonatal survival. Therefore, a large array of developmental defaults in a number of physiological systems must be considered in the analysis of mouse mutants with no overt phenotypes that die neonatally.

The complexity in the analysis of mouse mutants with neonatal lethal phenotypes can be explained by two reasons: 1) a single gene mutation can affect more than one physiological system that are essential for surviving birth; 2) abnormalities within a single physiological system can affect more than one physiological process in newborns, including respiration, suckling or homeostasis, which can be responsible for the lethality observed during the first 24 hours. Nevertheless, with a precise determination of the time of neonatal death and an understanding of the various systems important for survival of the newborn, it should become easier to study neonatal lethal mouse mutants. In addition to these physiological considerations, special experimental concerns related to this age group must be considered. Fortunately, the repertoire of techniques available for phenotyping mouse neonates is growing and includes sophisticated imaging methods [161].

Analysis of neonatal lethal phenotypes has proven highly informative in dissecting and analyzing gene functions. First, it allows the identification of genes that are essential for embryonic processes for which loss of function is only revealed at birth. Second, it obviously identifies genes involved in the development and function of organs or physiological processes

that are essential for extra-uterine life. Third, it contributes to the elaboration of signaling pathways through the establishment of phenocopies between mutants. In addition to their contribution to understanding gene function in development, mutants presenting neonatal lethal phenotypes provide extremely valuable models of neonatal syndromes in human. They are the models of choice for the study of human diseases that are the first to occur during extra-uterine life.

ACKNOWLEDGMENTS

We apologize to authors whose interesting work we could not be cited owing to space limitations. All the references for a given gene mutation are easily accessible at the MGI database (www.informatics.jax.org) through the use of the official gene symbols presented here.

B. Turgeon is recipient of a studentship from the Fonds de la recherche en santé du Québec. S. Meloche holds a Canada Research Chair in Cellular Signaling. The work performed in the author's laboratory is supported by grants from the Canadian Institutes for Health Research and the National Cancer Institute of Canada.

Table 1. Typical neonatal lethal mutations in mice associated with respiratory failure

Gene	Gene Product	Mutation	Time of death	Comments	References
Neuromuscular					
Neural					
Atp1a2	Na+/K+ transporter subunit	Null	10-15min	Phenocopy Scl12a5	[25][26]
Egr2	Zinc finger transcription factor	Null-LacZ	18hrs	30% survival	[23][24]
Kif1b	Kinesin motor protein	Null	30 min	Kyphosis/Human model syndrome	[34]
Mafb	bZip transcription factor	Null-GFP	2 hours	Apnea	[27]
Pbx3	Homeodomain transcription factor	Null	Few hours	Phenocopy Tlx3 KO	[29]
Slc6a9	Solute carrier	Null	6-14 hours	Human syndrome model	[30][31]
Stbxbp1	Syntaxin binding protein	Null	Immediate	Paralysis	[33]
Tlx3	Homeobox protein	Null	24 hours	human syndrome model	[28]
Neuromuscular junction					
Agrn	Agrin	Null	Immediate	Akinesia	[37]
Chat	Choline acetyltransferase	Null	Immediate	Kyphosis	[43]
Musk	Receptor tyrosine kinase	Null	Immediate	Phenocopy Agrin KO	[36]
Nrg1	Neuregulin 1	Knockin	Few Minutes	Akinesia	[44]
Rapsn	Synapse receptor	Null	Few hours	Weak breathing	[39]
Slc5a7	Choline transporter	Null-R	Immediate	Limited movement	[38]
Respiratory muscles					
Atp2a1	Sarcoplasmic ATPase	Null	30 min-2 hours	Abnormal contraction	[42]
Myog	Myogenin	Null	Neonatal, birth	Kyphosis	[40][41]
Lungs					
Branching morphogenesis					
Hhip	Hedgehog-interacting protein	Null-R	Few hours	Only 2 lobes	[49]
Fgf9	Fibroblast growth factor 9	Null-R	30 min	Hypoplastic lung	[47]
Wnt7b	Secreted Wnt factor	Null-R	10 min	Hypoplastic lung	[46]
Tcf21	Transcription factor	Null-R	5-15 min	hypoplastic lung	[48]
Maturation				Models of human RDS	
Crh	Corticotropin releasing hormone	Null	12 hours	Homozygous parents	[56]
Nfib	Transcription factor	Null-R	15 min	Hypoplastic lung	[50][51]
Nr3c1	Nuclear receptor	Null	1-2 hours	Delayed sacculation	[55]
Ndst1	N-deacetylase/N-sulfotransferase	Null	Less 10 hours	Immature type II cells	[53]
Pdpn	Podoplanin	Null	3-10 min	Type I cells defects	[52]

Table 1 (continued)

Gene	Gene Product	Mutation	Time of death	Comments	References
Gaz exchange				Models of human RDS	
Sftpb	Surfactant associated protein	Null	20 min	Surfactant deficiency	[58]
Scnn1a	Nonvoltage-gated Na+ channel	Null	5-40 hours	Lung clearance	[60]
Other					
Aldh1a3	Aldehyde dehydrogenase	Null-C	10 hours	Upper airways	[61]
Cardiovascular				Models of human CHD	
Outflow tract					
Sema3c	Semaphorin	Null-R	Soon after birth	Various penetrance	[67]
Foxc2	Forkhead transcription factor	Null	10 min of birth	Aortic arch anomalies	[68]
Plxnd1	Plexin	Null	24 hours	Truncus arteriosus	[69]
Ductus arteriosus					
Hpgd	Prostaglandine dehydrogenase	Null	12-24 hours	Model of human disease	[74]
Ptger4	Prostaglandin receptor	Null	12-48 hours		[72][73]
Ptgs1/2	Prostaglandin synthase	2ble null	30min-12hours	Secondary lung anomalies	[75]
Skeletal					
Rib cage				Models of chondrodysplasia	
Ctgf	Secreted factor	Null	Few minutes		[84]
Pthlh	Hormonal peptide	Null	Few minutes	Secondary to hormonal defec	[85]
Runx2	Runt domain transcription factor	Null-R	20 min	Model of human syndrome	[79][80]
Tbx18	T-box transcription factor	Null-R	Few minutes		[83]
Uncx4.1	Homeodomain transcription factor	Null-C	Few minutes	Similar to Tbx18 KO	[81][82]
Vertebraes					
Bapx1	Homeodomain trascription factor	Null-R	Few hours	yes	[86][87]
Col2a1	Collagen component	Null	Immediate	Model of human disease	[88]

C: conditional allele; R:reporter knockin (GFP or LacZ)

Table 2. Neonatal lethal mutations in mice associated with the inability to suckle and underlying defects

Gene	Gene product	Mutation	Time of Death	Comments	References
Neuromuscular					
Olfactory					
Ascl1	bHLH transcription factor	Null	24 hours	Possible breathing defect	[100]
Cnga2	Cyclin nucleotie-gated NG channel	Null	24 or 48 hours	Model of anosmia	[102]
Ebf2	rHlH transcription factor	Null-R	24 or 48 hours		[99]
Edg2	G-protein-coupled receptor	Null-C	Imm or Few days	Partial survival	[98]
Fyn	Src family tyrosine kinase	Null-R	Few days	Homozygous crosses	[103]
Gnal	Guanine nucleotide binding protein	Null	48 hours	Downstream of Cnga2	[101]
SensoryMotor					
Bdnf	Neurotrophic factor	Null	2 days	Partial survival	[105]
Chrng	Achetycholine receptor	Null	Imm or 2 days	Kiphosis	[107]
Cntfr	Neurotrophic factor receptor	Null	12-24 hours	Motor defects	[91]
Grin2b	Glutamate receptor	Null	24 hours	Sensory defects / Can be fed	[104]
Pip5k1c	Phosphatidylinositol kinase	Null	24 hours	Impaired mobility	[106]
Pou4f1	POU domain transcription factor	Null	24 hours	Sensory-motor	[108][109]
Nr2f1	Nuclear receptor	Null	max 36 hours	Swallowing defects	[110]
Hypothalamic					
Hap1	Huntingtin-associated protein	Null	Most 48 hours	Post natal apetite	[111][112]
Muscular					
Jph1	Junctophilin	Null	24 hours	Feeding / muscular	[114]
Craniofacial				Models of Cleft palate	
Lhx8	Lim domain Homeobox protein	Null	24 hours	Partial survival	[117]
Osr2	Zinc finger transcription factor	Null-R	24 hours	Palatal shelfs proliferation	[119]
Tgfb3	Transforming growth factor	Null	10-24 hours	Partial shelf fusion	[118]

C: conditional allele; R:reporter knockin (GFP or LacZ)

Table 3. Selected mutations associated with homeostasis deficiencies leading to neonatal death in mice

Symbol	Gene product	Mutation	Time of Death	Comments	References
Hypoglycemia					
Autophagy					
Atg5	autophagy-related 5	Null	10-14 hours	Abnormal feeding	[131]
Atg7	autophagy-related 7	Null-C	10-15 hours		[132]
Glucose homeostasis					
Arx	Homeodomain transcription factor	Null-R	48-72 hours	Pancreas defects	[135]
Cebpa	CCAAT/enhancer binding protein	Null	8 hours	Liver defects	[133]
Eif2s1	Translation initiation factor	Knockin	18 hours	Rescued by glucose injection	[134]
Hmgb1	HMG-box protein	Null	24 hours	Partial survival	[136]
Transepidermal water loss					
Spink5	Serine peptidase inhibitor	null	2 hours	Human syndrome model	[141][142]
Cldn1	Claudin	Null	24 hours	Rapid loss of weight	[143]
Klf4	Kruppel-transcription factor	Null	15 hours	Rapid loss of weight	[93]
Tgm1	Transglutaminase	Null	5 hours	Human syndrome model	[140]
Scd2	Stearoyl-CoA desaturase	null	24 hours	Few survival	[144]
Kydney failure					
Kydney ontogeny					
Itga3	Integrin	Null	24 hours or later	Dehydration	[153]
Pou3f3	POU transcription factor	Null	36 hours	Smaller kineys	[154]
Foxd1	Forkhead transcription factor	Null-R	24 hours		[151]
Itga8	Integrin	Null	1 or 2 days	One or two kydney missing	[152]
Fluid-electrolyte balance				Models of kydney failure	
Nphs1	Nephrin	Null-R	24 hours	Proteinuria, Human model syndrome	[156][157]
Podxl	CD34-related Membranal protein	Null	24 hours	Anuria	[158]
Scnn1b	sodium channel	Null	10-48 hours	Hyperkalemia	[159]

C: conditional allele R:reporter knockin (GFP or LacZ)

REFERENCES

1 Austin, C. P., Battey, J. F., Bradley, A., Bucan, M., Capecchi, M., Collins, F. S., Dove, W. F., Duyk, G., Dymecki, S., Eppig, J. T., Grieder, F. B., Heintz, N., Hicks, G., Insel, T. R., Joyner, A., Koller, B. H., Lloyd, K. C., Magnuson, T., Moore, M. W., Nagy, A., Pollock, J. D., Roses, A. D., Sands, A. T., Seed, B., Skarnes, W. C., Snoddy, J., Soriano, P., Stewart, D. J., Stewart, F., Stillman, B., Varmus, H., Varticovski, L., Verma, I. M., Vogt, T. F., von Melchner, H., Witkowski, J., Woychik, R. P., Wurst, W., Yancopoulos, G. D., Young, S. G. and Zambrowicz, B. (2004) The knockout mouse project. Nat Genet **36**, 921-924

2 Grimm, D. (2006) Mouse genetics. A mouse for every gene. Science **312**, 1862-1866

3 Zhao, Q., Behringer, R. R. and de Crombrugghe, B. (1996) Prenatal folic acid treatment suppresses acrania and meroanencephaly in mice mutant for the Cart1 homeobox gene. Nat Genet **13**, 275-283

4 Wallingford, J. B. (2005) Neural tube closure and neural tube defects: studies in animal models reveal known knowns and known unknowns. Am J Med Genet C Semin Med Genet **135**, 59-68

5 Greene, N. D. and Copp, A. J. (2005) Mouse models of neural tube defects: investigating preventive mechanisms. Am J Med Genet C Semin Med Genet **135**, 31-41

6 Shimizu, Y., Thumkeo, D., Keel, J., Ishizaki, T., Oshima, H., Oshima, M., Noda, Y., Matsumura, F., Taketo, M. M. and Narumiya, S. (2005) ROCK-I regulates closure of the eyelids and ventral body wall by inducing assembly of actomyosin bundles. J Cell Biol **168**, 941-953

7 Weir, E. (2003) Congenital abdominal wall defects. Cmaj **169**, 809-810

8 Chiang, C., Litingtung, Y., Lee, E., Young, K. E., Corden, J. L., Westphal, H. and Beachy, P. A. (1996) Cyclopia and defective axial patterning in mice lacking Sonic hedgehog gene function. Nature **383**, 407-413

9 Yamaguchi, T. P., Bradley, A., McMahon, A. P. and Jones, S. (1999) A Wnt5a pathway underlies outgrowth of multiple structures in the vertebrate embryo. Development **126**, 1211-1223

10 Satoh, K., Kasai, M., Ishidao, T., Tago, K., Ohwada, S., Hasegawa, Y., Senda, T., Takada, S., Nada, S., Nakamura, T. and Akiyama, T. (2004) Anteriorization of neural fate by inhibitor of beta-catenin and T cell factor (ICAT), a negative regulator of Wnt signaling. Proc Natl Acad Sci U S A **101**, 8017-8021

11 Min, H., Danilenko, D. M., Scully, S. A., Bolon, B., Ring, B. D., Tarpley, J. E., DeRose, M. and Simonet, W. S. (1998) Fgf-10 is required for both limb and lung development and exhibits striking functional similarity to Drosophila branchless. Genes Dev **12**, 3156-3161

12 Sekine, K., Ohuchi, H., Fujiwara, M., Yamasaki, M., Yoshizawa, T., Sato, T., Yagishita, N., Matsui, D., Koga, Y., Itoh, N. and Kato, S. (1999) Fgf10 is essential for limb and lung formation. Nat Genet **21**, 138-141

13 Copp, A. J. (1995) Death before birth: clues from gene knockouts and mutations. Trends Genet **11**, 87-93

14 Bader, B. L., Rayburn, H., Crowley, D. and Hynes, R. O. (1998) Extensive vasculogenesis, angiogenesis, and organogenesis precede lethality in mice lacking all alpha v integrins. Cell **95**, 507-519

15 Soriano, P. (1994) Abnormal kidney development and hematological disorders in PDGF beta-receptor mutant mice. Genes Dev **8**, 1888-1896

16 Tallquist, M. D., French, W. J. and Soriano, P. (2003) Additive effects of PDGF receptor beta signaling pathways in vascular smooth muscle cell development. PLoS Biol **1**, E52

17 Tachibana, K., Hirota, S., Iizasa, H., Yoshida, H., Kawabata, K., Kataoka, Y., Kitamura, Y., Matsushima, K., Yoshida, N., Nishikawa, S., Kishimoto, T. and Nagasawa, T. (1998) The chemokine receptor CXCR4 is essential for vascularization of the gastrointestinal tract. Nature **393**, 591-594

18 Jalbert, L. R., Rosen, E. D., Moons, L., Chan, J. C., Carmeliet, P., Collen, D. and Castellino, F. J. (1998) Inactivation of the gene for anticoagulant protein C causes lethal perinatal consumptive coagulopathy in mice. J Clin Invest **102**, 1481-1488

19 Cui, J., O'Shea, K. S., Purkayastha, A., Saunders, T. L. and Ginsburg, D. (1996) Fatal haemorrhage and incomplete block to embryogenesis in mice lacking coagulation factor V. Nature **384**, 66-68

20 Rosen, E. D., Chan, J. C., Idusogie, E., Clotman, F., Vlasuk, G., Luther, T., Jalbert, L. R., Albrecht, S., Zhong, L., Lissens, A., Schoonjans, L., Moons, L., Collen, D., Castellino, F. J. and Carmeliet, P. (1997) Mice lacking factor VII develop normally but suffer fatal perinatal bleeding. Nature **390**, 290-294

21 Mackman, N. (2005) Tissue-specific hemostasis in mice. Arterioscler Thromb Vasc Biol **25**, 2273-2281

22 Richter, D. W. and Spyer, K. M. (2001) Studying rhythmogenesis of breathing: comparison of in vivo and in vitro models. Trends Neurosci **24**, 464-472

23 Jacquin, T. D., Borday, V., Schneider-Maunoury, S., Topilko, P., Ghilini, G., Kato, F., Charnay, P. and Champagnat, J. (1996) Reorganization of pontine rhythmogenic neuronal networks in Krox-20 knockout mice. Neuron **17**, 747-758

24 Swiatek, P. J. and Gridley, T. (1993) Perinatal lethality and defects in hindbrain development in mice homozygous for a targeted mutation of the zinc finger gene Krox20. Genes Dev **7**, 2071-2084

25 Ikeda, K., Onimaru, H., Yamada, J., Inoue, K., Ueno, S., Onaka, T., Toyoda, H., Arata, A., Ishikawa, T. O., Taketo, M. M., Fukuda, A. and Kawakami, K. (2004) Malfunction of respiratory-related neuronal activity in Na+, K+-ATPase alpha2 subunit-deficient mice is attributable to abnormal Cl- homeostasis in brainstem neurons. J Neurosci **24**, 10693-10701

26 Moseley, A. E., Lieske, S. P., Wetzel, R. K., James, P. F., He, S., Shelly, D. A., Paul, R. J., Boivin, G. P., Witte, D. P., Ramirez, J. M., Sweadner, K. J. and Lingrel, J. B. (2003) The Na,K-ATPase alpha 2 isoform is expressed in neurons, and its absence disrupts neuronal activity in newborn mice. J Biol Chem **278**, 5317-5324

27 Blanchi, B., Kelly, L. M., Viemari, J. C., Lafon, I., Burnet, H., Bevengut, M., Tillmanns, S., Daniel, L., Graf, T., Hilaire, G. and Sieweke, M. H. (2003) MafB deficiency causes defective respiratory rhythmogenesis and fatal central apnea at birth. Nat Neurosci **6**, 1091-1100

28 Shirasawa, S., Arata, A., Onimaru, H., Roth, K. A., Brown, G. A., Horning, S., Arata, S., Okumura, K., Sasazuki, T. and Korsmeyer, S. J. (2000) Rnx deficiency results in congenital central hypoventilation. Nat Genet **24**, 287-290

29 Rhee, J. W., Arata, A., Selleri, L., Jacobs, Y., Arata, S., Onimaru, H. and Cleary, M. L. (2004) Pbx3 deficiency results in central hypoventilation. Am J Pathol **165**, 1343-1350

30 Gomeza, J., Hulsmann, S., Ohno, K., Eulenburg, V., Szoke, K., Richter, D. and Betz, H. (2003) Inactivation of the glycine transporter 1 gene discloses vital role of glial glycine uptake in glycinergic inhibition. Neuron **40**, 785-796

31 Tsai, G., Ralph-Williams, R. J., Martina, M., Bergeron, R., Berger-Sweeney, J., Dunham, K. S., Jiang, Z., Caine, S. B. and Coyle, J. T. (2004) Gene knockout of glycine transporter 1: characterization of the behavioral phenotype. Proc Natl Acad Sci U S A **101**, 8485-8490

32 Gaultier, C., Matrot, B. and Gallego, J. (2006) Transgenic models to study disorders of respiratory control in newborn mice. Ilar J **47**, 15-21

33 Verhage, M., Maia, A. S., Plomp, J. J., Brussaard, A. B., Heeroma, J. H., Vermeer, H., Toonen, R. F., Hammer, R. E., van den Berg, T. K., Missler, M., Geuze, H. J. and Sudhof, T. C. (2000) Synaptic assembly of the brain in the absence of neurotransmitter secretion. Science **287**, 864-869

34 Zhao, C., Takita, J., Tanaka, Y., Setou, M., Nakagawa, T., Takeda, S., Yang, H. W., Terada, S., Nakata, T., Takei, Y., Saito, M., Tsuji, S., Hayashi, Y. and Hirokawa, N. (2001) Charcot-Marie-Tooth disease type 2A caused by mutation in a microtubule motor KIF1Bbeta. Cell **105**, 587-597

35 Kummer, T. T., Misgeld, T. and Sanes, J. R. (2006) Assembly of the postsynaptic membrane at the neuromuscular junction: paradigm lost. Curr Opin Neurobiol **16**, 74-82

36 DeChiara, T. M., Bowen, D. C., Valenzuela, D. M., Simmons, M. V., Poueymirou, W. T., Thomas, S., Kinetz, E., Compton, D. L., Rojas, E., Park, J. S., Smith, C., DiStefano, P. S., Glass, D. J., Burden, S. J. and Yancopoulos, G. D. (1996) The receptor tyrosine kinase MuSK is required for neuromuscular junction formation in vivo. Cell **85**, 501-512

37 Gautam, M., Noakes, P. G., Moscoso, L., Rupp, F., Scheller, R. H., Merlie, J. P. and Sanes, J. R. (1996) Defective neuromuscular synaptogenesis in agrin-deficient mutant mice. Cell **85**, 525-535

38 Ferguson, S. M., Bazalakova, M., Savchenko, V., Tapia, J. C., Wright, J. and Blakely, R. D. (2004) Lethal impairment of cholinergic neurotransmission in hemicholinium-3-sensitive choline transporter knockout mice. Proc Natl Acad Sci U S A **101**, 8762-8767

39 Gautam, M., Noakes, P. G., Mudd, J., Nichol, M., Chu, G. C., Sanes, J. R. and Merlie, J. P. (1995) Failure of postsynaptic specialization to develop at neuromuscular junctions of rapsyn-deficient mice. Nature **377**, 232-236

40 Hasty, P., Bradley, A., Morris, J. H., Edmondson, D. G., Venuti, J. M., Olson, E. N. and Klein, W. H. (1993) Muscle deficiency and neonatal death in mice with a targeted mutation in the myogenin gene. Nature **364**, 501-506

41 Nabeshima, Y., Hanaoka, K., Hayasaka, M., Esumi, E., Li, S., Nonaka, I. and Nabeshima, Y. (1993) Myogenin gene disruption results in perinatal lethality because of severe muscle defect. Nature **364**, 532-535

42 Pan, Y., Zvaritch, E., Tupling, A. R., Rice, W. J., de Leon, S., Rudnicki, M., McKerlie, C., Banwell, B. L. and MacLennan, D. H. (2003) Targeted disruption of the ATP2A1 gene encoding the sarco(endo)plasmic reticulum Ca2+ ATPase isoform 1 (SERCA1) impairs diaphragm function and is lethal in neonatal mice. J Biol Chem **278**, 13367-13375

43 Misgeld, T., Burgess, R. W., Lewis, R. M., Cunningham, J. M., Lichtman, J. W. and Sanes, J. R. (2002) Roles of neurotransmitter in synapse formation: development of neuromuscular junctions lacking choline acetyltransferase. Neuron **36**, 635-648

44 Wolpowitz, D., Mason, T. B., Dietrich, P., Mendelsohn, M., Talmage, D. A. and Role, L. W. (2000) Cysteine-rich domain isoforms of the neuregulin-1 gene are required for maintenance of peripheral synapses. Neuron **25**, 79-91

45 Cardoso, W. V. (2000) Lung morphogenesis revisited: old facts, current ideas. Dev Dyn **219**, 121-130

46 Shu, W., Jiang, Y. Q., Lu, M. M. and Morrisey, E. E. (2002) Wnt7b regulates mesenchymal proliferation and vascular development in the lung. Development **129**, 4831-4842

47 Colvin, J. S., White, A. C., Pratt, S. J. and Ornitz, D. M. (2001) Lung hypoplasia and neonatal death in Fgf9-null mice identify this gene as an essential regulator of lung mesenchyme. Development **128**, 2095-2106

48 Quaggin, S. E., Schwartz, L., Cui, S., Igarashi, P., Deimling, J., Post, M. and Rossant, J. (1999) The basic-helix-loop-helix protein pod1 is critically important for kidney and lung organogenesis. Development **126**, 5771-5783

49 Chuang, P. T., Kawcak, T. and McMahon, A. P. (2003) Feedback control of mammalian Hedgehog signaling by the Hedgehog-binding protein, Hip1, modulates Fgf signaling during branching morphogenesis of the lung. Genes Dev **17**, 342-347

50 Grunder, A., Ebel, T. T., Mallo, M., Schwarzkopf, G., Shimizu, T., Sippel, A. E. and Schrewe, H. (2002) Nuclear factor I-B (Nfib) deficient mice have severe lung hypoplasia. Mech Dev **112**, 69-77

51 Steele-Perkins, G., Plachez, C., Butz, K. G., Yang, G., Bachurski, C. J., Kinsman, S. L., Litwack, E. D., Richards, L. J. and Gronostajski, R. M. (2005) The transcription factor gene Nfib is essential for both lung maturation and brain development. Mol Cell Biol **25**, 685-698

52 Ramirez, M. I., Millien, G., Hinds, A., Cao, Y., Seldin, D. C. and Williams, M. C. (2003) T1alpha, a lung type I cell differentiation gene, is required for normal lung cell proliferation and alveolus formation at birth. Dev Biol **256**, 61-72

53 Fan, G., Xiao, L., Cheng, L., Wang, X., Sun, B. and Hu, G. (2000) Targeted disruption of NDST-1 gene leads to pulmonary hypoplasia and neonatal respiratory distress in mice. FEBS Lett **467**, 7-11

54 Han, R. N., Babaei, S., Robb, M., Lee, T., Ridsdale, R., Ackerley, C., Post, M. and Stewart, D. J. (2004) Defective lung vascular development and fatal respiratory distress in endothelial NO synthase-deficient mice: a model of alveolar capillary dysplasia? Circ Res **94**, 1115-1123

55 Cole, T. J., Blendy, J. A., Monaghan, A. P., Krieglstein, K., Schmid, W., Aguzzi, A., Fantuzzi, G., Hummler, E., Unsicker, K. and Schutz, G. (1995) Targeted disruption of the glucocorticoid receptor gene blocks adrenergic chromaffin cell development and severely retards lung maturation. Genes Dev **9**, 1608-1621

56 Muglia, L., Jacobson, L., Dikkes, P. and Majzoub, J. A. (1995) Corticotropin-releasing hormone deficiency reveals major fetal but not adult glucocorticoid need. Nature **373**, 427-432

57 Nasonkin, I. O., Ward, R. D., Raetzman, L. T., Seasholtz, A. F., Saunders, T. L., Gillespie, P. J. and Camper, S. A. (2004) Pituitary hypoplasia and respiratory distress syndrome in Prop1 knockout mice. Hum Mol Genet **13**, 2727-2735

58 Clark, J. C., Wert, S. E., Bachurski, C. J., Stahlman, M. T., Stripp, B. R., Weaver, T. E. and Whitsett, J. A. (1995) Targeted disruption of the surfactant protein B gene disrupts surfactant homeostasis, causing respiratory failure in newborn mice. Proc Natl Acad Sci U S A **92**, 7794-7798

59 Olver, R. E., Walters, D. V. and S, M. W. (2004) Developmental regulation of lung liquid transport. Annu Rev Physiol **66**, 77-101

60 Hummler, E., Barker, P., Gatzy, J., Beermann, F., Verdumo, C., Schmidt, A., Boucher, R. and Rossier, B. C. (1996) Early death due to defective neonatal lung liquid clearance in alpha-ENaC-deficient mice. Nat Genet **12**, 325-328

61 Dupe, V., Matt, N., Garnier, J. M., Chambon, P., Mark, M. and Ghyselinck, N. B. (2003) A newborn lethal defect due to inactivation of retinaldehyde dehydrogenase type 3 is prevented by maternal retinoic acid treatment. Proc Natl Acad Sci U S A **100**, 14036-14041

62 Cole, F. S., Hamvas, A. and Nogee, L. M. (2001) Genetic disorders of neonatal respiratory function. Pediatr Res **50**, 157-162

63 Wallis, C. (2000) Clinical outcomes of congenital lung abnormalities. Paediatr Respir Rev **1**, 328-335

64 Rossant, J. (1996) Mouse mutants and cardiac development: new molecular insights into cardiogenesis. Circ Res **78**, 349-353

65 Conway, S. J., Kruzynska-Frejtag, A., Kneer, P. L., Machnicki, M. and Koushik, S. V. (2003) What cardiovascular defect does my prenatal mouse mutant have, and why? Genesis **35**, 1-21

66 Gruber, P. J. and Epstein, J. A. (2004) Development gone awry: congenital heart disease. Circ Res **94**, 273-283

67 Feiner, L., Webber, A. L., Brown, C. B., Lu, M. M., Jia, L., Feinstein, P., Mombaerts, P., Epstein, J. A. and Raper, J. A. (2001) Targeted disruption of semaphorin 3C leads to persistent truncus arteriosus and aortic arch interruption. Development **128**, 3061-3070

68 Iida, K., Koseki, H., Kakinuma, H., Kato, N., Mizutani-Koseki, Y., Ohuchi, H., Yoshioka, H., Noji, S., Kawamura, K., Kataoka, Y., Ueno, F., Taniguchi, M., Yoshida, N., Sugiyama, T. and Miura, N. (1997) Essential roles of the winged helix transcription factor MFH-1 in aortic arch patterning and skeletogenesis. Development **124**, 4627-4638

69 Gitler, A. D., Lu, M. M. and Epstein, J. A. (2004) PlexinD1 and semaphorin signaling are required in endothelial cells for cardiovascular development. Dev Cell **7**, 107-116

70 Vaughan, C. J. and Basson, C. T. (2000) Molecular determinants of atrial and ventricular septal defects and patent ductus arteriosus. Am J Med Genet **97**, 304-309

71 Tada, T. and Kishimoto, H. (1990) Ultrastructural and histological studies on closure of the mouse ductus arteriosus. Acta Anat (Basel) **139**, 326-334

72 Nguyen, M., Camenisch, T., Snouwaert, J. N., Hicks, E., Coffman, T. M., Anderson, P. A., Malouf, N. N. and Koller, B. H. (1997) The prostaglandin receptor EP4 triggers remodelling of the cardiovascular system at birth. Nature **390**, 78-81

73 Segi, E., Sugimoto, Y., Yamasaki, A., Aze, Y., Oida, H., Nishimura, T., Murata, T., Matsuoka, T., Ushikubi, F., Hirose, M., Tanaka, T., Yoshida, N., Narumiya, S. and Ichikawa, A. (1998) Patent ductus arteriosus and neonatal death in prostaglandin receptor EP4-deficient mice. Biochem Biophys Res Commun **246**, 7-12

74 Coggins, K. G., Latour, A., Nguyen, M. S., Audoly, L., Coffman, T. M. and Koller, B. H. (2002) Metabolism of PGE2 by prostaglandin dehydrogenase is essential for remodeling the ductus arteriosus. Nat Med **8**, 91-92

75 Loftin, C. D., Trivedi, D. B., Tiano, H. F., Clark, J. A., Lee, C. A., Epstein, J. A., Morham, S. G., Breyer, M. D., Nguyen, M., Hawkins, B. M., Goulet, J. L., Smithies, O., Koller, B. H. and Langenbach, R. (2001) Failure of ductus arteriosus closure and remodeling in neonatal mice deficient in cyclooxygenase-1 and cyclooxygenase-2. Proc Natl Acad Sci U S A **98**, 1059-1064

76 Karsenty, G. and Wagner, E. F. (2002) Reaching a genetic and molecular understanding of skeletal development. Dev Cell **2**, 389-406

77 Colnot, C. (2005) Cellular and molecular interactions regulating skeletogenesis. J Cell Biochem **95**, 688-697

78 Monsoro-Burq, A. H. (2005) Sclerotome development and morphogenesis: when experimental embryology meets genetics. Int J Dev Biol **49**, 301-308

79 Komori, T., Yagi, H., Nomura, S., Yamaguchi, A., Sasaki, K., Deguchi, K., Shimizu, Y., Bronson, R. T., Gao, Y. H., Inada, M., Sato, M., Okamoto, R., Kitamura, Y., Yoshiki, S. and Kishimoto, T. (1997) Targeted disruption of Cbfa1 results in a complete lack of bone formation owing to maturational arrest of osteoblasts. Cell **89**, 755-764

80 Otto, F., Thornell, A. P., Crompton, T., Denzel, A., Gilmour, K. C., Rosewell, I. R., Stamp, G. W., Beddington, R. S., Mundlos, S., Olsen, B. R., Selby, P. B. and Owen, M. J. (1997) Cbfa1, a candidate gene for cleidocranial dysplasia syndrome, is essential for osteoblast differentiation and bone development. Cell **89**, 765-771

81 Mansouri, A., Voss, A. K., Thomas, T., Yokota, Y. and Gruss, P. (2000) Uncx4.1 is required for the formation of the pedicles and proximal ribs and acts upstream of Pax9. Development **127**, 2251-2258

82 Leitges, M., Neidhardt, L., Haenig, B., Herrmann, B. G. and Kispert, A. (2000) The paired homeobox gene Uncx4.1 specifies pedicles, transverse processes and proximal ribs of the vertebral column. Development **127**, 2259-2267

83 Bussen, M., Petry, M., Schuster-Gossler, K., Leitges, M., Gossler, A. and Kispert, A. (2004) The T-box transcription factor Tbx18 maintains the separation of anterior and posterior somite compartments. Genes Dev **18**, 1209-1221

84 Ivkovic, S., Yoon, B. S., Popoff, S. N., Safadi, F. F., Libuda, D. E., Stephenson, R. C., Daluiski, A. and Lyons, K. M. (2003) Connective tissue growth factor coordinates chondrogenesis and angiogenesis during skeletal development. Development **130**, 2779-2791

85 Karaplis, A. C., Luz, A., Glowacki, J., Bronson, R. T., Tybulewicz, V. L., Kronenberg, H. M. and Mulligan, R. C. (1994) Lethal skeletal dysplasia from targeted disruption of the parathyroid hormone-related peptide gene. Genes Dev **8**, 277-289

86 Akazawa, H., Komuro, I., Sugitani, Y., Yazaki, Y., Nagai, R. and Noda, T. (2000) Targeted disruption of the homeobox transcription factor Bapx1 results in lethal skeletal dysplasia with asplenia and gastroduodenal malformation. Genes Cells **5**, 499-513

87 Lettice, L. A., Purdie, L. A., Carlson, G. J., Kilanowski, F., Dorin, J. and Hill, R. E. (1999) The mouse bagpipe gene controls development of axial skeleton, skull, and spleen. Proc Natl Acad Sci U S A **96**, 9695-9700

88 Li, S. W., Prockop, D. J., Helminen, H., Fassler, R., Lapvetelainen, T., Kiraly, K., Peltarri, A., Arokoski, J., Lui, H., Arita, M. and et al. (1995) Transgenic mice with targeted inactivation of the Col2 alpha 1 gene for collagen II develop a skeleton with membranous and periosteal bone but no endochondral bone. Genes Dev **9**, 2821-2830

89 Li, Y. and Olsen, B. R. (1997) Murine models of human genetic skeletal disorders. Matrix Biol **16**, 49-52

90 Papaioannou, V. E. and Behringer, R. (2005) Mouse phenotypes : a handbook of mutation analysis. Cold Spring Harbor Laboratory Press, Cold Spring Harbor. N.Y.

91 DeChiara, T. M., Vejsada, R., Poueymirou, W. T., Acheson, A., Suri, C., Conover, J. C., Friedman, B., McClain, J., Pan, L., Stahl, N., Ip, N. Y. and Yancopoulos, G. D. (1995) Mice lacking the CNTF receptor, unlike mice lacking CNTF, exhibit profound motor neuron deficits at birth. Cell **83**, 313-322

92 Mizushima, N., Yamamoto, A., Hatano, M., Kobayashi, Y., Kabeya, Y., Suzuki, K., Tokuhisa, T., Ohsumi, Y. and Yoshimori, T. (2001) Dissection of autophagosome formation using Apg5-deficient mouse embryonic stem cells. J Cell Biol **152**, 657-668

93 Segre, J. A., Bauer, C. and Fuchs, E. (1999) Klf4 is a transcription factor required for establishing the barrier function of the skin. Nat Genet **22**, 356-360

94 Blass, E. M. and Teicher, M. H. (1980) Suckling. Science **210**, 15-22

95 Westneat, M. W. and Hall, W. G. (1992) Ontogeny of feeding motor patterns in infant rats: an electromyographic analysis of suckling and chewing. Behav Neurosci **106**, 539-554

96 Kandel, E. R., Schwartz, J. H., and Jessell, T. M. (1991) Principles of Neuroscience. Elsevier, New York

97 Risser, J. M. and Slotnick, B. M. (1987) Nipple attachment and survival in neonatal olfactory bulbectomized rats. Physiol Behav **40**, 545-549

98 Contos, J. J., Fukushima, N., Weiner, J. A., Kaushal, D. and Chun, J. (2000) Requirement for the lpA1 lysophosphatidic acid receptor gene in normal suckling behavior. Proc Natl Acad Sci U S A **97**, 13384-13389

99 Wang, S. S., Lewcock, J. W., Feinstein, P., Mombaerts, P. and Reed, R. R. (2004) Genetic disruptions of O/E2 and O/E3 genes reveal involvement in olfactory receptor neuron projection. Development **131**, 1377-1388

100 Guillemot, F., Lo, L. C., Johnson, J. E., Auerbach, A., Anderson, D. J. and Joyner, A. L. (1993) Mammalian achaete-scute homolog 1 is required for the early development of olfactory and autonomic neurons. Cell **75**, 463-476

101 Belluscio, L., Gold, G. H., Nemes, A. and Axel, R. (1998) Mice deficient in G(olf) are anosmic. Neuron **20**, 69-81

102 Brunet, L. J., Gold, G. H. and Ngai, J. (1996) General anosmia caused by a targeted disruption of the mouse olfactory cyclic nucleotide-gated cation channel. Neuron **17**, 681-693

103 Yagi, T., Aizawa, S., Tokunaga, T., Shigetani, Y., Takeda, N. and Ikawa, Y. (1993) A role for Fyn tyrosine kinase in the suckling behaviour of neonatal mice. Nature **366**, 742-745

104 Kutsuwada, T., Sakimura, K., Manabe, T., Takayama, C., Katakura, N., Kushiya, E., Natsume, R., Watanabe, M., Inoue, Y., Yagi, T., Aizawa, S., Arakawa, M., Takahashi, T., Nakamura, Y., Mori, H. and Mishina, M. (1996) Impairment of suckling response, trigeminal neuronal pattern formation, and hippocampal LTD in NMDA receptor epsilon 2 subunit mutant mice. Neuron **16**, 333-344

105 Jones, K. R., Farinas, I., Backus, C. and Reichardt, L. F. (1994) Targeted disruption of the BDNF gene perturbs brain and sensory neuron development but not motor neuron development. Cell **76**, 989-999

106 Di Paolo, G., Moskowitz, H. S., Gipson, K., Wenk, M. R., Voronov, S., Obayashi, M., Flavell, R., Fitzsimonds, R. M., Ryan, T. A. and De Camilli, P. (2004) Impaired PtdIns(4,5)P2 synthesis in nerve terminals produces defects in synaptic vesicle trafficking. Nature **431**, 415-422

107 Takahashi, M., Kubo, T., Mizoguchi, A., Carlson, C. G., Endo, K. and Ohnishi, K. (2002) Spontaneous muscle action potentials fail to develop without fetal-type acetylcholine receptors. EMBO Rep **3**, 674-681

108 Xiang, M., Gan, L., Zhou, L., Klein, W. H. and Nathans, J. (1996) Targeted deletion of the mouse POU domain gene Brn-3a causes selective loss of neurons in the brainstem and trigeminal ganglion, uncoordinated limb movement, and impaired suckling. Proc Natl Acad Sci U S A **93**, 11950-11955

109 McEvilly, R. J., Erkman, L., Luo, L., Sawchenko, P. E., Ryan, A. F. and Rosenfeld, M. G. (1996) Requirement for Brn-3.0 in differentiation and survival of sensory and motor neurons. Nature **384**, 574-577

110 Qiu, Y., Pereira, F. A., DeMayo, F. J., Lydon, J. P., Tsai, S. Y. and Tsai, M. J. (1997) Null mutation of mCOUP-TFI results in defects in morphogenesis of the glossopharyngeal ganglion, axonal projection, and arborization. Genes Dev **11**, 1925-1937

111 Chan, E. Y., Nasir, J., Gutekunst, C. A., Coleman, S., Maclean, A., Maas, A., Metzler, M., Gertsenstein, M., Ross, C. A., Nagy, A. and Hayden, M. R. (2002) Targeted disruption of Huntingtin-associated protein-1 (Hap1) results in postnatal death due to depressed feeding behavior. Hum Mol Genet **11**, 945-959

112 Dragatsis, I., Zeitlin, S. and Dietrich, P. (2004) Huntingtin-associated protein 1 (Hap1) mutant mice bypassing the early postnatal lethality are neuroanatomically normal and fertile but display growth retardation. Hum Mol Genet **13**, 3115-3125

113 Sheng, G., Chang, G. Q., Lin, J. Y., Yu, Z. X., Fang, Z. H., Rong, J., Lipton, S. A., Li, S. H., Tong, G., Leibowitz, S. F. and Li, X. J. (2006) Hypothalamic huntingtin-associated protein 1 as a mediator of feeding behavior. Nat Med **12**, 526-533

114 Ito, K., Komazaki, S., Sasamoto, K., Yoshida, M., Nishi, M., Kitamura, K. and Takeshima, H. (2001) Deficiency of triad junction and contraction in mutant skeletal muscle lacking junctophilin type 1. J Cell Biol **154**, 1059-1067

115 Hilliard, S. A., Yu, L., Gu, S., Zhang, Z. and Chen, Y. P. (2005) Regional regulation of palatal growth and patterning along the anterior-posterior axis in mice. J Anat **207**, 655-667

116 Francis-West, P., Ladher, R., Barlow, A. and Graveson, A. (1998) Signalling interactions during facial development. Mech Dev **75**, 3-28

117 Zhao, Y., Guo, Y. J., Tomac, A. C., Taylor, N. R., Grinberg, A., Lee, E. J., Huang, S. and Westphal, H. (1999) Isolated cleft palate in mice with a targeted mutation of the LIM homeobox gene lhx8. Proc Natl Acad Sci U S A **96**, 15002-15006

118 Kaartinen, V., Voncken, J. W., Shuler, C., Warburton, D., Bu, D., Heisterkamp, N. and Groffen, J. (1995) Abnormal lung development and cleft palate in mice lacking TGF-beta 3 indicates defects of epithelial-mesenchymal interaction. Nat Genet **11**, 415-421

119 Lan, Y., Ovitt, C. E., Cho, E. S., Maltby, K. M., Wang, Q. and Jiang, R. (2004) Odd-skipped related 2 (Osr2) encodes a key intrinsic regulator of secondary palate growth and morphogenesis. Development **131**, 3207-3216

120 Wang, T., Tamakoshi, T., Uezato, T., Shu, F., Kanzaki-Kato, N., Fu, Y., Koseki, H., Yoshida, N., Sugiyama, T. and Miura, N. (2003) Forkhead transcription factor Foxf2 (LUN)-deficient mice exhibit abnormal development of secondary palate. Dev Biol **259**, 83-94

121 Caruana, G. and Bernstein, A. (2001) Craniofacial dysmorphogenesis including cleft palate in mice with an insertional mutation in the discs large gene. Mol Cell Biol **21**, 1475-1483

122 Wilson, J. B., Ferguson, M. W., Jenkins, N. A., Lock, L. F., Copeland, N. G. and Levine, A. J. (1993) Transgenic mouse model of X-linked cleft palate. Cell Growth Differ **4**, 67-76

123 Wilkie, A. O. and Morriss-Kay, G. M. (2001) Genetics of craniofacial development and malformation. Nat Rev Genet **2**, 458-468

124 Peters, H., Neubuser, A., Kratochwil, K. and Balling, R. (1998) Pax9-deficient mice lack pharyngeal pouch derivatives and teeth and exhibit craniofacial and limb abnormalities. Genes Dev **12**, 2735-2747

125 Jiang, R., Lan, Y., Chapman, H. D., Shawber, C., Norton, C. R., Serreze, D. V., Weinmaster, G. and Gridley, T. (1998) Defects in limb, craniofacial, and thymic development in Jagged2 mutant mice. Genes Dev **12**, 1046-1057

126 Houdayer, C. and Bahuau, M. (1998) Orofacial cleft defects: inference from nature and nurture. Ann Genet **41**, 89-117

127 Girard, J. and Pegorier, J. P. (1998) An overview of early post-partum nutrition and metabolism. Biochem Soc Trans **26**, 69-74

128 Darlington, G. J. (1999) Molecular mechanisms of liver development and differentiation. Curr Opin Cell Biol **11**, 678-682

129 Desvergne, B., Michalik, L. and Wahli, W. (2006) Transcriptional regulation of metabolism. Physiol Rev **86**, 465-514

130 Kotoulas, O. B. (2006) Glycogen autophagy in glucose homeostasis. Pathology – Research and Practice **in press**

131 Kuma, A., Hatano, M., Matsui, M., Yamamoto, A., Nakaya, H., Yoshimori, T., Ohsumi, Y., Tokuhisa, T. and Mizushima, N. (2004) The role of autophagy during the early neonatal starvation period. Nature **432**, 1032-1036

132 Komatsu, M., Waguri, S., Ueno, T., Iwata, J., Murata, S., Tanida, I., Ezaki, J., Mizushima, N., Ohsumi, Y., Uchiyama, Y., Kominami, E., Tanaka, K. and Chiba, T. (2005) Impairment of starvation-induced and constitutive autophagy in Atg7-deficient mice. J Cell Biol **169**, 425-434

133 Wang, N. D., Finegold, M. J., Bradley, A., Ou, C. N., Abdelsayed, S. V., Wilde, M. D., Taylor, L. R., Wilson, D. R. and Darlington, G. J. (1995) Impaired energy homeostasis in C/EBP alpha knockout mice. Science **269**, 1108-1112

134 Scheuner, D., Song, B., McEwen, E., Liu, C., Laybutt, R., Gillespie, P., Saunders, T., Bonner-Weir, S. and Kaufman, R. J. (2001) Translational control is required for the unfolded protein response and in vivo glucose homeostasis. Mol Cell **7**, 1165-1176

135 Collombat, P., Mansouri, A., Hecksher-Sorensen, J., Serup, P., Krull, J., Gradwohl, G. and Gruss, P. (2003) Opposing actions of Arx and Pax4 in endocrine pancreas development. Genes Dev **17**, 2591-2603

136 Calogero, S., Grassi, F., Aguzzi, A., Voigtlander, T., Ferrier, P., Ferrari, S. and Bianchi, M. E. (1999) The lack of chromosomal protein Hmg1 does not disrupt cell growth but causes lethal hypoglycaemia in newborn mice. Nat Genet **22**, 276-280

137 Clement, S., Krause, U., Desmedt, F., Tanti, J. F., Behrends, J., Pesesse, X., Sasaki, T., Penninger, J., Doherty, M., Malaisse, W., Dumont, J. E., Le Marchand-Brustel, Y., Erneux, C., Hue, L. and Schurmans, S. (2001) The lipid phosphatase SHIP2 controls insulin sensitivity. Nature **409**, 92-97

138 Hardman, M. J., Sisi, P., Banbury, D. N. and Byrne, C. (1998) Patterned acquisition of skin barrier function during development. Development **125**, 1541-1552

139 Nemes, Z. and Steinert, P. M. (1999) Bricks and mortar of the epidermal barrier. Exp Mol Med **31**, 5-19

140 Matsuki, M., Yamashita, F., Ishida-Yamamoto, A., Yamada, K., Kinoshita, C., Fushiki, S., Ueda, E., Morishima, Y., Tabata, K., Yasuno, H., Hashida, M., Iizuka, H., Ikawa, M., Okabe, M., Kondoh, G., Kinoshita, T., Takeda, J. and Yamanishi, K. (1998) Defective stratum corneum and early neonatal death in mice lacking the gene for transglutaminase 1 (keratinocyte transglutaminase). Proc Natl Acad Sci U S A **95**, 1044-1049

141 Descargues, P., Deraison, C., Bonnart, C., Kreft, M., Kishibe, M., Ishida-Yamamoto, A., Elias, P., Barrandon, Y., Zambruno, G., Sonnenberg, A. and Hovnanian, A. (2005) Spink5-deficient mice mimic Netherton syndrome through degradation of desmoglein 1 by epidermal protease hyperactivity. Nat Genet **37**, 56-65

142 Hewett, D. R., Simons, A. L., Mangan, N. E., Jolin, H. E., Green, S. M., Fallon, P. G. and McKenzie, A. N. (2005) Lethal, neonatal ichthyosis with increased proteolytic processing of filaggrin in a mouse model of Netherton syndrome. Hum Mol Genet **14**, 335-346

143 Furuse, M., Hata, M., Furuse, K., Yoshida, Y., Haratake, A., Sugitani, Y., Noda, T., Kubo, A. and Tsukita, S. (2002) Claudin-based tight junctions are crucial for the mammalian epidermal barrier: a lesson from claudin-1-deficient mice. J Cell Biol **156**, 1099-1111

144 Miyazaki, M., Dobrzyn, A., Elias, P. M. and Ntambi, J. M. (2005) Stearoyl-CoA desaturase-2 gene expression is required for lipid synthesis during early skin and liver development. Proc Natl Acad Sci U S A **102**, 12501-12506

145 Segre, J. A. (2006) Epidermal barrier formation and recovery in skin disorders. J Clin Invest **116**, 1150-1158

146 Horster, M. F., Braun, G. S. and Huber, S. M. (1999) Embryonic renal epithelia: induction, nephrogenesis, and cell differentiation. Physiol Rev **79**, 1157-1191

147 Miyamoto, N., Yoshida, M., Kuratani, S., Matsuo, I. and Aizawa, S. (1997) Defects of urogenital development in mice lacking Emx2. Development **124**, 1653-1664

148 Pellegrini, M., Mansouri, A., Simeone, A., Boncinelli, E. and Gruss, P. (1996) Dentate gyrus formation requires Emx2. Development **122**, 3893-3898

149 Bullock, S. L., Fletcher, J. M., Beddington, R. S. and Wilson, V. A. (1998) Renal agenesis in mice homozygous for a gene trap mutation in the gene encoding heparan sulfate 2-sulfotransferase. Genes Dev **12**, 1894-1906

150 Schuchardt, A., D'Agati, V., Larsson-Blomberg, L., Costantini, F. and Pachnis, V. (1994) Defects in the kidney and enteric nervous system of mice lacking the tyrosine kinase receptor Ret. Nature **367**, 380-383

151 Stark, K., Vainio, S., Vassileva, G. and McMahon, A. P. (1994) Epithelial transformation of metanephric mesenchyme in the developing kidney regulated by Wnt-4. Nature **372**, 679-683

152 Muller, U., Wang, D., Denda, S., Meneses, J. J., Pedersen, R. A. and Reichardt, L. F. (1997) Integrin alpha8beta1 is critically important for epithelial-mesenchymal interactions during kidney morphogenesis. Cell **88**, 603-613

153 Kreidberg, J. A., Donovan, M. J., Goldstein, S. L., Rennke, H., Shepherd, K., Jones, R. C. and Jaenisch, R. (1996) Alpha 3 beta 1 integrin has a crucial role in kidney and lung organogenesis. Development **122**, 3537-3547

154 Nakai, S., Sugitani, Y., Sato, H., Ito, S., Miura, Y., Ogawa, M., Nishi, M., Jishage, K., Minowa, O. and Noda, T. (2003) Crucial roles of Brn1 in distal tubule formation and function in mouse kidney. Development **130**, 4751-4759

155 Hatini, V., Huh, S. O., Herzlinger, D., Soares, V. C. and Lai, E. (1996) Essential role of stromal mesenchyme in kidney morphogenesis revealed by targeted disruption of Winged Helix transcription factor BF-2. Genes Dev **10**, 1467-1478

156 Putaala, H., Soininen, R., Kilpelainen, P., Wartiovaara, J. and Tryggvason, K. (2001) The murine nephrin gene is specifically expressed in kidney, brain and pancreas: inactivation of the gene leads to massive proteinuria and neonatal death. Hum Mol Genet **10**, 1-8

157 Rantanen, M., Palmen, T., Patari, A., Ahola, H., Lehtonen, S., Astrom, E., Floss, T., Vauti, F., Wurst, W., Ruiz, P., Kerjaschki, D. and Holthofer, H. (2002) Nephrin TRAP mice lack slit diaphragms and show fibrotic glomeruli and cystic tubular lesions. J Am Soc Nephrol **13**, 1586-1594

158 Doyonnas, R., Kershaw, D. B., Duhme, C., Merkens, H., Chelliah, S., Graf, T. and McNagny, K. M. (2001) Anuria, omphalocele, and perinatal lethality in mice lacking the CD34-related protein podocalyxin. J Exp Med **194**, 13-27

159 McDonald, F. J., Yang, B., Hrstka, R. F., Drummond, H. A., Tarr, D. E., McCray, P. B., Jr., Stokes, J. B., Welsh, M. J. and Williamson, R. A. (1999) Disruption of the beta subunit of the epithelial Na+ channel in mice: hyperkalemia and neonatal death associated with a pseudohypoaldosteronism phenotype. Proc Natl Acad Sci U S A **96**, 1727-1731

160 Saito, A., Yamazaki, H., Nakagawa, Y. and Arakawa, M. (1997) Molecular genetics of renal diseases. Intern Med **36**, 81-86

161 Kulandavelu, S., Qu, D., Sunn, N., Mu, J., Rennie, M. Y., Whiteley, K. J., Walls, J. R., Bock, N. A., Sun, J. C., Covelli, A., Sled, J. G. and Adamson, S. L. (2006) Embryonic and neonatal phenotyping of genetically engineered mice. Ilar J **47**, 103-117

CHAPITRE 2

ARTICLE

Clonage et caractérisation du produit du gène *Erk3* chez la souris, une protéine de 100 kDa

Article publié dans: *Biochem J.* **346** Pt 1:169-75; Février 2000

MISE EN SITUATION

À l'époque de mon arrivée dans le laboratoire du Dr Meloche, deux isoformes de ERK3 avaient été identifiées par clonages moléculaires chez les mammifères. J'ai reçu comme mandat de cloner le gène (ou les gènes) encodant ces isoformes et d'en déterminer la structure. En effet, connaître la structure du gène nous permettrait d'atteindre 2 objectifs : Le premier était de comprendre comment deux isoformes de ERK3 pourrait être encodée dans le génome et ainsi établir la relation génique entre ces deux isoformes. La connaissance de l'organisation du gène (ou des gènes) *Erk3* permettrait également de générer une stratégie d'invalidation génique. Pour atteindre cet objectif, il était nécessaire d'isoler des ADNc encodant des isoformes de ERK3 chez la souris. En effet, la séquence d'un ADNc représente un outil expérimental important pour le clonage d'un gène, de même que l'étude de la biologie moléculaire d'une protéine. Le clonage moléculaire de ces ADNc devenait donc important.

Au cours de ces travaux, mon collègue Phillipe Coulombe a porté à mon attention un rapport déposé à la banque publique de séquences nucléotidiques du NCBI qui suggérait l'existence d'une erreur potentielle dans la séquence publiée de l'ADNc de ERK3 du rat. Vérifier expérimentalement cette hypothèse devenait un préalable pour la recherche de gènes encodant une isoforme de 62 kDa de même que pour l'étude de la biologie moléculaire de ERK3.

Ce chapitre rapporte donc le clonage d'un ADNc possédant un cadre de lecture complet pour la protéine ERK3 chez la souris. Cet ADNc a permis d'étudier l'expression de l'ARNm de *Erk3* chez la souris, de caractériser son produit comme étant une protéine de 100 kDa et de localiser son gène sur le chromosome 9 de la souris. De façon importante, ce travail fourni les premières évidences expérimentales que ERK3 est une protéine de 100 kDa chez les mammifères, permettant de résoudre la controverse de l'existence d'un gène encodant une isoforme de 62 kDa

Cloning and characterization of mouse ERK3 as a unique gene product of 100 kiloDaltons

Benjamin Turgeon[*], Marc K. Saba-El-Leil[†] and Sylvain Meloche[*,†,1]

Research Centre, Centre hospitalier de l'Université de Montréal and [*] Department of Molecular Biology and [†] Pharmacology, University of Montreal, Montreal, Quebec, Canada H2W 1T8.

Short Title: Molecular cloning of mouse ERK3

[1]To whom correspondence should be addressed:

Dr. Sylvain Meloche
Research Centre
Centre hospitalier de l'Université de Montréal
Hotel-Dieu Campus
3850 St. Urbain Street
Montreal (Quebec) Canada H2W 1T8
Phone : (514) 843-2733
Fax: : (514) 843-2715
E-mail : [redacted]

ABSTRACT

Mitogen activated protein (MAP) kinases are a family of serine/threonine kinases which play a pivotal role in signal transduction. Here, we report the cloning and characterization of a mouse homolog of ERK3. The mouse ERK3 cDNA encodes a predicted protein of 720 amino acids, which displays 94% identity with human ERK3. *In vitro* transcription-translation of this cDNA generates a 100-kDa protein similar to the human ERK3 gene product. Immunoblot analysis with an antibody raised to a unique sequence of ERK3 also recognizes a 100-kDa protein in mouse tissues. A single transcript of *Erk3* was detected in every adult mouse tissue examined, with the highest expression found in the brain. Interestingly, expression of *Erk3* mRNA is acutely regulated during mouse development, with a peak of expression observed at embryonic day 11. The mouse *Erk3* gene was mapped to a single locus on central mouse Chromosome 9, adjacent to the *dilute* mutation locus and in a region syntenic to human chromosome 15q21. Finally, we provide several lines of evidence to support the existence of a unique *Erk3* gene product of 100 kDa in mammalian cells.

Keywords: Protein kinase; MAP kinase; gene cloning; chromosomal localization.

INTRODUCTION

Eukaryotic cells have the ability to respond to a wide variety of extracellular signals through the activation of specific transduction pathways. Among them are the extensively studied mitogen-activated protein (MAP) kinase pathways, which are involved in a vast repertoire of responses, including cell proliferation and differentiation, adaptation to environmental stress, apoptosis and embryonic morphogenesis (For reviews see [1-3]). MAP kinase pathways are organized into three-kinase module architecture, which transmit signals by sequential phosphorylation and activation of the specific components of the module. Many components of these cascades have been conserved from yeast to metazoan cells.

In mammalian cells, six MAP kinase modules have been identified so far. The best described are the extracellular signal-regulated kinase (ERK) pathway, which regulates cell growth and differentiation, and the c-Jun N-terminal kinase (JNK) and p38 pathways, which are mainly associated with the response to stress and inflammation [1-5]. Other protein kinases with high homology to ERK1/2 have been identified, which define three distinct subfamily of MAP kinases. These include ERK3 [6-8] and $p63^{MAPK}$ [9, 10], ERK5 [11, 12] and ERK7 [13]. Much less is known about the regulation and functions of these protein kinases. ERK3 was first cloned from a rat cDNA library as a 543-amino acid protein with a predicted molecular mass of 62 kDa [6]. The ERK3 protein is ~50% identical to ERK1/2 within the kinase catalytic domain and has similar lengths of inserts between conserved subdomains. However, one important structural feature that distinguishes ERK3 (and $p63^{MAPK}$) from the other MAP kinases is the presence of a SEG motif instead of the highly conserved TXY motif within the activation loop. It has been shown that ERK3 autophosphorylates *in vitro* and is phosphorylated *in vivo* on Ser-189 [14, 15], the residue equivalent to the activating phosphorylation site Thr-183 in ERK2. Later on, two groups isolated a cDNA encoding a human homolog of ERK3 [7, 8]. Sequence analysis revealed that human and rat ERK3 are 92 % identical over their shared length, but the human protein contains a unique C-terminal extension of 178 amino acids. *In vitro* translation of the human ERK3 cDNA generates a protein of ~100 kDa [7]. Intriguingly, the human and rat ERK3 sequences display high nucleotide homology (~82%) at their carboxy terminus, despite the fact that the two open reading frames are not parallel. The relationship between the two ERK3 orthologs has remained obscure and it has been hypothesized that multiple ERK3-related genes may exist or that the *Erk3* gene is alternatively spliced to generate two protein products [7, 14].

In this paper, we report the cloning and initial characterization of a mouse ERK3 homolog. The mouse ERK3 is a 720-amino acid protein that exhibits high identity to the human enzyme. Expression of ERK3 varies significantly in adult mouse tissues and is acutely regulated during mouse embryonic development. Importantly, we now provide compelling evidence for the existence of a single ERK3 gene product of ~ 100 kDa.

MATERIALS AND METHODS

Isolation and sequencing of murine *Erk3* cDNA clones

A mouse pituitary ATt-20 cDNA library constructed in λgt11 vector (kindly provided by Dr. Jacques Drouin, IRCM) was screened with a 198-bp AccI fragment derived from the first exon of the murine Erk3 gene (Turgeon B and Meloche S, unpublished) as probe. Hybridization and washing of the nylon filters were performed as described previously [16]. Positive clones were plaque-purified and the insert cDNAs were subcloned into pBK-CMV vector (Stratagene). The nucleotide sequences of the clones were determined using the Thermo Sequenase Cycle sequencing kit (Amersham Pharmacia). Sequence data were compiled and analyzed with the GeneWorks software (IntelliGenetics).

Reverse transcription (RT)-PCR and genomic PCR

Total RNA from rat tissues was isolated by the guanidinium thyocyanate acid extraction procedure [17]. For synthesis of first-strand cDNA, 5 μg of RNA was heat-denatured at 70°C for 10 min, chilled on ice, and added to a reaction mix containing 50 μM random hexamers, 1 mM dNTPs, 5 mM $MgCl_2$, 20 U RNAsin (Pharmacia), and 200 U M-MLV reverse transcriptase (Gibco BRL) in first-strand buffer (Gibco BRL) in a total volume of 20 μl. The RT reaction was carried out at 37°C for 90 min, followed by heat-inactivation of the enzyme at 94°C for 10 min. Rat genomic DNA was isolated from cultured rat aortic smooth muscle cells using standard methods [18].

Erk3 sequences were amplified by PCR using the oligonucleotide primers 5'-GGGACACTGAGCTATTCAAG-3' (forward) and 5'-GTAGCCATACTTGTAACTAC-3' (reverse) based on the published rat cDNA sequence [6]. Five μl of the RT reaction or 5 μg of genomic DNA was amplified in 100 μl reaction volume using the GenAmp PCR kit (Perkin Elmer Cetus) according to the manufacturer's instructions. PCR conditions used were: 94°C for 5 min followed by 30 cycles at 94°C for 45 sec, 52°C for 30 sec and 72°C for 2 min. Extension of the PCR products was performed at 72°C for an additional 10 min. The PCR products were purified by agarose gel electrophoresis and directly sequenced as described above.

Northern and Southern blot analysis

Total RNA from adult mouse tissues and embryos at different developmental stages was prepared as described above. Twenty micrograms of each RNA was resolved by

electrophoresis in a 1% agarose gel containing 1.8% formaldehyde, transferred to Hybond-N membrane (Amersham), and hybridized to a ^{32}P-labeled 0.9-kb BamHI fragment from the mouse ERK3 cDNA. Hybridization was carried out in hybridization buffer (5 X SSC, 0.1 % SDS, 5 X Denhardt's solution, 50% formamide, and 1 μg/ml ssDNA) containing the labeled probe (2 x 10^6 cpm/ml) for 16 h at 42°C. The membrane was washed at a final stringency of 0.1 X SSC, 0.1 % SDS at 60°C and analyzed by autoradiography.

Mouse genomic DNA (20 μg) was digested with various restriction endonucleases, fractionated on a 0.8% agarose gel, and transferred to Hybond-N membrane. The membrane was hybridized with a ^{32}P-labeled 200-bp genomic probe corresponding to the 3' exon-intron boundary of the mouse *Erk3* gene exon encoding amino acids 235-288 of the protein (Turgeon B and Meloche S, unpublished). Hybridization was carried out as described above.

In vitro transcription/translation

The full-length mouse and human [8] ERK3 cDNAs were subcloned in pBK-CMV vector (Stratagene) . *In vitro* transcription was performed using T7 RNA polymerase followed by translation with a rabbit reticulocyte lysate (Promega) in the presence of [^{35}S]methionine. The labeled proteins were resolved by SDS-gel electrophoresis, transferred to a nitrocellulose membrane, and visualized with a PhosphorImager (Molecular Dynamics).

Western blot analysis

Protein extracts of mouse embryos were prepared by homogenization of the whole embryo in Triton X-100 lysis buffer (50 mM Tris-HCl, pH 7.4, 100 mM NaCl, 50 mM NaF, 5 mM EDTA, 0.1 mM phenylmethylsulfonyl fluoride, 10^{-6} M leupeptin, 10^{-6} M pepstatin A, 1% Triton X-100) for 1 min at 4°C. Homogenates were clarified by centrifugation at 13,000 x g for 10 min. Equal amounts of lysate proteins (100 μg) were resolved by SDS-gel electrophoresis on 7.5% acrylamide gel and transferred to Hybond-C nitrocellulose membrane (Amersham). The membrane was blocked for 1 h at 37°C in Tris-buffered saline (TBS) containing 0.1% Tween-20 and 1% bovine serum albumin (BSA) prior to incubation at 25°C for 1 h with anti-ERK3 antibody (sc-156; Santa-Cruz Biotechnology) diluted 1:1,000 in blocking solution. After extensive washing in TBS, 0.1 % Tween-20, the membrane was incubated for 1 h at 25°C with horseradish peroxidase-conjugated anti-IgG (1:3,000 dilution) in blocking solution. Immunoreactive bands were visualized by enhanced chemiluminescence (Amersham).

Chromosomal mapping

The mouse *Erk3* gene was mapped using The Jackson Laboratory interspecific backcross panel (C57BL/6JEi x SPRET/Ei)F_1 x SPRET/Ei (Jackson BSS)[19]. A total of 94 backcross progeny mice were used to map *Erk3* using a MspI restriction fragment length polymorphism (RFLP). The MspI digestion identified a 6 kb allele fragment for C57BL/6J DNA and a fragment of 3.6 kb for *M. spretus* DNA. Mouse genomic DNA digested with MspI was analyzed by southern blot using the genomic probe described above. The presence or absence of the 6 kb C57BL/6J-specific band was scored in backcross mice. The mapping data were analyzed by Mary Barter at The Jackson Laboratory.

RESULTS AND DISCUSSION

Molecular cloning of a murine ERK3 homolog

To isolate a mouse homolog of ERK3, we screened a mouse pituitary cDNA library with a 198-bp AccI fragment derived from the first exon of the murine *Erk3* gene (Turgeon B and Meloche S, unpublished). Among 1 x 10^6 phage plaques, four positive clones were isolated with inserts ranging from 0.8 to 2.6 kb. Partial characterization of these clones confirmed that they were highly homologous to previously cloned ERK3 cDNAs. The largest clone (λMmK3) was further characterized. Nucleotide sequence analysis showed that this clone extends over 2683 nucleotides and contains both initiation and termination codons for translation (Fig. 1A). A continuous open reading frame of 2160 nucleotides encodes a deduced protein of 720 amino acids with a calculated molecular mass of 82.1 kDa (Fig. 1A). The coding sequence is preceded by a 505-base 5'-untranslated region (UTR), which contains an in-frame stop codon, and is followed by a very short 3'UTR. Protein sequence alignments revealed that mouse ERK3 shares 93% amino acid identity with human ERK3 and also possesses a C-terminal extension of 177 residues compared to the published rat ERK3 sequence (Fig. 1B). Like the human and rat proteins, mouse ERK3 contains the SEG motif in the activation loop and the sequence SPR rather than APE in subdomain VIII, features that distinguish ERK3 from other MAP kinase subfamilies.

Expression of ERK3 in embryonic and adult mouse tissues

The expression pattern of *Erk3* mRNA in various adult tissues and at distinct developmental stages of the mouse was determined by Northern blot analysis. Total RNA was extracted from multiple mouse tissues and hybridized with a radiolabeled 0.9-kb probe from the 3' end of the mouse ERK3 cDNA. A single transcript of 4.5 kb was detected in every adult tissue examined, but the relative level of expression varied considerably from one tissue to another (Fig. 2A). The highest expression was found in the brain.

A developmental study revealed that ERK3 expression is acutely regulated during mouse ontogeny. The expression of *Erk3* mRNA dramatically increases from embryonic day 9 to 11, followed by a gradual downregulation up to birth (Fig. 2B). These findings are in agreement with previous observations that *ERK3* mRNA is expressed at highest levels in the developing spinal cord and hippocampus of the rat [6]. It was also shown that *Erk3* transcripts strongly increase upon differentiation of P19 embryonal carcinoma cells toward the neuronal or muscle lineage [6]. All these observations support the idea that ERK3 may play unique signaling roles in cell differentiation and development. It is interesting to note

that the induction of ERK3 expression, which is detected by day 9 to 11 after fertilization, is coincident with the period of early organogenesis in the mouse embryo.

ERK3 is a unique gene product of 100 kDa

As mentioned above, two forms of ERK3 have been described so far, a short form of 62 kDa cloned from the rat [6] and a human homolog which encodes a longer protein of ~ 97 kDa [7, 8]. We carried out a series of experiments to characterize the mouse ERK3 protein and to help resolve the ambiguity about the existence of two putative forms of the enzyme. *In vitro* transcription-translation of the mouse and human ERK3 cDNAs generated a specific protein product with an apparent molecular mass of ~100 kDa (Fig. 3A). To identify ERK3 in intact mouse tissues, we used a commercially available antibody raised to an internal sequence of ERK3 conserved in mouse, rat and human ERK3, but not in the related protein $p63^{MAPK}$. Immunoblot analysis of whole embryo extracts detected a protein of 100 kDa, as well as a few other bands which may represent degradation products (Fig. 3B). No band was detected at 62 kDa. Similarly, analysis of cellular extracts from more than 40 human cell lines of diverse histogenesis using the same antibody identified an immunoreactive band at 100 kDa, but no 62-kDa protein (Coulombe P and Meloche S, unpublished observations). The results presented in Fig. 3B also confirmed that ERK3 protein abundance is maximal at embryonic day 11 and subsequently decreases to very low levels in late embryos and neonates.

Nucleotide sequence alignment of rat, mouse and human ERK3 cDNAs revealed that the published rat sequence [6] has a missing nucleotide between codons 502 and 503. Addition of a single nucleotide at this position shifts the reading frame of rat ERK3, which now becomes parallel to the mouse cDNA (and human) protein and translates into a protein of 720 amino acids with 98% overall amino acid identity. To clarify this issue, a pair of primers encompassing the region encoding amino acids 440 to 555 of rat ERK3 was used to amplify reverse transcribed cDNA prepared from rat brain, heart and kidney RNA, as well as rat genomic DNA. A single PCR product of the expected size was obtained with all four templates. Sequence analysis of several PCR products showed that they all contain an additional guanosine residue at codon 503 (Fig. 4). The rat *Erk3* gene is therefore unlikely to encode a 62 kDa protein.

In addition to the results presented above, a number of observations are also inconsistent with the hypothesis of two distinct forms of ERK3. Northern blot analysis of RNA from various tissues and cell lines detects only one transcript ([6-8]; this study). The possibility that the human genome contains two ERK3-related genes (other than $p63^{MAPK}$)

is also unlikely, since fluorescence *in situ* hybridization analysis with the full-length human ERK3 cDNA revealed a single chromosomal locus [8]. Also, a recent BLAST search of the dbEST database of the NCBI failed to identify any ERK3-related sequences other than $p63^{MAPK}$. We conclude from these observations that ERK3 is a unique gene product of 100 kDa.

Chromosomal localization of the murine *Erk3* gene

We have used the interspecific backcross panel BSS from The Jackson Laboratory to determine the chromosomal localization of the gene encoding mouse ERK3. A 200-bp DNA product corresponding to the mouse *Erk3* exon encoding amino acids 235 to 288 was used as probe for Southern blot analysis of C57BL/6J and *M. spretus* parental strain DNA. A single hybridization band was detected in each digestion, indicating that the *Erk3* gene is present at a single locus in the mouse genome (Fig. 5A). An informative RFLP was found with this probe in a MspI digest (Fig 5A) and used to type 94 progeny from the Jackson BSS. The position of the *Erk3* gene (approved name *Prkm6*) was unambiguously assigned to central Chromosome 9 based on the results of haplotype analysis (Fig. 5B). The position and intergenic distances for *Prkm6* relative to other DNA markers on mouse Chromosome 9 are shown in Fig. 5C. *Prkm6* cosegregates with previously mapped loci that include *Adam10* and *Myo1e*. *Myo5a,* a marker of the mouse mutation *dilute,* also maps to this region of the Jackson BSS panel. However, this locus presents one double crossover typing that is believed to be a typing error. If the double crossover typing is an error, *Myo5a* cosegregates with *Adam10*, *Myo1e*, and *Prkm6*. Comparing the location of *Prkm6* with Chromosome 9 data in the Mouse Genome Database (http://www.informatics.jax.org) therefore suggests that *Prkm6* is located near the mouse mutation *dilute*. The *dilute* locus is associated with abnormal melanocyte morphology, neurological defects and, in some mutant forms, early death [20]. The human *ERK3* gene has been mapped by fluorescence *in situ* hybridization to Chromosome 15q21 [8] and *MYO5A*, also maps within this region. Thus, mutations at *Prkm6* could contribute to some of the phenotypes associated with the mouse mutations *dilute*.

ACKNOWLEDGEMENTS

We thank P. Coulombe for valuable discussions, L. Rowe and M. Barter for their generous help in interpreting mapping data. We also thank J. Vacher for the rpL32 probe. This work was supported in part by a grant from the Medical Research Council of Canada. B. Turgeon and M. K. Saba-El-Leil are recipients of studentships from the Heart and Stroke Foundation of Canada and MRC/Rhone Poulenc Rorer, respectively. S. Meloche is a Scientist of the Medical Research Council of Canada.

FOOTNOTES

The abbreviations used are: MAP, mitogen-activated protein; ERK, extracellular signal-regulated kinase; JNK, c-Jun N-terminal kinase; RT, reverse transcription; PCR, polymerase chain reaction; TBS, Tris-buffered saline; RFLP, restriction fragment length polymorphism.

A

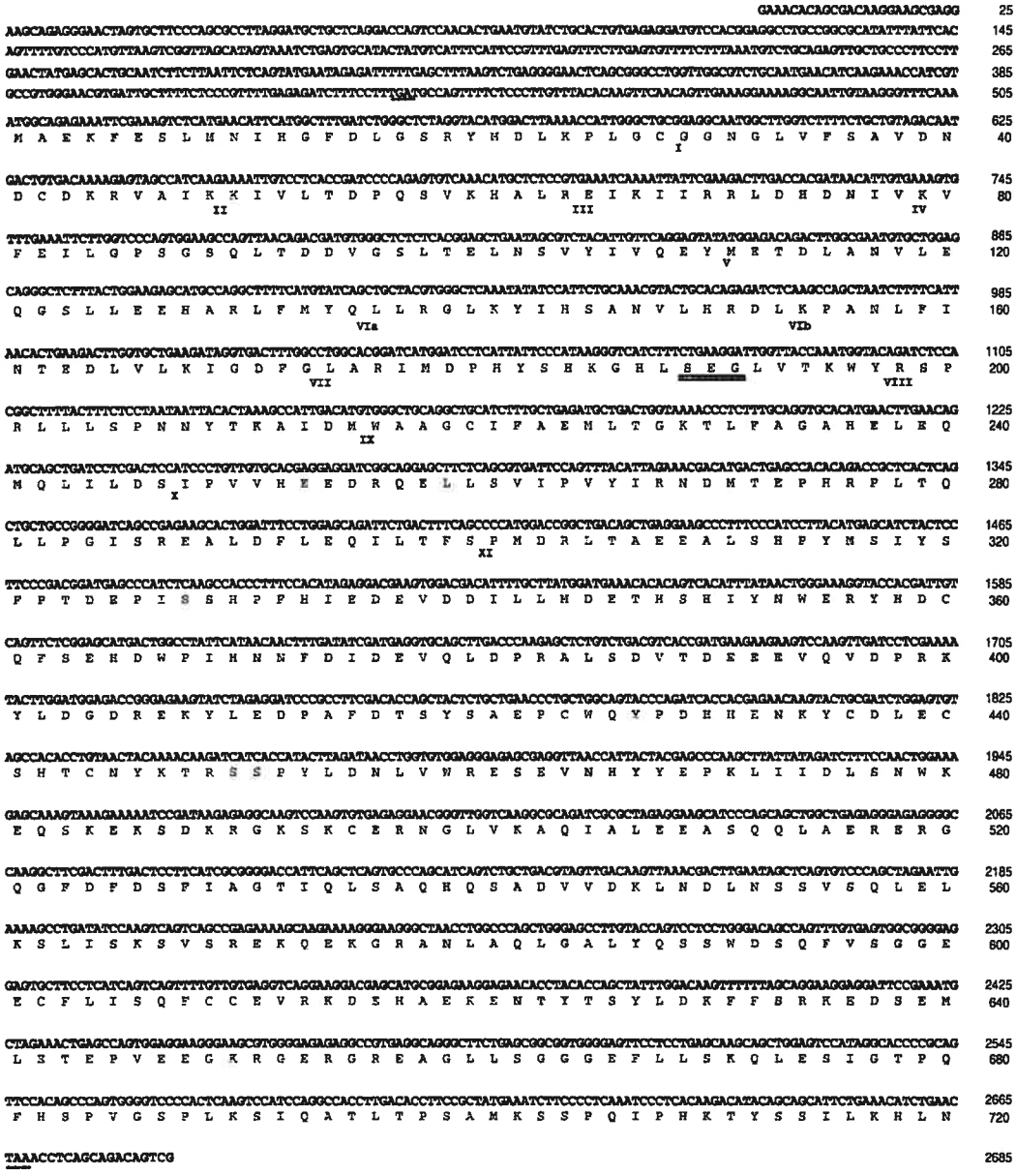

Fig. 1: Mouse ERK3 cDNA encodes a predicted protein of 720 amino acids highly homologous to human ERK3. **A)** Nucleotide and deduced amino acid sequence of the mouse ERK3 cDNA. Stop codons are underlined. Locations of conserved protein kinase subdomains are indicated by roman numerals. The SEG motif is underlined twice. The Genbank accession number for this sequence is AF132850. **B)** See below.

B

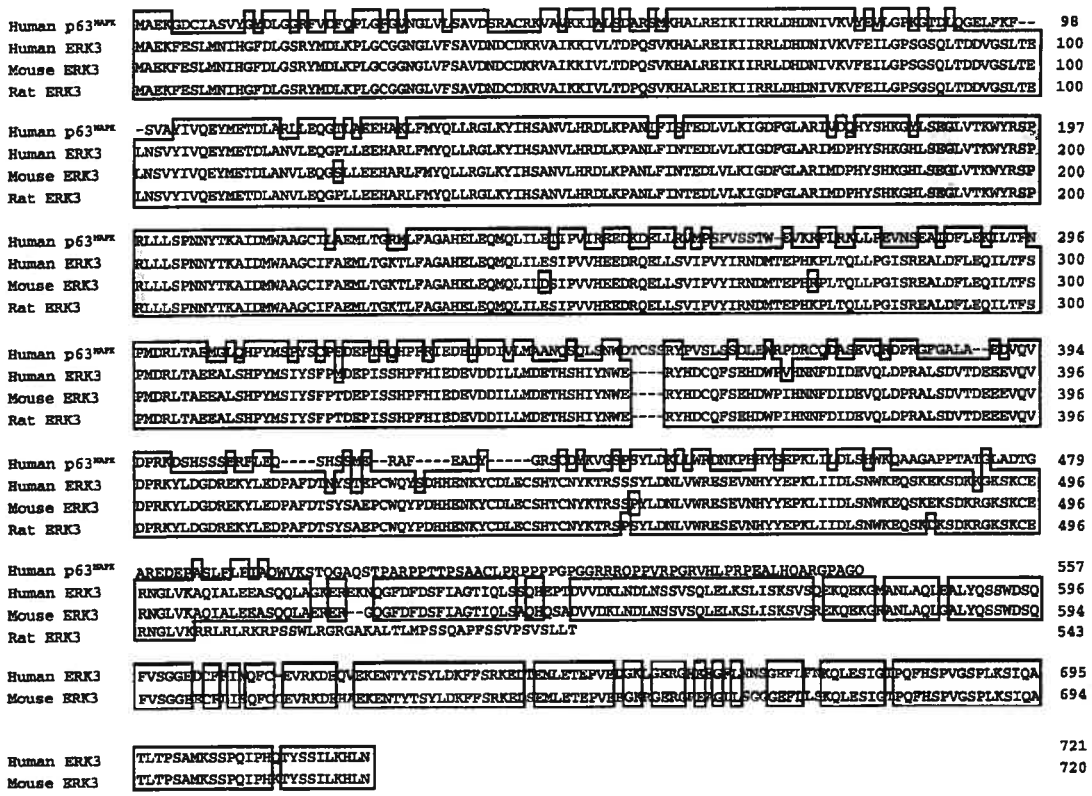

Fig. 1: Cont'd

B) Comparison of mouse ERK3 with others ERK3 homologs and p63^{MAPK}. The protein sequences were aligned using the GeneWorks software. Amino acid residues that are identical between proteins are boxed. SEG and SPR motifs are shaded.

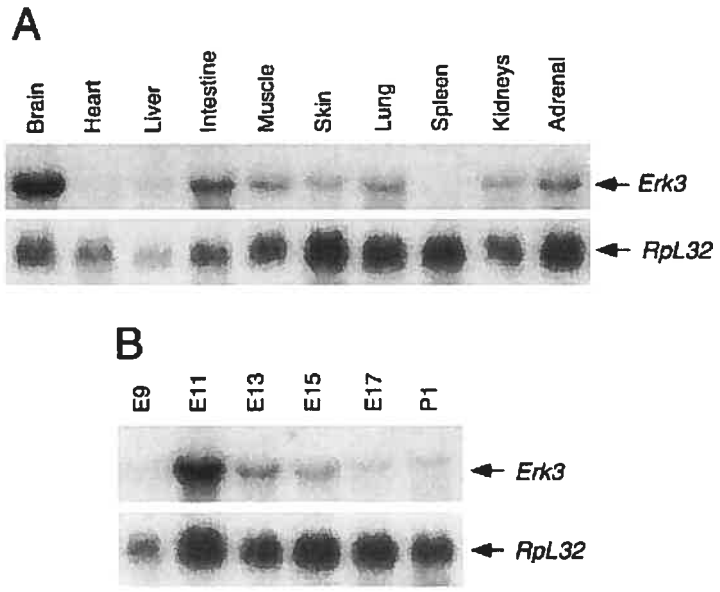

Fig. 2: Northern blot analysis of *Erk3* mRNA expression in the mouse. Total RNA (20 μg) isolated from various adult mouse tissues **(A)** and from embryos **(B)** at different developmental stages (E9 to E17 and P1) was analyzed by Northern hybridization using a ^{32}P-labeled ERK3 cDNA probe. RNA levels were normalized by rehybridization of the blot with a ribosomal protein L32 probe. E: embryonic day; P: postnatal day. The results are representative of two independent experiments.

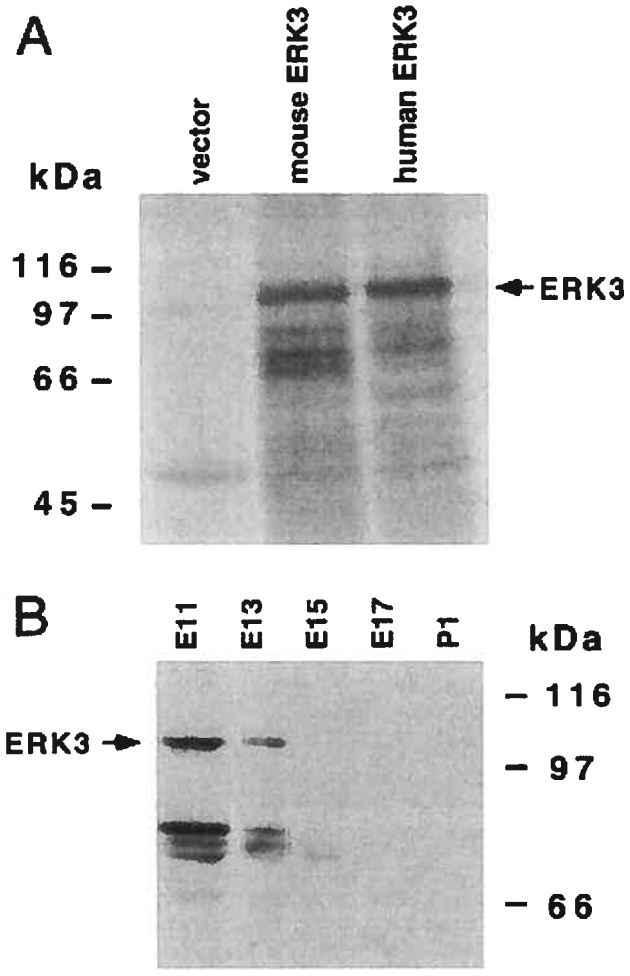

Fig. 3: Mouse ERK3 is a unique protein of 100 kDa. **A)** *In vitro* translation of mouse ERK3 cDNA. The full-length mouse and human [8] ERK3 cDNAs subcloned in pBK-CMV were translated *in vitro* using a coupled transcription/translation rabbit reticulocyte system in the presence of ^{35}S methionine. Labeled proteins were resolved by SDS- gel electrophoresis, transferred to a nitrocellulose membrane and visualized with a PhosphorImager. **B)** Immunoblot analysis. Protein extracts (100 μg) of whole mouse embryos at different developmental stages were resolved by SDS-gel electrophoresis and electrotransferred to nitrocellulose membrane. The membrane was probed with an ERK3-specific antibody and the proteins visualized by chemiluminescence detection. The position of ERK3 is indicated by an arrow. The results are representative of three independent experiments.

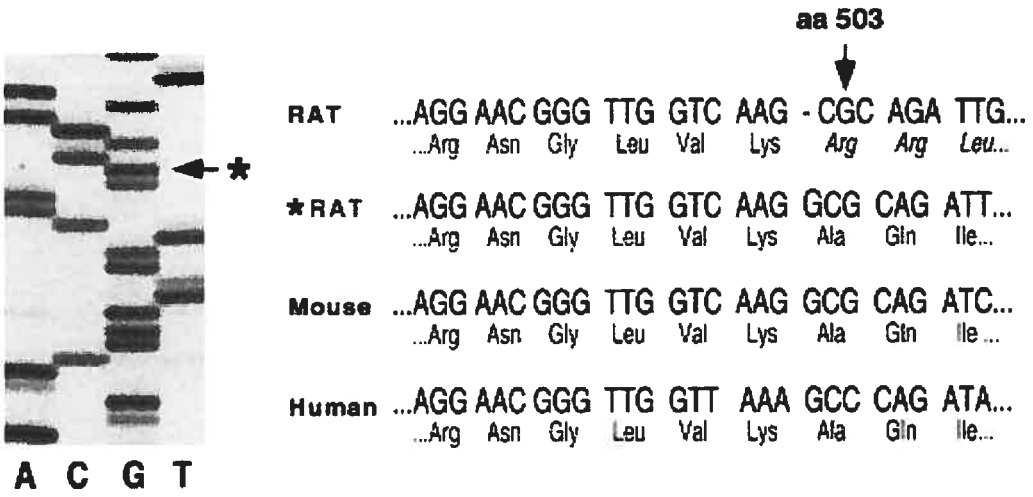

Fig. 4: Partial nucleotide sequence of rat *Erk3* cDNA and gene. Total RNA from rat brain, kidney and heart were used as template for the synthesis of first-strand cDNA using the M-MLV reverse transcriptase. Genomic DNA was isolated from rat vascular smooth muscle cells. This material was amplified by PCR using a combination of primers spanning nucleotides 1710 to 2056 of rat ERK3 cDNA sequence [6]. A unique DNA fragment of 345 bp was amplified from each template (data not shown). The PCR products were directly sequenced in the presence of dITP instead of dGTP. Sequences of both *Erk3* cDNAs and gene show the presence of an additional guanosine residue at codon 503 (shown by an asterisk) as compared to the published rat ERK3 nucleotide sequence. The frameshift predicted for this insertion in the rat ERK3 amino acid sequence is shown on the right. The homologous sequences of mouse and human cDNAs are also shown below.

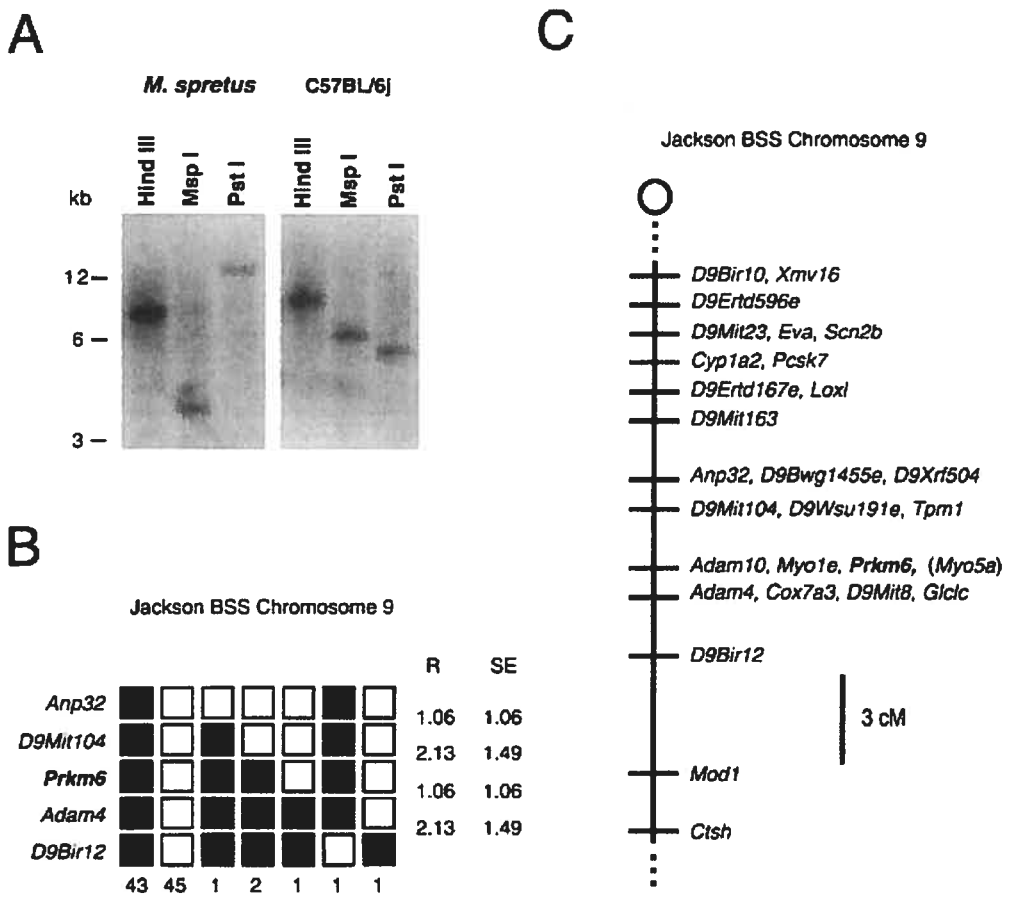

Fig. 5: *Prkm6* maps to the central region of mouse Chromosome 9. **A)** Southern blot analysis of *Mus spretus* and C57BL/6J genomic DNA digested with various enzymes. The blot was probed with a 200-bp genomic probe corresponding to the exon encoding amino acids 235 to 288 of mouse ERK3. **B)** Haplotype figure from The Jackson BSS backcross showing part of Chromosome 9 with loci linked to *Prkm6*. Loci are listed in order with the most proximal at the top. The black boxes represent the C57BL6/JEi allele and the white boxes the SPRET/Ei allele. The number of animals with each haplotype is given at the bottom of each column of boxes. The percent recombination (R) between adjacent loci is given to the right of the figure with the standard error (SE) for each R. Missing typings were inferred from surrounding data where assignment was unambiguous. **C)** Map figure from The Jackson BSS backcross showing part of Chromosome 9. The map is depicted with the centromere toward the top. A 3 cM scale bar is shown to the right of the figure. Loci mapping to the same position are listed in alphabetical order. Raw data from The Jackson Laboratory were obtained from the World Wide Web address http://www.jax.org/resources/documents/cmdata. *Myo5a*, listed in parentheses, has one double crossover typing that is believed to be a typing error. The mouse loci symbol *Prkm6* has been approved by the Mouse Nomenclature Committee.

REFERENCES

1 Robinson, M. J. and Cobb, M. H. (1997) Curr. Opin. Cell Biol. **9**, 180-186

2 Ip, Y. T. and Davis, R. J. (1998) Curr. Opin. Cell Biol.**10**, 205-219

3 Widmann, C., Gibson, S., Jarpe, M. B. and Johnson, G. L. (1999) Physiol. Rev. **79**, 143-180

4 Kyriakis, J. M. and Avruch, J. (1996) J. Biol. Chem. **271**, 24313-24316

5 Lewis, T. S., Shapiro, P. S. and Ahn, N. G. (1998) Adv. Cancer Res. **74**, 49-139

6 Boulton, T. G., Nye, S. H., Robbins, D. J., Ip, N. Y., Radziejewska, E., Morgenbesser, S. D., DePinho, R. A., Panayotatos, N., Cobb, M. H. and Yancopoulos, G. D. (1991) Cell **65**, 663-675

7 Zhu, A. X., Zhao, Y., Moller, D. E. and Flier, J. S. (1994) Mol. Cell. Biol. **14**, 8202-8211

8 Meloche, S., Beatty, B. G. and Pellerin, J. (1996) Oncogene **13**, 1575-1579

9 Garcia, J. I., Zalba, G., Detera-Wadleigh, S. D. and de Miguel, C. (1996) Mamm. Genome **7**, 810-814

10 Gonzalez, F. A., Raden, D. L., Rigby, M. R. and Davis, R. J. (1992) FEBS Lett. **304**, 170-178

11 Lee, J. D., Ulevitch, R. J. and Han, J. (1995) Biochem. Biophys. Res. Commun. **213**, 715-724

12 Zhou, G., Bao, Z. Q. and Dixon, J. E. (1995) J. Biol. Chem. **270**, 12665-12669

13 Abe, M. K., Kuo, W. L., Hershenson, M. B. and Rosner, M. R. (1999) Mol. Cell. Biol. **19**, 1301-1312

14 Cheng, M., Boulton, T. G. and Cobb, M. H. (1996) J. Biol. Chem. **271**, 8951-8958

15 Cheng, M., Zhen, E., Robinson, M. J., Ebert, D., Goldsmith, E. and Cobb, M. H. (1996) J. Biol. Chem. **271**, 12057-12062

16 Meloche, S., Pages, G. and Pouyssegur, J. (1992) Mol. Biol. Cell **3**, 63-71

17 Chomczynski, P. and Sacchi, N. (1987) Anal. Biochem. **162**, 156-159

18 Sambrook, J., Fritsch, E. F. and Maniatis, T. (1989) Molecular Cloning: a laboratory manual, Cold Spring Harbor Laboratory Press, New York

19 Rowe, L. B., Nadeau, J. H., Turner, R., Frankel, W. N., Letts, V. A., Eppig, J. T., Ko, M. S., Thurston, S. J. and Birkenmeier, E. H. (1994) Mamm. Genome **5**, 253-274

20 Strobel, M. C., Seperack, P. K., Moore, K. J., Copeland, N. G. and Jenkins, N. A. (1988) Prog. Clin. Biol. Res. **256**, 297-305

CHAPITRE 3

ARTICLE

Analyse génomique de la sous-famille ERK3 des MAP kinases

Arcticle : Genomics **80**(6):673-80; Décembre 2002

MISE EN SITUATION

Après avoir fait la démonstration que ERK3 est le produit unique d'un seul gène, notre objectif de clonage du gène *Erk3* chez la souris s'en trouvait simplifié. Le chapitre 3 rapporte donc le clonage du gène *Erk3* chez la souris et la détermination de son organisation intron-exon. De plus, un pseudogène de *Erk3* a été identifié par clonage moléculaire.

Ce travail rapporte également l'étude de la sous-famille ERK3 des MAP kinase chez l'humain, à partir des séquences humaines disponibles à ce moment. Cette analyse a tout d'abord permis d'identifier un nombre important de pseudogène de ERK3 dans la séquence génomique humaine. Par ailleurs, la structure du gène ERK3 a pu être comparée à celle de ERK4 pour confirmer que ces deux gènes sont des paralogues. De façon importante, ce travail confirme l'existence d'un seul gène fonctionnel encodant ERK3 chez l'humain et la souris.

The MAP kinase ERK3 is Encoded by a Unique Functional Gene: Genomic Analysis of the ERK3 Gene Family

Benjamin Turgeon[1], B. Franz Lang[2], and Sylvain Meloche[1,*]

[1] Institut de recherches cliniques de Montréal and Departments of Pharmacology and Molecular Biology, Université de Montréal, Montréal, Québec, Canada H2W 1R7
[2] Program in Evolutionary Biology, Canadian Institute for Advanced Research, Department of Biochemistry, Université de Montréal, Montréal, Québec, Canada H3T 1J4

Sequence data from this article have been deposited in GenBank under Accession Nos. AY134879, AY134880, AY134881, AY134882, AY134660, AY134883 (*Mapk6*) and AY134661 (*Mapk6-ps1*).

* Corresponding author: Dr. Sylvain Meloche
Institut de recherches cliniques de Montréal
110 Pine Avenue West
Montréal (Québec) H2W 1R7
Canada
Tel.: (514) 987-5783
Fax: (514) 987-5536

E-mail: [redacted]

ABSTRACT

Extracellular signal-regulated kinase 3 (ERK3) is a distantly related member of the mitogen-activated protein (MAP) kinase family of serine/threonine kinases. Here, we report the characterization of the genomic loci encoding ERK3 in mice and humans. The mouse ERK3 gene (*Mapk6*) spans more than 20 kb and is split into six exons. Its structure is similar to the human *MAPK6* gene, which extends over 40 kb. We also identified and characterized a mouse *Mapk6* processed pseudogene. In humans, database analysis has revealed the presence of six *MAPK6* processed pseudogenes localized on four different chromosomes. We further show that the structure of *MAPK6* is closely related to the gene encoding the homologous protein kinase $p63^{MAPK}$ (*MAPK4*), suggesting that the two genes arose by duplication. Our analysis demonstrates that the ERK3 subfamily of MAP kinase genes is composed of two functional genes, *MAPK6* and *MAPK4*, and several pseudogenes.

Keywords: MAP kinase, ERK3, $p63^{MAPK}$, cloning, gene family, pseudogenes.

INTRODUCTION

Mitogen-activated protein (MAP) kinases are a superfamily of serine/threonine kinases that play a major role in transducing extracellular chemical and physical signals into intracellular responses [reviewed in 1-3]. These enzymes are components of signaling pathways that control a wide variety of biological responses including embryonic development, cell proliferation, differentiation, cell survival, and adaptation [1, 2, 4]. MAP kinase pathways are conserved through evolution and homologues of many of the mammalian kinases have been found in yeast, *C. elegans* and *D. melanogaster* [3]. In mammals, nearly 20 genes encoding conventional MAP kinases and related protein kinases have been identified so far [2, 5].

Extracellular signal-regulated kinase 3 (ERK3) is a MAP kinase homologue that was first identified a decade ago by screening of a rat cDNA library using an ERK1-derived probe [6]. Later, the sequences of the human [7, 8] and mouse [9] homologs were reported. Human ERK3 is a 721-amino acid protein that shares about 50% amino acid identity with the MAP kinases ERK1/2 in the catalytic domain. However, several features distinguish ERK3 from other family members. First, ERK3 contains a single phospho-acceptor site (SEG) in its activation loop, instead of the highly conserved Thr-X-Tyr motif found in conventional MAP kinases. This structural characteristic is shared by the ERK3-related protein $p63^{MAPK}$, which displays 73% amino acid identity with ERK3 in the kinase domain [10]. Second, ERK3 and $p63^{MAPK}$ have the amino acid sequence SPR instead of APE in subdomain VIII of the kinase domain. Third, ERK3 has a long C-terminal extension rich in serine and threonine residues. Although the exact cellular function of ERK3 is unknown, a number of observations suggest that the kinase may regulate cell differentiation. We found that expression of *Erk3* mRNA increases markedly from days 9 to 11 in the developing mouse embryo, followed by a gradual decrease up to birth [9]. *Erk3* transcripts are up-regulated upon differentiation of P19 embryonal carcinoma cells to neuronal or muscle cells [6], and by treatment of the Burkitt lymphoma cell line Raji with growth inhibitory gangliosides [11]. In addition, it was recently reported that the luteolytic factor prostaglandin $F_{2\alpha}$ ($PGF_{2\alpha}$) stimulates the accumulation of *Erk3* mRNA in the rat corpus luteum in vivo [12].

A single gene encoding ERK3 (*MAPK6*) has been mapped to chromosome 15q21 in the human genome [7]. In the mouse, the ERK3 gene (*Mapk6*) was mapped to a single locus on central chromosome 9, adjacent to the *dilute* mutation and in a region syntenic to human chromosome 15q21 [9]. No homologs of ERK3 have been identified in invertebrates. Intriguingly, Southern blot analysis with ERK3-specific probes has revealed the presence of multiple hybridizing bands in human genomic DNA [6, 7], suggesting the existence of several ERK3-related gene loci. In this study, we have cloned the mouse ERK3 gene (*Mapk6*),

determined its organization, and compared it to the structure of human MAP kinase genes. We show that the genomic structures of the mouse and human ERK3 genes are evolutionarily conserved, and are similar to that of the human $p63^{MAPK}$ gene (*MAPK4*). Furthermore, we provide evidence for the existence of at least one ERK3 pseudogene in the mouse genome and six pseudogenes in the human genome. Our analysis demonstrates that the ERK3 subfamily of MAP kinase genes is composed of *MAPK6*, *MAPK4*, and several pseudogenes.

RESULTS AND DISCUSSION

Organization of the mouse *Mapk6* gene

To isolate genomic clones encoding mouse ERK3, we screened a mouse 129Sv genomic library in λGem12 with a human ERK3 cDNA probe [7]. This first screen yielded two positive non-overlapping clones designated λK3-2 and λK3-11. Sequence analysis revealed that λK3-2 contains the translation initiation codon of ERK3 and downstream coding sequences, interrupted by a single intron. The second clone encodes a full-length intronless copy of the ERK3 cDNA and will be described below. Using probes derived from the λK3-2 clone, we searched for additional genomic clones that overlap with λK3-2 by chromosomal walking. From this second screen, we were able to reconstitute most of the Mapk6 gene, except for the 3'-end of the gene that was still missing. In order to obtain the complete sequence of the gene, we screened BAC filters with a 198 bp exon-intron genomic probe [9] and isolated a positive BAC clone (LP39E18). Southern blot analysis and DNA sequencing confirmed that this BAC clone contains the entire Mapk6 gene.

The mouse Mapk6 gene spans 20 kb and comprises 6 exons (Fig. 1A). The exons range in size from 140 to 2207 bp (Table 1). The first exon encodes part of the 5' non-coding sequence and is separated from the second exon, that contains the translation initiation codon, by an intron of approximately 11 kb. The catalytic domain of ERK3 is encoded by exons 2, 3, 4 and 5. Exon 6 encodes the C-terminal extension of the kinase in addition to the 3' untranslated region, which includes a number of putative polyadenylation signals. DNA sequence analysis confirmed that the intron-exon junctions conform to the consensus splice donor-acceptor rule [13] and that the invariable AG at the 3' splice site is always preceded by a characteristic pyrimidine tract. The size of introns was estimated by PCR amplification using primers located in the corresponding flanking exons (Table 1). Primer extension experiments localized the predominant transcription start site of Mapk6 gene to a guanosine nucleotide 140 bp from the 3' end of the first exon (data not shown).

Identification of a mouse *Erk3* pseudogene

The screening for genomic clones containing the 3' end of the *Mapk6* gene was complicated by the presence of highly similar sequences. Several positive clones that did not correspond to the *Mapk6* gene were isolated and found to overlap into an independent contig. Restriction analysis and DNA sequencing strongly suggests that this locus represents a *Mapk6* processed pseudogene referred to as *Mapk6-ps1* (Fig. 1B). Processed pseudogenes usually display four main features: they lack introns, they represent a copy of a processed

transcript of the functional gene from which they were derived, they have a poly (A) sequence at the 3' end, and they are flanked by direct repeats which correspond to the integration sites of the pseudogene [14, 15]. Sequence comparison with the mouse ERK3 cDNA [9] revealed that, in addition to lacking introns, the *Mapk6-ps1* pseudogene is truncated at the 5' untranslated region, and contains a 5 bp insertion in the coding sequence that causes a frameshift introducing a premature termination codon. The translation initiation codon is conserved and the two sequences present a sequence identity of 97% in the coding region. A poly (A) tail is present at the 3' end of *Mapk6-ps1* sequence, and direct repeats are found at the 5' and 3' junctions. The high sequence similarity between the *Mapk6* and *Mapk6-ps1* suggests that the pseudogene results from a recent retrotransposition event.

Southern analysis suggests that additional *Mapk6*-related sequences are unlikely to be found in the mouse genome. Hybridization with a cDNA fragment corresponding to exon 6 of *Mapk6* reveals only two bands, whereas an intron-containing probe hybridizes to a single fragment corresponding to the functional gene [data not shown and 9]. Thus, our analysis suggests that there are only two *Mapk6*-like sequences in the mouse genome: the functional *Mapk6* gene mapping to central chromosome 9, and the *Mapk-ps1* sequence that displays the hallmarks of a processed pseudogene. We have not determined whether *Mapk-ps1* is expressed, which, however, is unlikely as no cDNA or EST clone with this sequence have been isolated yet. Furthermore, Northern blot analysis of mouse tissues identified a single ERK*3* transcript [9]. The chromosomal localization of *Mapk-ps1* remains to be established.

The *ERK3* gene family in human

Southern blot analysis of human genomic DNA with ERK3 cDNA probes identified multiple strongly hybridizing fragments, suggesting that the human genome contains numerous ERK3-related sequences [6, 7]. To clarify this issue, we performed a comprehensive analysis of the human genome database. BLAST searches of the database with the full-length human ERK3 cDNA [7, 8] revealed the presence of eight ERK3-related sequences (Fig. 2). Only two of these sequences contain introns. One sequence that localizes to chromosome 15 band q21 represents the genuine *MAPK6* gene encoding ERK3. A second homolog on chromosome 18q21.1 corresponds to *MAPK4*, which encodes the ERK3-related protein kinase $p63^{MAPK}$. The localization of the two genes is in perfect agreement with previously reported FISH analysis [7, 16]. The other six loci correspond to *MAPK6* pseudogenes (see below).

We also used the catalytic domain protein sequences of ERK3 and $p63^{MAPK}$ to perform an iterative search against the translated human genomic sequences available in public databases. No gene other than known members of the MAP kinase family was identified from

this search. We conclude from our analysis that the human genome, as currently sequenced, contains only two functional genes that encode members of the ERK3 subfamily of MAP kinases: *MAPK6* and the $p63^{MAPK}$ gene *MAPK4*.

Human *ERK3* pseudogenes

In addition to the *MAPK6* and *MAPK4* genes, BLAST searches with the ERK3 cDNA revealed the presence of six *MAPK6*-related sequences localized on four different chromosomes (Fig. 2 and Table 2). Three of the sequences were found on chromosome 8. Sequence analysis indicates that all these loci contain intronless copies of *MAPK6* that display the hallmarks of processed pseudogenes. Notably, four of the loci are localized near centromeric regions (Fig. 2), that represent a pseudogene hot spot [17].

The six pseudogene sequences, *MAPK6-PS1 to MAPK6-PS6*, are close to 90% identical to the ERK3 cDNA in the coding region (Table 2). However, they all contain numerous nucleotide insertions, deletions and substitutions that result in the introduction of multiple termination codons in all reading frames (Fig. 3). *MAPK6-PS1*, *MAPK6-PS2* and *MAPK6-PS5* display simlarity throughout the entire ERK3 cDNA sequence, whereas *MAPK6-PS3* lacks the 5' half of the sequence. The *MAPK-PS4* and *MAPK-PS6* pseudogenes are also characterized by large deletions. ATG codons are absent in *MAPK-PS3*, *MAPK-PS4*, *MAPK-PS5* and *MAPK-PS6*, but they all have a conserved stop codon (TAA) at a position corresponding to the ERK3 cDNA. *MAPK-PS2* and *MAPK-PS4* also contain large insertions of an endogenous retroviral sequence (HERV-K). Among all pseudogenes, only *MAPK-PS6* has a complete open reading frame (ORF). However, this ORF does not coincide with that of ERK3.

All the pseudogene sequences contain an adenine-rich region, but the position of the poly (A) tract differs with respect to the ERK3 cDNA. The *MAPK6* gene contains 4 putative polyadenylation signals that are located 205, 590, 1124 and 1242 nucleotides after the stop codon. *MAPK-PS1*, *MAPK-PS3* and *MAPK-PS4* possess a poly (A) tract that is downstream of the second polyadenylation signal, whereas the poly (A) sequence of the three other pseudogenes is after the third signal. Since pseudogenes arise by retrotransposition of a processed mRNA, these observations implicate that two transcripts of *MAPK6* gene likely exist in cells, and consequently that the two putative polyadenylation signals are functional. We also analyzed the regions surrounding the pseudogene integration sites. Processed pseudogenes are non-autonomous transposable elements that are dependent on other transposable elements for their mobility [18]. Computer searches revealed that all pseudogene sequences are flanked by interspersed repeats [19] of various types, including LINEs, SINEs and LTR elements (Fig.

3). It has been reported that LINE retrotransposons can mobilize pseudogenes in mammalian cells [20]. All these observations are consistent with the idea that *MAPK-PS1* to *MAPK-PS6* pseudogenes were generated by retrotransposition in the human genome. It is not known whether the pseudogenes originated from a single retrotranspositional event, or if some of them have been duplicated or evolved from one another.

We have not addressed experimentally if the human *MAPK6* pseudogenes are transcribed. However, as for the mouse *Mapk6-ps1* pseudogene, no cDNA clone corresponding to these sequences has been isolated and no EST clone has been retrieved from available databases. In support of these observations, Northern blot analysis with ERK3-specific probes identified a unique transcript in various human cell lines [7, 8]. Further analysis of the human genome sequence database also failed to reveal the presence of *MAPK4* pseudogene.

Comparison of the mouse and human *ERK3* genes

The organization of the human *MAPK6* gene is very similar to that of the mouse *Mapk6* gene, except that the human gene is more than twice the length of its mouse counterpart. The position of the exon/intron boundaries is well conserved between the two orthologous genes and the sizes of exons are comparable (Fig. 4). The first and last exons have different sizes due to variations in the length of the UTR regions between human and mouse. The *MAPK6* gene contains a large intron in the leader region upstream the second exon that includes the initiation codon, a feature shared with the mouse ortholog gene *Mapk6*, but that is not observed in the *MAPK4* gene. Such particular organization may confer to the *MAPK6* gene transcriptional regulatory properties distinct from *MAPK4* or from conventional MAP kinase genes. In addition to the conservation of their gene structure, the mouse and human ERK3 proteins are highly similar sharing 94% overall amino acid identity [9]. In the catalytic kinase domain, the similarity raises to 99%. This high level of evolutionary conservation suggests that ERK3 protein fulfills important cellular functions that are likely to be conserved among species.

Evolutionary origin of the *MAPK6* gene

The structural organization of the *MAPK6* gene is different from that of genes encoding conventional MAP kinases and related protein kinases. Athough ERK3 is more similar to ERK1 in its catalytic domain than to any other protein kinase (with the exception of $p63^{MAPK}$), the gene encoding ERK3 does not retain the basic exon/intron structure of the ERK1 gene, notably with regard to the exonic organization of kinase subdomains (Fig. 5). The kinase domain of ERK3 is encoded by 4 exons, whereas the ERK1 kinase domain spreads over 7

exons. While kinase subdomains I to VIII are encoded by a single exon in ERK3 gene, they are split into 4 exons in the ERK1 gene. The structure of the *MAPK6* gene is more closely related to *MAPK4*, and the two genes have a similar organization of exon/intron boundaries (Fig. 4). The high amino acid identity between ERK3 and p63^{MAPK} within the kinase domain, together with their conserved structural organization, strongly suggest that the *MAPK6* and *MAPK4* genes arose by duplication of a common ancestor gene. This further substantiates the idea that ERK3 and p63^{MAPK} define a distinct subfamily of MAP kinases.

Gene structure conservation is also observed within other MAP kinase subfamilies. The ERK1 and ERK2 genes present a similar organization, as well as the three JNK and the four p38 MAP kinase genes. In addition, exon correspondence is observed between genes from different subfamilies. For example, the genes encoding JNK1, p38α and NLK all have 2 exons of similar sizes encoding kinase subdomains II, III and IV (Fig. 5). This implies that these genes present an evolutionary connection, as would be expected for a gene superfamily.

The homology of ERK3 and p63^{MAPK} with conventional MAP kinases in the catalytic domain argues that the two enzymes are members of the superfamily of MAP kinases. However, it has proven to be difficult to retrace the origin of the common ancestor gene for *MAPK6* and *MAPK4* within the MAP kinase gene family. First, very few sequences of ERK3 and p63^{MAPK} are available and, contrary to conventional MAP kinases, there are no homologues of ERK3 or p63^{MAPK} in invertebrates. Second, as mentioned above, the structure of the genes encoding ERK3 and p63^{MAPK} is different from that of other MAP kinases. Third, rigorous phylogenetic analysis of MAP kinase-related protein sequences has been limited by the difficulty of clustering the ERK3, p63^{MAPK} and ERK7 sequences with other conventional MAP kinases [21]. Despite the fact that sequence signatures common to MAP kinases are also found in ERK3 [22], phylogenic analysis do not enable us to demonstrate a significant relationship between the ERK3 subfamily and other subfamilies of MAP kinases. It is clear however that ERK3 and p63^{MAPK} cluster together with strong support (data not shown), suggesting that they define a typical gene family. A meaningful analysis of the evolutionary relationship of ERK3 with other MAP kinases requires the identification of ERK3 orthologs from several non-mammalian vertebrate species.

MATERIALS AND METHODS

General molecular cloning techniques

The preparation of genomic DNA and hybridizations were performed as described previously [9]. λphage DNA was prepared by standard methods [23]. DNA sequences were determined using the ThermoSequenase terminator cycle sequencing kit (Amersham-Pharmacia). The sequences were assembled using the Sequencher 3.1 software (GeneCodes Corporation).

Isolation of mouse *Mapk6* genomic clones

Mouse *Mapk6* genomic clones were isolated by screening of a 129Sv genomic library in λGem12 as described in detail elsewhere [9]. The library was initially screened with a 0.2 kb *Acc*I/*Apa*I fragment derived from the human ERK3 cDNA [7]. Then, additional probes were derived from a genomic clone containing the central part of the *Mapk6* gene to isolate clones containing the 5' and 3' ends of the gene. To obtain the complete sequence of the gene, mouse genomic high-density BAC filters (96021; Research Genetics) were screened with a 198 bp kb genomic probe, corresponding to an exon-intron boundary of the gene [9] according to the manufacturer's recommendations. The clones were analyzed by restriction mapping, Southern hybridization, and DNA sequencing.

Analysis of *Mapk6* introns

The size of introns was determined by PCR using flanking primers derived from the ERK3 cDNA sequence. PCR amplification conditions were: 94°C at 2 min.; followed by 30 cycles of denaturation (94°C for 30 sec), annealing (55°C for 30 sec), and extension (72°C for 3 min) using Taq DNA polymerase (Gibco). Intron 1 was amplified with Klentac (Sigma) according to the manufacturer's specifications.

Database search and sequence analysis

To identify ERK3-related sequences, we performed similarity searches between the human ERK3 cDNA sequence (acc. # L77964) and the human genome sequence database at the NCBI using the basic local alignment search tool (BLASTN) in addition to the BLAT search engine at the UCSC (http://genome.ucsc.edu). All sequences were downloaded and analyzed using the Sequencher software. The sequences mapping to human chromosomes 15q21.2 and 18.21.1 were analyzed for exon-intron organization by comparison with the human ERK3 or $p63^{MAPK}$ (acc. # NM_002748 and NM_002748) cDNA sequences. Pseudogene sequences

including flanking genomic regions were analyzed for the presence of interspersed repeats with the RepeatMasker program (http://ftp.genome.washington.edu/RM/RepeatMasker.html). To search for novel protein kinases similar to ERK3, an iterative BLAST search (PSI-BLAST) was carried out with the kinase domain sequence (amino acids 1 to 316) of ERK3 using standard parameters.

To obtain information about the structure of the different human MAP kinase genes, the human genome sequence database was searched using the BLAST program. The accession numbers of the representative MAP kinase cDNA sequences used for the search are: ERK1 (XM_055766), ERK5 (XM_008323), p38α (NM_001315), JNK2 (NP_002752), and NLK (NM_016231). Gene structure was provided by the evidence viewer at NCBI.

Sequence alignments and phylogenetic analysis

Protein alignments were performed with the CLUSTAL W program [24], which was launched from GDE (Genetic Data Environment; [25]). Only unambiguously aligned amino acid positions, with at least 10% amino acid identity among the selected species, were used in the phylogenetic analysis. For tree construction, we used either a maximum likelihood (PUZZLE 4.02; [26]) or distance approaches. A distance table was calculated using the most recent implementation of PROTDIST, which allows a Jin/Nei correction for unequal rates of change at different amino acid positions (Phylogeny Inference Package Version 3.6 a2; Felsenstein, J.,University of Washington, Seattle), and the tree topology was inferred using WEIGHBOUR [27]. Bootstrap analysis (1000 replicates) was performed according to Felsenstein [28].

ACKNOWLEDGEMENTS

We are grateful to Jean Vacher (IRCM) for help with BAC library analysis. We also thank Marc Saba-El-Leil and Jean-René Basque for critical review of the manuscript. B. Turgeon is recipient of a studentship from the National Cancer Institute of Canada. S. Meloche is an Investigator of the Canadian Institutes for Health Research (CIHR). This work was supported by a grant (MOP-38010) from the CIHR.

TABLE 1: Exon-intron boundaries of the mouse Mapk6 gene

intron boundary sequences		Intron size	Exon	Exon size
5' boundary	3' boundary	kb	no.	bp
AGTCCC gt tgtatc	cacccc ag GTTGTA	11	1	140
CATAAG gt acgtag	ttttcc ag GGTCAT	2	2	1172
TTGCAG gt acgtag	tcactc ag GTGCAC	2	3	145
GAGAAG gt atgggg	cccctt ag CACTGG	3	4	165
GGAAAG gt gggtaa	tgcttc ag GTACCA	1	5	205
			6	2207

TABLE 2: Human *MAPK6* processed pseudogenes

Gene Symbol	Locus	Introns	Poly A	ORF	Homology	Acc. number
MAPK6-PS1	8q11.21	no	yes[1]	no	92%	NT_023678
MAPK6-PS2	8q11.23	no	yes	no	93%	NT_023795
MAPK6-PS3	8q24.12	no	yes[1]	no	96%	NT_008048
MAPK6-PS4	10q11.21	no	yes[1]	no	94%	NT_017696
MAPK6-PS5	13q14.13	no	yes	no	93%	NT_009910
MAPK6-PS6	21q11.12	no	yes	yes[2]	89%	NT_011512

[1] The position of poly(A) tails varies among pseudogenes

[2] The putative ORF do not correspond to that of ERK3

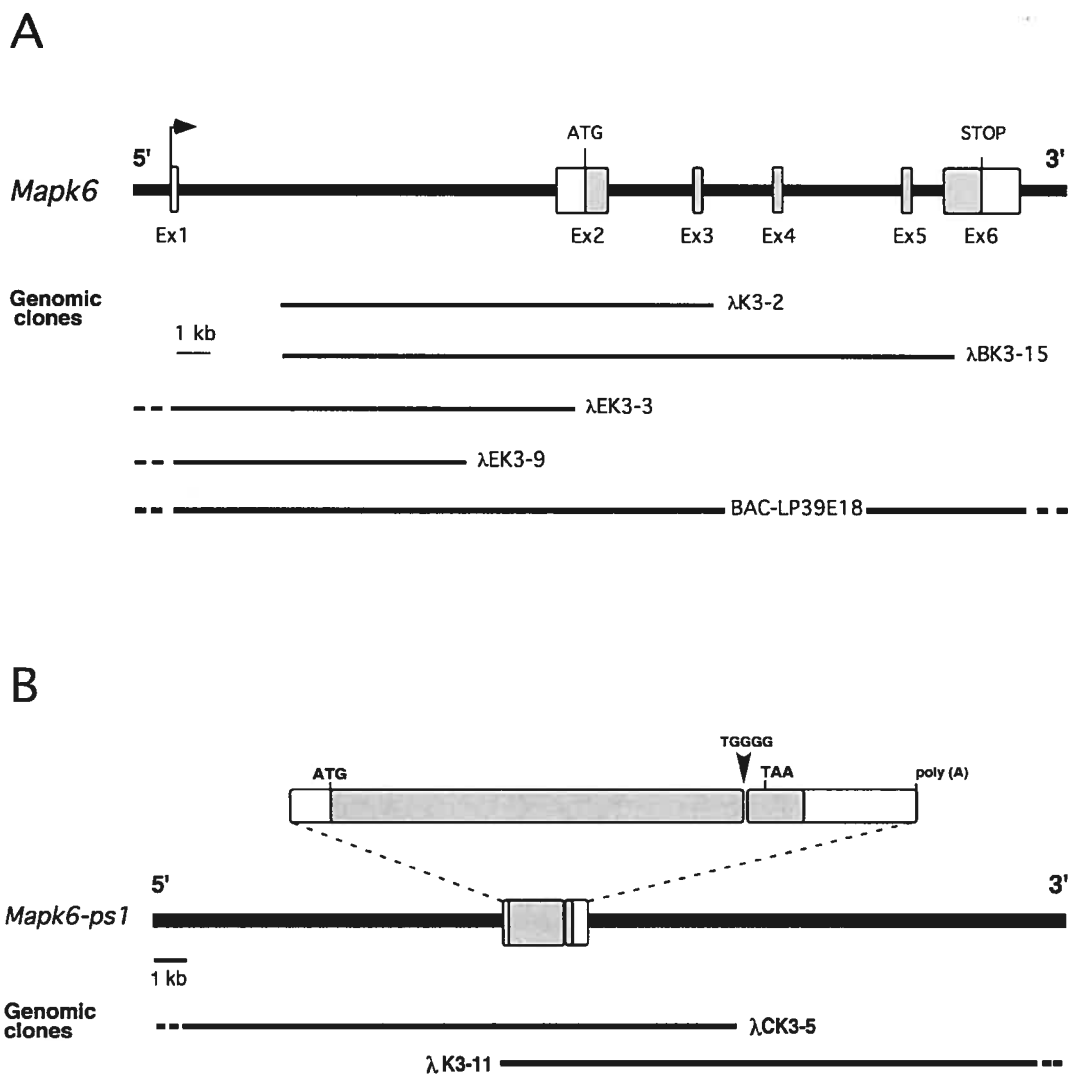

Fig. 1: Genomic organization of the Mapk6 gene family. (A) Structure of the *Mapk6* gene. Exons are represented by dark boxes for the coding sequence, and by open boxes for the 5' and 3'untranslated regions. The introns are indicated by single lines. The size of introns was estimated by PCR using flanking primers. The complete *Mapk6* genomic locus was isolated in a single BAC clone as shown at the bottom. (B) Schematic diagram of the mouse *Mapk6-ps1* pseudogene. The sequence homologous to ERK3 cDNA is shown: the coding region is represented by a dark box and untranslated regions by open boxes. The insertion of an in-frame stop codon, as well as the poly (A) tail is shown.

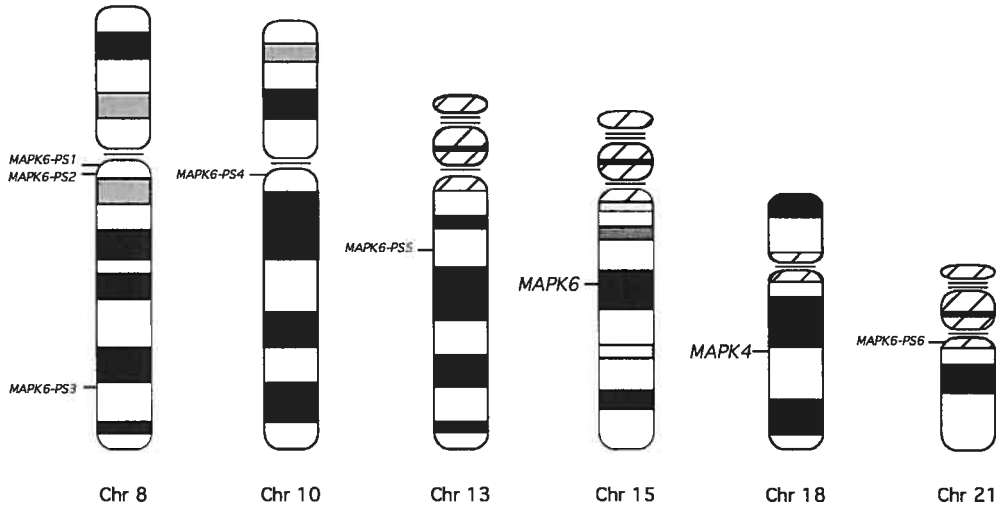

Fig. 2: Distribution of ERK3-related sequences in the human genome. Ideograms of G-banded chromosomes are shown with the localization of ERK3-related genomic sequences. *MAPK6* pseudogenes are symbolized by *MAP6-PS1* to *MAPK6-PS6.*

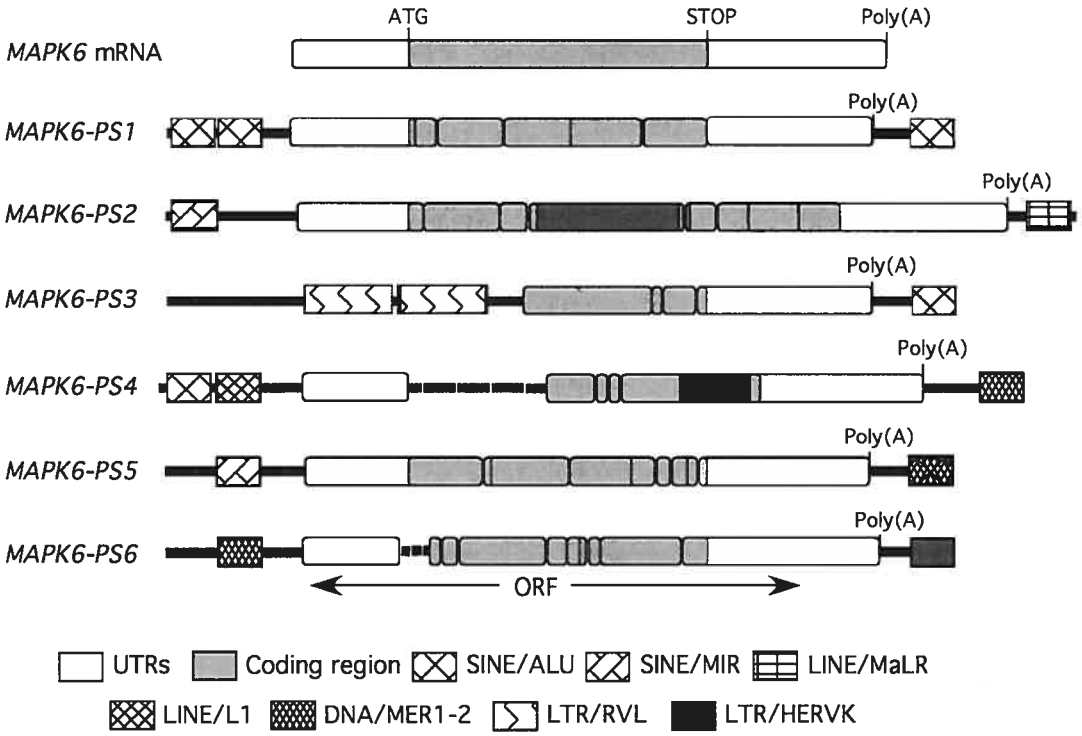

Fig. 3: Structural organization of human *MAPK6* pseudogenes and flanking regions. The structure of the human ERK3 cDNA is shown for comparison. Sequences homologous to ERK3 cDNA are represented by dark (coding) and open (untranslated) boxes. Gaps represent deletions and vertical lines correspond to insertions in the coding region (substitutions were omitted). The different types of interspersed repeats flanking the pseudogene sequences are shown.

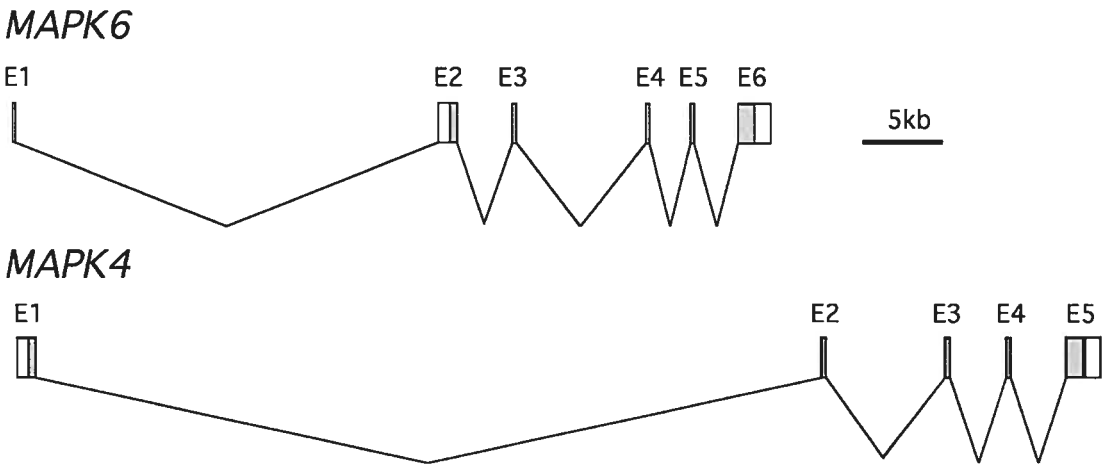

Fig. 4: The human ERK3 subfamily of MAP kinase genes. Structural organization of the human *MAPK6* and *MAPK4* genes. Exons are represented by dark boxes for the coding sequence, and by open boxes for the 5' and 3'untranslated regions. The introns are indicated by single lines. Human sequences from chromosome 15 and 18 were downloaded from the human genome sequence database at NCBI. Gene organization was confirmed by comparison with the ERK3 and $p63^{MAPK}$ cDNA sequences.

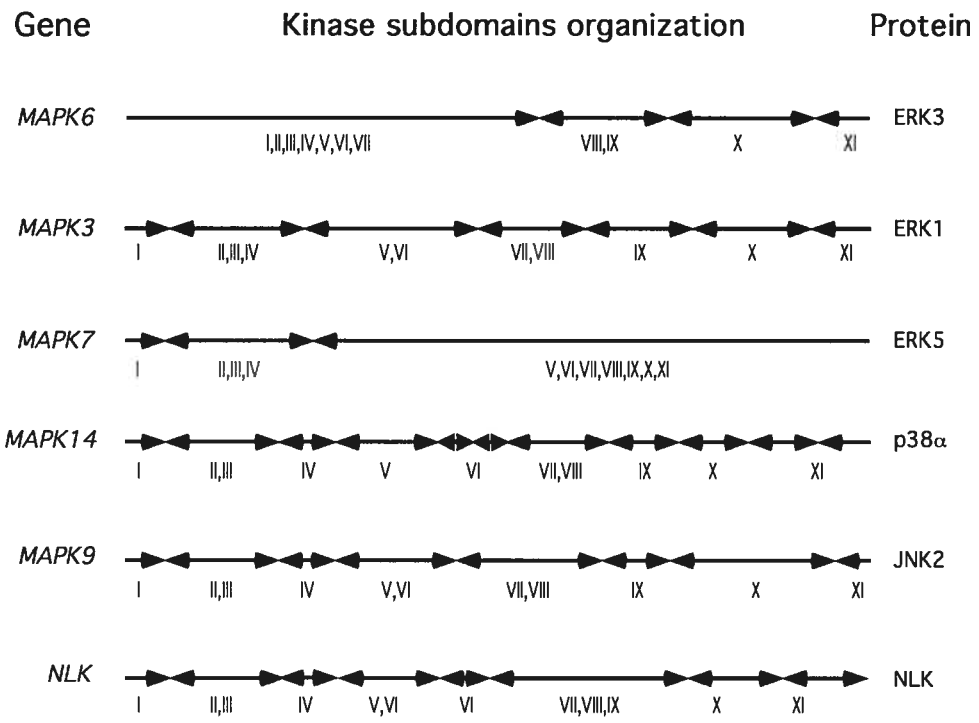

Fig. 5: Comparative analysis of human MAP kinase gene structures. Comparison of the exonic organization of protein kinase subdomains in *MAPK6* gene and other representative members of the MAP kinase gene superfamily. Exons are represented by arrows. Protein kinase subdomains are indicated by roman numerals.

REFERENCES

1. Lewis, T.S., P.S. Shapiro, and A.N. G., *Signal transduction through MAP kinase cascades.* Adv Cancer Res, 1998. **74**: p. 49-139.

2. Pearson, G., et al., *Mitogen-activated protein (MAP) kinase pathways: regulation and physiological functions.* Endocr Rev, 2001. **22**(2): p. 153-83.

3. Widmann, C., et al., *Mitogen-activated protein kinase: conservation of a three-kinase module from yeast to human.* Physiol Rev, 1999. **79**(1): p. 143-80.

4. Chang, L. and M. Karin, *Mammalian MAP kinase signalling cascades.* Nature, 2001. **410**(6824): p. 37-40.

5. Miyata, Y. and E. Nishida, *Distantly related cousins of MAP kinase: biochemical properties and possible physiological functions.* Biochem Biophys Res Commun, 1999. **266**(2): p. 291-295.

6. Boulton, T.G., et al., *ERKs: a family of protein-serine/threonine kinases that are activated and tyrosine phosphorylated in response to insulin and NGF.* Cell, 1991. **65**(4): p. 663-75.

7. Meloche, S., B.G. Beatty, and J. Pellerin, *Primary structure, expression and chromosomal locus of a human homolog of rat ERK3.* Oncogene, 1996. **13**(7): p. 1575-9.

8. Zhu, A.X., et al., *Cloning and characterization of p97MAPK, a novel human homolog of rat ERK-3.* Mol Cell Biol, 1994. **14**(12): p. 8202-11.

9. Turgeon, B., M.K. Saba-El-Leil, and S. Meloche, *Cloning and characterization of mouse extracellular-signal-regulated protein kinase 3 as a unique gene product of 100 kDa.* Biochem J, 2000. **346 Pt 1**: p. 169-75.

10. Gonzalez, F.A., et al., *Heterogeneous expression of four MAP kinase isoforms in human tissues.* FEBS Lett, 1992. **304**(2-3): p. 170-8.

11. Kleines, M., et al., *Early steps in termination of the immortalization state in Burkitt lymphoma: induction of genes involved in signal transduction, transcription, and trafficking by the ganglioside IV(3)NeuAc- nLcOse(4)Cer.* Biochim Biophys Acta, 2000. **1492**(1): p. 139-44.

12. Stocco, C., E. Callegari, and G. Gibori, *Opposite effect of prolactin and prostaglandin F(2 alpha) on the expression of luteal genes as revealed by rat cDNA expression array.* Endocrinology, 2001. **142**(9): p. 4158-61.

13. Mount, S.M., *A catalogue of splice junction sequences.* Nucleic Acids Res, 1982. **10**(2): p. 459-72.

14. Tchenio, T., E. Segal-Bendirdjian, and T. Heidmann, *Generation of processed pseudogenes in murine cells.* Embo J, 1993. **12**(4): p. 1487-97.

15. Vanin, E.F., *Processed pseudogenes: characteristics and evolution.* Annu Rev Genet, 1985. **19**: p. 253-272.

16. Li, L., et al., *Genomic loci of human mitogen-activated protein kinases.* Oncogene, 1994. **9**(2): p. 647-9.

17. Harrison PM, H.H., Balasubramanian S, Luscombe NM, Bertone P, Echols N, Johnson T, Gerstein M., *Molecular fossils in the human genome: identification and analysis of the pseudogenes in chromosomes 21 and 22.* Genome research, 2002. **12**(2): p. 272-80.

18. Prak ET, K.H.J., *Mobile elements and the human genome.* Nature reviews in genetics, 2000. **1**(2): p. 134-144.

19. Smit, A.F., *Interspersed repeats and other mementos of transposable elements in mammalian genomes.* Curr Opin Genet Dev., 1999. **9**(6): p. 657-663.

20. Esnault, C., J. Maestre, and T. Heidmann, *Human LINE retrotransposons generate processed pseudogenes.* Nat Genet., 2000. **24**(4): p. 363-367.

21. Caffrey, D.R., L.A. O'Neill, and D.C. Shields, *The evolution of the MAP kinase pathways: coduplication of interacting proteins leads to new signaling cascades.* J Mol Evol, 1999. **49**(5): p. 567-82.

22. Kultz, D., *Phylogenetic and functional classification of mitogen- and stress- activated protein kinases.* J Mol Evol, 1998. **46**(5): p. 571-88.

23. Sambrook, J., E.F. Fritsch, and T. Maniatis, *Molecular Clonong: a laboratory manual.* 1989, New-York: Cold Spring Harbor Laboratory Press.

24. Thompson, J.D., D.G. Higgins, and T.J. Gibson., *CLUSTAL W: improving the sensitivity of progressive multiple sequence alignment through sequence weighting, position specific gap penalties and weight matrix choice.* Nucleic Acids Res., 1994. **22**: p. 4673-4680.

25. Smith, S.W., et al., *The genetic data environment, an expandable GUI for multiple sequence analysis.* Comput. Appl. Biosci., 1994. **10**: p. 671-675.

26. Strimmer, K. and A. von Haeseler, *Quartet puzzling: a quartet maximum-likelihood method for reconstructing tree topologies.* Mol. Biol. Evol., 1996. **13**: p. 964-969.

27. Bruno, W.J., N.D. Socci, and A.L. Halpern, *Weighted neighbor joining: a likelihood-based approach to distance-based phylogeny reconstruction.* Mol. Biol. Evol., 2000. **17**: p. 189-197.

28. Felsenstein, J., *Confidence limits on phylogenies: an approach using the bootstrap.* Evolution, 1985. **39**: p. 783-791.

CHAPITRE 4

MANUSCRIT EN PRÉPARATION

Invalidation génique de la MAP kinase ERK3 : rôle physiologique et étude de l'expression du gène

MISE EN SITUATION

Les résultats présentés dans les chapitres précédents démontrent l'existence d'un gène unique encodant la protéine ERK3 chez la souris, le rat et l'humain. Une question importante demeurait quant à la fonction biologique de cette protéine et donc de l'importance physiologique du gène *Erk3*. Cette question a été adressée par l'invalidation génique de *Erk3* chez la souris. Ce chapitre rapporte donc les résultats de cette étude.

Suite au clonage moléculaire et à l'analyse de la structure du gène *Erk3,* il a été possible de concevoir une stratégie d'invalidation génique chez la souris. L'inactivation du gène *Erk3* a été obtenue par insertion d'un rapporteur *LacZ* au locus *Erk3*. En plus d'inactiver le gène, cette insertion a permis l'étude de l'expression du gène *Erk3* au cours du développement intra-utérin. Ce modèle a également permis de mettre en évidence les conséquences de la perte de ERK3 chez la souris. Ainsi, l'absence de ERK3 a pour conséquence la létalité néonatale. Cette mortalité est associée à la détresse respiratoire et l'incapacité des nouveaux-nés à se nourrir. De plus, un retard de croissance intra-utérin ainsi qu'une intolérance au glucose ont été observés chez les animaux mutants. De façon importante, ce travail est le premier à démontrer l'importance biologique de ERK3.

Loss of the *Erk3* Gene in Mice Leads to *In-utero* Growth Retardation, Neonatal Lethality and Impaired Glucose Tolerance

Benjamin Turgeon[1] and Sylvain Meloche[1,*]

[1] Institut de Recherche en Immunologie et Cancérologie and Departments of Pharmacology and Molecular Biology, Université de Montréal, Montréal, Québec, Canada

Running title: ERK3 is essential for neonatal survival

* Corresponding author: Dr. Sylvain Meloche
Institut de Recherches en immunologie et Cancérologie
2940 chemin de la Polytechnique
Montréal (Québec)
Canada
Tel.: (514) 343-6966
Fax: (514) 343-6843

E-mail: [redacted]

ABSTRACT

Extracellular signal regulated protein kinase (ERK) 3 is an atypical member of the MAP kinase family of signaling molecules. No function has yet been ascribed to this atypical MAP kinase. To determine the role played by ERK3 during development, we generated mice bearing a mutant *Erk3* allele in which the *LacZ* coding region replaces the coding region of the first exon. Expression studies using the *LacZ* reporter reveal that *Erk3* is specifically expressed during organogensis at high levels in neural tissue and branchial arches. During fetal development, *Erk3* is strongly expressed both in muscle tissues as well as in the epithelium of multiple organs. Interestingly, *Erk3* expression is regulated in time and space as monitored by detection of β-galactosidase in multiple organs at various stages of their development. Mice with the *LacZ* insertion do not express ERK3, they survive until birth but die neonatally from respiratory failure or inability to feed. Surprisingly, histological studies of homozygous *Erk3*-deficient mutants failed to exhibit major developmental defects in any of the $Erk3^{LacZ}$ highest expression domains during development. However, loss of ERK3 results into *in-utero* growth restriction that is dependent on gene dosage, consistent with an important role of ERK3 during development. In addition, newborn mutants have a defective glucose tolerance after birth, suggesting that they could develop diabetes melitus. These data represent the first genetic evidence of an essential role of ERK3 in mouse development and physiology.

Keywords: MAP kinase, ERK3, mice, knockout, phenotype, neonatal lethality, suckling, respiratory distress, glucose tolerance.

INTRODUCTION

Mitogen-activated protein (MAP) kinases are intermediates in signal transduction pathways that are essential for an increasing number of cellular processes required for normal development [1]. Based on their mechanism of activation, MAP kinases can be classified into two categories. The *classical* MAP kinases are activated by dual phosphorylation by kinases of the MAP kinase kinase family and include the well characterized ERK1/2, ERK5 as well as the JNK and $p38^{MAPK}$ isoforms [2-5]. The atypical group of MAP kinases includes ERK7 (ERK8 in human), NLK and ERK3/4. Much less is known about the biology of these proteins, but available data indicate that they are regulated in a different manner from that of classical MAP kinases [6].

ERK3 was isolated 15 years ago by sequence identity to ERK1 and initially proposed to be a 63 kDa protein based on sequence prediction and immunoreactivity [7]. Surprisingly, the human counterpart was found to be a protein of 100 kDa characterized by an identical kinase domain but with longer C-terminal extension [8, 9]. The controversy surrounding the ERK3 sequence was finally resolved after the cloning of the mouse *Erk3* cDNA which predicts a 100 kDa gene product together with the resequencing of the *Erk3* mRNA and gene sequences from the rat [10]. Further analysis of the mouse and human genome confirmed the existence of a single functional gene. In addition, numerous inactive pseudogenes are found in mouse and human genomes [11]. It was recently proposed that a shorter isoform of ERK3 could however be generated as the result of C-terminal truncation of ERK3 by proteolytic cleavage [12].

Although ERK3 shares 51% identity with ERK1 in the catalytic domain, it possesses many striking features that make it unique among the MAP kinase family. First, the phosphorylation motif of ERK3 is S-E-G instead of the well conserved T-X-Y which is a the hallmark of MAP kinases [7]. Second, the motif S-P-R replaces the motif A-P-E, which is conserved in the subdomain VIII of many kinases, including the MAP kinases. These characteristics are also shared by ERK4, a close relative of ERK3 of 62 kDa [11, 13]. Finally, ERK3 is characterized by a short half-life and its stability is controlled by the ubiquitin-proteasome pathway [14, 15].

Despite the fact that ERK3 was one of the first MAP kinases identified by molecular cloning, its function is still poorly understood. ERK3 expression increases during *in vitro* differentiation of neurons and muscle cells [7, 14] and overexpression of a stable mutant of ERK3 in many cell lineages limits proliferation [14]. ERK3 was recently found to interact with and to activate specifically the mitogen-activated protein kinase activated protein kinase

5 (MAPKAPK5 or MK5) [16, 17]. In accordance with a role of ERK3 as a biological activator of MK5, changes in expression level of ERK3 are associated with differences in MK5 activity [16, 17]. MK5 deletion in mice is partially embryonic lethal in the C57BL/6 background during embryogenesis [17], suggesting that MK5 could play a role during development. In accordance with ERK3 and MK5 being on the same genetic pathway, MK5 and ERK3 are coexpressed during embryonic development including E11.5 dpc [17], which corresponds to a time point of high levels of *Erk3* expression [10]. Interestingly, mouse embryonic fibroblasts (MEFs) deficient for MK5 were found to express lower levels of ERK3 [17]. Together, these results suggest that ERK3 could be important for mouse development.

In order to reveal ERK3 biological function, we generated *Erk3*-deficient mice by targeted replacement of the *Erk3* coding region with the *LacZ* reporter gene. Heterozygous embryos showed strong expression of the reporter gene in the epithelium compartment of several tissues during fetal development. $Erk3^{lacZ}$ is expressed in a temporally and spatially specific pattern during organ development, consistent with a role of ERK3 during mouse ontogeny. Loss of ERK3 is associated with respiratory distress and inability to suckle after birth, which are incompatible with neonatal survival. Surprisingly, *Erk3*-deficient newborns failed to exhibit major developmental defects. However, *Erk3* mutants are growth restricted and present glucose homeostasis defects after birth.

RESULTS

Targeted inactivation of the *Erk3* gene

The *Erk3* gene spans 6 exons and is found on mouse chromosome 9. Its organization is similar to *Erk4* with conserved intronic organization [11]. To generate an *Erk3*-null allele, we inserted a *LacZ* reporter gene in frame with the ATG initiation codon located in exon 2 using conventional targeting procedures. The coding sequence contained in exon 2, 3 and 4 was deleted by this insertion. The *LacZ* gene provides a stop codon and a polyadenylation signal predicted to result into a null allele (Fig. 1A). Chimeric mice from two independently derived homologous recombinant R1 ES cells transmitted the disrupted *Erk3* allele to the germ line as determined by Southern-blot analysis using the indicated probe (Fig.1B). Quantitative RT-PCR was carried out with E18.5 dpc *Erk3* WT and KO embryonic lung mRNA to detect possible *Erk3* transcript. As shown in figure 1E, we did not detect *Erk3* mRNA in null embryos.

We have previously shown that the *Erk3* gene predicts a single protein of approximately 100 kDa in mammalian cells [10, 11]. The ERK3 protein was shown to be lost in mouse embryonic fibroblast generated from our *Erk3* deficient mice. Furthermore, the loss of a single allele of *Erk3* was sufficient to decrease ERK3 expression by half [16]. To confirm that no ERK3 protein is produced in *Erk3* (-/-) cells, we analyzed ERK3 levels using a monoclonal antibody against ERK3 in MEF cells. Consistent with previous observations, no ERK3 protein is detected in null MEFs (Fig. 1F). Together, these results confirm the generation of a null allele of *Erk3*.

$Erk3^{LacZ}$ expression during mouse development

The insertion of *LacZ* in the coding region of *Erk3* allowed us to carry out a detailed examination of *Erk3* expression during mouse development. Taking advantage of the high sensitivity of the β-gal staining technique, we sought to identify the sites for functional analysis. To allow the *LacZ* gene to recapitulate *Erk3* endogenous expression, we excised the neomycin resistance cassette to avoid possible influence of its strong promoter that could interfere with β-galactosidase expression. Heterozygous mice for the $Erk3^{LacZNeo}$ mutation were therefore breed with a CRE recombinase transgenic mouse. Successful recombination of the *Erk3* allele in the progeny ($Erk3^{LacZ}$) was confirmed by southern analysis (Fig. 1C). Embryos derived from recombinant mice presented stronger β-gal staining than $Erk3^{LacZNeo}$ embryos. However, we did not note differences in the general pattern of β–gal expression between $Erk3^{LacZ}$ or $Erk3^{LacZNeo}$ embryos (data not shown).

Previous analysis of mRNA levels using Northern blot hybridization indicated that *Erk3* expression is the highest around embryonic day 11 in mouse [10]. We first decided to determine the pattern of $Erk3^{LacZ}$ expression during embryogenesis. Staining of E9.5-13.5 embryos for β-galactosidase activity is presented in figure 2. $Erk3^{LacZ}$ expression could be detected as soon as E9.5 in the neural tube of the embryo (Fig. 2A). At E11.5, $Erk3^{lacZ}$ expression is substantially increased compared with E9.5 (Fig. 2B,C and D), in agreement with a high level of expression *Erk3* mRNA at E11.5 dpc. Only low levels of β-galactosidase activity could be detected in primitive internal organs with no apparent expression in the primitive liver (Fig. 2B). However, expression was strong in the neural tissue and it was found specifically within the mantle zone of the spinal cord and the hindbrain. Also, $Erk3^{lacZ}$ was highly expressed in the thin outer rim of the marginal layer of the neural tube rather than the ependymal layer, the head mesenchyme and the cranial ganglia (Fig. 2C and D). Robust expression was observed in the otic vesicles (Fig. 2C) and within the mandibular component of the first branchial arch (Fig. 2D). E13.5 embryo presented a similar pattern of $Erk3^{LacZ}$ expression. As shown in figure 2E, areas of high expression included the striatum of the forebrain but not the trigeminal ganglion, the spine and primitive internal organs and intervertebral disks. Again, no β-galactosidase activity could be detected in the liver (Fig. 2D).

The specificity in the $Erk3^{lacZ}$ expression pattern became more apparent during fetal development. Using time course of β-galactosidase staining, we were able to determine the site with the highest $Erk3^{LacZ}$ expression at E15.5 (Table 1). The sites of highest *Erk3* expression were the choroid plexuses of the brain. Other relevant sites included muscle tissues such as the heart, tongue and the thick muscular wall of the bladder. In the primitive brain, high expression was detected in the neopallial cortex but few staining is observed in the olfactory lobe (Fig.3A). Dorsal root ganglia are among the site of highest $Erk3^{LacZ}$ expression in neural tissues but moderate staining was also observed in cranial ganglia. Furthermore, strong β-galactosidase staining was also found in the developing inter-vertebral disks of the distal part of the spine (Fig. 3A). Interestingly, intense β-galactosidase staining was detected in the epithelium of many structures including the choroid plexus, the sub-maxillary gland and the gut (Fig. 3B, C and D). In organs that develop through epithelial-mesenchymal interactions, the expression of $Erk3^{LacZ}$ was also confined to the epithelial compartment. These included the lung, the testis, the kidney and the pancreas (Fig. 3E, F, G and H). The liver remained the only organ presenting weak β-galactosidase activity. Interestingly, spotted staining was observed in the liver, which likely represents hematopoietic cells at this stage of development (Fig. 3I).

An interesting feature of *Erk3* expression during fetal development was its epithelial expression in most organs examined. To determine if *Erk3* expression could also be regulated in space within the epithelial compartment, we stained the sub-maxilary gland for β-galactosidase activity. At E16.5, this organ presents a proximal to distal tubular organization. $Erk3^{LacZ}$ was highly expressed in the distal buds of the epithelial tubules (Fig. 4A). Spatial expression of $Erk3^{LacZ}$ was also addressed in non-tubular epithelia such as the nasal epithelia. As shown in figure 4B, a clear transition in β-gal staining between the olfactory epithelium and respiratory epithelium was observed. These findings indicate that *Erk3* is expressed in a specific pattern during the development of both tubular and non-tubular epithelia.

The analysis of β-galactosidase expression during mid development suggests that *Erk3* expression is regulated in a dynamic manner. To evaluate how *Erk3* expression is regulated during organ development, we determined β-galactosidase activity at various stages of organ development in chosen tissues (Fig. 5). $Erk3^{LacZ}$ expression is the most robust in the choroid plexus (CP) of the fetus and therefore represents an ideal site to study temporal regulation of *Erk3* expression. We therefore examined β-galactosidase activity in the CP of the IV^{th} ventricule. When the CP is only rudimentary at E12.5, $Erk3^{LacZ}$ expression was very low (Fig 5A), compared with robust expression during the fetal stages of development (Fig. 5B and C). However, the β-galactosidase activity was found to a lesser extent in the adult gland (Fig. 5D). Another site of high $Erk3^{LacZ}$ expression during development was the heart. Similarly, at an early stage of development, $Erk3^{LacZ}$ expression was low in the heart (Fig. 5E). However, expression in the cardiac muscle dramatically increases in embryos during fetal development (Fig. 5F and G). Consistent with Northern analysis in adult tissues [10], no $Erk3^{LacZ}$ expression was observed in the adult heart (Fig. 5H).

The lung is a site of moderate *Erk3* expression in adult mouse but represents an example of an organ that develops through epithelial-mesenchymal interaction. $Erk3^{LacZ}$ expression was detected as soon as E12.5 in the primitive lung (Fig. 5I). Again, increased β-gal staining occurred during fetal development (Fig. 5J and K). Interestingly, the pattern of $Erk3^{lacZ}$ expression changes at the end of gestation in the lung, being highest in epithelial cells of proximal airways (compare 5J and K). Low levels of expression were found in the adult lung, compared to the fetal lung (Fig. 5L).

The tissue of highest expression of *Erk3* mRNA in adult mouse was reported to be the retina and therefore represent another site of interest [7]. Although *Erk3* expression seems to remain constant throughout eye development, specific expression was found in pigmented retina and ganglion cells of the neural retina (Fig. 5M, N, O). In contrast with other tissues

examined, *Erk3*^{lacZ} expression remains high in the adult retina, especially in the pigmented epithelium, the outer and inner cell layers as well as the ganglionic layer (Fig. 5P).

Loss of ERK3 leads to neonatal death

Heterozygous mice for the *Erk3*^{LacZNeo} mutation were viable and fertile. In mice examined for 18 months, heterozygous mutant demonstrated no abnormal phenotypes or lethality. Genotypes of mice at weaning from heterozygous crosses are presented in table 2. There were no *Erk3* (-/-) mice as demonstrated by genotyping by PCR analysis of tail DNA, indicating a lethal phenotype. Furthermore, disruption of *Erk3* leads to lethality in all genetic background observed, indicating that *Erk3* is essential for mouse survival. Interestingly, *Erk3* (+/+) and *Erk3* (+/-) genotypes in a pure background (CD1 and 129sv) were significantly different from the expected ratio ($P<0.001$, Pearson's chi-square test), suggesting that the loss of a single allele of ERK3 can challenge post-natal survival.

To determine the developmental timing of death of homozygous mutants, we analyzed litters from heterozygous parents in a mixed genetic background at various time points. Pregnancies were first interrupted between E12.5 to E18.5 to determine the percentage of *Erk3* (-/-) present. Although a subtle overrepresentation of *Erk3* (-/-) animal was observed before E15.5, the expected Mandelian ratio was obtained at E18.5 dpc (Fig. 6A). The day after birth, dead mutant were usually found in the litters of newborn mice (Fig. 6B). However, no *Erk3* (-/-) could be found between post-natal day 2-5 (Fig. 6C), indicating that *Erk3*-null mutant die during the first day after birth. Similar results were observed with animals of mixed background derived from the two independent ES targeted cell lines tested.

Respiratory distress in *Erk3*-deficient newborns

In order to determine the precise onset of mortality and underlying cause of neonatal death, newborn litters were closely observed and revealed a normal ratio of null animals. *Erk3*-deficient mice were being born alive with no gross apparent defects. However, a proportion of null pups experienced respiratory distress after birth as indicated by cyanosis (Fig. 6D). Indeed, *Erk3*-null mice presented characteristic features of respiratory distress; they remained cyanotic after birth and gasped for air but failed to breathe properly. Consequently, 39% (12/31) of the *Erk3*-null pups died immediately after birth. The lung of these animals were dissected and compared to wild-type littermates. The wild-type lungs were well inflated in contrast to mutant lungs that had a liver-like appearance (Fig. 6E and F) and sank when put in PBS, suggesting that these null pups did not breathe.

Many tissue defects can account for respiratory distress at birth including lungs immaturity, heart and skeletal malformations, as well as neuromuscular dysfunction. Pathological examination of mutant mice did not reveal any gross malformation in heart or any other tissue examined including the diaphragm muscle (see suppl. data). Moreover, no skeletal defects were found in the rib cage of dead mutants (see suppl. data). However, we have found indications of neuromuscular and lung defects in *Erk3*-deficient newborns (see below).

Histological analysis of the lungs from dead newborns showed that saccular space was markedly reduced (athelectasis) compared to the lung from neonates that breathed (Fig. 7A-C). Nevertheless, mutant lungs morphology was normal and they presented a normal number of lobes. Furthermore, mutant lungs filled the thoracic cavity, suggesting normal branching at later stages of development (data not shown). To verify if *Erk3* (-/-) lung have developmental defects of the saccular structures that are involved in gas exchange, we verified the normal differentiation of the peripheral epithelium. We first tested the distensibility of the lungs to determine if the type I pneumocytes are present. At E18.5 dpc, when instillated with cryopreservative or fixative, the mutant lung histology was comparable to the control lungs (Fig. 7D and E). This suggests that the type I pneumocytes are differentiated in *Erk3*-null mice and can form functional respiratory saccules. The second epithelial population in the respiratory saccules is composed of the type II pneumocytes responsible for surfactant secretion. Ultrastructure analysis from E18.5 dpc lungs by EM indicates that the type II pneumocytes from *Erk3* (-/-) lungs contained abundant glycogen pools and presented attenuated villi when compared with controls (Fig. 7F and G). This indicates that type II pneumocytes are immature in *Erk3* (-/-) lungs. Immature type II pneumocytes normally contain abundant glycogen stores that they convert into surfactant phospholipids prior to birth [18]. This suggests that some *Erk3* (-/-) lungs collapse after birth due to insufficient surfactant production.

Surviving *Erk3*-deficient pups are unable to feed

Observation of *Erk3*-deficient pups that survived respiratory distress revealed an empty stomach (Fig. 6I), indicating a suckling defect. Since suckling depends mainly on neural reflexes [31], we performed a simple behavioral test on *Erk3*-mutant pups to assess normal development of the neuromuscular system. Touch stimulation induces suckling-like responses, including rhythmic mouth opening. The *Erk3*-deficient neonates did not moved their jaws as notably as control littermate after a stimulation by a tail pinch. To confirm that a suckling defect could be the cause of inability to feed, we analyzed the feeding behavior of newborn mice using anesthetized mothers (Table 3). When put into close contact with the

nipple, the control pups were able to identify the nipple, to rapidly reach it by themselves and to grab it. They could suckle within seconds. However, mutant pups presented problems in all aspect of the feeding process. Most of the homozygous mutants had the olfactory reflex to identify the nipple but failed to reach it because of uncoordinated movements, suggesting a possible neuromuscular defect. The only mutants who could grab the nipple could not make an effort to suckle. This indicates that inability to feed is a consequence of an inability to suckle as well as an uncoordination problems of the *Erk3*(-/-) pups.

In addition to an uncoordination problem, mutant pups usually had a curled appearance or kyphosis (Suppl. Fig.1). When stimulated, *Erk3*-null newborns showed struggling response to pinch but they developed infirm voices. Finally, *Erk3*-deficient mice presented carpoptosis (Fig. 6G). Consequently, when forced to stand on their limbs, mutant pups cannot use their forepaws properly (data not shown). All these observation are consistent with neuromuscular defects in *Erk3*-null pups.

To verify that the death of *Erk3* mutants was caused by absence of nourishment, we determined the survival curve of *Erk3* mutant mice. Non-suckling mice usually die in a window of 12-24 hours. As mentioned above, a proportion of *Erk3* deficient mice died immediately after birth (Fig 6H). Like the control littermate, the remaining mutants could survive for at least 14 hours after birth. We conclude from these observations that the second cause of death of the *Erk3*-null pups is a consequence of their failure to feed, due to a neuromuscular problem. The etiology of the neuromuscular defects remains to be determined.

Erk3 (-/-) mice display intrauterine growth restriction (IUGR)

At birth, *Erk3* mutant pups appeared smaller than their wild-type counterpart. To verify that *Erk3* mutants are growth retarded, we analyzed the weight of E18.5 dpc fetuses. Indeed, *Erk3*-deficient mice exhibited, on average, a 10-15% reduction in weight relative to their wild-type counterpart [*Erk3*(+/+), 1.34 ± 0.07g; *Erk3*(+/-), 1.27 ± 0.09g; *Erk3*(-/-), 1.18 ± 0.08g]. Interestingly, heterozygous mutant were also significantly smaller (Fig. 8A), indicating that the loss of a single allele of *Erk3* in sufficient to restrict growth *in-utero*.

Growth retardation can be a consequence of poor nutrient delivery to the embryo. We therefore evaluated the possibility that IUGR was caused by placental defects. The mature placenta in mice consists of three layers: the labyrinth, containing the network of fetal capillaries and maternal blood sinuses; the junctional zone, that contains spongiotrophoblasts cells; and the maternal decidua [19]. We first analyzed *Erk3* expression in the placenta using the *LacZ* transgene. β-gal staining at E15.5 dpc revealed a strong expression of $Erk3^{LacZ}$ in

the junctional zone of the placenta (Fig. 8B), consistent with a role of ERK3 in placental development. We next analyzed the placentas from E18.5 dpc fetuses. Interestingly, the placentas from *Erk3* (-/-) animals were found to be smaller than their wild-type counterparts (Fig. 8C and D). In addition, the *Erk3*-null placenta presented reduced vascularisation into the chorionic plate (Fig. 8E and H), suggesting a possible defect in the labyrinth vasculature. Nonetheless, histopathological examination of the *Erk3*-mutant placenta did not reveal any gross abnormalities (Fig. 8F and I). To determine the onset of the placental defects in mutant mice, we weighted the fetuses and placenta at various developmental times. Following dissection of embryos, we found that the mutant placenta were significantly lighter than their wild-type counterparts as soon as E13.5 dpc ($Erk3^{+/+}$, 76.7± 10.0 mg; $Erk3^{-/-}$, 65.1 ± 5.6 mg; $p< 0.01$)(see Fig 8G). Interestingly, no significant differences were measured at that time between the average fetal weight of wild type and mutant embryos (Fig. 8J). However, at E16.5 significant difference was found between the average fetal weight of wild-type and *Erk3*–null fetuses (Fig. 8J). These results indicate that growth and development of both placenta and embryo are impaired in *Erk3*-null mice.

Impaired glucose tolerance in *Erk3*-deficient mice

The in utero growth retardation in *Erk3*-null embryos is reminiscent of the one seen in insulin-deficient animals [20]. Interestingly, ERK3 was recently showed to be important for insulin secretion in response to glucose *in vitro* [21]. To determine if a decreased in insulin secretion could be associated with growth restriction in *Erk3*-null mice, we submitted neonatal mice to a glucose resistance test. Unfed newborn animals were injected with 2mg/g glucose intraperitoneally and blood glycemia was measured at time 0, 1 and 2 hours after injection. In accordance with an insulin secretion defect, *Erk3*-null newborns failed to decrease their glucose blood levels 2 hours after injection in comparison with control pups (Fig. 9). This result is consistent with a possible decreased in insulin levels in *Erk3* mutant mice and suggests that *Erk3*-deficient newborns could also develop diabetes.

DISCUSSION

Little is known about the function of ERK3, and failure to address ERK3 function for the last 15 years comes from the challenge encountered to identify ERK3 function using *in-vitro* approaches. First, discrepancies in cloned cDNAs as well as limited antibodies specificities could have led to confusion between ERK3 and the related ERK4. Second, atypical characteristic of ERK3, such as the constitutively phosphorylated motif (SEG) and protein stability have impeded the study of ERK3 biology in the same manner as classical MAP kinases. Finally, even though signals that increases ERK3 expression have been identified, their effect on ERK3 activity are currently unknown and interacting protein and possible substrates are just being discovered [16, 17, 21, 22]. Gene deletion in mice would be expected to overcome these limitations and to address the specific function of ERK3. Moreover, our *LacZ* knock-in model should allow a better understanding of tissue-specific *Erk3* expression and possible sites of ERK3 function.

Erk3 expression

Erk3 expression was initially studied in the adult rat. *Erk3* mRNA was detected in all tissues examined with the highest levels of the mRNA in the neural tissues such as the brain, spine and retina [7]. These results are in agreement with *Erk3* expression in the adult mouse [10]. In human, *ERK3* mRNA was found at the highest levels in the brain and skeletal muscle [8]. These observations proposed an ubiquitous expression of the gene. *Erk3* expression during development was first addressed by Northern blot analysis on total mouse embryo mRNAs and a high level of *Erk3* mRNA was found around embryonic day 11 [10]. Our $Erk3^{LacZ}$ expression is in good agreement with Northern analysis of *Erk3* expression. Indeed, adult tissues that are known to express low levels of *Erk3* mRNA, such as the heart and lung, expressed only low levels of β-galactosidase. Moreover, high expression of $Erk3^{LacZ}$ was observed during organogenesis around E11.5 dpc, consistent with detection *Erk3* mRNA by in-situ hybridization during mid-development [17].

Based on *Erk3* expression, one could predict that ERK3 is involved in various aspects of development in all organs with the exception of the liver. Unexpectedly, *Erk3* expression was found to be relatively high in epithelia compared to other cell types during fetal development. This leads to two possibilities: 1) ERK3 is involved in epithelial-mesenchymal interactions governing the development of specific organs. 2) Since epithelial cells play critical roles in tissue homeostasis, ERK3 could play a role in epithelium biology. These include acting as a physical barrier, secretion or host defense. It is interesting that ERK3 expression was indeed the strongest in secretory epithelia, such as the choroids plexus, respiratory nasal epithelium

(but not the olfactory epithelium) and glands such as the salivary glands and the pancreas. Whether ERK3 plays a role in secretion will require further studies. In addition, expression of *Erk3* is lower in adult tissues than embryos. Therefore, one could predict that ERK3 is more important to epithelium development than epithelium homeostasis. However, it would be of interest to evaluate the effects of the loss of ERK3 in epithelial cells in adult mice using conditional knockout strategies.

ERK3 is essential for neonatal survival

Erk3 mutant mice are born without apparent defects beside modest growth impairment (approximately 85-90% of wild type) and hyperflexed forelimbs. However, a proportion of mutants died of respiratory distress and the surviving KO had no milk in their stomach. The neonatal death of *Erk3* deficient mice therefore indicates that ERK3 is indispensable for mouse survival after birth. Beside respiratory distress, inability to feed can explain the lethality of *Erk3*-deficient pups with the first day after birth. Accordingly, *Erk3*-null animal die in a window of time consistent with inability to feed. In addition to respiratory distress and inability to feed, we observed impaired glucose tolerance in *Erk3*-deficient mice after birth, which indicate that *Erk3*-deficient mice could develop diabetes mellitus. Important models of diabetes mellitus include deletion of the insulin genes as well as the insulin receptor in mice [20, 23, 24]. Lethality of these mutant animals occurs 48 hours after birth as a result of ketoacidosis. However, there are few chances that this phenotype is associated with death of the *Erk3*-null pups. Indeed, *Erk3*-mutant mice cannot feed, therefore preventing a dramatic increase in their glucose blood levels that could result in ketoacidosis. In addition, glycemia was normal in *Erk3*-deficient mice a few hours after birth in absence of feeding, indicating that glucose homeostasis of non-feeding mutants is normal. However, we can predict that *Erk3*-null mutants would develop diabetes mellitus if they could suckle.

Respiratory distress in *Erk3*-deficient mice

An important proportion of *Erk3*-null animals died immediately after birth from respiratory distress. No defects were observed in the heart and skeleton, raising the possibility that the defect is pulmonary in origin. Indeed, *Erk3*-null animals that did not survive birth sometimes presented collapsed lung or in rare cases, partially inflated lung (data not shown). Intrinsic lung defects associated with abnormal lung inflation at birth can be due to delayed lung maturation. Indeed, abnormal differentiation of type I pneumocytes (PNI), can result in absence of distal saccular structures, as seen in the *Pdpn* gene knockout [25]. Consistent with an abnormal saccular structure in these mice, E19.5 dpc lungs cannot be inflated by instillation

with fixative. On the contrary, *Erk3*-deficient lung showed a normal morphology compared to wild-type counterpart when instillated, which is indicative of normal development of PNI cells.

Abnormal production of surfactant by type II pneumocytes (PNII) is associated with a collapsed lung at birth as demonstrated by the loss of Surfactant protein B, which is essential for surfactant production [26]. Immaturity of PNII cells (revealed by high glycogen content) is associated with decreased surfactant production and poor neonatal survival, as demonstrated in the *Ndst1*-null mice [27]. Increased glycogen content in type II pneumocytes of the *Erk3*-null lung would be indicative of decreased surfactant production in these mice. ERK3 expression was recently described in epithelial immature cells of the fetal rat rather than surfactant producing cells, as well as the clara cells that line the proximal airways [28]. We have observed $Erk3^{LacZ}$ expression in proximal airways as well. The possibility that *Erk3* is expressed in PNII remains however to be clarified. Further studies will be required to determine if the lung defects in *Erk3* mutant mice are cell autonomous or a consequence of growth restriction in these mice (see below). Nevertheless, the *Erk3*-null mice represent a new model of respiratory distress syndrome (RDS) in human.

Neuromuscular defects in *Erk3*-mutant mice

All *Erk3*-mutants that survived birth never had milk in their stomach. Monitoring the suckling behavior in newborn pups revealed that no *Erk3*-null pups could suckle properly. Mutant animals were probably unable to reach the nipple by themselves because of uncoordinated movement. Since we have frequently observed small heterozygous or wild-type pups with milk in their stomach, it is unlikely that inability to feed is a consequence of the smaller size of *Erk3*-null pups. Neuromuscular defects could instead account for inability to feed or suckle. Accordingly, *Erk3*-null animals could not open their jaws as notably as their littermates in reflex to stimulation. This phenotype was observed in a number of mouse mutants such as the *Cntfr* and *Grin2b* KO mice [29, 30], that were found to have specific neuronal defects associated with inability to suckle. Important neural structures involved in suckling include the olfactory epithelia, the olfactory bulb and cortex, the brainstem as well as the cranial nerves involved in rhythmic mouth contraction and swallowing [31]. Sites of high expression of *Erk3* in neural tissues include the brain cortex, spinal cord, dorsal root ganglia and the cranial ganglia. However, defects in these structures remain to be found in the *Erk3*-deficient mice. The brainstem is involved in the rhythmic neuronal activity of both breathing and suckling. Interestingly, *Erk3*-deficient mice showed both defect in these physiological processes, indicating that neuronal function within the brainstem could be affected in the *Erk3*-null mice.

Erk3-deficient newborns also presented forepaw defects that were not associated with skeletal malformation (see suppl data). This problem was characterized by an inability to achieve extension of the forepaws that remained in a hyperflexed position. This defect has also been associated with neuronal defects in mice with a deletion of the *Kif1b* gene, that encodes a kinesin motor protein involved in axonal transport. Similar to the *Erk3*-deficient mice, *Kif1b*-null pups die of respiratory distress, are not responsive to stimuli and have a curled appearance [32], suggesting that *Erk3*-deficient mice could have a mild form of neuropathy. The forepaw defects observed in *Erk3*-deficient pups is also reminiscent of a punctual mutation in the *Met* gene, which encodes the receptor for hepatocyte growth factor/ scatter factor (HGF/SF). Forepaw defects in these mice are rather associated with abnormal development of muscle of the forelimbs than neuronal anomalies. This mutation, that affects signaling downstream of Grb2 in response to HGF, is also associated with limited neonatal survival, due to diaphragm muscle defects [33]. High expression of *Erk3* in muscle tissue was observed during fetal development. We therefore cannot exclude a possible muscular defect in *Erk3*-null mice. Specifically, defects in the jaw muscles would explain the inability of *Erk3*-deficient pups to open their mouth and failure to raise squeaky voices in response to stimuli. Such defects were observed in the *Jph1* KO mice. Notably, muscles defects in these mice are limited to the jaw muscles [34]. Similarly, muscle defects in *Erk3*-deficient mice could be limited to specific regions such as the forearms and the head.

A model of intrauterine growth restriction (IUGR).

Erk3-null animals showed modest but significant growth retardation at birth. Analysis of a large number of animals at E18.5 indicates that the whole population of mutant animal presented lower weights. This decrease is proportional with the number of gene copies, indicating that growth retardation of the *Erk3* deficient mice is a fully penetrant phenotype. *Erk3* (-/-) placentas were smaller at E18.5 dpc. However, no gross abnormalities were found in the placenta that could explain smaller *Erk3* mutant embryos. Placental development is influenced by non cell-autonomous environmental factors such as nutrient and oxygenation [19]. Consequently, one could hypothesize that growth defects in the *Erk3* (-/-) embryos influences late placental development. However, decreased embryo size does not necessarily accompany placental growth retardation as shown by the *Igf1* knockout mutant. These mutants reach birth with 40% growth retardation with normal placental size [35]. In addition, we observed that placental growth impairment precedes that of embryos, suggesting that impairment in the embryos is a consequence of abnormal development of the placenta. Therefore, growth retardation could be a consequence of cell autonomous placental defects in the *Erk3* mutants. The mechanism of this placental phenotypes remains to be clarified.

IUGR is a common cause of neonatal morbidity in human newborn and gene deletions affecting placental development and transport function are currently seen has models of IUGR [36]. However, the placenta is highly sensitive to developmental disturbance and most mutations that affect its development or its component lineages leads to death at mid-gestation [19]. Interestingly, analysis of time pregnancies from *Erk3* (+/-) crosses did not reveal embryonic losses. Lethality at birth is usually a consequence of important growth retardation or defects in the fetuses as well. Indeed, growth retardation due to placental defects correlates well with neonatal survival of *Wnt2* and *Cited1* null mutants [37, 38]. In the targeted deletion of the *Cul7* and *Lifr* genes, neonatal lethality is associated with a combination of defect in both placenta and embryos [39, 40]. However, placental defects that occur at the latest stage of labyrinth development or those limiting placental growth can allow neonatal survival, as shown by deletion of the *Esx1* gene and the loss of the placental-specific isoform of IGF-II [41, 42]. Although these mutants are born significantly smaller than their control littermates, they bypass neonatal lethality and reach a normal weight by maturity. These studies suggest that neonatal death in *Erk3* (-/-) mice could be the consequence of defects in both the placenta and the fetuses. Tetraploid rescue experiments need to be performed to evaluate the contribution of the placental phenotypes on neonatal survival of the *Erk3*-null mice.

Deletion of the insulin genes also result in impaired fetal growth [20] and ERK3 was recently reported to be important for insulin production in rat [21]. In accordance with a role of ERK3 in insulin secretion, *Erk3*-deficient mice have impaired glucose tolerance. However, it is unknown at this time if insulin levels are decreased in *Erk3*-deficient mice. Many diseases, including Type II diabetes can also be associated with abnormal tissue programming resulting from the IUGR [43]. We therefore cannot exclude the possibility that the impaired glucose tolerance observed in *Erk3*-deficient mice is a secondary consequence of IUGR resulting from abnormal placental nutrition.

Compensatory mechanisms to ERK3 loss

The phenotype of *Erk3*-null animals is surprisingly mild in comparison to its expression pattern. It is possible that functional redundancy is masking other roles of *Erk3* during mid-development. A genetic pathway or even a single gene could compensate for *Erk3* loss. The best candidate would be the *Erk3* closest relative *Erk4*. Indeed, the *Erk3* and *Erk4* genes have similar structures and both proteins present high identity in their catalytic domain [7, 11, 13]. In addition, recent reports suggest that ERK3 and ERK4 can participate in a same molecular pathway. Indeed, both genes are co-expressed in fetal tissues during development [44]. Similar to ERK3, ERK4 can bind, activate and translocate MK5 from the

nucleus to the cytoplasm in transfected cells. Finally, ERK3 and ERK4 were both shown to be physiological activator of MK5 kinase activity *in vivo* [44, 45]. These data indicate that ERK3 and ERK4 could participate in a common signaling pathway involving MK5. Further studies, such as the generation of a null allele of *Erk4* will be required to determine if ERK4 can compensate for the loss of ERK3 during early development.

Loss of MK5 was previously reported and these *Mapkapk5*-deficient mice are viable in a mixed 129Sv x C57Bl/6 genetic background [17]. However, in a pure C57Bl/6 background, embryonic loss were documented during mid-development [17], a stage where expression of *Erk3* is high [10, this study]. Interestingly, mouse embryonic fibroblasts deficient for MK5 showed an important decrease in ERK3 levels, raising the possibility that loss of ERK3 expression could be associated with some of the phenotypes observed. Preliminary analysis in the *Erk3* null mutation in the C57BL/6 genetic background does not suggest embryonic loss of *Erk3* null mutants. Together, the phenotypes of *Erk3* or *Mapkapk5* null mice suggest that both proteins can fulfill independent functions during development. Alternatively, decreased ERK3 expression in *Mapkapk5*-deficient mice could be insufficient to explain the phenotype of these mice. It will be of interest to determine if *Mapkapk5/Erk3* double knockout mice have the same phenotype has the *Mapkapk5* deletion alone in a pure C57BL/6 genetic background.

In summary, our findings present physiological evidence that *Erk3* is a gene essential for mouse development and survival. Our data demonstrate that *Erk3* is expressed in embryos and fetuses in a manner that is consistent with a role of ERK3 during development. Indeed, *Erk3* mutants reach birth with intra-uterine growth restriction and die of respiratory distress and inability to feed thereafter. Furthermore, *Erk3*-deficient newborns have glucose homeostasis defects. Initial characterization of these phenotypes allowed us to identify organ defects including lungs immaturity and placental hypotrophy, as well as to uncover neuromuscular problems in homozygous mutant newborns. Importantly, this model should allow a better understanding of ERK3 biological function and provide a new tool to study ERK3 at the molecular level.

MATERIALS AND METHODS

Construction of the targeting vector

The murine *Erk3* gene was isolated previously [11]. A targeting vector was designed to replace a 5kb genomic fragment containing the N-terminal region of the ERK3 kinase domain, which is encoded by exon 2, 3 and 4. The *LacZ* reporter gene containing a polyadenylation signal was inserted in-frame with the ERK3 initiation codon. The Neomycin resistance cassette (Neo) was inserted in the targeting vector 3' of the *LacZ* gene in the antisense orientation to *Erk3* transcription. *LacZ-Neo* was flanked by 4.5 kb of *Erk3* genomic DNA on both sides. The targeting vector was linearized with NotI and electroporated into R1 ES cells [46]. After selection with 180 μg/ml G418, homologous recombinants were screened by southern blot analysis. DNA sample were digested with EcoR1 and probed with a 5' external probe (KpnI-XbaI, genomic fragment). Homologous recombination was detected in 3% of the clones (7/214).

Generation of *Erk3*-deficient mice

Two correctly targeted ES clones (103K3 and 127K3) were separately injected into C57Bl/6 host blastocysts to generate chimeric animals. Male chimeras were bred with C57BL/6 females and both clones gave germ line transmission, as determined by Southern blot analysis. Germ line transmitting mice from the two ES clones were mated with either C57BL/6 or 129/Sv mice to produce heterozygous mutant mice on either mixed C57BL/6x129/Sv or pure 129Sv background. Subsequent progeny were genotyped by PCR. *Erk3* specific intronic primers (forward:GTTGCTCATAAACACAAACCTCC, reverse: GGGATGGGTTATGTTTTCTAGAC) amplifies a 300 bp fragment corresponding to exon the 5' intron exon boundary of exon 3 of the gene. The mutated allele was amplified using *Lac-Z* specific primers (forward: TAAACCGACTACACAAATCAGCG, reverse: GCAGCAGCAGACCATTTTCAATC) that results in a 600 bp PCR product. *Erk3* Heterozygous mice were backcrossed with C57Bl/B6 or CD1 mice for ten generations to obtain pure genetic C57Bl/6 or CD1 backgrounds. To remove the neomycin resistance cassette within the *Erk3* locus, *Erk3* heterozygous mice were crossed with a CRE deleter mice (of unknown genetic background) for 2 generations. Progeny were genotyped by Southern blot analysis.

Western blotting

Isolation of mouse embryonic fibroblasts (MEFs) was described previously [16]. 100 µg of protein were separated by SDS-PAGE and western blotting as described previously [10]. ERK3 protein was detected using a monoclonal antibody generated against the full-length rat ERK3 (USBiological). The membrane was stripped and reblotted with a monoclonal anti-actin antibody (Sigma).

RNA analysis

Total RNA was isolated from E18.5 dpc lung tissue and purified using silica-gel-based spin columns (RNeasy, Quiagen). Total RNA were reverse transcribed in a final volume of 100 µL using the High Capacity cDNA Archive Kit with random primers (Applied Biosystems, Foster City, CA) as described by the manufacturer. Sense and antisense oligonucleotide (ACTGGTAAAACCCTCTTTGCAG and GGAATCACGCTGAGAAGCTC) specific for *Mapk6* were used for real-time PCR performed in triplicate using 2 µl of cDNA samples (50 ng), 5 µl of the TaqMan PCR Master Mix (Applied Biosystems, CA), 2 µM of each primer and 1 µM of the Universal TaqMan probe in a total volume of 10 µl. The ABI PRISM® 7900HT Sequence Detection System (Applied Biosystems) was used to detect the amplification level. The human GAPDH (glyceraldehyde-3-phosphate dehydrogenase), ACTB (Beta Actin) or 18S ribosomal RNA were used as endogenous controls.

Tissue preparation and *LacZ* detection

Embryos were harvested at 9.5 to 18.5 days after detection of a coital plug and fixed in PBS containing 0.2% glutaraldehyde, 5 mM EGTA (pH 7.3), and 0.1 M MgCl2 for 1 h on ice and rinsed three times for 15 min with cold PBS. For adequate penetration of fixative of 15.5 dpc embryos and older, the rib cage, peritoneum and skull were opened. Aldult mice were transcardiacally perfused with 4% paraformaldehyde. Fixed embryos or tissues were cryoprotected overnight in cold 30% sucrose in 1x PBS and then embedded in OCT embedding medium (Tissue-Tek) and frozen on dry ice. Cryostat sections of frozen tissue (10 µm) were loaded onto polylysine-coated slides and allowed to dry at room temperature for 2 h. Sections were re-fixed in 0.2% glutaraldehyde on ice and washed in wash buffer (PBS contaning 2 mM MgCl2, 0.01% sodium deoxycholate, 0.02% NP-40) prior to incubation in ß-Gal solution (5 mM potassium ferricyanide, 5 mM potassium ferrocyanide, 1 mg of X-Gal [5-bromo-4-chloro-3-indolyl-ß-D-galactopyranoside]) in wash buffer, at 37°C for a few

hours to O/N. Stained sections were washed three times in PBS and then counterstained with nuclear fast red and topped with coverslips for analysis. ß-galactosidase expressing tissues were photographed under a dissecting microscope.

Histological staining procedures

Newborns or E18.5 dpc fetuses were incubated overnight in 10% buffered formalin after opening of the rib cage and peritoneum to allow penetration of the fixative. Placentas were cut in half before incubation in fixative. Samples were dehydrated and embedded in paraffin, sectioned on a microtome to a 5µm thickness and stained using a conventional hematoxylin-eosin (H&E) protocol.

Lung inflation

E18.5 fetuses were dissected to remove the abdomen from the upper body part. The diaphragm was gently dissected out from the rib cage to allow maximal inflation of the lung. The lungs were inflated with a 0.5X solution of OCT embedding medium (Tissue-Tek) in PBS by injection through the trachea using a 25G blunted needle, until the lung filled completely the thoracic cavity. After inflation, the trachea was knotted with a surgical suture and the upper body was immediately covered with OCT and frozen on dry ice. Cryostat sections of the samples (7 µm) were loaded onto polylysine-coated slides and allowed to dry at room temperature for 2 h. Sections were fixed in 4% paraformaldehyde and stained using a conventional hematoxylin-eosin (H&E) protocol.

Lung ultrastructure

Lung tissues were fixed by immersion with 1% (v/v) glutaraldehyde in 0.1 M phosphate buffer, pH 7.4, for 2 hours at 4°C. Tissues were then washed in phosphate buffer, dehydrated in a series of graded methanol solutions at decreasing temperature until –30oC and embedded in Lowicryl K4M (CANEMCO, St-Laurent, Qc, Canada) as described previously [47]. Epon embedding was also carried out after post-fixation of the tissue with 1% osmium tetroxide for 1h at 4°C, dehydration in ethanol and propylene oxide. Thin tissue sections (70 nm) were mounted on Parlodion and carbon-coated nickel grids. Examination was carried out with a Philips 410LS electron microscope (FEI Systems Canada Inc, St-Laurent, Qc, Canada).

Glucose resistance

Blood glucose levels were measured from 3 µl of tail blood with a portable glucose-measuring device (Bayer). Glucose tolerance tests were performed in starved newborn animals 4-6 hours after birth. Newborns were injected intraperitoneally with 2mg/g body weight glucose in a volume of 20µl/g, and blood glucose levels were determined at intervals thereafter.

AKNOWLEDGEMENTS

The authors would like to thank David Lohnes for providing the ES cells, Kim Levesque for outstanding technical assistance, Marc K Saba-El-Leil and Philippe Coulombe for discussion, Diane Gingras for electron microscopy, Christian Charbonneau for microscopic assistance and Geoffrey Woods for pathological analysis. Benjamin Turgeon is a recipient of a FRSQ doctoral fellowship.

Table. 1 Levels of *Erk3*^{LacZ} expression at E15.5

Systems	Tissues	Levels
Head/Neck	Teeth	+++
	Nasal cavities	+++
	Submax. gland	+++
Cardiovascular/ Pulmonary	Heart	+++
	Lungs	++
Nervous	Choroid plexus	++++
	Dorsal root ganglia	+++
	Neocotex	++
	Retina	+++
Digestive	Eosophagus	+++
	Pancreas	++
	Intestins	++
Urogenital	Bladder	+++
	Kydneys	+++
Skeletal muscle	Tongue	+++

Table 2. Genotyping of *Erk3* (+/-) intercrosses at weaning

Background	Genotype					Total
	(+/+)	(%)	(+/-)	(%)	(-/-)	(100%)
(103K3) Mixed*	106	(31)	236	(69)	0	342
(103K3) CD1**	69	(41)	101	(59)	0	170
(103K3) 129Sv	65	(45)	81	(55)	0	146
(127K3) Mixed*	68	(37)	114	(63)	0	182

*C57Bl/6.129Sv mixed genetic background; **backcross N10

Table 3. Suckling test in *Erk3* mutant mice

Aspect	+/+	+/-	-/-
Reflex	100%	100%	64%
Seaking	100%	100%	55%*
Grabbing	100%	100%	20%
Suckling	100%	100%	0%

+/+, n = 6; +/-, n = 21; -/-, n = 11. *atypical, uncoordination

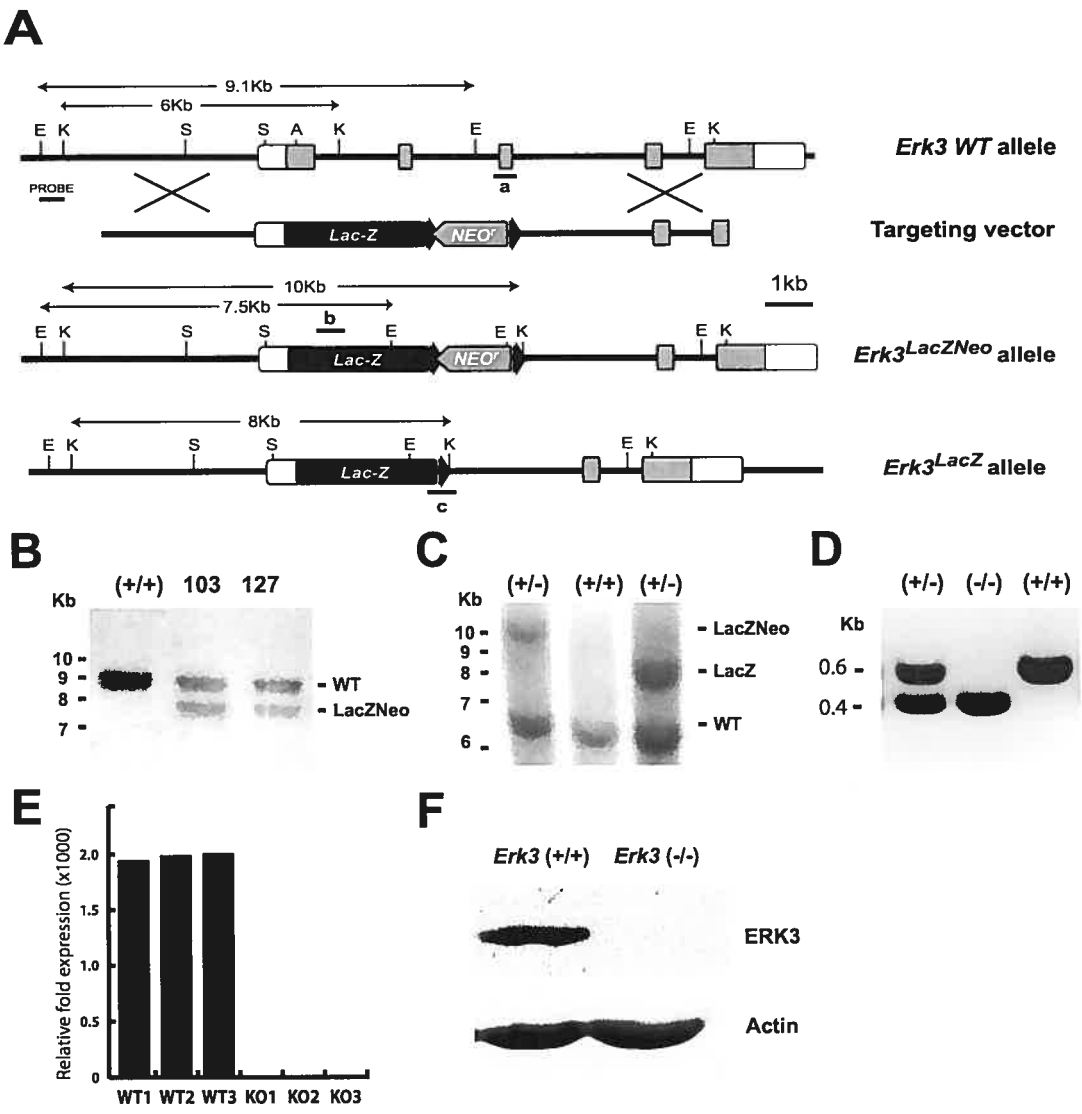

Fig. 1: Targeting strategy for generation of the *Erk3*^{NeoLacZ} and *Erk3*^{LacZ} mice. (A) Schematic representation of the *Erk3* locus, targeting construct, and recombinant alleles. The targeting vector carried a neomycin resistance cassette (Neo^r) and a *E. coli LacZ* gene that has been fused in frame with the *Erk3* coding sequence, 12 amino acids downstream of its initiation codon. Exon 2, 3, 4, 5 and 6 and restriction sites are shown (E:EcoR1; K:Kpn1; etc). Open boxes represent UTRs and dark boxes indicate coding regions. Introns are shown as bars. (B) Southern blot analysis of DNA from two of the correctly targeted ES clones (left panel), indicating the wild type allele (9.1kb) and the mutant allele (7.5kb), resulting from an EcoR1 digest (C) Southern blot analysis of tail DNA from heterozygous mice before and after breeding with a CRE deleter mice, showing the wild type allele (6kb), the *LacZNeo* allele (10kb) and the *LacZ* allele (8kb), resulting from a Kpn1 digest. (D) PCR amplification of WT and mutant alleles from tail DNA. (E) Real-time quantitative RT-PCR analysis of *Erk3* mRNA isolated from E18.5 mouse lungs. Data are expressed relative to WT1. (F) Western analysis of protein lysates from mutant and control embryonic fibroblasts showing absence of the ERK3 protein in null embryos.

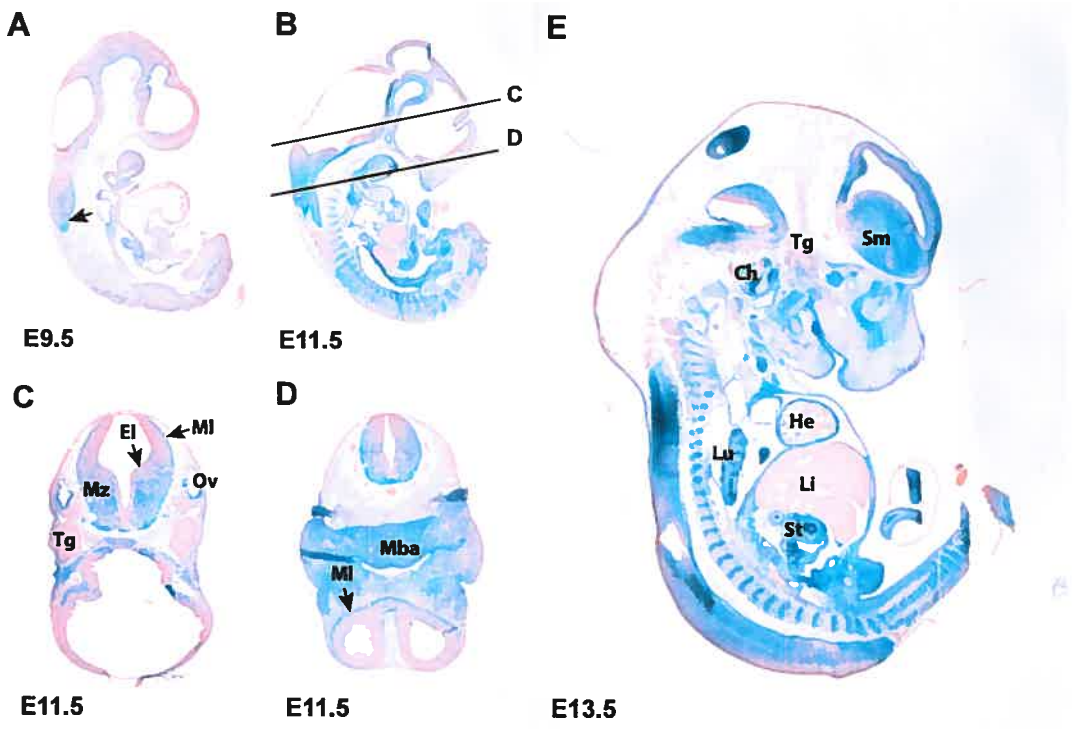

Fig. 2: Expression of *Erk3*^{LacZ} during mid-development. ß-galactosidase activity was detected in cryotome-sectioned heterozygous embryos at E9.5 (A), E11.5 (B,C,D), and E13.5 (E). Sections are either sagital (A,B,E) or transverse (C,D). The lines in B represent the level of section of the C and D panels. No β-gal staining was observed for wild-type littermate under identical conditions. Ch: Choclea; El: Ependimal layer; He: Primitive heart; Li: Primitive liver; Lu: Lung; Mba: Mandibular component of the first branchial arch; Ml: marginal layer; Mz: Mantle zone; Ov: Otic vesicle; St: Stomach; Sm: Striatum; Tg: Trigeminal (V) ganglion.

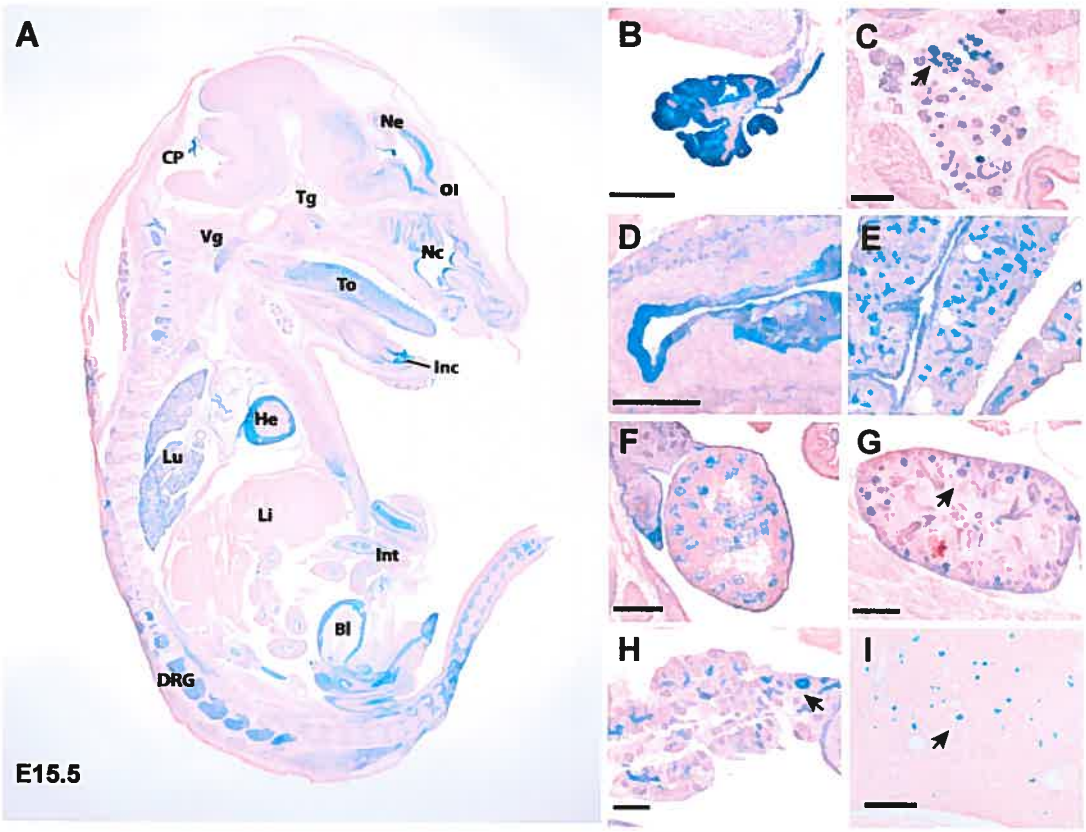

Fig. 3: Expression of *Erk3*^{lacZ} during fetal development. ß-galactosidase activity was detected at embryonic day 15.5. in whole embryos (A). Staining was found in the developing epithelium of the choroids plexus of the 4th ventricle (B), sub-maxillary gland (arrow in C), stomach (D), lung (E), testis (F), kidney (arrow in G) and pancreas (arrow in H). (I) Characteristic punctual ß-galactosidase staining in the liver (arrow in I). Abbreviations: Bl: Bladder; CP: Choroid plexus; Drg: Dorsal root ganglion; He: Heart; Inc: Incisor; Int: Intestine; Li: Liver; Lu: Lung; Ne: Neocortex; Nc: Nasal cavity; Ol: Olfactory lobe; Vg: Vagal (X) ganglion; Tg: Trigeminal (V) ganglion; To: Tongue. Scale bar: 200 µm.

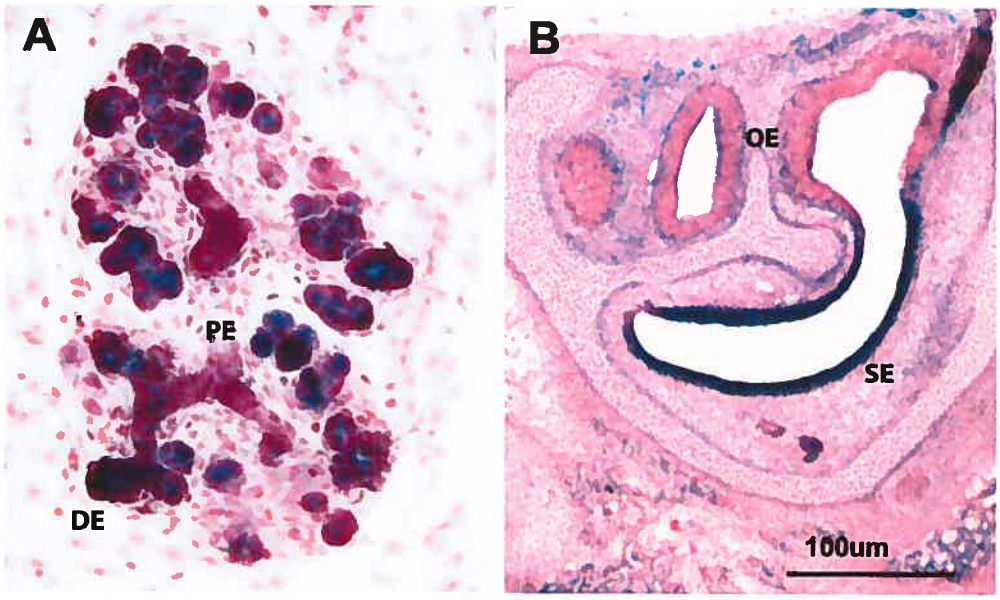

Fig. 4: Spatial expression of *Erk3*^{LacZ} within epithelia. ß-galactosidase staining in the sub-maxillary gland at E16.5 (A) and in the nasal cavity at E15.5 dpc (B). PE: Proximal epithelium; DE: Distal epithelium; OE: Olfactory epithelium; SE; Secretory epithelium.

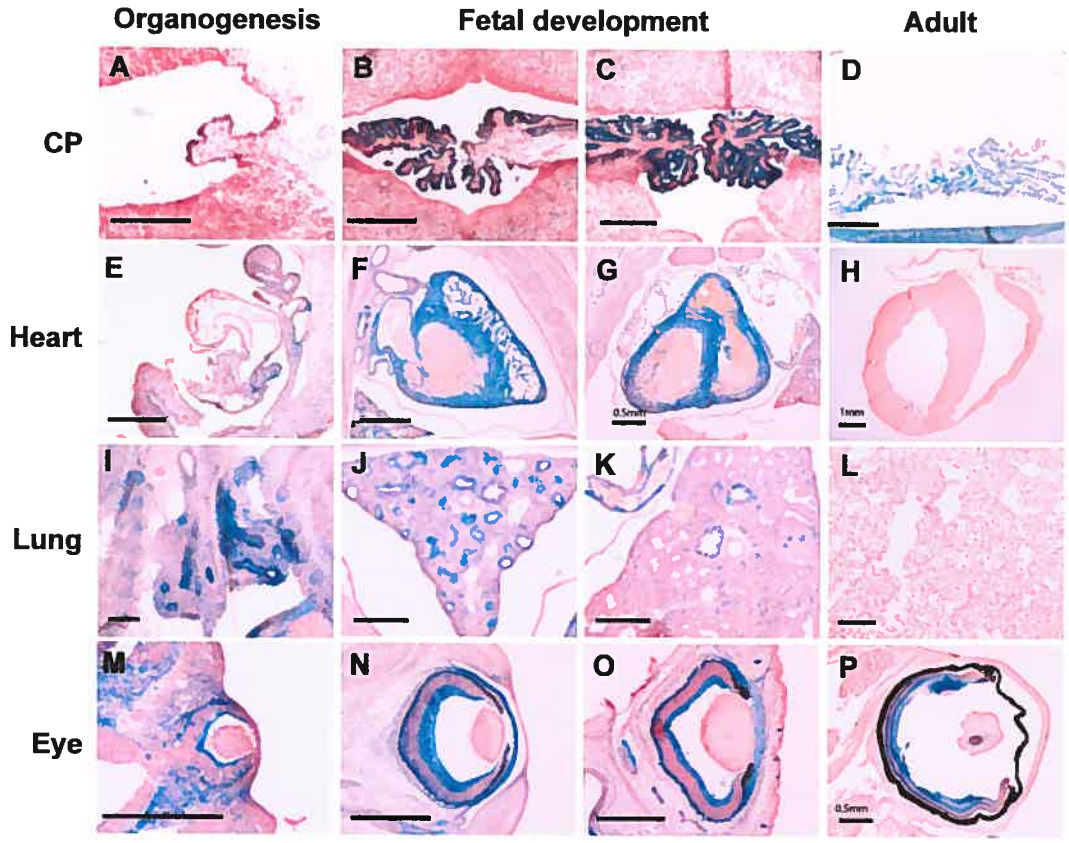

Fig. 5: Temporal expression of *Erk3*^{lacZ} during organ development. ß-galactosidase activity was detected in the choroid plexus of the 4th ventricle (A,B,C,D), the heart (E,F,G,H), the lungs (I,J,K,L) and the eye (M,N,O,P) at various stage of their development: (A,E) E11.5; (I,M) 12.5; (B,F,J,N) E15.5; (C,G,K,O) E18.5 and adult (D,H,L,P). Scale bar is 200 µm unless specified.

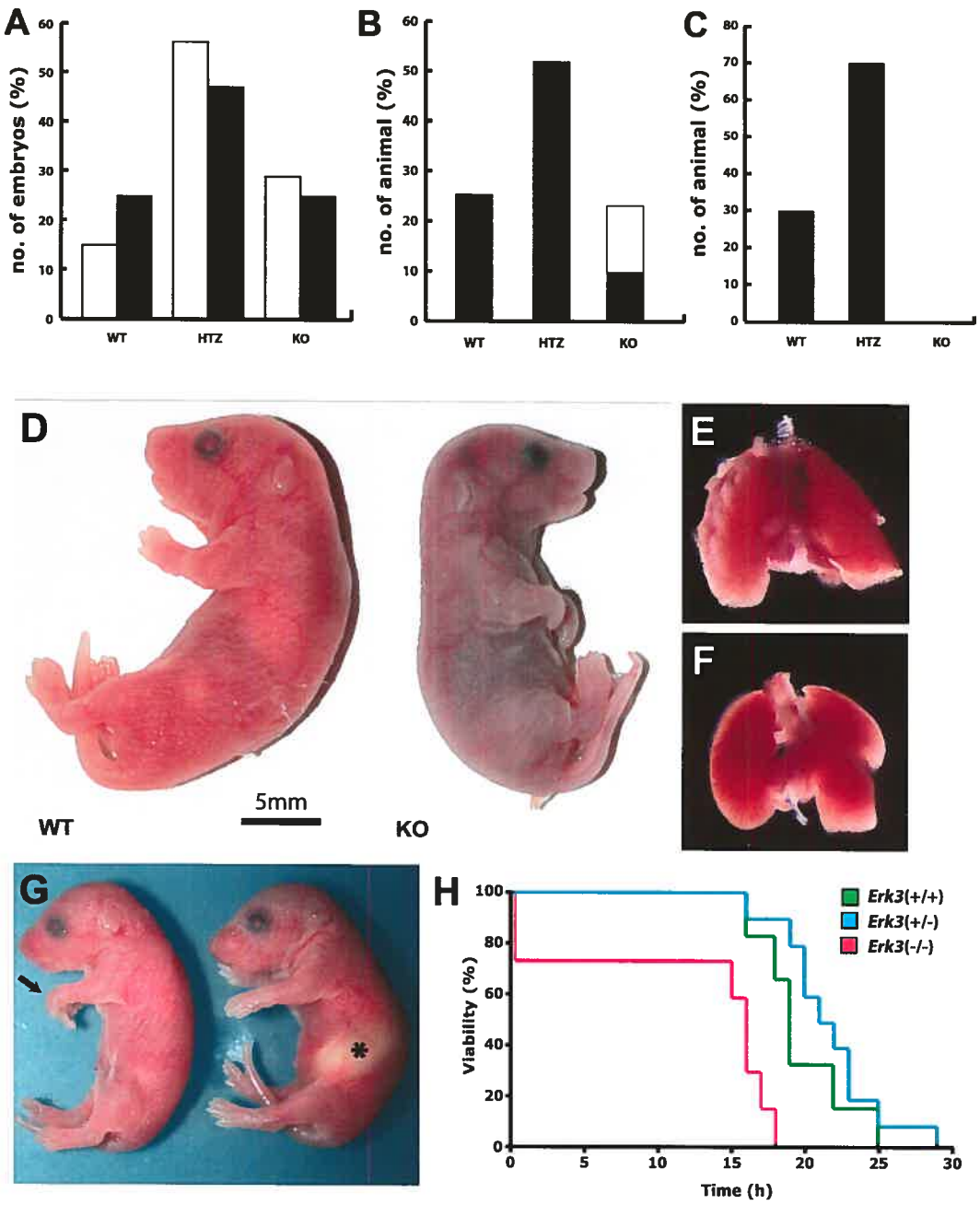

Fig. 6: *Erk3* deletion leads to neonatal lethality. (A) Genotype distribution of embryos from heterozygous crosses isolated between E12.5 and E15.5 dpc (opened bars [n=80]) and E18.5 dpc (filled bars [n=173]). (B) Relative distribution of alive newborn mice the day after birth (n=149). (C) Genotype distribution of litters at P2 (n=57). (D) Gross morphology of pups immediately after birth representing a normal *Erk3* (+/+) or a cyanosed *Erk3* (-/-) newborn. (E) Lungs isolated from a wild type newborn are well inflated compared to a dead homozygous mutant pup (F) that have a collapsed liver-like appearance. (G) Wild-type pups have milk in their stomach whether surviving *Erk3*-null pups lack a milk spot (* in G). Note the carpoptosis (arrow in G) in the *Erk3*-null mice. (H) Survival curves of newborns from heterozygous crosses in absence of feeding [*Erk3* (+/+): n=6; *Erk3* (+/-): n= 11; *Erk3* (-/-): n=7].

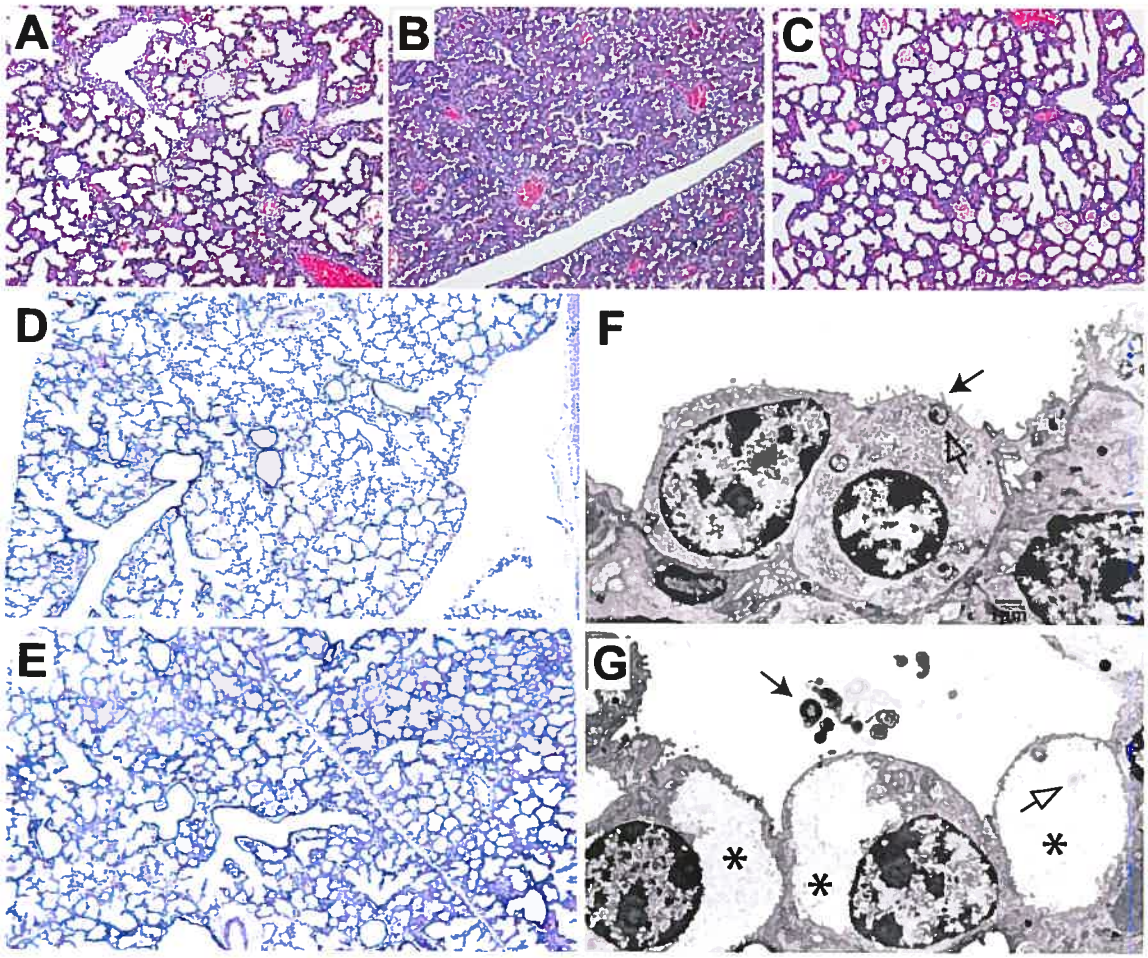

Fig. 7: Lung immaturity in *Erk3*-null mice. (A-C) Hematoxylin-eosin coloration of lungs from breathing *Erk3* (+/+)(A), non-breathing *Erk3* (-/-)(B) and breathing *Erk3* (-/-)(C) neonates at 5X magnification. (D) Histology of E18.5 *Erk3* (+/+) and *Erk3* (-/-)(E) lungs inflated with cryopreservative at 5X magnification. (F-G) Ultrastructure of *Erk3* (+/+)(F) or *Erk3* (-/-)(G) lungs. Mature type II cells present characteristic villi (black arrow in F) and contain lamellar bodies (open arrow in F). Type II cells from *Erk3* (-/-) lungs contain an abundant pool of glycogen (* in G) and present attenuated villi. A lamellar body within the glycogen pool is indicated by an open arrow in G. Alveolar secreted surfactant is observed in *Erk3* (-/-) mice (black arrow in G).

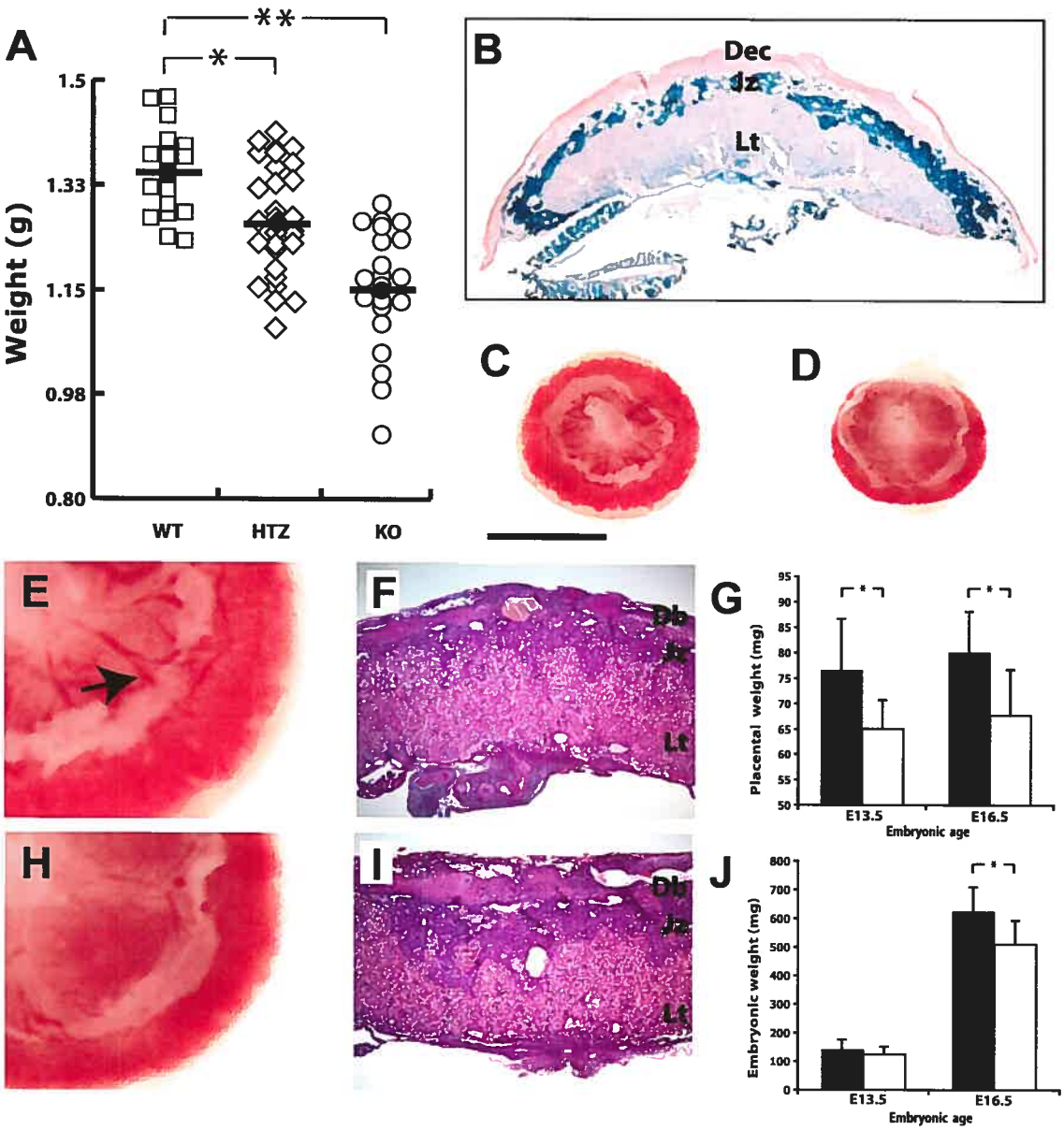

Fig. 8: Intrauterine growth restriction in *Erk3*-mutant mice. (A) Body weights distribution as determined at E18.5 dpc after delivery by c-section. The mean body weight is also presented for each genotype. (B) Expression of $Erk3^{lacZ}$ in the placenta at E15.5 dpc. (C) Morphology of the *Erk3*(+/+) or *Erk3*(-/-)(D) placenta at E18.5 dpc. Scale bar: 5mm. (E) Ventral face of the *Erk3*(+/+) or *Erk3* (-/-)(H) placentas showing the blood vessels of the chorionic plate (arrow in E). (F) Hematoxylin-eosin coloration of E18.5 *Erk3*(+/+) or *Erk3*(-/-)(I) placenta at 10X magnification. (G) Placental or embryonic (J) weights from *Erk3*(+/+) and *Erk3*(-/-) as determined at E13.5 [*Erk3*(+/+): n=10; KO: n=12] or E16.5 dpc [*Erk3*(+/+): n=12; *Erk3*(-/-): n=10] after delivery by C-section. The mean ± SEM is presented for *Erk3*(+/+)(filled bars) or *Erk3*(-/-)(open bars). *: T student test, $p < 0.05$; **: $p < 0.01$. Db: Decidua basalis; Lz: Labyrinthine zone; Jz: Junctional zone.

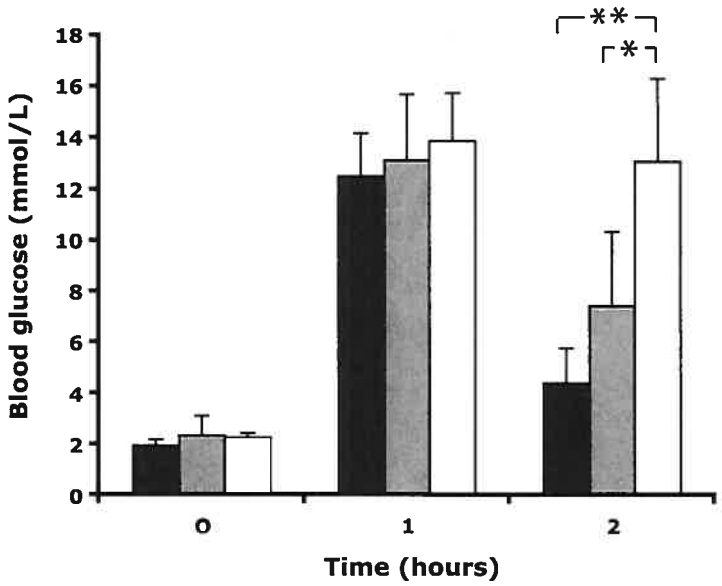

Fig. 9: Glucose homeostasis defects in *Erk3*-mutant mice. Glucose was injected in starved newborns 4 hours after birth, and glycemia was measured at 0, 1 and 2 hours after injection. Each bar represents the mean ± SEM of n = 4 pups [*Erk3*(+/+), filled bars; *Erk3*(+/-), grey bars; *Erk3*(-/-), open bars]. *: T Student test, $p < 0.05$; **: $p < 0.01$.

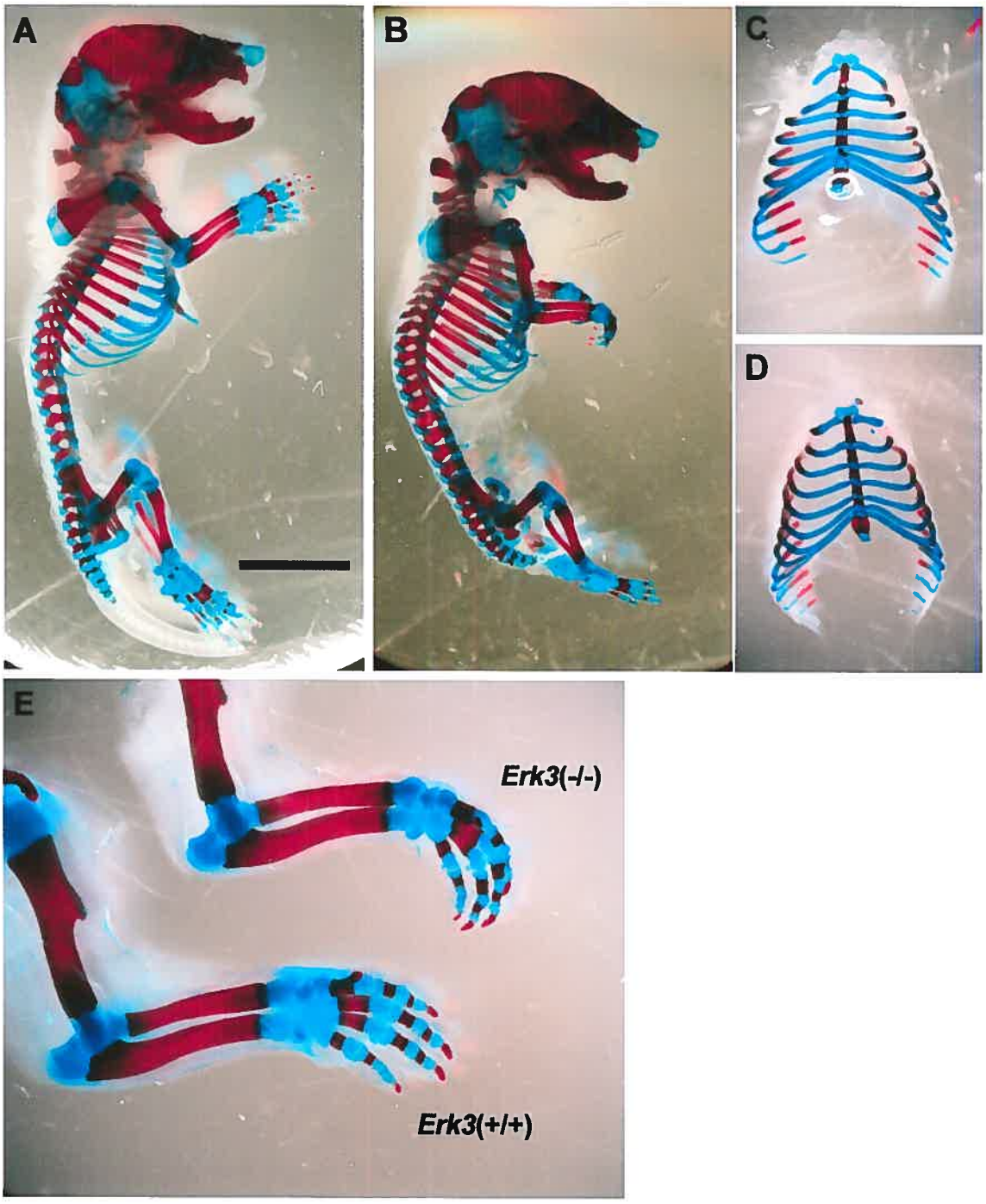

Suppl Fig. 1: The skeletal system of the *Erk3*-null mice. Newborn mice were double stained with Alizarin red and Alcian blue and cleared. Lateral view of whole skeletal preparation of *Erk3*(+/+)(A) or *Erk3*(-/-)(B) mouse. Note the more pronounced curvature of the spine in the *Erk3*(-/-). Ventral view of the rib cage of *Erk3*(+/+) (C) or *Erk3*(-/-)(D) mice. (E) Skeletal staining of forearm showing normal staining of bone and cartilage of the forepaw in KO mice.

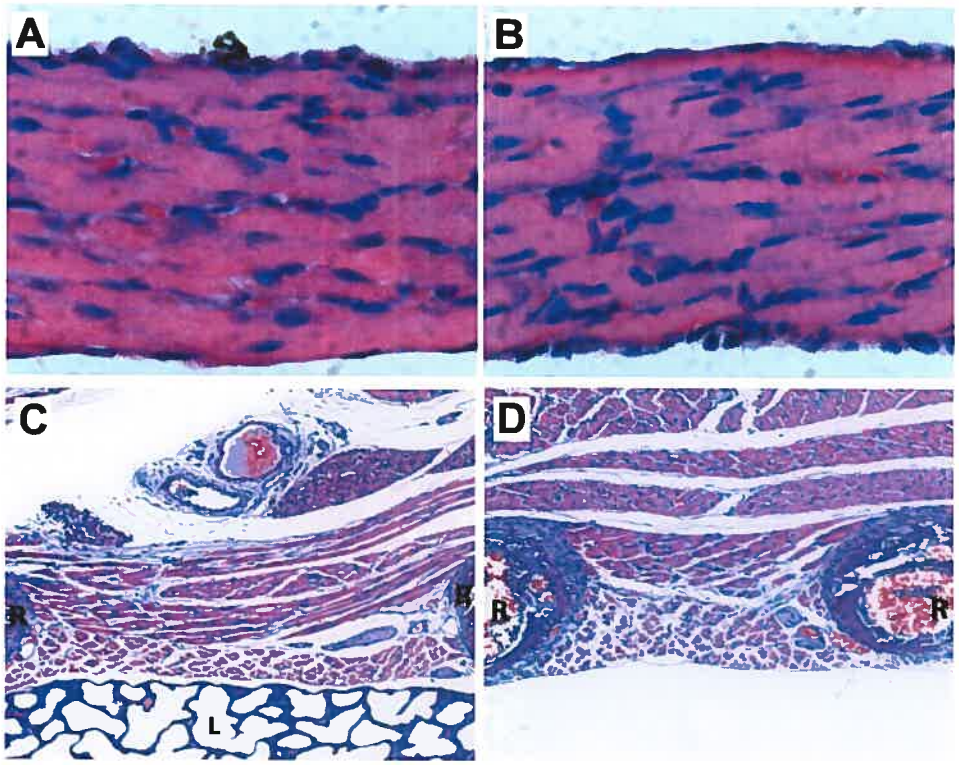

Suppl Fig. 2: Respiratory muscles in the *Erk3*-null pups. Newborn mice were fixed in formalin, embedded in paraffin and sectioned in the coronal plane. (A) Diaphragm muscle from a *Erk3*(+/+) animal (B) Diaphragm muscle from a *Erk3*(-/-) pup. (C) Intercostal muscle of a *Erk3*(+/+) pup. (D) Intercostal muscle of a *Erk3*(-/-) newborn. L:Lung; R: Ribs.

REFERENCES

1 Krens, S. F., Spaink, H. P. and Snaar-Jagalska, B. E. (2006) Functions of the MAPK family in vertebrate-development. FEBS Lett **580**, 4984-4990

2 Zarubin, T. and Han, J. (2005) Activation and signaling of the p38 MAP kinase pathway. Cell Res **15**, 11-18

3 Wang, X. and Tournier, C. (2006) Regulation of cellular functions by the ERK5 signalling pathway. Cell Signal **18**, 753-760

4 Rubinfeld, H. and Seger, R. (2005) The ERK cascade: a prototype of MAPK signaling. Mol Biotechnol **31**, 151-174

5 Karin, M. and Gallagher, E. (2005) From JNK to pay dirt: jun kinases, their biochemistry, physiology and clinical importance. IUBMB Life **57**, 283-295

6 Coulombe, P. and Meloche, S. (2007) Atypical mitogen-activated protein kinases: Structure, regulation and functions. Biochim Biophys Acta **1773**, 1376-1387

7 Boulton, T. G., Nye, S. H., Robbins, D. J., Ip, N. Y., Radziejewska, E., Morgenbesser, S. D., DePinho, R. A., Panayotatos, N., Cobb, M. H. and Yancopoulos, G. D. (1991) ERKs: a family of protein-serine/threonine kinases that are activated and tyrosine phosphorylated in response to insulin and NGF. Cell **65**, 663-675

8 Zhu, A. X., Zhao, Y., Moller, D. E. and Flier, J. S. (1994) Cloning and characterization of p97MAPK, a novel human homolog of rat ERK-3. Mol Cell Biol **14**, 8202-8211

9 Meloche, S., Beatty, B. G. and Pellerin, J. (1996) Primary structure, expression and chromosomal locus of a human homolog of rat ERK3. Oncogene **13**, 1575-1579

10 Turgeon, B., Saba-El-Leil, M. K. and Meloche, S. (2000) Cloning and characterization of mouse extracellular-signal-regulated protein kinase 3 as a unique gene product of 100 kDa. Biochem J **346** Pt 1, 169-175

11 Turgeon, B., Lang, B. F. and Meloche, S. (2002) The protein kinase ERK3 is encoded by a single functional gene: genomic analysis of the ERK3 gene family. Genomics **80**, 673-680

12 Bind, E., Kleyner, Y., Skowronska-Krawczyk, D., Bien, E., Dynlacht, B. D. and Sanchez, I. (2004) A novel mechanism for mitogen-activated protein kinase localization. Mol Biol Cell **15**, 4457-4466

13 Gonzalez, F. A., Raden, D. L., Rigby, M. R. and Davis, R. J. (1992) Heterogeneous expression of four MAP kinase isoforms in human tissues. FEBS Lett **304**, 170-178

14 Coulombe, P., Rodier, G., Pelletier, S., Pellerin, J. and Meloche, S. (2003) Rapid turnover of extracellular signal-regulated kinase 3 by the ubiquitin-proteasome pathway defines a novel paradigm of mitogen-activated protein kinase regulation during cellular differentiation. Mol Cell Biol **23**, 4542-4558

15 Coulombe, P., Rodier, G., Bonneil, E., Thibault, P. and Meloche, S. (2004) N-Terminal ubiquitination of extracellular signal-regulated kinase 3 and p21 directs their degradation by the proteasome. Mol Cell Biol **24**, 6140-6150

16 Seternes, O. M., Mikalsen, T., Johansen, B., Michaelsen, E., Armstrong, C. G., Morrice, N. A., Turgeon, B., Meloche, S., Moens, U. and Keyse, S. M. (2004) Activation of MK5/PRAK by the atypical MAP kinase ERK3 defines a novel signal transduction pathway. Embo J **23**, 4780-4791

17 Schumacher, S., Laass, K., Kant, S., Shi, Y., Visel, A., Gruber, A. D., Kotlyarov, A. and Gaestel, M. (2004) Scaffolding by ERK3 regulates MK5 in development. Embo J **23**, 4770-4779

18 Ridsdale, R. and Post, M. (2004) Surfactant lipid synthesis and lamellar body formation in glycogen-laden type II cells. Am J Physiol Lung Cell Mol Physiol **287**, L743-751

19 Watson, E. D. and Cross, J. C. (2005) Development of structures and transport functions in the mouse placenta. Physiology (Bethesda) **20**, 180-193

20 Duvillie, B., Cordonnier, N., Deltour, L., Dandoy-Dron, F., Itier, J. M., Monthioux, E., Jami, J., Joshi, R. L. and Bucchini, D. (1997) Phenotypic alterations in insulin-deficient mutant mice. Proc Natl Acad Sci U S A **94**, 5137-5140

21 Anhe, G. F., Torrao, A. S., Nogueira, T. C., Caperuto, L. C., Amaral, M. E., Medina, M. C., Azevedo-Martins, A. K., Carpinelli, A. R., Carvalho, C. R., Curi, R., Boschero, A. C. and Bordin, S. (2006) ERK3 associates with MAP2 and is involved in glucose-induced insulin secretion. Mol Cell Endocrinol **251**, 33-41

22 Sun, M., Wei, Y., Yao, L., Xie, J., Chen, X., Wang, H., Jiang, J. and Gu, J. (2006) Identification of extracellular signal-regulated kinase 3 as a new interaction partner of cyclin D3. Biochem Biophys Res Commun **340**, 209-214

23 Joshi, R. L., Lamothe, B., Cordonnier, N., Mesbah, K., Monthioux, E., Jami, J. and Bucchini, D. (1996) Targeted disruption of the insulin receptor gene in the mouse results in neonatal lethality. Embo J **15**, 1542-1547

24 Accili, D., Drago, J., Lee, E. J., Johnson, M. D., Cool, M. H., Salvatore, P., Asico, L. D., Jose, P. A., Taylor, S. I. and Westphal, H. (1996) Early neonatal death in mice homozygous for a null allele of the insulin receptor gene. Nat Genet **12**, 106-109

25 Ramirez, M. I., Millien, G., Hinds, A., Cao, Y., Seldin, D. C. and Williams, M. C. (2003) T1alpha, a lung type I cell differentiation gene, is required for normal lung cell proliferation and alveolus formation at birth. Dev Biol **256**, 61-72

26 Clark, J. C., Wert, S. E., Bachurski, C. J., Stahlman, M. T., Stripp, B. R., Weaver, T. E. and Whitsett, J. A. (1995) Targeted disruption of the surfactant protein B gene disrupts surfactant homeostasis, causing respiratory failure in newborn mice. Proc Natl Acad Sci U S A **92**, 7794-7798

27 Fan, G., Xiao, L., Cheng, L., Wang, X., Sun, B. and Hu, G. (2000) Targeted disruption of NDST-1 gene leads to pulmonary hypoplasia and neonatal respiratory distress in mice. FEBS Lett **467**, 7-11

28 Kling, D. E., Brandon, K. L., Sollinger, C. A., Cavicchio, A. J., Ge, Q., Kinane, T. B., Donahoe, P. K. and Schnitzer, J. J. (2006) Distribution of ERK1/2 and ERK3 during normal rat fetal lung development. Anat Embryol (Berl) **211**, 139-153

29 Kutsuwada, T., Sakimura, K., Manabe, T., Takayama, C., Katakura, N., Kushiya, E., Natsume, R., Watanabe, M., Inoue, Y., Yagi, T., Aizawa, S., Arakawa, M., Takahashi, T., Nakamura, Y., Mori, H. and Mishina, M. (1996) Impairment of suckling response, trigeminal neuronal pattern formation, and hippocampal LTD in NMDA receptor epsilon 2 subunit mutant mice. Neuron **16**, 333-344

30 DeChiara, T. M., Vejsada, R., Poueymirou, W. T., Acheson, A., Suri, C., Conover, J. C., Friedman, B., McClain, J., Pan, L., Stahl, N., Ip, N. Y. and Yancopoulos, G. D. (1995) Mice lacking the CNTF receptor, unlike mice lacking CNTF, exhibit profound motor neuron deficits at birth. Cell **83**, 313-322

31 Kandel, E. R., Schwartz, J. H., and Jessell, T. M. (1991) Principles of Neuroscience. Elsevier, New York

32 Zhao, C., Takita, J., Tanaka, Y., Setou, M., Nakagawa, T., Takeda, S., Yang, H. W., Terada, S., Nakata, T., Takei, Y., Saito, M., Tsuji, S., Hayashi, Y. and Hirokawa, N. (2001) Charcot-Marie-Tooth disease type 2A caused by mutation in a microtubule motor KIF1Bbeta. Cell **105**, 587-597

33 Maina, F., Casagranda, F., Audero, E., Simeone, A., Comoglio, P. M., Klein, R. and Ponzetto, C. (1996) Uncoupling of Grb2 from the Met receptor in vivo reveals complex roles in muscle development. Cell **87**, 531-542

34 Ito, K., Komazaki, S., Sasamoto, K., Yoshida, M., Nishi, M., Kitamura, K. and Takeshima, H. (2001) Deficiency of triad junction and contraction in mutant skeletal muscle lacking junctophilin type 1. J Cell Biol **154**, 1059-1067

35 Baker, J., Liu, J. P., Robertson, E. J. and Efstratiadis, A. (1993) Role of insulin-like growth factors in embryonic and postnatal growth. Cell **75**, 73-82

36 Sibley, C. P., Turner, M. A., Cetin, I., Ayuk, P., Boyd, C. A., D'Souza, S. W., Glazier, J. D., Greenwood, S. L., Jansson, T. and Powell, T. (2005) Placental phenotypes of intrauterine growth. Pediatr Res **58**, 827-832

37 Rodriguez, T. A., Sparrow, D. B., Scott, A. N., Withington, S. L., Preis, J. I., Michalicek, J., Clements, M., Tsang, T. E., Shioda, T., Beddington, R. S. and Dunwoodie, S. L. (2004) Cited1 is required in trophoblasts for placental development and for embryo growth and survival. Mol Cell Biol **24**, 228-244

38 Monkley, S. J., Delaney, S. J., Pennisi, D. J., Christiansen, J. H. and Wainwright, B. J. (1996) Targeted disruption of the Wnt2 gene results in placentation defects. Development **122**, 3343-3353

39 Ware, C. B., Horowitz, M. C., Renshaw, B. R., Hunt, J. S., Liggitt, D., Koblar, S. A., Gliniak, B. C., McKenna, H. J., Papayannopoulou, T., Thoma, B. and et al. (1995) Targeted disruption of the low-affinity leukemia inhibitory factor receptor gene causes placental, skeletal, neural and metabolic defects and results in perinatal death. Development **121**, 1283-1299

40 Arai, T., Kasper, J. S., Skaar, J. R., Ali, S. H., Takahashi, C. and DeCaprio, J. A. (2003) Targeted disruption of p185/Cul7 gene results in abnormal vascular morphogenesis. Proc Natl Acad Sci U S A **100**, 9855-9860

41 Li, Y. and Behringer, R. R. (1998) Esx1 is an X-chromosome-imprinted regulator of placental development and fetal growth. Nat Genet **20**, 309-311

42 Constancia, M., Hemberger, M., Hughes, J., Dean, W., Ferguson-Smith, A., Fundele, R., Stewart, F., Kelsey, G., Fowden, A., Sibley, C. and Reik, W. (2002) Placental-specific IGF-II is a major modulator of placental and fetal growth. Nature **417**, 945-948

43 Fowden, A. L., Ward, J. W., Wooding, F. P., Forhead, A. J. and Constancia, M. (2006) Programming placental nutrient transport capacity. J Physiol **572**, 5-15

44 Kant, S., Schumacher, S., Singh, M. K., Kispert, A., Kotlyarov, A. and Gaestel, M. (2006) Characterization of the atypical MAPK ERK4 and its activation of the MAPK-activated protein kinase MK5. J Biol Chem **281**, 35511-35519

45 Aberg, E., Perander, M., Johansen, B., Julien, C., Meloche, S., Keyse, S. M. and Seternes, O. M. (2006) Regulation of MAPK-activated protein kinase 5 activity and subcellular localization by the atypical MAPK ERK4/MAPK4. J Biol Chem **281**, 35499-35510

46 Nagy, A., Rossant, J., Nagy, R., Abramow-Newerly, W. and Roder, J. C. (1993) Derivation of completely cell culture-derived mice from early-passage embryonic stem cells. Proc Natl Acad Sci U S A **90**, 8424-8428

47 Bendayan, M. (1995) Colloidal gold post-embedding immunocytochemistry. Prog Histochem Cytochem **29**, 1-159

CHAPITRE 5

Conclusions et directions futures

MISE EN SITUATION

Le chapitre 5 est une discussion de l'importance des résultats présentés dans cette thèse de même que des limitations du modèle génétique présenté. De plus, ce chapitre adresse les avenues de recherche envisageables dans l'étude future de la fonction de ERK3, tant au niveau moléculaire que physiologique.

5.1 ERK3 : il ne peut y en avoir qu'un

5.1.1 Confusion ERK3-ERK4 : la malédiction du SEG

On a longtemps cru que deux isoformes de ERK3 pouvait exister dans les cellules de mammifères. Le premier ADNc de ERK3 rapporté prédisait en effet une protéine de 546 a.a. (62 kDa), alors que d'autres ADNc prédisaient une protéine de 720 a.a (100 kDa). Cependant, mes travaux ont permis de démontrer qu'il n'existe qu'un gène encodant la protéine ERK3, et que le produit de ce gène est une protéine de 100 kDa chez le rat, la souris et l'homme (chapitres 2 et 3).

Il est plutôt difficile d'évaluer l'impact de cette confusion pour la recherche sur ERK3, qui pourrait être à l'origine d'interprétations expérimentales erronées. Par exemple, il a été rapporté que ERK3 interagit avec B-Raf [1] et qu'il existe une corrélation entre l'activité de ERK3 et celle de la PKC [2]. De plus, les premières études de localisation cellulaire de ERK3 suggère qu'il s'agit d'une protéine constitutivement nucléaire [3]. Ces études font référence à une protéine de 62 kDa qui réagit avec des anticorps générés contre une protéine ERK3 recombinante. Cependant, puisque le gène ERK3 prédit une protéine de 100 kDa, les conclusions de ces études sont donc à revoir. D'ailleurs, aucune autres études n'ont fait suite à ces résultats. La détection d'une protéine de 62 kDa pourrait être associée à la reconnaissance de ERK4 par des anticorps générés contre ERK3. Il semblerait que cette controverse soit encore aujourd'hui d'actualité. Plusieurs études récentes font en effet référence à des protéines de différentes tailles (de 62 kDa jusqu'à 120kDa) reconnues par des anticorps contre ERK3 et d'une éventuelle confusion avec ERK4 [4-7].

Contre toute attente, des erreurs dans la séquence primaire de ERK4 ont récemment été rapportées [8, 9]. La correction de la séquence prédit une protéine plus longue de quelque 30 acides aminés. Cette erreur pourrait être à l'origine d'une divergence de résultats expérimentaux quant à l'association de ERK4 avec MK5 [10, 11] et cette interaction a récemment été revérifiée [8].

Ces confusions expliquent en partie pourquoi ERK3 demeure une des MAPK les moins bien caractérisés de toute cette famille. Ainsi, il a fallu attendre les dernières années avant la mise en évidence de modes de régulation de ERK3 ainsi que de l'identification de substrats potentiels. En conséquence, l'architecture de cette voie demeure encore un mystère, plus de 15 ans après la découverte de cette MAP kinase.

5.1.2 Clivage par protéolyse

Le groupe de I. Sanchez a récemment confirmé mes résultats démontrant que ERK3 est une protéine de 100 kDa chez le rat [6]. Par ailleurs, ce groupe a proposé qu'une isoforme courte de ERK3 pouvait être générée suite à la protéolyse de sa partie C-terminale. Ainsi, la surexpression d'une chimère recombinante GFP-ERK3 (stable) dans des cellules Hela a permis de mettre en évidence une forme GFP-ERK3 plus courte que celle attendue, puisque des anticorps générés contre la partie C-terminale de ERK3 ne permette pas sa détection par immunofluorescence. La forme endogène tronquée de ERK3 a également pu être révélée par analyse *western* à partir d'extrait de cellules Hela en présence d'un inhibiteur du protéasome, le MG132 [6].

Cette protéine pourrait avoir une demi-vie très courte, et les conditions nécessaires à sa stabilisation pourraient être associées au stade de prolifération de la cellule. En effet, cette isoforme GFP-ERK3 tronquée est détectée uniquement dans le noyau des cellules s'approchant de la mitose [6]. Les souris déficientes en ERK3 devraient permettre une meilleure compréhension du rôle de cette isoforme. Tout d'abord, la disponibilité de cellules ou tissus déficients en ERK3 est un contrôle négatif important pour prouver l'existence de cette protéine lors d'expériences d'immunolocalisation et d'études *western*. Ensuite, les souris déficientes en ERK3 représentent un outil important pour déterminer le rôle cellulaire de ERK3 (voir ci-bas). Ainsi, connaître la fonction cellulaire de ERK3 devrait permettre de comprendre l'importance de cette isoforme potentielle de ERK3.

5.1.3 ERK3 à l'ère post-génomique

Les analyses *in silico* de la sous-famille ERK3 des MAP kinases que j'ai effectuées ont précédé la publication de la séquence du génome humain, ainsi que l'analyse du kinome [12]. Ces derniers travaux ont confirmé l'existence d'un seul gène fonctionnel encodant ERK3 chez l'humain. Par contre, nous avons caractérisé un nombre de pseudogènes pour *ERK3* de deux fois supérieur à celui rapporté lors de l'analyse du kinome humain [12]. Ceci peut s'expliquer par des différences entre les méthodes d'analyse utilisées. Ainsi, ayant utilisé la séquence complète de l'ADNc de *ERK3* pour mes analyses, la probabilité d'identifier des séquences génomiques pour *ERK3* spécifiques était augmentée.

Il est toutefois surprenant que *ERK3* soit le seul gène MAP kinase à avoir autant de pseudogènes, alors qu'il est probablement l'un des gènes les plus jeunes de la famille MAP kinase. Ce grand nombre de pseudogènes pourrait être associé à la stabilité de son ARNm, sa compétence traductionnelle ou sa localisation [13]. Les rétro-pseudogènes sont

des copies de l'ARNm d'un gène rétrotranscrites et intégrées dans le génome. Ces séquences sont couramment considérées comme non-fonctionnelles [14]. Toutefois, ces pseudogènes pourraient être impliqués dans la regulation de l'expression de ERK3, dans la mesure où ils sont exprimés [15]. Alternativement, ces séquences pourraient être vues comme des *potogènes*, i.e, des séquences ayant le potentiel de devenir des gènes fonctionnels [16]. La famille de gènes ERK3 pourrait ainsi être en évolution rapide.

5.2 Rôles physiologiques de ERK3

5.2.1 Rôle dans les interactions épithélio-mésenchymateuses

L'étude de l'expression de *Erk3* et l'analyse des phénotypes des souris *Erk3*(-/-) ont amené une hypothèse intéressante quand à une fonction inattendu de ERK3 au cours du développement murin. En effet, la forte expression de *Erk3* au niveau de l'épithélium des tissus se développant via des interactions entre un épithélium et le mésenchyme de ces tissus suggère un rôle de ERK3 dans les interactions épithélo-mésenchymateuse (E-M). Par ailleurs, des fissures palatines ont été observées chez 10% des homozygotes mutants dont un fond génétique hétérogène (129/Sv x C57BL/6) x CD1 (Figure 1). Puisque le développent du palais est contrôlé par des interactions E-M, cette observation est également en accord avec l'hypothèse d'un rôle de ERK3 dans les interactions E-M.

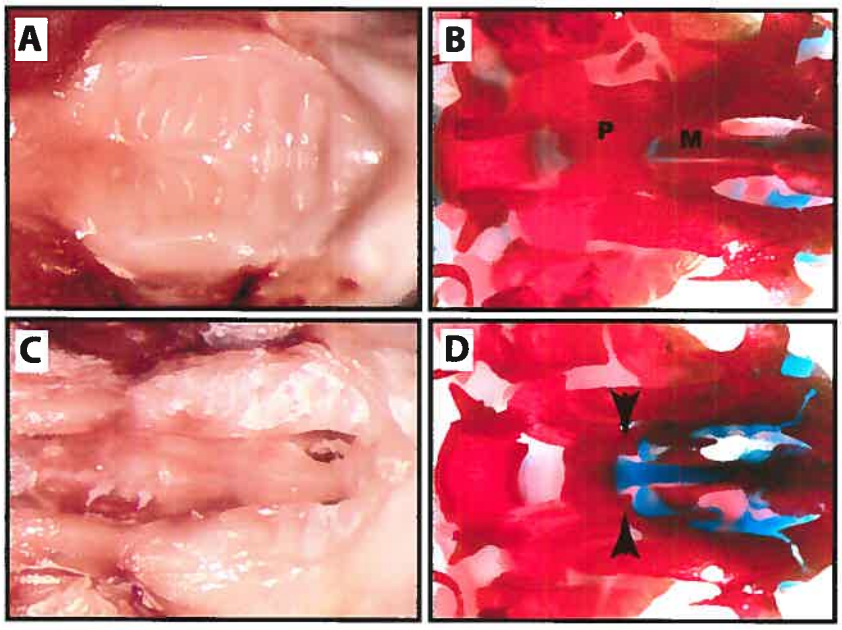

Figure 1: Fissure palatine des souris déficientes en ERK3 dans un fond mixte (129/Sv x C57BL/6) x CD1. Analyse macroscopique des palais d'une souris de type sauvage (A) et homozygote mutante (C). Coloration des os et cartilage de la tête d'une souris homozygote mutante présentant une fissure palatine (D) en comparaison avec une souris de type sauvage (B). L'absence de fusion des os du palais secondaire est indiquée par des flèches. P :Palatal shelves, M : Maxilary shelves.

Cette hypothèse prédit l'existence potentielle d'un signal provenant des cellules du mésenchyme pouvant activer ERK3 au niveau de l'épithélium d'un organe en formation. En accord avec cette hypothèse, nous avons mis à jour un signal provenant d'une lignée cellulaire d'origine non-épithéliale (fibroblaste) capable d'induire l'expression de ERK3 dans une ligné de type épithéliale (Figure 2). Bien que l'identité de ce facteur reste inconnue, ces donnés préliminaires sont en faveurs de l'existence d'un tel signal et d'un rôle de ERK3 dans les interactions E-M. La concentration et la purification de ce facteur à partir du milieu conditionné permettront de déterminer l'identité de ce facteur de façon à caractériser le rôle de ERK3 dans les interactions E-M ou d'autre types d'interactions cellules-cellules.

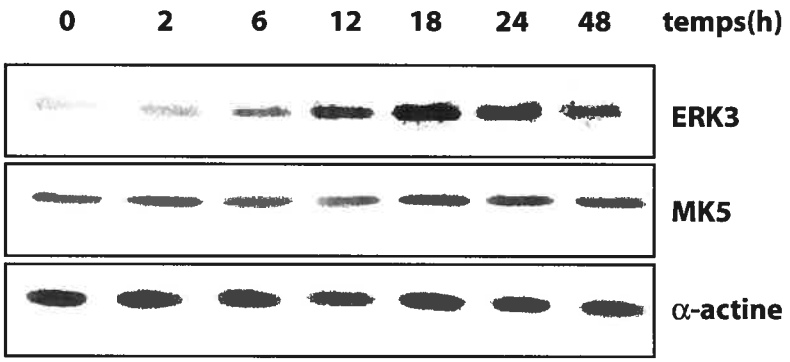

Figure 2: Cinétique d'expression de ERK3 en réponse à un facteur extracellulaire d'identité inconnue. Analyse *western* de lysats protéiques provenant de cellules HEK293 en présence d'un milieu conditionné provenant de cellules L en absence de sérum. L'expression de ERK3 est maximale au temps 18h, alors que l'expression de MK5 n'est pas modifiée par le milieu conditionné. Une quantité comparable de protéines à été analysée à chaque point tel que démontré par les niveaux d'α-actine.

5.2.2 Implication dans le cycle cellulaire

Plusieurs observations expérimentales sont à l'origine de l'hypothèse que ERK3 est impliqué dans le contrôle de la prolifération cellulaire. Tout d'abord, la surexpression d'un mutant stable de ERK3 est associée à une diminution de la synthèse d'ADN [17]. De plus, l'augmentation de l'expression de ERK3 lors de la différenciation cellulaire est parallèle à celle des niveaux d'expression de $p21^{CIP1}$, un inhibiteur du cycle cellulaire [17]. Par ailleurs, des expériences de double-hybride et de purification par affinité en tandem (TAP) effectuées dans notre laboratoire ont permis de mettre en évidence une interaction entre ERK3 et des protéines régulatrices du cycle cellulaire, les kinases Cdc7 et Nek2. Cdc7 est impliquée dans la progression de la phase S [18], alors que Nek2 participe à la régulation de la transition G2/M

[19]. Finalement, la caractérisation de l'interaction entre ERK3 et la cycline D3 a récemment été rapportée [20] et confirmée par notre laboratoire. On ignore cependant l'importance physiologique de l'interaction entre ERK3 et ces protéines et, conséquemment, si ERK3 joue un rôle de régulateur positif ou négatif du cycle cellulaire. L'inhibition de prolifération observée en réponse à la surexpression d'un mutant stable de ERK3 pourrait être causée par un effet dominant négatif. Par contre, puisque $p21^{CIP}$ est un marqueur de différenciation terminale [21], ceci suggère que ERK3 pourrait être associée à la sortie du cycle cellulaire qui accompagne la différenciation cellulaire terminale.

Il est difficile à ce niveau de déterminer si les phénotypes observés chez les souris *Erk3* mutantes peuvent être attribués à des défauts de prolifération ou de différenciation cellulaire. En effet, l'examen pathologique des souris mutantes n'a pas révélé de malformations associées à des défauts de prolifération ou de différenciation. Une caractérisation approfondie des défauts cellulaires associés aux phénotypes des souris *Erk3* mutantes permettra de répondre à cette question. Par ailleurs, dans le but de mettre en évidence des problèmes de prolifération cellulaires en absence de ERK3, nous avons établi des lignées primaires de fibroblastes embryonnaires (MEFs) à partir d'embryons mutants. Cependant, la prolifération des cellules mutantes (3 lignées pour chaque génotype) n'est pas affectée sur une période de 30 passages (non-illustré).

La connaissance du patron d'expression de *Erk3* au cours du développement murin représente une information importante pour comprendre le rôle de ERK3 dans la prolifération et/ou différenciation. Ainsi, il serait important de corréler l'expression de ERK3 avec la différenciation cellulaire *in vivo*. La glande sous-maxillaire représente un tissu approprié pour ce genre d'étude. En effet, la formation des embranchements de l'épithélium de la glande en développement requiert plusieurs processus cellulaires, dont la prolifération et la différentiation cellulaire, coordonnés par des interactions E-M [22]. De façon intéressante, *Erk3* est exprimé de manière spécifique dans l'épithélium de la glande en développement (chapitre 4). Il sera important de déterminer si cette expression corrèle avec la prolifération ou la différenciation des cellules épithéliales, de même qu'évaluer l'effet de la perte de ERK3 sur la formation de cette glande. Les souris *Erk3* mutantes demeurent donc un modèle important pour comprendre l'implication de ERK3 lors de la prolifération ou la différenciation cellulaire.

5.2.3 Rôle dans la sécrétion

Les sites d'expression les plus importants de *Erk3* sont sans équivoque les tissus impliqués dans la sécrétion. Par exemple, l'expression de *Erk3* est la plus forte dans les plexus choroïdes du cerveau foetal. Le plexus choroïde est la glande dont la sécrétion est la plus importante dans tout l'organisme, avec une production de 500 ml de liquide céphalorachidien par jour chez l'homme [23]. D'autres sites d'expression de *Erk3* comme la glande sous-maxillaire, le pancréas et les muqueuses gastrique et nasale sont en accord avec un rôle de ERK3 dans la sécrétion.

Il a récemment été suggéré que ERK3 est important pour la production d'insuline chez le rat [7]. On pourrait donc s'attendre à ce que ERK3 soit important pour la sécrétion d'insuline chez la souris. En accord avec ce rôle de ERK3, une résistance anormale au glucose chez les souris *Erk3(-/-)* a été observée. Toutefois, plusieurs expériences seront nécessaires pour confirmer l'importance de ERK3 dans la production et/ou sécrétion d'insuline. Des protocoles permettant de mesurer les niveaux d'insuline chez les nouveaux-nés sont présentement en élaboration dans notre laboratoire et devraient permettre de déterminer l'effet de la perte de ERK3 sur la production d'insuline en réponse au glucose. La diminution des niveaux d'insuline chez les souris déficientes en ERK3 sera une évidence importante que ERK3 est important pour la sécrétion.

La détresse respiratoire chez les nouveaux-nés *Erk3(-/-)* pourrait également être causé par des défauts de sécrétion de surfactant pulmonaire, étant donné que nos analyses préliminaires suggèrent une structure normale des poumons. Comme dans le cas de l'insuline, il sera important de vérifier la production de surfactant des souris *Erk3(-/-)*.

5.2.4 Réponse aux stress du réticulum endoplasmique

Plusieurs résultats expérimentaux suggèrent indirectement un rôle de ERK3 dans la réponse au stress du réticulum endoplasmique (RE). Ainsi, les niveaux d'expression de ERK3 sont augmentés dans plusieures lignées cellulaires par des inhibiteurs spécifiques du protéasome tels que le MG132, MG115, PS341, PSI, lactacystin et lactacystin-β-lactone [24]. L'inhibition du protéasome représente un stress pour le RE et des réponses cellulaires, dont l'apoptose, y sont associées [26-28]. Par ailleurs, cette augmentation est dépendante de l'activité de $p38^{MAPK}$, une MAP kinase également induite en réponse au stress du RE [25]. Les gangliosides peuvent également induirent un stress du RE [29] et certains sont responsables de l'augmentation des niveaux de ERK3 dans les cellules RAJI [30]. La colocalisation de ERK3 avec la protéine ERGIC-53 dans le compartiment ERGIC [6], suggère également un

rôle dans la réponse au stress du réticulum endoplasmique. En effet, l'expression de cette protéine est augmentée par des agents induisant des stress du RE [31].

D'un point de vue physiologique, la réponse au stress du RE est importante pour le développement normal des cellules sécrétrices [32], mais également impliquée dans certaines pathologies dont le diabète [33]. De façon intéressante, une forte expression du gène *Erk3* a été observée dans les tissus dont les cellules possèdent un RE très spécialisé et très développé, dont les cellules sécrétrices ainsi que dans le muscle squelettique (chapitre 4). Finalement, une résistance anormale au glucose qui caractérise le diabète est observée chez les souris *Erk3*(-/-). Ces observations sont également en accord avec un rôle de ERK3 dans la réponse au stress du RE.

L'importance de ERK3 dans la réponse au stress du RE pourrait être évaluée de plusieurs façons grâce aux souris *Erk3* mutantes. Ainsi, la sensibilité des MEFs *Erk3*(-/-) à des agents inducteurs de stress du RE pourrait être évaluée. De manière semblable, la sensibilité à des dommages tissulaires provoqués par l'induction de stress du RE pourrait être examinée dans les embryons *Erk3* mutants. Par ailleurs, la souris transgénique ERAI pourrait être exploitée. Cette lignée exprime un rapporteur fluorescent (GFP) dont l'expression est basée sur le clivage de l'ARNm de XBP-1, un indicateur de stress du RE [34]. La présence de ce transgène dans un fond *Erk3* nul permettrait de quantifier les niveaux de réponse au stress du RE chez les embryons mutants et de les comparer avec ceux d'embryons normaux.

5.2.5 Point de vue de la localisation chromosomique

Le gène *Erk3* murin a été localisé sur la partie centrale du chromosome 9, près du locus associé aux phénotypes *dilute* chez la souris (chapitre 2). Les allèles *dilute* sont associés principalement à des défauts mélanocytaires. De plus, comme pour les souris *Erk3*(-/-), des problèmes neurologiques ainsi que la mortalité précoce sont caractéristiques des phénotypes *dilute* [35]. Toutefois, il est peu probable que des mutations du gène *Erk3* contribuent au phénotype *dilute*. En effet, le gène responsable du phénotype *dilute*, *Myo5a*, qui encode une myosine non-conventionnelle [36], est situé à plus de 180 kb de *Erk3*.

5.2.6 Point de vue évolutif

L'analyse de la séquence protéique de ERK3 entre différentes espèces de vertébrés indique que ERK3 est fortement conservée chez les vertébrés (Figure 3). Cette forte conservation de ERK3 suggère que sa fonction est également conservée entre ces espèces. Mes résultats indiquent que ERK3 est essentiel pour la survie néonatale chez la souris

(chapitre 4). Cependant, survivre aux premières heures de la vie extra-utérine s'applique aux mammifères et une question demeure quant à l'extrapolation de ce rôle physiologique de ERK3 aux espèces de complexité inférieure.

Figure 3: Alignement de la séquence protéique du domaine kinase de ERK3 entre différentes espèces de vertébrés. Les séquences primaires correspondant au domaine kinase de ERK3 (317 premier a.a.) ont été comparées à l'aide du programme CLUSTALW (http://www.ebi.ac.uk/clustalw/). Les régions d'identité protéique sont soulignées en gris. Le motif de phosphorylation SEG est souligné en jaune.

Il a été démontré que l'absence de ERK3 mène à des troubles respiratoires à la naissance. Bien que la cause de ce phénotype n'a pas encore été identifiée, la détresse respiratoire pourrait être associée à des défauts neurologiques ou à la production insuffisante de surfactant dans les poumons (à démontrer). Toutefois, on devrait s'attendre à l'absence de ce phénotype chez l'amphibien ou le poisson, pour qui le système nerveux ou les poumons sont moins importants pour l'oxygénation du sang que chez la souris.

Un phénotype important associé à la létalité des souris *Erk3* mutantes est l'incapacité à se nourrir et les tests neurologiques effectués chez les nouveaux-nés déficients en ERK3 indiquent un problème neuromusculaire chez ces mutants. ERK3 est donc important pour le développement ou la fonction du système neuromusculaire (voir ci-bas). L'importance de cette fonction est mise en évidence facilement à la naissance chez la souris. En effet, l'intégrité du système neuromusculaire est dispensable au développement intra-utérin [37],

mais absolument essentielle à l'adaptation à la vie extra-utérine (chapitre 1, partie 2). Ainsi, cette fonction de ERK3 peut être extrapolée jusqu'au poisson zèbre, où l'absence de ERK3 devrait également mener à des défauts du système neuromusculaire, qui pourrait être mis en évidence par des problèmes dans le mouvement. Le gène ERK3 pourrait être apparu au cours de l'évolution en association avec une fonction neuromusculaire essentielle.

5.3 La souris *Erk3(-/-)* comme modèle d'étude: forces et limitations

La façon la plus simple de mettre en évidence la fonction biologique d'un gène demeure l'invalidation de celui-ci chez un organisme modèle. Nous avons donc choisi d'invalider le gène *Erk3* chez la souris. Or, depuis la génération des premiers modèles d'invalidation géniques chez la souris à la fin des années 90, plusieurs stratégies ont été développées pour inactiver les gènes murins [38, 39]. La stratégie présentée dans cette thèse pour la génération des souris *Erk3*(-/-) implique le remplacement de la région codante de *Erk3* par le rapporteur *LacZ*, donc la génération d'un allèle nul.

Cette approche possède plusieurs avantages. Tout d'abord, la protéine ERK3 est hautement conservée entre la souris et l'humain. La souris représente donc un modèle de choix pour l'étude de ERK3. Deuxièmement, l'approche d'invalidation génique permet de contourner les limitations liées à l'étude de ERK3. Ainsi, l'invalidation du gène fait abstraction du caractère atypique de ERK3 ainsi que des controverses liées aux études de localisation cellulaire, d'isoformes et de substrats. De façon importante, ce modèle devrait permettre de résoudre des controverses dont la localisation subcellulaire de ERK3. En effet, les tissus qui n'expriment pas ERK3 sont des contrôles important lors d'étude de la localisation subcellulaire de ERK3 dans un tissus donné. Finalement, cet outil génétique est adapté pour l'étude de l'expression du gène *Erk3*. Cet outil pourrait même être utilisé pour mettre en évidence des différences histologiques entre des tissus affectés (-/-) et normaux (+/-).

Deux limitations majeures sont toutefois associées à ce modèle. Tout d'abord, l'observation des phénotypes associés à une mutation chez la souris peut prendre de quelques mois à quelques années. Le poisson zèbre est un modèle alternatif où la fonction d'un gène important pour le développement peut être mise en évidence en quelques jours par l'utilisation d'oligonucléotides antisens morpholinos [40]. Une étude structure-fonction d'une protéine est donc préférable chez le poisson zèbre. D'autres limitations de notre modèle concernent l'analyse des phénotypes. Ainsi, l'invalidation de *Erk3* résulte en la mortalité néonatale, un phénotype complexe. En effet, plusieurs organes sont importants pour la survie néonatale. De plus, les phénotypes observés peuvent être secondaires à des défauts primaires. Par ailleurs, il nous est impossible d'adresser l'importance de ERK3 pour la croissance post-natale ainsi

que l'homéostasie chez l'adulte. Dans cette optique, la génération d'un modèle de délétion génique conditionnelle permettrait de palier à ces limitations.

Plusieurs questions concernant la biologie d'un gène sont souvent à l'origine de l'élaboration d'un modèle murin. Or, est-il préférable de générer un mutant pour répondre à plusieurs questions ou de générer plusieurs mutants pour répondre à plusieurs questions? La réponse à cette question est simple, il n'existe pas de modèle de délétion génique parfait. Le meilleur modèle demeure celui qui permet de répondre à une question expérimentale en peu de temps, à peu de frais ainsi qu'avec la meilleure valeur scientifique. Dans le cas présent, le modèle *Erk3(-/-)* permet de répondre rapidement à la question de l'importance de ce gène, de même qu'à la question d'expression du gène. Cependant le modèle ne permet pas d'adresser rapidement la fonction biologique de ERK3, principalement à cause de la complexité des phénotypes de létalité néonatale. Par contre, ce modèle a permis de corréler l'absence de ERK3 avec le développement de plusieurs pathologies.

5.4 Perspectives d'études futures

5.4.1 Caractérisation du rôle moléculaire de ERK3

Lorsque la fonction biologique d'un gène reste inconnue, l'objectif à long terme de l'invalidation de ce gène est de déterminer le rôle moléculaire de la protéine encodée par ce gène. Cependant, il existe plusieurs étapes expérimentales séparant les observations initiales du phénotype et l'étude directe de la fonction moléculaire de la protéine (Figure 4). Une approche expérimentale basée sur la fenêtre de mortalité néonatale a permis de mettre en évidence les systèmes touchés chez les souris *Erk3*(-/-) (Chapitre 4). Ceci permettra de caractériser des anomalies tissulaires et conséquemment de mettre en évidence les défauts cellulaires responsables du phénotype de mortalité néonatale. Finalement, la connaissance des évènements moléculaires impliqués dans ces processus cellulaires défaillants permettront de positionner ERK3 dans une voie métabolique connue, ou encore de définir une nouvelle voie métabolique.

Toutefois, bien que ce schème représente une approche expérimentale alléchante pour identifier la fonction moléculaire de ERK3, il pourrait mener à un cul de sac expérimental. En effet, dans le cas d'une analyse de phénotypes de souris mutantes, particulièrement dans le cas de phénotypes néonataux, il est primordial de déterminer si les phénotypes représentent une conséquence d'un défaut primaire avant de poursuivre la caractérisation moléculaire de ces phénotypes en question. Dans le cas des souris déficientes en ERK3, il serait nécessaire de déterminer si les phénotypes observés sont secondaires à des problèmes de placenta. Les

souris déficientes en p38α^{MAPK} et en Rb, un régulateur du cycle cellulaire, illustrent bien ce concept d'effet secondaire. La mort embryonnaire des souris déficientes en p38α^{MAPK} est associée à des défauts cardiaques et vasculaires. Cependant ces défauts sont secondaires à un développement anormal du placenta [41]. De la même façon, des défauts d'érythropoïèse et neuronaux au cours du développement sont associés à la perte de Rb [42-44]. Comme pour p38α^{MAPK}, ces phénotypes résultent de problèmes de développement du placenta [45]. On ne peut malheureusement pas exclure à ce stade la possibilité que des problèmes extra-

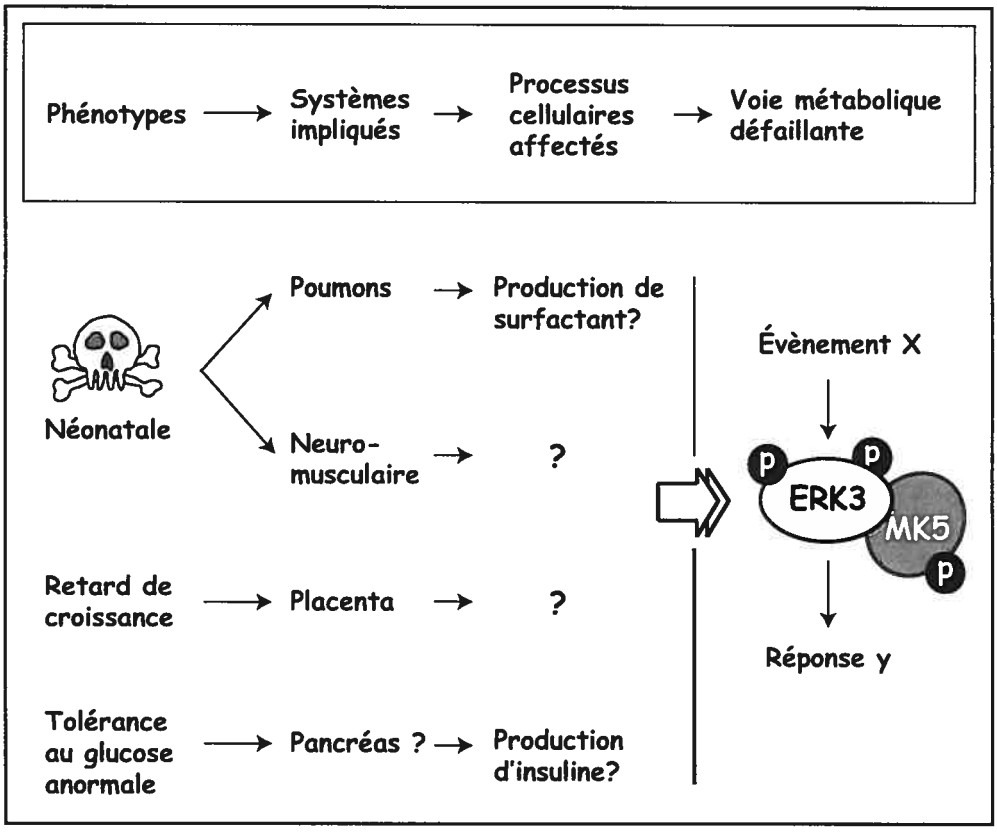

Figure 4: Schème d'étude de la fonction moléculaire de ERK3 à partir des phénotypes associés à l'invalidation du gène *Erk3* chez la souris.

embryonnaires, mis en évidence par un retard de croissance du placenta et des foetus, puissent affecter le développement du système nerveux, retarder le développement pulmonaire ainsi qu'interférer avec la programmation intra-utérine des organes impliqués dans l'homéostasie du glucose chez les souris *Erk3(-/-)*. Ainsi, le choix des tissus qui serviront à déterminer la fonction moléculaire de ERK3 devra se faire avec distinction.

Finalement, des lignées cellulaires établies à partir d'embryons *Erk3*(-/-) représentent un modèle important pour l'étude de la fonction moléculaire de ERK3. Ainsi, des fibroblastes embryonnaires déficients en ERK3 ont déjà été utilisés pour démontrer une relation entre les

niveaux de ERK3 et les niveaux de phosphorylation de la protéine MK5 (Annexe 1). Cependant, on peut se demander si ce modèle cellulaire est idéal pour l'étude de la fonction moléculaire de ERK3. Basée sur les données d'expression de ERK3, d'autres lignées cellulaires tel que les épithéliums, représentent probablement de meilleurs modèles cellulaires.

5.4.2 Déterminer l'effet du fond génétique sur la mutation *Erk3*-nulle

Toutes les mutations chez la souris, qu'elles soient naturelles, induites ou ciblées, peuvent résulter en des phénotypes très différents en relation avec le fond génétique de la mutation [38]. L'exemple classique de l'effet du fond génétique sur le phénotype d'une mutation est la délétion du gène *Egfr*, qui encode le récepteur de l'EGF. En effet, le temps de létalité des souris *Egfr* (-/-) varie considérablement en fonction du fond génétique, débutant à 7.5 dpc en fond CF-1, en passant par la mortalité fœtale en fond 129/Sv, perinatale en fond CD1 et postnatale dans le fond mixte 129/Sv x C57Bl/6 [46, 47]. Dans notre cas, un exemple

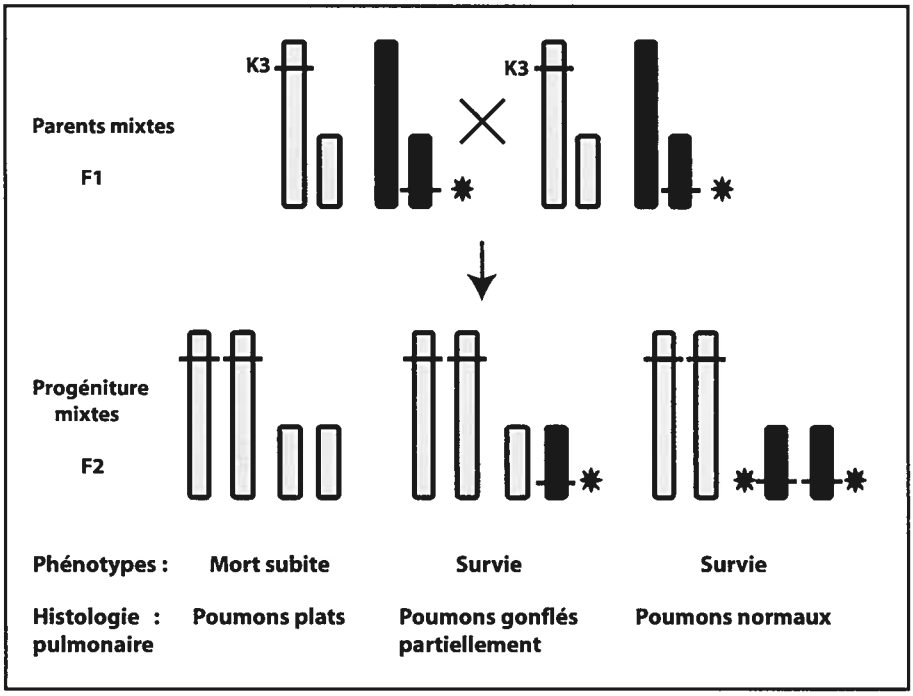

Figure 5: Origine et ségrégation théorique d'un allèle modificateur d'un phénotype associé à la mutation *Erk3(-/-)* dans un fond mixte C57BL/6 x 129/Sv. Les animaux homozygotes mutants issus du croisement F1 possèdent une ségrégation différente d'un allèle modificateur potentiel. Cette distribution pourrait être associée à une variabilité de certains phénotypes, par exemple la détresse respiratoire. K3- : allèle nul d'un chromosome 129/Sv. Astérix : allèle modificateur provenant d'un chromosome C57BL/6.

approprié est l'inactivation du gène de MK5. En effet, les souris déficientes en MK5 sont viables dans un fond génétique mixte 129/Sv x C57BL/6, alors qu'une mortalité embryonnaire partielle est observée avec un enrichissement en C57BL/6 [11]. Étant donné la relation moléculaire entre MK5 et ERK3, on pourrait s'attendre à un effet du fond génétique sur le phénotype de la mutation *Erk3*(-/-). Aucun des fonds génétiques testés jusqu'à maintenant ne permet aux souris déficientes en ERK3 de survivre, tel que démontré par l'absence de mutants homozygotes trois semaines après la naissance. Toutefois, une variabilité du phénotype est observée chez les nouveaux-nés *Erk3(-/-)* dans le fond génétique mixte, où seulement le tiers des animaux meurent de détresse respiratoire. Il n'est pas impossible qu'un gène modificateur soit responsable de la variabilité de ce phénotype dans le fond mixte (Figure 5).

Il est important de déterminer l'influence du fond génétique à ce stade, dans le but de choisir le fond génétique le plus approprié pour poursuivre la caractérisation des phénotypes associés à l'invalidation du gène *Erk3*. Par ailleurs, ceci pourrait permettre d'identifier un schème expérimental pour identifier des gènes modificateurs potentiels.

5.4.3 Adresser la redondance ERK3-ERK4

Aucun défauts tissulaires marqués chez les souris *Erk3(-/-)* au cours du développement embryonnaire n'ont pu être mis en évidence par des analyses pathologiques. On aurait pu toutefois s'attendre à des défauts de développement majeurs dans au moins un des tissus exprimant fortement le gène *Erk3,* et ce pour plusieurs raisons. Tout d'abord, l'expression de ERK3 coïncide avec des stades importants du développement cardiaque. Des défauts de développement du coeur causent des phénotypes sévères dans d'autres modèles de délétion génique chez la souris, et sont également associés à la mortalité néonatale (voir chapitre 1). De façon similaire *Erk3* est exprimé dans le tissu dont l'intégrité est critique pour la survie de l'embryon, le placenta. Comme pour le cœur, des défauts appréciables du placenta ont été décrits lors d'analyse de mutants murins présentant une mortalité néonatale [48]. Finalement, la perte de MK5 corrèle avec une diminution des niveaux de ERK3 [10, 11] et la létalité embryonnaire partielle des souris déficientes en MK5 dans le fond génétique C57Bl/6 corrèle avec un stade d'expression élevé de ERK3 (chapitre 1 et 4).

Il semble donc probable qu'un gène puisse compenser pour la perte de ERK3 lors du développement embryonnaire chez la souris. Un candidat potentiel pour remplir ce rôle est sans contredit la protéine ERK4, un paralogue de ERK3 (voir discussion chapitre 4). Toutefois, contrairement à ERK3, l'absence de ERK4 n'affecte pas la survie de la souris dans un fond génétique mixte (Rousseau *et al*, en préparation). Il pourrait exister une forme de redondance entre ERK3 et ERK4 à certaines étapes du développement. Il est toutefois

difficile de prédire à ce moment s'il y a redondance entre ces deux gènes. Tout d'abord, bien que ces deux gènes soient co-exprimés dans certain organes lors du développement foetal [8], la stabilité protéique de ces deux protéines est différente. En effet, la demi-vie de ERK4 est beaucoup plus élevée que celle de ERK3 qui est activement dégradée par le protéasome [8, 9, 17]. La co-expression de ces protéines dans les tissues fœtaux restent donc à être vérifiée. Par ailleurs, ERK3 possède une extension C-terminale beaucoup plus grande que ERK4 et leur région commune ne partage seulement qu'une identité protéique modeste [49]. En comparaison, les MAP kinases JNK1 et JNK2, qui sont redondantes pour le développement murin (chapitre 1), partagent près de 85% d'identité protéique et ce, sur toute leur longueur.

La disponibilité des souris déficientes en ERK3 ou ERK4 permettra toutefois d'adresser de façon élégante la redondance entre ces deux protéines. Ainsi, les niveaux d'expression de ERK4 en absence de ERK3 (et vice-versa) pourraient être déterminés. Par exemple, l'augmentation d'expression de ERK4 chez les embryons *Erk3(-/-)* pourrait suggérer une compensation par ERK4. Dans ce cas, il serait pertinent de générer des embryons mutants composés pour les mutations inactivant les gènes *Erk3* et *Erk4*. Étant donnés les phénotypes des souris déficientes en ERK3, on pourrait donc s'attendre à une mortalité embryonnaire ou foetale dans le cas de redondance entre ERK3 et ERK4.

5.4.4 Interaction génétique MK5-ERK3

Plusieurs évidences expérimentales suggèrent que ERK3 et MK5 font partie d'une même voie de signalisation (discussion chapitre 4), qui pourrait également impliquer ERK4 [8, 9]. Il existe toutefois une différence majeure entre les phénotypes des souris *Erk3(-/-)* et déficientes en MK5 dans le fond mixte 129/Sv x C57BL/6. En effet, l'invalidation de *Erk3* est absolument létale alors que la perte de MK5 ne l'est pas. Ceci est plutôt surprenant puisque la perte de MK5 conduit à une diminution des niveaux de ERK3 endogènes [10, 11]. La viabilité des souris déficientes en MK5 suggère donc que la diminution des niveaux de ERK3 n'est pas suffisante pour conduire à la létalité néonatale. Alternativement, la baisse de ERK3 dans les mutants MK5 pourrait être compensée par ERK4 (voir ci-haut). Finalement, il est possible que ERK3 possède une fonction biologique qui ne soit pas associée à son interaction/activation de MK5.

Il est trop tôt pour tirer des conclusions concernant l'organisation hiérarchique de la voie ERK3/ERK4-MK5 et d'autres études seront nécessaires pour comprendre l'interaction génétique entre ces gènes. Il serait par ailleurs intéressant de vérifier les niveaux d'expression de ERK3 et ERK4 dans les embryons MK5 mutants et de générer des mutants composés de ces allèles.

5.4.5 Rôle biologique de l'activité catalytique de ERK3

L'activité biologique de ERK3 en tant que kinase représente encore un sujet de controverse. Bien que les niveaux de ERK3 soient associés aux niveaux de phosphorylation de MK5 [10, 11], la relation enzyme-substrat de ERK3-MK5 reste incertaine. L'association entre MK5 et ERK3 pourrait être suffisante pour l'activation de MK5 [8, 11], mais l'activité kinase de ERK3 semble également être nécessaire pour l'activation maximale de MK5 [10]. En accord avec un rôle important de l'activité catalytique de ERK3, son domaine kinase est hautement conservé au cours de l'évolution, tel que démontré par un alignement de la séquence primaire du domaine kinase de ERK3 de divers organismes modèles (Figure 3).

Les souris déficientes en ERK3 représentent toutefois un modèle limité pour l'étude de sa fonction catalytique. Bien qu'il soit possible de corréler une diminution de phosphorylation de substrats potentiels chez les souris *Erk3*(-/-), cela ne démontre pas que ERK3 est une kinase pour ces substrats. Le cas du substrat potentiel MK5 représente un bon exemple de

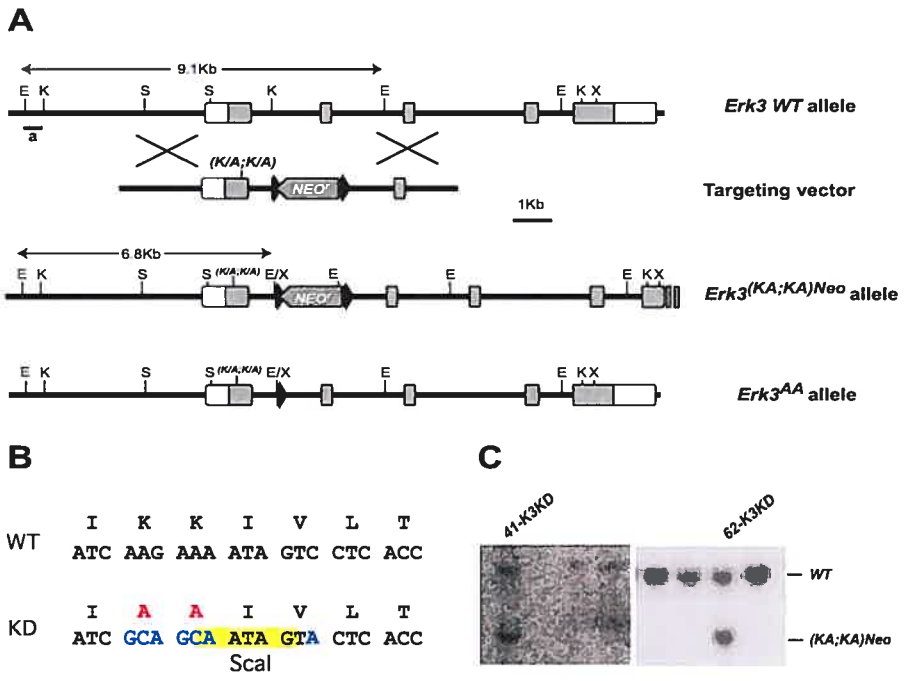

Figure 6 : Iinactivation de l'activité catalytique de ERK3 chez la souris. (A) Pour générer l'allèle *kinase dead (KD),* un vecteur de ciblage à été conçu de façon à muter les residus lys^{49} et lys^{50} encodés dans l'exon 2 du gene *Erk3* par recombinaison homologue dans les cellules ES (B) Séquence des locus de type sauvage (WT) et mutant (KD) (C) Analyse *Southern* à l'aide d'une sonde située en 5' du vecteur de ciblage démontrant un évènement de recombinaison homologue pour deux clones ES.

ce concept, puisque l'interaction entre ERK3 et MK5 pourrait suffire à activer MK5. Un modèle animal approprié impliquerait plutôt la mutation du gène *Erk3* de façon à générer une forme catalytiquement inactive de ERK3. En ce sens, nous avons généré cette mutation dans des cellules souches embryonniaires, qui serviront à la génération de lignées de souris exprimant une forme catalytiquement inactive de ERK3 (Figure 6). Puisque l'analyse des souris *Erk3*(-/-) a permis de démontrer son importance pour le développement et la survie, la perte d'activité catalytique de ERK3 pourra être évaluée en comparant les phénotypes entre les souris *Erk3*(-/-) et *Erk3*(KA,KA). Une phénocopie indiquerait que l'activité kinase de ERK3 est essentielle pour sa fonction biologique. De plus, l'analyse de l'expression de *Erk3* a permis d'identifier des tissus où les effets de la perte de l'activité catalytique de ERK3 pourrait être évaluée. Ces tissus pourraient donc être utilisés pour établir les lignées cellulaires appropriées pour l'étude de l'activité catalytique de ERK3.

5.5 Conclusions

L'objectif principal de cette thèse était de générer un modèle d'invalidation génique de *Erk3* chez la souris dans le but de mettre en évidence son rôle biologique. De plus, de façon à rendre l'outil plus intéressant, il a été adapté pour l'étude de l'expression de *Erk3*. Préalablement, j'ai démontré l'existence d'un seul gène pouvant encoder la protéine unique ERK3 chez les mammifères. À la lumière des résultats obtenus, on peut affirmer que *Erk3* est un gène essentiel pour le développement normal de la souris, sa perte conduisant à la mort néonatale. Celle-ci est causée par une détresse respiratoire à la naissance ainsi qu'à une incapacité des nouveaux-nés à téter. Par ailleurs, la perte de fonction du gène *Erk3* est associée à un retard de croissance *in utero* ainsi qu'à une tolérance anormale au glucose chez les nouveaux-nés. La souris *Erk3*(-/-) représente donc un modèle pour l'étude du retard de croissance intra-utérin, la détresse respiratoire du nouveau-né ainsi que pour l'étude de l'intolérance au glucose. De façon importante, mes résultats ont permis de fournir des bases solides pour les études futures de cette MAP kinases atypique, et ce pour tous les aspects de sa biologie moléculaire, ainsi que d'associer la perte de ce gène avec le développement de pathologies chez l'humain.

5.6 Références

1 Kim, S. H. and Yang, Y. C. (1996) A specific association of ERK3 with B-Raf in rat hippocampus. Biochem Biophys Res Commun 229, 577-581

2 Sauma, S. and Friedman, E. (1996) Increased expression of protein kinase C beta activates ERK3. J Biol Chem 271, 11422-11426

3 Cheng, M., Boulton, T. G. and Cobb, M. H. (1996) ERK3 is a constitutively nuclear protein kinase. J Biol Chem 271, 8951-8958

4 Kling, D. E., Brandon, K. L., Sollinger, C. A., Cavicchio, A. J., Ge, Q., Kinane, T. B., Donahoe, P. K. and Schnitzer, J. J. (2006) Distribution of ERK1/2 and ERK3 during normal rat fetal lung development. Anat Embryol (Berl) 211, 139-153

5 Bogoyevitch, M. A. and Court, N. W. (2004) Counting on mitogen-activated protein kinases--ERKs 3, 4, 5, 6, 7 and 8. Cell Signal 16, 1345-1354

6 Bind, E., Kleyner, Y., Skowronska-Krawczyk, D., Bien, E., Dynlacht, B. D. and Sanchez, I. (2004) A novel mechanism for mitogen-activated protein kinase localization. Mol Biol Cell 15, 4457-4466

7 Anhe, G. F., Torrao, A. S., Nogueira, T. C., Caperuto, L. C., Amaral, M. E., Medina, M. C., Azevedo-Martins, A. K., Carpinelli, A. R., Carvalho, C. R., Curi, R., Boschero, A. C. and Bordin, S. (2006) ERK3 associates with MAP2 and is involved in glucose-induced insulin secretion. Mol Cell Endocrinol 251, 33-41

8 Kant, S., Schumacher, S., Singh, M. K., Kispert, A., Kotlyarov, A. and Gaestel, M. (2006) Characterization of the atypical MAPK ERK4 and its activation of the MAPK-activated protein kinase MK5. J Biol Chem 281, 35511-35519

9 Aberg, E., Perander, M., Johansen, B., Julien, C., Meloche, S., Keyse, S. M. and Seternes, O. M. (2006) Regulation of MAPK-activated protein kinase 5 activity and subcellular localization by the atypical MAPK ERK4/MAPK4. J Biol Chem 281, 35499-35510

10 Seternes, O. M., Mikalsen, T., Johansen, B., Michaelsen, E., Armstrong, C. G., Morrice, N. A., Turgeon, B., Meloche, S., Moens, U. and Keyse, S. M. (2004) Activation of MK5/PRAK by the atypical MAP kinase ERK3 defines a novel signal transduction pathway. Embo J 23, 4780-4791

11 Schumacher, S., Laass, K., Kant, S., Shi, Y., Visel, A., Gruber, A. D., Kotlyarov, A. and Gaestel, M. (2004) Scaffolding by ERK3 regulates MK5 in development. Embo J 23, 4770-4779

12 Manning, G., Whyte, D. B., Martinez, R., Hunter, T. and Sudarsanam, S. (2002) The protein kinase complement of the human genome. Science 298, 1912-1934

13 Pavlicek, A., Gentles, A. J., Paces, J., Paces, V. and Jurka, J. (2006) Retroposition of processed pseudogenes: the impact of RNA stability and translational control. Trends Genet 22, 69-73

14 Zhang, Z., Carriero, N. and Gerstein, M. (2004) Comparative analysis of processed pseudogenes in the mouse and human genomes. Trends Genet 20, 62-67

15 Hirotsune, S., Yoshida, N., Chen, A., Garrett, L., Sugiyama, F., Takahashi, S., Yagami, K., Wynshaw-Boris, A. and Yoshiki, A. (2003) An expressed pseudogene regulates the messenger-RNA stability of its homologous coding gene. Nature 423, 91-96

16 Balakirev, E. S. and Ayala, F. J. (2003) Pseudogenes: are they «junk» or functional DNA? Annu Rev Genet 37, 123-151

17 Coulombe, P., Rodier, G., Pelletier, S., Pellerin, J. and Meloche, S. (2003) Rapid turnover of extracellular signal-regulated kinase 3 by the ubiquitin-proteasome pathway defines a novel paradigm of mitogen-activated protein kinase regulation during cellular differentiation. Mol Cell Biol 23, 4542-4558

18 Kim, J. M., Yamada, M. and Masai, H. (2003) Functions of mammalian Cdc7 kinase in initiation/monitoring of DNA replication and development. Mutat Res 532, 29-40

19 Lu, K. P. and Hunter, T. (1995) Evidence for a NIMA-like mitotic pathway in vertebrate cells. Cell 81, 413-424

20 Sun, M., Wei, Y., Yao, L., Xie, J., Chen, X., Wang, H., Jiang, J. and Gu, J. (2006) Identification of extracellular signal-regulated kinase 3 as a new interaction partner of cyclin D3. Biochem Biophys Res Commun 340, 209-214

21 Guo, K., Wang, J., Andres, V., Smith, R. C. and Walsh, K. (1995) MyoD-induced expression of p21 inhibits cyclin-dependent kinase activity upon myocyte terminal differentiation. Mol Cell Biol 15, 3823-3829

22 Patel, V. N., Rebustini, I. T. and Hoffman, M. P. (2006) Salivary gland branching morphogenesis. Differentiation 74, 349-364

23 Emerich, D. F., Skinner, S. J., Borlongan, C. V., Vasconcellos, A. V. and Thanos, C. G. (2005) The choroid plexus in the rise, fall and repair of the brain. Bioessays 27, 262-274

24 Zimmermann, J., Lamerant, N., Grossenbacher, R. and Furst, P. (2001) Proteasome- and p38-dependent regulation of ERK3 expression. J Biol Chem 276, 10759-10766

25 Liang, S. H., Zhang, W., McGrath, B. C., Zhang, P. and Cavener, D. R. (2006) PERK (eIF2alpha kinase) is required to activate the stress-activated MAPKs and induce the expression of immediate-early genes upon disruption of ER calcium homoeostasis. Biochem J 393, 201-209

26 Lee, A. H., Iwakoshi, N. N., Anderson, K. C. and Glimcher, L. H. (2003) Proteasome inhibitors disrupt the unfolded protein response in myeloma cells. Proc Natl Acad Sci U S A 100, 9946-9951

27 Kawazoe, Y., Nakai, A., Tanabe, M. and Nagata, K. (1998) Proteasome inhibition leads to the activation of all members of the heat-shock-factor family. Eur J Biochem 255, 356-362

28 Bush, K. T., Goldberg, A. L. and Nigam, S. K. (1997) Proteasome inhibition leads to a heat-shock response, induction of endoplasmic reticulum chaperones, and thermotolerance. J Biol Chem 272, 9086-9092

29 Tessitore, A., del, P. M. M., Sano, R., Ma, Y., Mann, L., Ingrassia, A., Laywell, E. D., Steindler, D. A., Hendershot, L. M. and d'Azzo, A. (2004) GM1-ganglioside-mediated activation of the unfolded protein response causes neuronal death in a neurodegenerative gangliosidosis. Mol Cell 15, 753-766

30 Kleines, M., Gartner, A., Ritter, K. and Schaade, L. (2000) Early steps in termination of the immortalization state in Burkitt lymphoma: induction of genes involved in signal transduction, transcription, and trafficking by the ganglioside IV(3)NeuAc-nLcOse(4)Cer. Biochim Biophys Acta 1492, 139-144

31 Nyfeler, B., Nufer, O., Matsui, T., Mori, K. and Hauri, H. P. (2003) The cargo receptor ERGIC-53 is a target of the unfolded protein response. Biochem Biophys Res Commun 304, 599-604

32 Rutkowski, D. T. and Kaufman, R. J. (2004) A trip to the ER: coping with stress. Trends Cell Biol 14, 20-28

33 Marciniak, S. J. and Ron, D. (2006) Endoplasmic reticulum stress signaling in disease. Physiol Rev 86, 1133-1149

34 Iwawaki, T., Akai, R., Kohno, K. and Miura, M. (2004) A transgenic mouse model for monitoring endoplasmic reticulum stress. Nat Med 10, 98-102

35 Strobel, M. C., Seperack, P. K., Moore, K. J., Copeland, N. G. and Jenkins, N. A. (1988) The dilute coat-color locus of mouse chromosome 9. Prog Clin Biol Res 256, 297-305

36 Mercer, J. A., Seperack, P. K., Strobel, M. C., Copeland, N. G. and Jenkins, N. A. (1991) Novel myosin heavy chain encoded by murine dilute coat colour locus. Nature 349, 709-713

37 Copp, A. J. (1995) Death before birth: clues from gene knockouts and mutations. Trends Genet 11, 87-93

38 Muller, U. (1999) Ten years of gene targeting: targeted mouse mutants, from vector design to phenotype analysis. Mech Dev 82, 3-21

39 Glaser, S., Anastassiadis, K. and Stewart, A. F. (2005) Current issues in mouse genome engineering. Nat Genet 37, 1187-1193

40 Beis, D. and Stainier, D. Y. (2006) In vivo cell biology: following the zebrafish trend. Trends Cell Biol 16, 105-112

41 Adams, R. H., Porras, A., Alonso, G., Jones, M., Vintersten, K., Panelli, S., Valladares, A., Perez, L., Klein, R. and Nebreda, A. R. (2000) Essential role of p38alpha MAP kinase in placental but not embryonic cardiovascular development. Mol Cell 6, 109-116

42 Lee, E. Y., Chang, C. Y., Hu, N., Wang, Y. C., Lai, C. C., Herrup, K., Lee, W. H. and Bradley, A. (1992) Mice deficient for Rb are nonviable and show defects in neurogenesis and haematopoiesis. Nature 359, 288-294

43 Jacks, T., Fazeli, A., Schmitt, E. M., Bronson, R. T., Goodell, M. A. and Weinberg, R. A. (1992) Effects of an Rb mutation in the mouse. Nature 359, 295-300

44 Clarke, A. R., Maandag, E. R., van Roon, M., van der Lugt, N. M., van der Valk, M., Hooper, M. L., Berns, A. and te Riele, H. (1992) Requirement for a functional Rb-1 gene in murine development. Nature 359, 328-330

45 Wu, L., de Bruin, A., Saavedra, H. I., Starovic, M., Trimboli, A., Yang, Y., Opavska, J., Wilson, P., Thompson, J. C., Ostrowski, M. C., Rosol, T. J., Woollett, L. A., Weinstein, M., Cross, J. C., Robinson, M. L. and Leone, G. (2003) Extra-embryonic function of Rb is essential for embryonic development and viability. Nature 421, 942-947

46 Threadgill, D. W., Dlugosz, A. A., Hansen, L. A., Tennenbaum, T., Lichti, U., Yee, D., LaMantia, C., Mourton, T., Herrup, K., Harris, R. C. and et al. (1995) Targeted disruption of mouse EGF receptor: effect of genetic background on mutant phenotype. Science 269, 230-234

47 Sibilia, M. and Wagner, E. F. (1995) Strain-dependent epithelial defects in mice lacking the EGF receptor. Science 269, 234-238

48 Watson, E. D. and Cross, J. C. (2005) Development of structures and transport functions in the mouse placenta. Physiology (Bethesda) 20, 180-193

49 Coulombe, P. and Meloche, S. (2006) Atypical mitogen-activated protein kinases: Structure, regulation and functions. Biochim Biophys Acta. doi:10.1016/ j.bbamcr.2006.11.001

ANNEXE I

Activation of MK5/PRAK by the atypical MAP kinase ERK3 defines a novel signal transduction pathway

MBO J. **23**(24): 4780-91. Décembre 2004
Erratum: EMBO J. **24**(4): 873. Février 2005

The EMBO Journal (2004) 23, 4780–4791 | © 2004 European Molecular Biology Organization | All Rights Reserved 0261-4189/04
www.embojournal.org

THE EMBO JOURNAL

Activation of MK5/PRAK by the atypical MAP kinase ERK3 defines a novel signal transduction pathway

Ole-Morten Seternes[1,*], Theresa Mikalsen[2], Bjarne Johansen[2], Espen Michaelsen[1], Chris G Armstrong[3,6], Nick A Morrice[3], Benjamin Turgeon[4], Sylvain Meloche[4], Ugo Moens[2] and Stephen M Keyse[5,*]

[1]Department of Pharmacology, Institute of Medical Biology, University of Tromsø, Tromsø, Norway, [2]Department of Biochemistry, Institute of Medical Biology, University of Tromsø, Tromsø, Norway, [3]MRC Protein Phosphorylation Unit, School of Life Sciences, University of Dundee, Dundee, UK, [4]Department of Molecular Biology, Institut de Recherche en Immunovirologie et Cancerologie, Universite de Montreal, Quebec, Canada and [5]Cancer Research UK, Molecular Pharmacology Unit, Biomedical Research Centre, Level 5, Ninewells Hospital, Dundee, UK

Extracellular signal-regulated kinase 3 (ERK3) is an atypical mitogen-activated protein kinase (MAPK), which is regulated by protein stability. However, its function is unknown and no physiological substrates for ERK3 have yet been identified. Here we demonstrate a specific interaction between ERK3 and MAPK-activated protein kinase-5 (MK5). Binding results in nuclear exclusion of both ERK3 and MK5 and is accompanied by ERK3-dependent phosphorylation and activation of MK5 *in vitro* and *in vivo*. Endogenous MK5 activity is significantly reduced by siRNA-mediated knockdown of ERK3 and also in fibroblasts derived from ERK3$^{-/-}$ mice. Furthermore, increased levels of ERK3 protein detected during nerve growth factor-induced differentiation of PC12 cells are accompanied by an increase in MK5 activity. Conversely, MK5 depletion causes a dramatic reduction in endogenous ERK3 levels. Our data identify the first physiological protein substrate for ERK3 and suggest a functional link between these kinases in which MK5 is a downstream target of ERK3, while MK5 acts as a chaperone for ERK3. Our findings provide valuable tools to further dissect the regulation and biological roles of both ERK3 and MK5.

The EMBO Journal (2004) **23**, 4780–4791. doi:10.1038/sj.emboj.7600489; Published online 2 December 2004
Subject Categories: signal transduction
Keywords: differentiation; ERK3; MK5; phosphorylation; signalling

*Corresponding authors. O-M Seternes, Department of Pharmacology, Institute of Medical Biology, University of Tromsø, 9037 Tromsø, Norway. Tel.: +47 77 64 65 06; Fax: +47 77 64 53 10; E-mail: [redacted] or SM Keyse, Cancer Research UK, Molecular Pharmacology Unit, Biomedical Research Centre, Level 5, Ninewells Hospital, Dundee DD1 9SY, UK. Tel.: +44 1382 632 622; Fax: +44 1382 669 993; E-mail: [redacted]
[6]Present address: Invitrogen, 501 Charmany Drive, Madison, WI, USA

Received: 9 July 2004; accepted: 28 October 2004; published online: 2 December 2004

Introduction

Mitogen-activated protein kinase (MAPK) cascades are highly conserved signal transduction pathways, which relay a wide variety of extracellular signals to elicit an appropriate biological response (Garrington and Johnson, 1999). In mammalian cells and tissues, these include proliferation, differentiation, inflammation and apoptosis. MAPK activation requires the phosphorylation of both the threonine and tyrosine residues of a conserved T-X-Y motif within the activation loop of the kinase by a dual-specificity MAPK kinase (MKK or MEK) (Marshall, 1994). Mammalian MAPKs are subdivided into three major classes based on sequence homology and differential activation by agonists (Davis, 2000; Kyriakis and Avruch, 2001; Johnson and Lapadat, 2002). These include the growth factor-activated extracellular signal-regulated kinase (ERK) 1 and 2 and two families of stress-activated MAPKs, the c-Jun amino-terminal kinases (JNKs) and the p38 MAPKs.

ERK3 was first identified by sequence homology to ERK1, showing identities as high as 83 and 72% within kinase subdomains V and IX, respectively, and with a subdomain structure placing it firmly within the MAPK family (Boulton *et al*, 1991; Zhu *et al*, 1994; Cheng *et al*, 1996; Meloche *et al*, 1996). Despite this, ERK3 exhibits striking differences compared with other MAPK isoforms. Most notably, the highly conserved T-E-Y motif is substituted by S-E-G and ERK3 also contains a unique C-terminal extension. Until recently, almost nothing was known about the regulation and function of ERK3. ERK3 mRNA is widely distributed in adult tissues, but is markedly upregulated during mouse development (Turgeon *et al*, 2000). In addition, ERK3 mRNA is also upregulated during differentiation of P19 embryonal carcinoma cells towards the neuronal or muscle lineages (Boulton *et al*, 1991). Taken together, these studies suggest a possible role for ERK3 during embryogenesis and cellular differentiation.

Many known MAPK substrates are not phosphorylated by ERK3 *in vitro*, indicating that it targets distinct and perhaps highly specific proteins *in vivo* (Cheng *et al*, 1996). Furthermore, serine 189 within the S-E-G motif of ERK3 is constitutively phosphorylated *in vivo*, indicating that ERK3 is not regulated like other MAPK family members (Cheng *et al*, 1996; Julien *et al*, 2003). The latter idea was reinforced by the finding that ERK3 is highly unstable, with rapid turnover mediated by ubiquitination and proteosomal degradation (Coulombe *et al*, 2003, 2004). Interestingly, ERK3 is stabilised on differentiation of both PC12 and C2C12 cells into the neuronal and muscle lineage, respectively, and expression of stable mutants of ERK3 caused cell cycle arrest in NIH3T3 cells. This suggests that rather than being regulated by inducible phosphorylation, the biological activity of ERK3 may be determined by its cellular abundance (Coulombe *et al*, 2003). Despite these advances, further progress in elucidating

the regulation, biochemical activity and physiological function of ERK3 is hampered by ignorance of its cellular targets.

We and others reported that both the activity and subcellular localisation of MAPK-activated protein kinase-5 (MK5 or PRAK) is subject to regulation by p38 (Seternes *et al*, 2002; New *et al*, 2003). However, these experiments relied on overexpression of MK5 and p38 in mammalian cells, and recent studies of endogenous MK5 do not support the idea that p38 is a physiological regulator of MK5 (Shi *et al*, 2003). In particular, endogenous MK5 was not activated in response to stimuli that activate p38, no interaction was detected between endogenous MK5 and p38 and, unlike MK2, MK5 did not display chaperoning properties towards p38 (Shi *et al*, 2003).

To address the interaction of MK5 with the MAPK family of enzymes, we performed a yeast two-hybrid screen in which MK5 was assayed against a comprehensive panel of MAPKs. Surprisingly, ERK3, but not p38, emerged as a specific binding partner for MK5. Binding was direct and the interaction of endogenous MK5 and ERK3 was confirmed. Interestingly, this also promoted the nuclear export of both ERK3 and MK5 and increased the activity of MK5 towards peptide substrates both *in vitro* and *in vivo*. To establish that ERK3 regulates MK5 *in vivo*, we employed siRNA to knock down endogenous ERK3 expression in HeLa cells and also derived mouse embryo fibroblasts (MEFs) from ERK3$^{-/-}$ mice. In both cases, we observed a significant reduction in the activity of endogenous MK5. Furthermore, we show that the elevated levels of ERK3 protein seen during PC12 cell differentiation are accompanied by increased MK5 activity *in vivo*. Conversely, experiments in which siRNA was used to knock down endogenous MK5 revealed that loss of MK5 protein was accompanied by a dramatic fall in the levels of endogenous ERK3, which could be rescued by ectopic expression of MK5. Finally, we demonstrate that activated MK5 is able to phosphorylate ERK3 both *in vitro* and *in vivo*, indicating that in addition to being an activator of MK5, ERK3 is also a physiological target for MK5. Our results identify the first physiological target for ERK3 in mammalian cells and indicate a strong functional link between these two protein kinases.

Results

MK5 interacts specifically and directly with ERK3

Yeast two-hybrid assays were used to determine the specificity of interactions between MK5 and a panel of nine distinct MAPK isoforms *in vivo*. Binding was determined by the activation of GAL4-dependent ADE2/HIS3/*lacZ* reporters. Activation of ADE2/HIS3 was assessed by selection on syn-

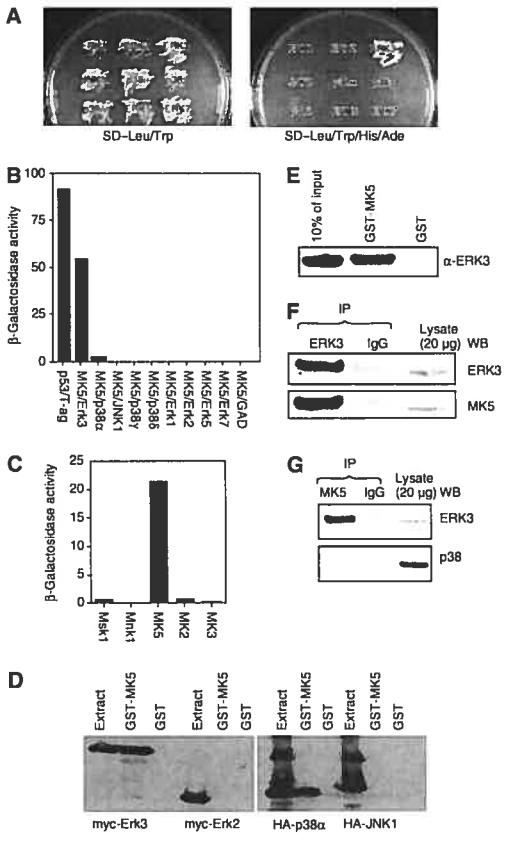

Figure 1 MK5 interacts specifically with ERK3. (**A**) Yeast two-hybrid assay. pGBKT7-MK5 was transformed into PJ69-2A and mated with Y187 expressing the indicated GAL4AD fusions. Yeast diploids expressing both DB and AD fusions were selected on synthetic dropout (SD) medium deficient for leucine and tryptophan (SD–leu/trp, left panel). Leu/trp positives were restreaked onto SD minus leucine, tryptophan, histidine and adenine (SD–leu/trp/his/ade, right panel), and protein–protein interactions were assessed by growth on this medium. (**B**) Semiquantitative analysis of induction of the β-galactosidase reporter for MK5 and the indicated MAPKs. Interactions between SV40 large T antigen and p53 and MK5 and GAL4-AD alone are used as positive and negative controls, respectively. Assays were performed in triplicate, and the results of a representative experiment are shown. (**C**) pGBKT7 expressing GAL4 DB fusions of the indicated MAPKAP-kinases were transformed into PJ69-2A and mated with Y187 expressing the GAL4 AD fusion pGADT7.ERK3. Semiquantitative analysis of induction of the β-galactosidase reporter was performed in triplicate and the results of a representative experiment are shown. (**D**) Lysates of COS-1 cells transfected with either Myc-tagged ERK3, Myc-tagged ERK2, HA-tagged p38α or HA-tagged JNK-1 were mixed with either GST-MK5 or GST alone. Bound MAPKs were detected by Western blotting using an anti-Myc antibody (ERK3 and ERK2, left panel) and an anti-HA antibody (p38α and JNK-1, right panel). (**E**) Direct interaction between ERK3 and MK5 *in vitro* assayed by GST pull-down. Recombinant ERK3 (1 μg) was mixed with 2 μg of either GST-MK5 or GST alone and glutathione agarose. Bound ERK3 was detected using an anti-ERK3 antibody. (**F**) Co-immunoprecipitation of ERK3 and MK5 in RAW 264.7 cells using an anti-ERK3 antibody. ERK3 was immunoprecipitated from cell lysates using a monoclonal anti-ERK3 antibody and protein G–Sepharose and immunoprecipitates analysed by Western blotting using either a polyclonal ERK3 antibody (upper panel) or a polyclonal MK5 antibody (lower panel). Control immunoprecipitations were performed using preimmune IgG antibodies. Total cell lysate (20 μg) was also analysed in parallel. (**G**) Co-immunoprecipitation of ERK3 but not p38 in RAW 264.7 cells using an anti-MK5 antibody. MK5 was immunoprecipitated from cell lysates using a polyclonal anti-MK5 antibody and protein G–Sepharose. Immunoprecipitates were then analysed by Western blotting using either a monoclonal ERK3 antibody (upper panel) or a monoclonal p38 antibody (lower panel). Control immunoprecipitations were performed using preimmune IgG antibodies. Total cell lysate (20 μg) was also analysed in parallel.

thetic dropout medium deficient for adenine and histidine and the strength of interaction was quantified in a β-galactosidase assay. MK5 interacts specifically with ERK3 with no significant interaction detected with p38α, p38δ, p38γ, JNK1, ERK1, ERK2, ERK5 or ERK7 (Figure 1A and B). To further examine the specificity of interaction between ERK3 and MK5, we used five MAPK-activated protein kinases (MAPKAP-kinases) as baits in the two-hybrid assay. These include MK2 and MK3, which are most highly related to MK5 (45 and 46% identity, respectively). ERK3 interacted specifically with MK5 showing no significant binding to MK2, MK3, MSK1 or MNK1 (Figure 1C). To confirm the specificity of MAPK binding, we used GST pulldown assays employing both transfected cell lysates and purified recombinant proteins. In agreement with the yeast two-hybrid results, MK5 binds to ERK3 and not to either ERK2 or JNK1 (Figure 1D). Furthermore, this interaction is direct as it is also detected using purified recombinant ERK3 and GST-MK5 (Figure 1E). In agreement with our previous study (Seternes *et al*, 2002), MK5 also interacted with p38α (Figure 1D). Finally, to determine the ability of endogenous MK5 to interact with either ERK3 or p38, we performed co-immunoprecipitation experiments using the RAW246.7 mouse macrophage cell line. Endogenous MK5 was readily detected in immunoprecipitates of endogenous ERK3 (Figure 1F) and endogenous ERK3, but not p38 was readily detected in immunoprecipitates of endogenous MK5 (Figure 1G). We conclude that MK5 binds specifically and directly to ERK3 both *in vitro* and *in vivo*. In contrast, although we could detect interactions between MK5 and p38 *in vitro*, we found no evidence of interaction between endogenous MK5 and p38.

Coexpression of ERK3 and MK5 causes the redistribution of both proteins from the nucleus to the cytoplasm

To examine the subcellular distributions of MK5 and ERK3, we expressed either wild-type ERK3 or an EGFP-MK5 fusion protein in HeLa cells. As described previously (Seternes *et al*, 2002), EGFP-MK5 is predominantly nuclear when expressed in these cells (Figure 2A). In contrast, ERK3 is distributed in both the nuclear and cytoplasmic compartments (Figure 2B). However, on coexpression, a profound change in the subcellular localisation of ERK3 and MK5 was seen, with both proteins now excluded from the nucleus (Figure 2C). Identical results were obtained in NIH3T3, HEK293 and COS-1 cells (data not shown). The kinase activities of either protein are not required for relocalisation, as 'kinase-dead' mutants of either MK5 or ERK3 are also predominantly cytoplasmic (Figure 2D). To examine the requirement for specific protein–protein interactions between MK5 and ERK3, we used two truncations of ERK3. The first of these (ERK3 1–330) no longer interacts with MK5 in GST pulldown assays, while the second (ERK3 1–340) readily binds to MK5 (Figure 3A). Although both proteins exhibit subcellular distributions that are indistinguishable from the full-length protein (Figure 3B), only ERK3 1–340 causes the redistribution of MK5 from the nucleus to the cytoplasm when the two proteins are coexpressed (Figure 3C).

We next determined if an active nuclear export pathway is essential for relocalisation of MK5 and ERK3. Both proteins were coexpressed in HeLa cells either in the absence or presence of leptomycin B (LMB), an inhibitor of CRM1-dependent nuclear export (Wolff *et al*, 1997; Kudo *et al*, 1998). LMB blocks the redistribution of both MK5 and ERK3, indicating that a leucine-rich NES present on either or both of these proteins is required to mediate the relocalisation seen on coexpression (Figure 4A and B). This is consistent with a recent report demonstrating CRM1-dependent export of ERK3 (Julien *et al*, 2003).

The export of MK5 in response to ERK3 is reminiscent of the effect of coexpressing p38 (Seternes *et al*, 2002). To ask if both events are mediated by a similar mechanism, we used mutated and truncated forms of MK5, which show differential binding to ERK3 and p38. Mutation of the nuclear localisation sequence in MK5 (GSTMK5mutNLS) reduces its ability to interact with p38 in GST pulldown assays, but permits interaction with ERK3 (Figure 5A and B). Conversely, a truncated form of MK5 (EGFP-MK5 1–423) no longer binds to ERK3, but can bind to p38 (Figure 5A and B). The latter form of MK5 is efficiently exported from the nucleus in response to activation of the p38 pathway (MKK6E/E + p38) but is unresponsive to expression of ERK3 (Figure 5C). To examine any possible connection between p38 activity and nuclear export of ERK3, we also coexpressed ERK3 alone with MKK6E/E + p38. We observed no change in ERK3 localisation, nor was this affected by treatment of cells with sodium arsenite (data not shown). Finally, the nuclear export of MK5 in response to activation of p38 requires phosphorylation of Thr182 (Seternes *et al*, 2002; New *et al*, 2003). To determine if this is also required for the relocalisation of MK5 by ERK3, we coexpressed a mutant form of MK5 in which this site was mutated to alanine (EGFP-MK5T182A) and either ERK3 or p38 plus MKK6E/E. As observed previously, MKK6E/E + p38 failed to cause nuclear export of MK5T182A (Figure 5D). In contrast, this mutant was exclusively cytoplasmic when coexpressed with ERK3, thus demonstrating no requirement for T182 phosphorylation for MK5 to relocalise in response to ERK3 binding.

ERK3 phosphorylates and activates MK5 both in vitro and in vivo

The interactions between ERK3 and MK5 strongly suggest an enzyme–substrate relationship between these two proteins. To investigate this, we expressed and purified wild-type ERK3 and a 'kinase-dead' mutant (ERK3 D171A) in insect Sf9 cells. When analysed by SDS–PAGE, both proteins migrated as a single band of approximately 100 kDa, indicating that they are full length and undegraded (Figure 6A). Furthermore, both proteins were recognised by an anti-phospho antibody against serine 189 of the S-E-G motif, demonstrating that this residue is constitutively phosphorylated in Sf9 cells (Figure 6A). We also produced ERK3 in which S189 was mutated to glutamic acid (S189E) and this serves as a negative control for the anti-phospho S189 antibody (Figure 6A).

To determine if ERK3 is capable of activating MK5 *in vitro*, we incubated either wild-type ERK3 or kinase-dead (ERK3D171A) protein with inactive recombinant MK5 in the presence of ATP and Mg^{2+} and monitored MK5 activity using PRAKtide (KKLRRTLSVA, derived from glycogen synthase). Wild-type ERK3, but not ERK3D171A, caused a significant increase in MK5 activity towards this substrate (Figure 6B). Furthermore, an antiserum specific for phosphorylation of

the regulatory site (T182) within the activation loop of MK5 demonstrates that activation of MK5 by ERK3 was accompanied by phosphorylation of Thr182 (Figure 6C). The ERK3 protein in which the putative regulatory serine (S189) of the S-E-G motif was mutated to glutamic acid (ERK3S189E) also activated MK5, albeit with lower efficiency, and activation was also accompanied by phosphorylation of Thr182 (Figure 6B and C). We conclude that ERK3 is capable of activating MK5 *in vitro*, and that this activation requires ERK3 kinase activity and is accompanied by phosphorylation of the key regulatory site (Thr182) of MK5. Furthermore, the result obtained using the S189E mutant of ERK3 suggests that phosphomimetic substitution of this residue is able to activate, at least in part, the kinase activity of ERK3 towards MK5.

To explore the ability of ERK3 to activate MK5 under more physiological conditions, HeLa cells were transfected with expression constructs encoding EGFP-MK5, either alone or in combination with either Myc-tagged wild-type or kinase-dead ERK3. EGFP-MK5 was then immunoprecipitated from these cells and assayed for activity towards PRAKtide as before. As positive controls for these experiments, EGFP-MK5 was also coexpressed with either p38 alone or p38 plus MKK6E/E, the latter combination having previously been demonstrated to activate MK5 in these cells (Seternes *et al*, 2002). Under these conditions, wild-type ERK3 but not the kinase-dead (D171A) mutant activates MK5. Furthermore, the level of MK5 activity is comparable with that seen following activation of p38 (Figure 7A) and is also dependent on phosphorylation of Thr182 in MK5, as mutation of this residue abolishes activation by ERK3 (Figure 7B). Finally, given the ability of p38 to activate MK5, it was critical to demonstrate that ERK3 was not activating MK5 indirectly by activating the p38 pathway. However, treatment of cells with SB203580, a specific p38 inhibitor (Cuenda *et al*, 1995), had no effect on the activation of MK5 achieved by cotransfection of ERK3. In contrast, the activation of MK5 by p38 plus MKK6E/E was completely abolished by this drug (Figure 7C). We conclude that ERK3 is capable of activating MK5 *in vivo*, that activation is mediated by phosphorylation of Thr182 in MK5 and that this is not dependent on the activity of p38.

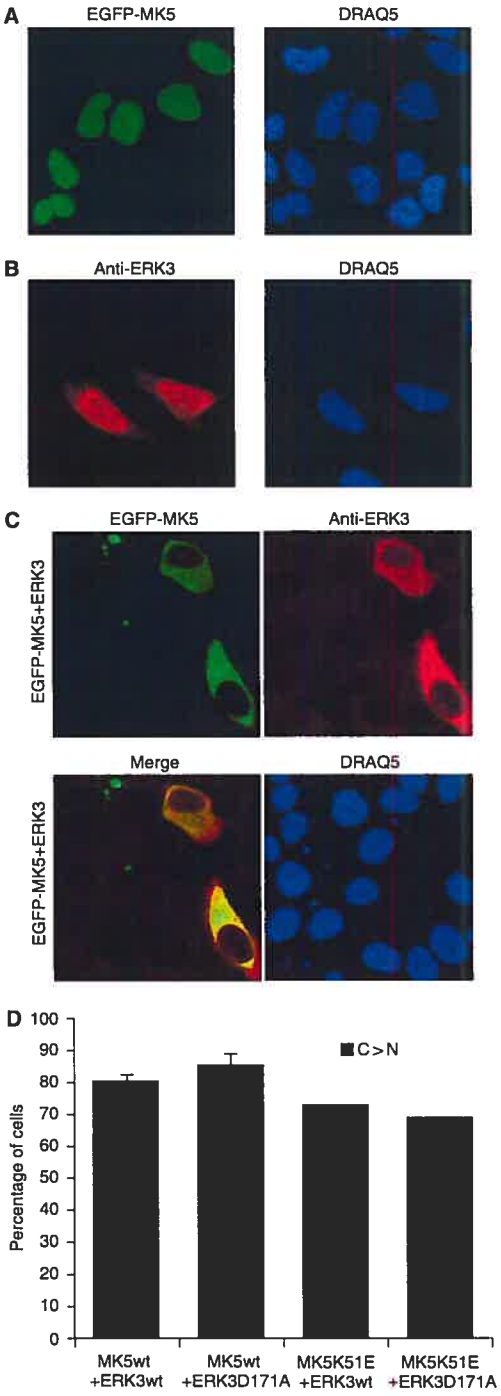

Figure 2 Coexpression of MK5 and ERK3 leads to relocalisation of both proteins. (**A**) HeLa cells were transfected with expression vector encoding EGFP-MK5. EGFP fluorescence was visualised directly (green channel on left) and cell nuclei were visualised by DRAQ5 staining (blue channel on right). (**B**) HeLa cells transfected with expression vector encoding ERK3. After 24 h, ERK3 expression was visualised by staining with an anti-ERK3 antibody and Alexa 594 anti-sheep antibody (red channel on left), while cell nuclei were visualised by DRAQ5 staining (blue channel on right). (**C**) HeLa cells were cotransfected with expression vectors encoding EGFP-MK5 and ERK3 and after 24 h cells were fixed. EGFP-MK5 was visualised directly (green channel on left), and ERK3 was visualised by staining with an anti-ERK3 antibody and Alexa 594 anti-sheep antibody (red channel on right). A merged image of the green and red channels is shown (lower left) and nuclei were visualised by DRAQ5 staining (blue channel on lower right). (**D**) HeLa cells were cotransfected with the indicated expression vectors and EGFP-MK5 and ERK3 were visualised as above. In all, 100 cells coexpressing both EGFP-MK5 and ERK3 from three independent transfections were counted and the distribution of both proteins was scored. The results are presented as the % of cells in which both EGFP-MK5 and ERK3 were predominantly cytosolic (C>N) and mean values with associated errors are shown. In all experiments, several fields of cells were examined and representative images are shown.

The activation of MK5 by ERK3 requires specific protein–protein interaction

To explore the necessity for physical docking between these two proteins in mediating the activation of MK5, we used the truncated forms of ERK3 characterised in Figure 3. As before, wild-type ERK3 led to significant activation of MK5. However, ERK3 1–330, which fails to bind to MK5, does not (Figure 7D). In contrast, ERK3 1–340, which retains the ability to bind to MK5, activates MK5 as efficiently as the wild-type protein (Figure 7D). Finally, the truncated form of MK5 (MK5 1–423), which is unable to bind to ERK3, but retains binding towards p38, is activated on coexpression of p38 and MKK6E/E but not by ERK3 (Figure 7E). We conclude that specific but distinct interactions between ERK3 and MK5 are necessary for both relocalisation and for the phosphorylation and activation of MK5 by ERK3.

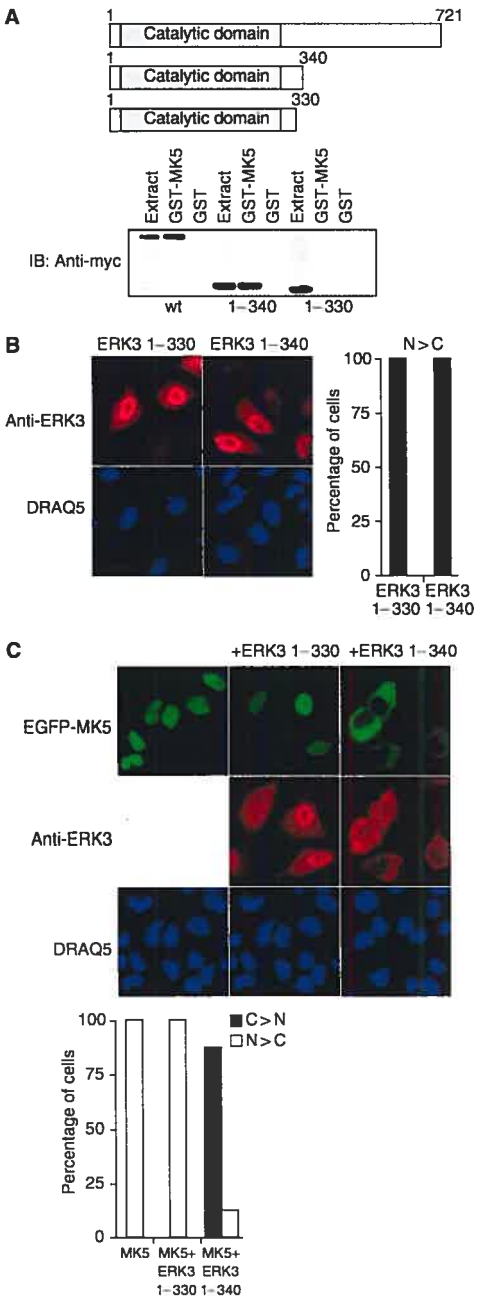

Loss of endogenous ERK3 protein causes a significant decrease in the activity of MK5, while elevated levels of ERK3 in differentiating PC12 cells are accompanied by an increase in MK5 activity

Although our overexpression studies suggest a functional link between ERK3 and MK5, they do not prove that ERK3 is a physiological activator of MK5. To address this, we first performed siRNA-mediated knockdown of endogenous ERK3 in HeLa cells. Using three distinct siRNAs directed against ERK3, we achieved significant reduction in the levels of endogenous ERK3 protein (Figure 8A). In contrast, levels of the related ERK2 MAPK were unchanged, as were levels of endogenous MK5. Immune complex kinase assays revealed that ERK3 knockdown resulted in a significant reduction (30–50%) in endogenous MK5 activity. To confirm an absolute link between ERK3 and MK5, we obtained primary MEFs derived from wild-type ($ERK3^{+/+}$), heterozygous ($ERK3^{+/-}$) and null ($ERK3^{-/-}$) animals. ERK3 protein levels were either reduced ($ERK3^{+/-}$) or absent ($ERK3^{-/-}$) in these cells, while MK5 protein levels were unchanged. However, endogenous MK5 activity was reduced by approximately

Figure 3 Amino acids 330–340 of ERK3 are required for interaction with and relocalisation of MK5. (**A**) COS-1 cells were transfected with expression vectors encoding Myc-tagged full-length, or C-terminal truncation mutants of ERK3 encoding either amino acids 1–340 or 1–330 of the protein. Cell lysates were then mixed with either recombinant GST-MK5 or GST alone. Binding of ERK3 was detected by Western blotting using an anti-Myc monoclonal antibody. (**B**) HeLa cells were transfected with expression vectors encoding either amino acids 1–330 or 1–340 of ERK3. ERK3 was visualised by staining with an anti-ERK3 antibody and an Alexa 594-coupled secondary (anti-sheep) antibody (red channel in upper panels) and cell nuclei were visualised by DRAQ5 staining (blue channel in lower panels). In all, 100 cells expressing the indicated mutant of ERK3 from each of three independent transfections were counted and the distribution of the ERK3 protein was scored. The results are presented as the % of cells in which the ERK3 protein was predominantly nuclear (N>C) and mean values with associated errors are shown. (**C**) HeLa cells were cotransfected with vectors encoding EGFP-MK5 and either ERK3 1–330 or 1–340. EGFP-MK5 was visualised directly (green channel in upper panels), ERK3 was visualised by staining with an anti-ERK3 antibody and an Alexa 594-coupled secondary (anti-sheep) antibody (red channel in middle panels) and cell nuclei were visualised by DRAQ5 staining (blue channel in lower panels). A total of 100 cells expressing either EGFP-MK5 alone or coexpressing both EGFP-MK5 and the indicated mutant of ERK3 from three independent transfections were counted and the distribution of MK5 was scored. The results are presented as the % of cells in which EGFP-MK5 was either predominantly nuclear (N>C) or predominantly cytoplasmic (C>N) and mean values with associated errors are shown. In all experiments, several fields of cells were examined and representative images are shown.

25% in the ERK3 heterozygous and 50% in the ERK3 null cells (Figure 8B). Our results demonstrate that ERK3 is responsible for a significant fraction of endogenous MK5 activity in mammalian cells. Finally, ERK3 protein accumulates during the differentiation of PC12 cells in response to nerve growth factor (NGF) (Coulombe *et al*, 2003). To determine if this influences MK5 activity, we exposed PC12 cells to NGF for 4 days and monitored differentiation as characterised by neurite outgrowth. These cells were also analysed for expression levels of ERK3, ERK2, p38 and MK5, and MK5 activity was assayed following immunoprecipitation. After 4 days of exposure to NGF, the levels of endogenous ERK3 protein increased significantly, while the levels of endogenous MK5 appeared to be stable (Figure 8C). However, the kinase activity of the endogenous MK5 protein increases approximately four-fold, indicating that increased levels of ERK3 protein result in activation of MK5 (Figure 8C). It is possible that this could be the result of p38 activation, as this MAPK has been implicated in PC12 cell differentiation in response to NGF (Morooka and Nishida, 1998). However, MK5 activity was unaffected by exposure of these cells to SB203580 and thus is not dependent on p38 (data not shown).

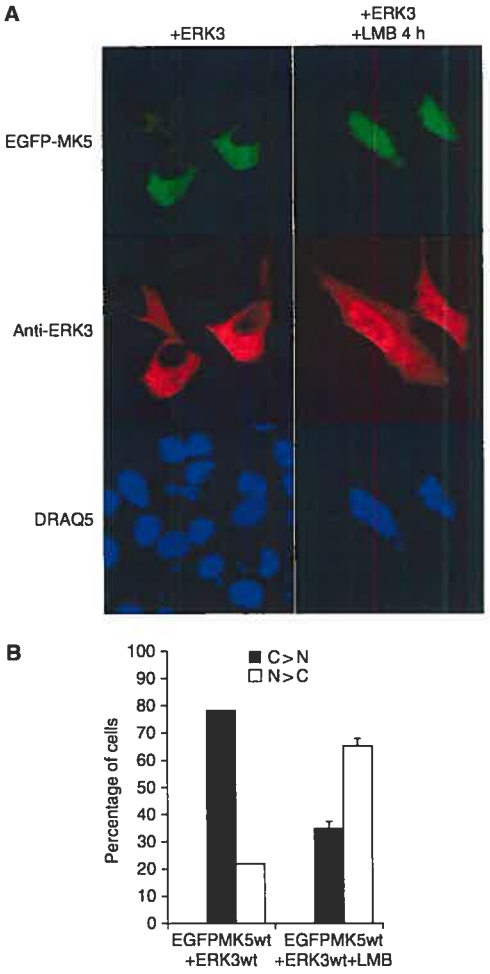

Figure 4 Relocalisation of both MK5 and ERK3 requires a CRM1-dependent nuclear export pathway. (**A**) HeLa cells were cotransfected with expression vectors encoding EGFP-MK5 and ERK3. After 24 h, cells were either left untreated (left panels) or exposed to LMB at a final concentration of 5 ng/ml for 4 h (right panels). Following fixation, EGFP-MK5 was visualised directly (green channel in upper panels), ERK3 was visualised by staining with an anti-ERK3 antibody and an Alexa 594-coupled secondary (anti-sheep) antibody (red channel in middle panels) and cell nuclei were visualised by DRAQ5 staining (blue channel in lower panels). Several fields of cells were examined and representative images are shown. (**B**) A total of 100 cells coexpressing both EGFP-MK5 and ERK3 from each of three independent transfections were counted and the distribution of both proteins was scored. The results are presented as the % of cells in which both EGFP-MK5 and ERK3 were either predominantly cytosolic (C>N) or predominantly nuclear (N>C) and mean values with associated errors are shown.

Chaperoning or nuclear-cytoplasmic cotransport activity of MK5 is required to maintain levels of endogenous ERK3

Deletion of MK2 causes a reduction in p38 protein, due to a lack of chaperoning and/or nucleo-cytoplasmic cotransport of p38 (Kotlyarov *et al*, 2002). In contrast, loss of MK5 has no effect on levels of p38, indicating that MK5 does not perform a similar function (Shi *et al*, 2003). To examine the effect of reducing MK5 on ERK3 protein levels, we have employed siRNA-mediated knockdown. Using this approach, we achieve a significant reduction in the levels of MK5 protein and this is reflected in a reduction of approximately 90% in endogenous MK5 kinase activity. In contrast, no change is seen in the levels of the closely related kinase MK2 (Figure 9A). Furthermore, in cells treated with MK5 siRNA, we consistently observe a dramatic reduction in the level of endogenous ERK3 protein (Figure 9B) and this can be rescued by expression of either an siRNA-resistant (murine) wild-type MK5 or T182A mutant of MK5.

ERK3 is a substrate for activated MK5 in vitro and in vivo

MK5 was first characterised as a kinase, which phosphorylated the small heat shock protein Hsp27 *in vitro* and *in vivo* (New *et al*, 1998). However, mice lacking MK2 suffer almost complete loss of Hsp27 kinase activity, making it extremely unlikely that Hsp27 is a physiological substrate for MK5 (Kotlyarov *et al*, 1999). Given that ERK3 and MK5 form a complex, which results in MK5 activation, we wanted to determine if ERK3 was itself a substrate for activated MK5. To examine this, we incubated activated MK5 and MK2 (1 U/ml) with either recombinant wild-type ERK3 or Hsp27, together with [γ-^{32}P]ATP and Mg^{2+}. We clearly observe that MK5, but not MK2, is able to phosphorylate ERK3 *in vitro*, while both kinases phosphorylate Hsp27 (Figure 10A). The stoichiometry of ERK3 phosphorylation by MK5 was also determined and demonstrated that ERK3 is not only a preferred substrate for MK5 over MK2, but is also efficiently phosphorylated to 1.5 mol/mol. These results suggest that ERK3 is a target for activated MK5 *in vivo*. To address this, we coexpressed either Myc-tagged wild-type or kinase-dead ERK3 with either EGFP alone, wild-type MK5 or MK5L337G, a constitutively active mutant of MK5 (Seternes *et al*, 2002). Cells were then labelled with

[^{32}P]orthophosphate and ERK3 was immunoprecipitated and analysed by SDS–PAGE. Both wild-type and kinase-dead ERK3 are phosphorylated by MK5, indicating that ERK3 is a physiological target for activated MK5 in mammalian cells (Figure 10).

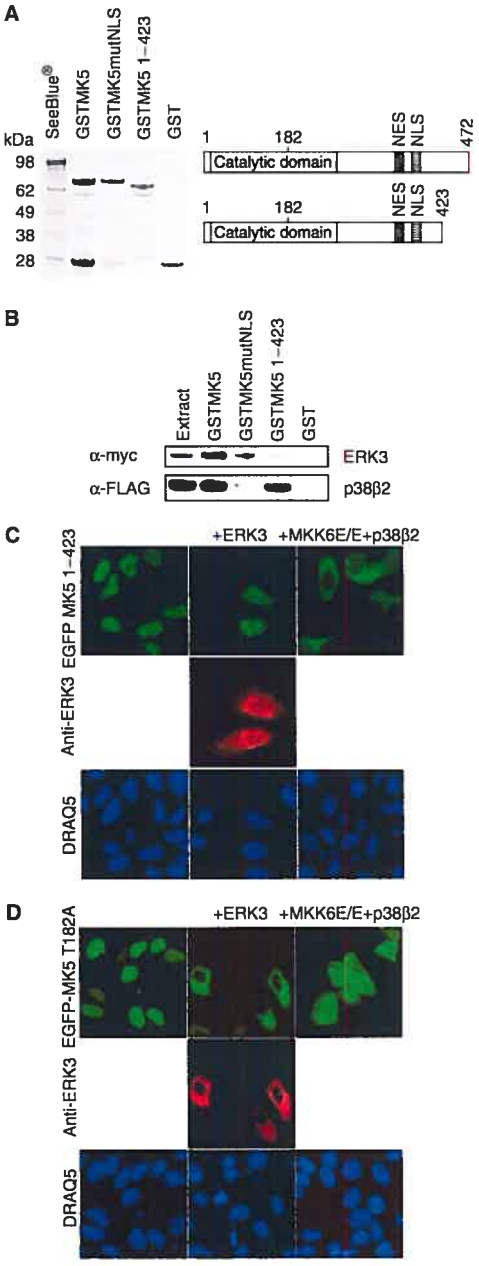

Discussion

We have established a functional link between the atypical MAPK ERK3 and the activity and localisation of MK5. MK5 was first characterised as p38-regulated/activated protein kinase (PRAK) (New *et al*, 1998; Ni *et al*, 1998). Subsequent work indicated that both the activity and the subcellular localisation of MK5 could be regulated by interaction with p38 (Seternes *et al*, 2002; New *et al*, 2003). However, these interactions were either demonstrated *in vitro* or following overexpression of p38 and MK5 in cultured cells. Subsequent attempts to demonstrate functional interactions between endogenous p38 and MK5 have proven difficult as highlighted by recent studies of endogenous MK5 activities in both wild-type and MK5 null mice (Shi *et al*, 2003). Firstly, endogenous MK5 activity was not increased by treatments that activated both endogenous p38 and its *bona fide* substrate MK2. Secondly, attempts to show binding of endogenous p38 using tandem affinity purification (TAP) of MK5 failed, whereas p38 was readily detected following TAP of MK2. Finally, p38 protein levels were unaffected by deletion of MK5, whereas loss of MK2 caused a significant reduction in p38, indicating that MK2, but not MK5, exhibits chaperoning properties towards p38 (Shi *et al*, 2003).

In the present study, we used a yeast two-hybrid assay to study interactions between MK5 and MAPKs and we identified ERK3, but not p38, as a specific binding partner for MK5. Furthermore, although we could readily demonstrate the presence of endogenous MK5 in ERK3 immunoprecipitates and endogenous ERK3 in MK5 immunoprecipitates, we repeatedly failed to detect endogenous p38 in the latter. Therefore, despite our ability to detect robust binding between p38 and MK5 both *in vitro* and when overexpressed in mammalian cells, the results of our protein–protein interac-

Figure 5 ERK3 and p38 mediate the translocation of MK5 through different mechanisms. (**A**) Recombinant GSTMK5, GSTMK5mutNLS, GSTMK5 1–423 and GST alone were expressed and purified from *Escherichia coli*. Each protein (2 μg) was then analysed by SDS–PAGE and Coomassie blue staining. This material represents the input in the GST pulldown assay described below and also those presented in Figures 1 and 3. (**B**) Lysates from COS-1 cells transfected with expression vectors encoding either Myc-tagged ERK3 or FLAG-tagged p38β2 were mixed with the indicated GST fusion proteins. Bound MAPKs were detected using an anti-Myc antibody (ERK3, upper panel) and an anti-FLAG antibody (p38β2, lower panel). The experiment was performed three times and a representative result is shown. (**C**) HeLa cells were cotransfected with expression vectors encoding a C-terminal truncation of EGFP-MK5 (EGFPMK5 1–423) and either ERK3 or constitutively active MKK6 together with p38β2 (MKK6E/E + p38β2). After 24 h, cells were fixed and EGFP-MK5 was visualised directly (green channel in upper panels), and ERK3 was visualised by staining with an anti-ERK3 antibody and an Alexa 594-coupled secondary (anti-sheep) antibody (red channel in the middle panel). Cell nuclei were visualised by DRAQ5 staining (blue channel in lower panels). (**D**) HeLa cells were cotransfected with expression vectors encoding EGFP-MK5 T182A, in which the phospho-acceptor site Thr182 was substituted by alanine together with either ERK3 or MKK6 plus p38β2 (MKK6E/E + p38β2). After 24 h, cells were fixed and EGFP-MK5 was visualised directly (green channel in upper panels), and ERK3 was visualised by staining with an anti-ERK3 antibody and an Alexa 594-coupled secondary (anti-sheep) antibody (red channel in middle panels). Cell nuclei were visualised by DRAQ5 staining (blue channel in lower panels). In all experiments, several fields of cells were examined and representative images are shown.

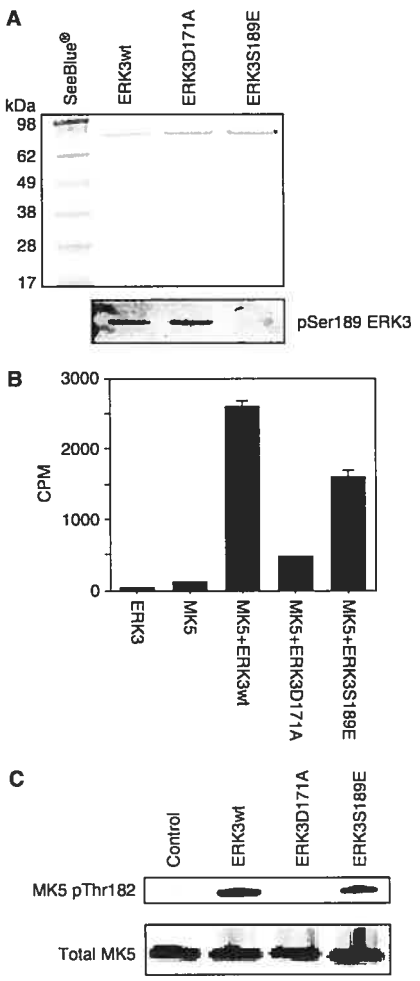

Figure 6 ERK3 activates MK5 *in vitro* by phosphorylating Thr182 within the activation loop of the kinase. (**A**) Recombinant wild-type ERK3 (ERK3wt), a kinase-dead mutant of ERK3 (ERK3D171A) or a mutant in which serine189 within ERK3 was mutated to glutamic acid (ERK3S189E) were expressed and purified from insect Sf-9 cells. Proteins (2 μg) were then analysed using SDS–PAGE and Coomassie blue staining (upper panel). Molecular mass markers are shown on the left. Proteins were also analysed by SDS–PAGE and Western blotting using a phospho-specific antibody raised against S189 of ERK3 (lower panel). (**B**) Activation of recombinant MK5 was assayed *in vitro* by incubation with either wild-type ERK3, the kinase-dead mutant of ERK3 (ERK3D171A) or ERK3S189E using PRAKtide as substrate and activities compared with those of either ERK3 or MK5 alone. Assays were performed in quadruplicate and mean activities are presented here as counts per minute (CPM) incorporated with associated errors. (**C**) Recombinant MK5 (1 μg) was incubated either alone or with 6 μg of each of the indicated recombinant ERK3 proteins in the presence of ATP and Mg^{2+}. After 60 min, a sample of MK5 (250 ng) was analysed by SDS–PAGE and Western blotting using a phospho-specific antibody raised against Thr182 (upper panel). As a loading control, the samples were also analysed by SDS–PAGE and Western blotting using an anti-MK5 antibody (lower panel).

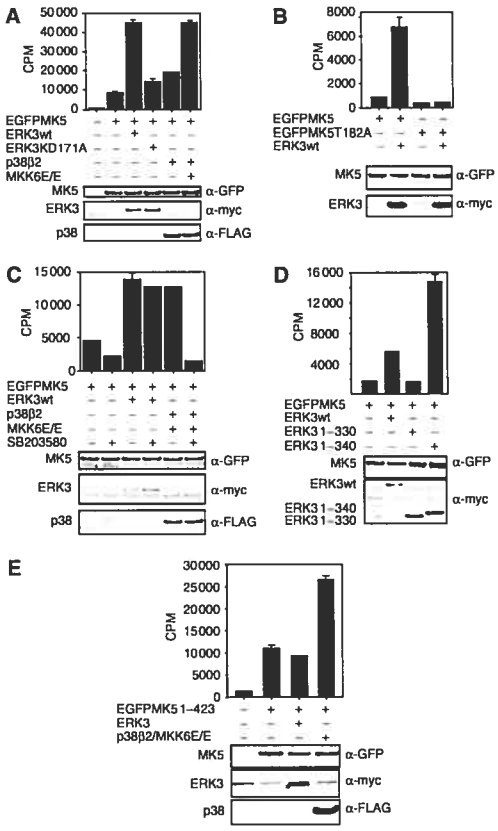

Figure 7 ERK3 activates MK5 *in vivo*. (**A**) HeLa cells were transfected with the indicated expression plasmids. After 24 h, cells were lysed and EGFPMK5 activity was assayed in an immune complex kinase assay using PRAKtide as substrate. Activity is expressed as counts per minute (CPM) incorporated. (**B**) HeLa cells were transfected with either wild-type MK5 (EGFPMK5) or the mutant EGFPMK5 T182A, either alone or in combination with wild-type ERK3 (ERK3wt). After 24 h, cells were lysed and the activity of the EGFP-MK5 fusion protein was assayed as before. (**C**) HeLa cells were transfected with the indicated plasmids as in (**A**). After 24 h, cells were treated (where indicated) with 10 μM of SB 203580 for 2 h before cell lysis and assay of EGFPMK5 kinase as before. (**D**) HeLa cells were transfected with EGFPMK5 either alone or in combination with either wild-type ERK3 (ERK3wt), a C-terminal truncation encoding residues 1–330 of ERK3 (ERK3 1–330) or a C-terminal truncation encoding residues 1–340 of ERK3 (ERK3 1–340). After 24 h, cells were lysed and the activity of the EGFP-MK5 fusion protein was assayed as before. (**E**) HeLa cells were transfected with a C-terminal truncation of MK5 (EGFPMK5 1–423) either alone or in combination with either wild-type ERK3 (*) or expression plasmids encoding p38β2 and MKK6E/E. After 24 h, cells were lysed and the activity of the EGFPMK5 1–423 fusion protein was assayed as before. All experiments were performed at least three times, and the results of a single representative experiment are shown. Kinase assays were performed in quadruplicate and mean values with associated errors are presented. Expression of wild-type and mutant forms of MK5 and ERK3 and of p38 was verified by Western blotting of cell lysates using appropriate antibodies (lower panels in A–E).

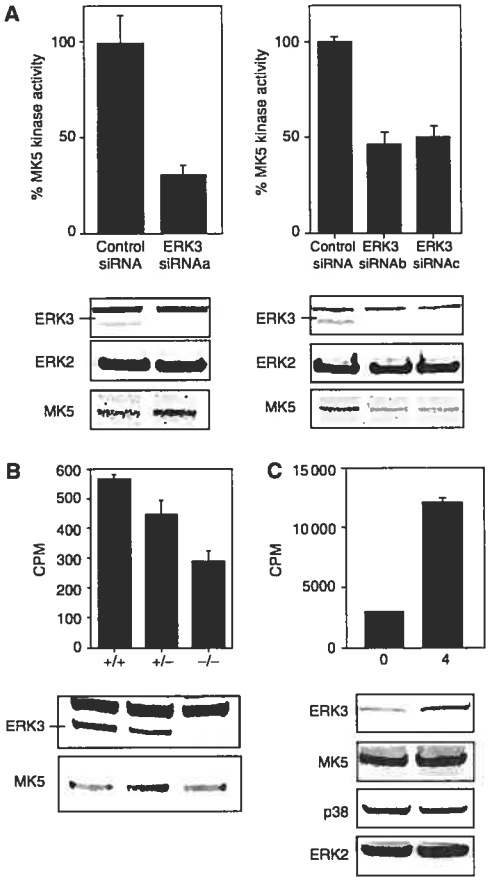

Figure 8 ERK3 is a physiological activator of MK5. **(A)** SiRNA-mediated knockdown of ERK3 decreases endogenous MK5 activity. HeLa cells were transfected with 10 nM of either a control (scrambled) siRNA or three distinct siRNAs against human ERK3. After 24 h, cells were lysed and endogenous MK5 was immunoprecipitated. MK5 activity was then assayed exactly as before and results are presented as relative kinase activity (%), where the activity in cells transfected with control siRNA is 100%. Total cell lysates (20 μg) were also analysed by SDS–PAGE and Western blotting to determine the levels of endogenous ERK3, ERK2 and MK5 using appropriate antibodies (lower panels). **(B)** MK5 activity is reduced in ERK3 knockout fibroblasts. Primary MEFs derived from wild-type (+/+), ERK3 heterozygous (+/−) or ERK3 null (−/−) mice were lysed and endogenous MK5 was immunoprecipitated. MK5 activity was then assayed as before. Total cell lysates (20 μg) were also analysed by SDS–PAGE and Western blotting to determine the levels of endogenous ERK3 and MK5 using appropriate antibodies (lower panels). **(C)** Differentiation of PC12 leads to increased ERK3 expression and MK5 activity. PC12 cells were either untreated (0) or stimulated with NGF (100 ng/ml) for 4 days (4) before cells were lysed. MK5 was immunoprecipitated and MK5 activity was then assayed as described before. Total lysates (20 μg) were also analysed by SDS–PAGE and Western blotting to determine the levels of ERK3, MK5, p38 and ERK2 expression using appropriate antibodies (lower panels). All experiments were performed at least three times, and the results of a single representative experiment are shown. Kinase assays were performed in quadruplicate and mean values with associated errors are presented.

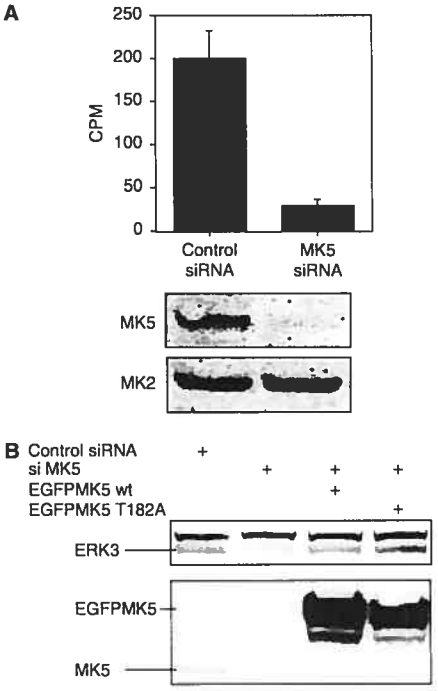

Figure 9 SiRNA-mediated knockdown of MK5 causes loss of endogenous ERK3 protein. **(A)** HeLa cells were transfected with 100 nM of the indicated siRNAs and lysed after 48 h. MK5 was immunoprecipitated using a polyclonal anti-MK5 antibody and the activity of the MK5 was assayed in an immune complex kinase assay as before. Experiments were performed at least three times, and the results of a single representative experiment are shown. Kinase assays were performed in quadruplicate and mean incorporations (CPM) with associated errors are presented. Cell lysates (20 μg) were also analysed by SDS–PAGE and Western blotting using antibodies against MK5 and MK2, respectively (lower panels). **(B)** HeLa cells were transfected with 100 nM of the indicated siRNAs. After 24 h, the cells were transfected with 1 μg of the indicated expression plasmids and 24 h later, the cells were harvested. Total lysates (20 μg) were analysed by SDS–PAGE and Western blotting using a rabbit polyclonal ERK3 antibody (E3-CT4, upper panel) and a polyclonal MK5 antibody, respectively (lower panel).

tion studies strongly favour a functional relationship between endogenous MK5 and the atypical MAPK ERK3 but not p38. This conclusion is further strengthened by our demonstration that this interaction causes both proteins to relocalise from the nucleus to the cytoplasm. Furthermore, recombinant ERK3, in which serine 189 within the S-E-G motif is phosphorylated, is able to activate MK5 *in vitro* and expression of wild-type ERK3, but not a kinase-dead mutant, is also able to activate MK5 *in vivo*. The activation of MK5 by ERK3 is absolutely dependent on the phosphorylation of Thr182 within the activation loop of MK5, requires specific protein–protein interactions between ERK3 and MK5 and is completely unaffected by a potent and specific inhibitor of p38.

To demonstrate a definitive physiological link between ERK3 and MK5 activation, we have used several approaches.

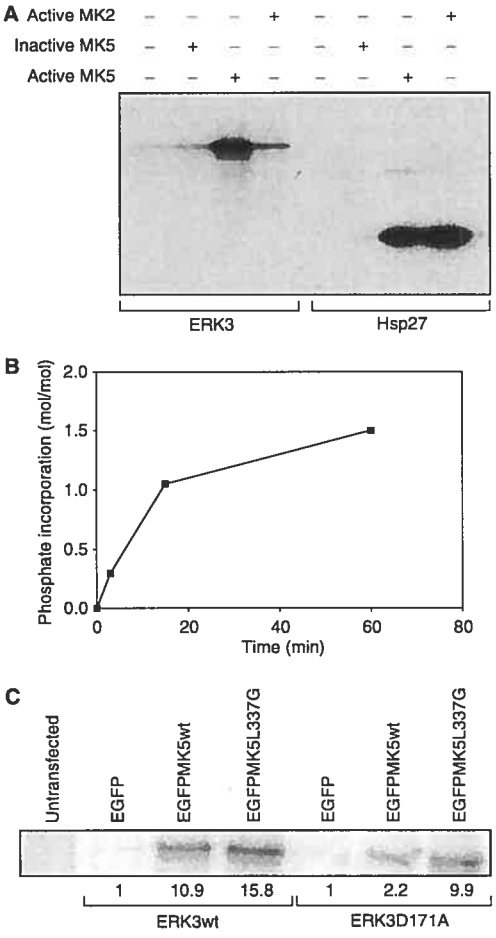

Figure 10 ERK3 is a substrate for MK5 *in vitro* and *in vivo*. (**A**) In all, 5 μg of either recombinant ERK3 (left) or Hsp27 (right) was incubated with either 1 U/ml activated MK5 or MK2 or 1 μg inactive MK5 for 20 min in the presence of Mg^{2+} and [γ-^{32}P]ATP. Radiolabelled proteins were then analysed by SDS–PAGE and autoradiography. (**B**) ERK3 was phosphorylated at 2 μM by 3 U/ml active MK5. Samples were removed at the indicated times and analysed by SDS–PAGE and autoradiography. Radiolabelled bands were excised and subjected to scintillation counting before calculation of the stoichiometry of ERK3 phosphorylation (phosphate incorporation in mol/mol). (**C**) Phosphorylation of ERK3 by MK5 *in vivo*. HeLa cells were either untransfected or cotransfected with expression plasmids encoding either Myc-tagged wild-type or kinase-dead ERK3 together with expression vectors encoding either EGFP alone, EGFPMK5 or constitutively active MK5 (EGFPMK5337G). After 24 h, cells were labelled for 4 h with [^{32}P]orthophosphate, lysed and ERK3 was immunoprecipitated using an anti-Myc monoclonal antibody. Immunoprecipitates were analysed by SDS–PAGE and radiolabelled ERK3 proteins were visualised and quantitated using a PhosphorImager. Incorporation of ^{32}P is expressed here relative to the amount detected in ERK3 when coexpressed with EGFP alone.

Firstly, we employed siRNA to knock down endogenous ERK3 protein in HeLa cells. Secondly, we obtained MEFs from animals in which the ERK3 gene has been deleted by homologous recombination. In both models, we see a significant reduction in endogenous MK5 activity. Finally, in agreement with recent studies (Coulombe *et al*, 2003), we have shown that PC12 cells induced to differentiate by NGF contain elevated levels of ERK3 protein and that this correlates with a significant increase in endogenous MK5 kinase activity.

Deletion of ERK3 does not abolish MK5 activity, causing a maximum reduction of approximately 40–50%. This suggests the existence of additional MK5 regulators in these cells. One possibility is that bound ERK3 prevents endogenous p38 from activating MK5. This might explain the finding that MK5 can be activated by p38 only when overexpressed, and suggests that in the absence of ERK3, p38 might interact with and activate endogenous MK5. We find that the sequence determinants for interaction between either ERK3 and MK5 or p38 and MK5 are distinct, and that mutated or truncated forms of both partner proteins exist, which affect interaction with ERK3 but not p38 and *vice versa*. Furthermore, whereas p38-mediated export of MK5 requires phosphorylation of Thr182 within MK5, ERK3-mediated export of MK5 did not require this modification. This indicates that although the relocalisation of MK5 by both ERK3 and p38 occurs via a CRM1-dependent export pathway, it is not mediated by a common mechanism. However, in preliminary experiments, we have been unable to demonstrate any effect of the p38 inhibitor SB203580 on endogenous MK5 activity in HeLa cells expressing specific siRNA against ERK3, indicating that p38 is not responsible for this residual MK5 activity.

A second possible regulator of MK5 activity was uncovered by a recent genomic analysis of ERK3. This revealed that, in addition to ERK3 (*MAPK6*), mice and humans possess a functional gene designated *MAPK4*, which encodes a 63 kDa ERK3 homologue (Turgeon *et al*, 2002). P63^{MAPK} displays 73% homology to ERK3 within the kinase domain and also contains the S-E-G motif. At present, nothing is known about the regulation and function of p63^{MAPK}, but expression is detected in human heart, brain and lung (Gonzalez *et al*, 1992). Future studies will examine the role of p63^{MAPK} in regulating MK5 activity.

Having demonstrated that ERK3 can activate MK5 *in vivo*, we wished to explore the possibility that, in addition to being activated by ERK3, MK5 also plays some role in regulating the function of ERK3 itself. This might be analogous to the dual role of MK2, which acts both as a substrate for p38 and as a chaperone to stabilise p38 protein levels (Kotlyarov *et al*, 2002). To approach this question, we have used siRNA to target endogenous MK5 in HeLa cells and have clearly shown that we can achieve a significant reduction in both protein level and associated MK5 kinase activity. Furthermore, loss of MK5 causes a dramatic reduction in the levels of endogenous ERK3 protein, which can be rescued by expression of siRNA-resistant murine MK5. In agreement with our results, a significant reduction in ERK3 protein levels is also detected in MEFs derived from MK5 knockout mice (Kotlyarov and Gaestel, personal communication). More interestingly, in the C57/B6 genetic background, MK5-deficient mice show embryonic lethality with incomplete penetrance, which results from embryonic death at about E11, the developmental stage where ERK3 expression is maximum (Kotlyarov and Gaestel, personal communication).

Finally, we have gone on to show that ERK3, in addition to activating MK5 and forming a complex that is translocated

from the nucleus to the cytoplasm, is also a potential substrate for the kinase activity of MK5. ERK3 is very efficiently phosphorylated by activated MK5 *in vitro* and *in vivo*. As yet it is unclear what the function of this modification might be. However, our demonstration that the T182A mutant of MK5 efficiently rescues the loss of ERK3 seen when endogenous MK5 is depleted and also relocalises to the cytoplasm as efficiently as the wild-type protein indicates that the kinase activity of MK5 towards ERK3 is not required for either the chaperoning or cotransport activities of MK5 towards ERK3.

In conclusion, we have presented convincing evidence for a functional link between the atypical MAPK ERK3 and the serine/threonine kinase MK5 and have identified the latter protein as the first *bona fide* physiological substrate for ERK3. At present, the functional consequences of this interaction and the resulting activation of MK5 are not clear. In the case of ERK3, elevated levels of protein are associated with the process of cellular differentiation (Boulton *et al*, 1991; Coulombe *et al*, 2003), and we have demonstrated a possible link between ERK3 accumulation and MK5 activity. ERK3 expression is also induced when human carcinoma cell lines are plated on type-IV collagen and correlated with decreased cell proliferation. Furthermore, overexpression of ERK3 inhibited cancer cell growth, migration and invasion (Crowe, 2004). All of the above point towards a negative role for ERK3 with respect to cell proliferation and this would be compatible with a key role for ERK3 and possibly MK5 during the process of tissue and cell differentiation. Our study provides important tools and suggests further experiments to probe the relationship between ERK3 and MK5 and the consequences of MK5 activation.

Materials and methods

SiRNA

All siRNAs were purchased as validated or predesigned from Ambion and transfected into HeLa cells using Lipofectamine 2000 according to the manufacturer's instructions. Precise details of the siRNAs used can be found in Supplementary data.

Localisation studies

Cells were fixed using 4% paraformaldehyde (PFA) and 0.3% Triton X-100 for 5 min and 4% PFA for 20 min. Cells were then incubated for 2 h with 3% BSA in phosphate-buffered saline before incubation with anti-ERK3 antibody at a final concentration of 2 μg/ml for 1 h. Immunostaining was developed using Alexa 594-conjugated anti-sheep IgG (1:400; Molecular Probes). Cell nuclei were visualised by staining with DRAQ5 (Biostatus Ltd, Leicestershire, UK). Images were collected using a Zeiss LSM510 confocal microscope. A detailed description of all other methods employed in this study can be found in Supplementary data of this paper.

Supplementary data

Supplementary data are available at *The EMBO Journal* Online.

Acknowledgements

We thank Geir Bjørkøy for confocal microscopy, and J Han and DR Alessi for plasmids. We acknowledge Andy Cassidy (University of Dundee) for DNA sequencing, professor P Cohen for advice and reagents, and the protein production and antibody purification teams (Division of Signal Transduction Therapy (DSTT), University of Dundee) coordinated by Hilary McLauchlan and James Hastie, for expression and purification of enzymes and affinity purification of antibodies. We also thank Alexey Kotlyarov and Matthias Gaestel (University of Hannover, Germany) for communicating results prior to publication. This work was supported by NFR (project numbers 151907/150,135823/310 and 16099/V40), DNK, the Aakres Foundation, CIHR (grant MOP-64320) and by Cancer Research UK.

References

Boulton TG, Nye SH, Robbins DJ, Ip NY, Radziejewska E, Morgenbesser SD, DePinho RA, Panayotatos N, Cobb MH, Yancopoulos GD (1991) ERKs: a family of protein-serine/threonine kinases that are activated and tyrosine phosphorylated in response to insulin and NGF. *Cell* **65:** 663–675

Cheng M, Boulton TG, Cobb MH (1996) ERK3 is a constitutively nuclear protein kinase. *J Biol Chem* **271:** 8951–8958

Coulombe P, Rodier G, Bonneil E, Thibault P, Meloche S (2004) N-terminal ubiquitination of extracellular signal-regulated kinase 3 and p21 directs their degradation by the proteasome. *Mol Cell Biol* **24:** 6140–6150

Coulombe P, Rodier G, Pelletier S, Pellerin J, Meloche S (2003) Rapid turnover of extracellular signal-regulated kinase 3 by the ubiquitin–proteasome pathway defines a novel paradigm of mitogen-activated protein kinase regulation during cellular differentiation. *Mol Cell Biol* **23:** 4542–4558

Crowe DL (2004) Induction of p97MAPK expression regulates collagen mediated inhibition of proliferation and migration in human squamous cell carcinoma lines. *Int J Oncol* **24:** 1159–1163

Cuenda A, Rouse J, Doza YN, Meier R, Cohen P, Gallagher TF, Young PR, Lee JC (1995) SB 203580 is a specific inhibitor of a MAP kinase homologue which is stimulated by cellular stresses and interleukin-1. *FEBS Lett* **364:** 229–233

Davis RJ (2000) Signal transduction by the JNK group of MAP kinases. *Cell* **103:** 239–252

Garrington TP, Johnson GL (1999) Organization and regulation of mitogen-activated protein kinase signaling pathways. *Curr Opin Cell Biol* **11:** 211–218

Gonzalez FA, Raden DL, Rigby MR, Davis RJ (1992) Heterogeneous expression of four MAP kinase isoforms in human tissues. *FEBS Lett* **304:** 170–178

Johnson GL, Lapadat R (2002) Mitogen-activated protein kinase pathways mediated by ERK, JNK, and p38 protein kinases. *Science* **298:** 1911–1912

Julien C, Coulombe P, Meloche S (2003) Nuclear export of ERK3 by a CRM1-dependent mechanism regulates its inhibitory action on cell cycle progression. *J Biol Chem* **278:** 42615–42624

Kotlyarov A, Neininger A, Schubert C, Eckert R, Birchmeier C, Volk HD, Gaestel M (1999) MAPKAP kinase 2 is essential for LPS-induced TNF-alpha biosynthesis. *Nat Cell Biol* **1:** 94–97

Kotlyarov A, Yannoni Y, Fritz S, Laass K, Telliez JB, Pitman D, Lin LL, Gaestel M (2002) Distinct cellular functions of MK2. *Mol Cell Biol* **22:** 4827–4835

Kudo N, Wolff B, Sekimoto T, Schreiner EP, Yoneda Y, Yanagida M, Horinouchi S, Yoshida M (1998) Leptomycin B inhibition of signal-mediated nuclear export by direct binding to CRM1. *Exp Cell Res* **242:** 540–547

Kyriakis JM, Avruch J (2001) Mammalian mitogen-activated protein kinase signal transduction pathways activated by stress and inflammation. *Physiol Rev* **81:** 807–869

Marshall CJ (1994) MAP kinase kinase kinase, MAP kinase kinase and MAP kinase. *Curr Opin Genet Dev* **4:** 82–89

Meloche S, Beatty BG, Pellerin J (1996) Primary structure, expression and chromosomal locus of a human homolog of rat ERK3. *Oncogene* **13:** 1575–1579

Morooka T, Nishida E (1998) Requirement of p38 mitogen-activated protein kinase for neuronal differentiation in PC12 cells. *J Biol Chem* **273:** 24285–24288

New L, Jiang Y, Han J (2003) Regulation of PRAK subcellular location by p38 MAP kinases. *Mol Biol Cell* **14:** 2603–2616

New L, Jiang Y, Zhao M, Liu K, Zhu W, Flood LJ, Kato Y, Parry GC, Han J (1998) PRAK, a novel protein kinase regulated by the p38 MAP kinase. *EMBO J* **17:** 3372–3384

Ni H, Wang XS, Diener K, Yao Z (1998) MAPKAPK5, a novel mitogen-activated protein kinase (MAPK)-activated protein kinase, is a substrate of the extracellular-regulated kinase (ERK) and p38 kinase. *Biochem Biophys Res Commun* **243:** 492–496

Seternes OM, Johansen B, Hegge B, Johannessen M, Keyse SM, Moens U (2002) Both binding and activation of p38 mitogen-activated protein kinase (MAPK) play essential roles in regulation of the nucleocytoplasmic distribution of MAPK-activated protein kinase 5 by cellular stress. *Mol Cell Biol* **22:** 6931–6945

Shi Y, Kotlyarov A, Laabeta K, Gruber AD, Butt E, Marcus K, Meyer HE, Friedrich A, Volk HD, Gaestel M (2003) Elimination of protein kinase MK5/PRAK activity by targeted homologous recombination. *Mol Cell Biol* **23:** 7732–7741

Turgeon B, Lang BF, Meloche S (2002) The protein kinase ERK3 is encoded by a single functional gene: genomic analysis of the ERK3 gene family. *Genomics* **80:** 673–680

Turgeon B, Saba-El-Leil MK, Meloche S (2000) Cloning and characterization of mouse extracellular-signal-regulated protein kinase 3 as a unique gene product of 100 kDa. *Biochem J* **346** (Part 1): 169–175

Wolff B, Sanglier JJ, Wang Y (1997) Leptomycin B is an inhibitor of nuclear export: inhibition of nucleo-cytoplasmic translocation of the human immunodeficiency virus type 1 (HIV-1) Rev protein and Rev-dependent mRNA. *Chem Biol* **4:** 139–147

Zhu AX, Zhao Y, Moller DE, Flier JS (1994) Cloning and characterization of p97MAPK, a novel human homolog of rat ERK-3. *Mol Cell Biol* **14:** 8202–8211

The EMBO Journal (2005) 24, 873–874 | © 2005 European Molecular Biology Organization | All Rights Reserved 0261-4189/05
www.embojournal.org

THE EMBO JOURNAL

Erratum

Activation of MK5/PRAK by the atypical MAP kinase ERK3 defines a novel signal transduction pathway

Ole-Morten Seternes, Theresa Mikalsen, Bjarne Johansen, Espen Michaelsen, Chris G Armstrong, Nick A Morrice, Benjamin Turgeon, Sylvain Meloche, Ugo Moens and Stephen M Keyse

The EMBO Journal (2005) **24,** 873–874. doi:10.1038/sj.emboj.7600591

Correction to: *The EMBO Journal* (2004) **23,** 4780–4791. doi:10.1038/sj.emboj.7600489

Due to a typesetting error, Figure 3c of the above article was published incorrectly in print. The correct Figure 3 is reproduced below in its entirety.

The Publisher would like to apologise for any inconvenience this may have caused.

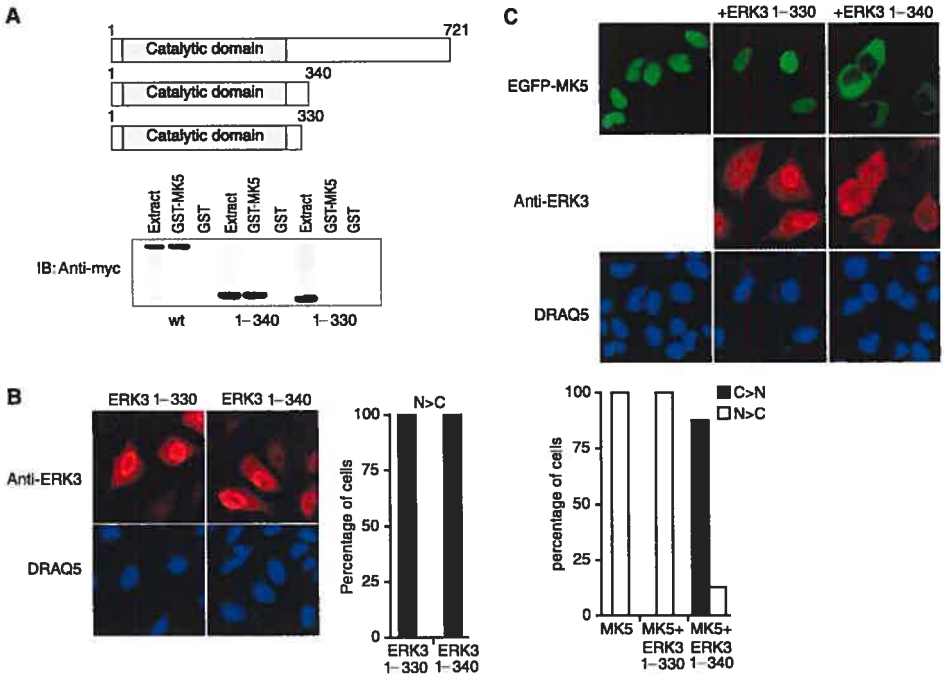

Figure 3 For Caption see next page

Figure 3 Amino acids 330–340 of ERK3 are required for interaction with and relocalisation of MK5. (**A**) COS-1 cells were transfected with expression vectors encoding Myc-tagged full-length, or C-terminal truncation mutants of ERK3 encoding either amino acids 1–340 or 1–330 of the protein. Cell lysates were then mixed with either recombinant GST-MK5 or GST alone. Binding of ERK3 was detected by Western blotting using an anti-Myc monoclonal antibody. (**B**) HeLa cells were transfected with expression vectors encoding either amino acids 1–330 or 1–340 of ERK3. ERK3 was visualised by staining with an anti-ERK3 antibody and an Alexa 594-coupled secondary (anti-sheep) antibody (red channel in upper panels) and cell nuclei were visualised by DRAQ5 staining (blue channel in lower panels). In all, 100 cells expressing the indicated mutant of ERK3 from each of three independent transfections were counted and the distribution of the ERK3 protein was scored. The results are presented as the % of cells in which the ERK3 protein was predominantly nuclear (N>C) and mean values with associated errors are shown. (**C**) HeLa cells were cotransfected with vectors encoding EGFP-MK5 and either ERK3 1–330 or 1–340. EGFP-MK5 was visualised directly (green channel in upper panels), ERK3 was visualised by staining with an anti-ERK3 antibody and an Alexa 594-coupled secondary (anti-sheep) antibody (red channel in middle panels) and cell nuclei were visualised by DRAQ5 staining (blue channel in lower panels). A total of 100 cells expressing either EGFP-MK5 alone or coexpressing both EGFP-MK5 and the indicated mutant of ERK3 from three independent transfections were counted and the distribution of MK5 was scored. The results are presented as the % of cells in which EGFP-MK5 was either predominantly nuclear (N>C) or predominantly cytoplasmic (C>N) and mean values with associated errors are shown. In all experiments, several fields of cells were examined and representative images are shown.